UNIVERSITY OF LONDON THESIS

Degree PhD Year 2006 Name of Author HOLMES Toby M

A study of the retinal vascular pathology in the Royal College of Surgeons Rat: A model of human retinal degeneration.

Toby M Holmes

Institute of Ophthalmology

PhD Thesis

ProQuest LLC
789 East Eisenhower Parkway
P.O. Box 1346
Ann Arbor, MI 48106-1346

Abstract

A study of the retinal vascular pathology in the Royal College of Surgeons Rat: A model of human retinal degeneration.

The leading causes of loss of vision in the developed world are the degenerative diseases of photoreceptors; in particular, age-related macular degeneration (AMD) and retinitis pigmentosa (RP). A common characteristic of these diseases is secondary damage affecting the vascular network, which is apparently initiated by photoreceptor loss. One problem with investigating the vascular consequences of these diseases has been the lack of a suitable animal model that can be used to investigate various potential treatments. This study has developed methods of quantifying retinal vascular damage in the pigmented Royal College of Surgeons (RCS) rat, which is characterised by the formation of vascular complexes and these methods have been used to explore strategies to retard or reverse this damage. This was done with the view to improving the retinal environment, thereby assisting other therapeutic strategies that target the primary defect causing the loss of photoreceptors. The work was divided into three areas: 1) investigation of the vascular effects of progressive photoreceptor loss and development of computerised image analysis to quantify changes, 2) pharmaceutical intervention to modify the normal sequence of events, 3) examination of the effects of RPE sub-retinal transplantation on the vascular network to determine how the retinal vasculature would react to the presence of transplanted human RPE cells at different time-points.

These three areas of study validate the use of naturally occurring events in the RCS rat to provide a model of vascular pathology in human retinal degenerative diseases. This contrasts with previous models, which have relied on creating wounds to simulate conditions that occurring in the diseased human retina.

Acknowledgement

There are two people in particular that I should thank for getting me started on this project, first Professor Raymond Lund for giving me the opportunity to register, the countless re-reads and putting up with me in his lab. Also Dr Jean Lawrence for giving me the initial encouragement to get started without which none of this would have happened.

There are many people that I should acknowledge starting with those members of the original lab who stayed in the Institute of Ophthalmology, Tim Pheby, Dr. David Keegan (whose ability to sing while performing transplants will always be remembered), Dr Tony Kwan, Dr Jean Lawrence and Dr Polly Litchfield. Outside of the lab there was John Peacock as the voice of sanity in the IOO administration and the voice of reason in the Fountain public house. Thank you to Dr Mike Cheethams lab at the IOO, especially Dr Paul Chapple for help with the western blot and encouragement over the years.

I will always be indebted to those members of the lab who made the journey to Utah for their patient advice and good humour. Dr Shaomei Wang for her years of unstinting support and many lunch boxes of steamed Chinese dumplings, Dr Lu Bin for his help performing the transplantation procedures. Dr Sergej Girman for his aura of calm when things did not go as they should and ability to build nearly anything out of other peoples junk. Dr Elsa Raibon for reminding me that it was worth the trek and lastly Nic for buying me the time to get this finished.

There are many others that I could mention who have given encouragement and support along the way such as my family and friends but this is already starting to read like an Oscar acceptance speech so I will stop here.

Contents

List of Figures

1.0 Literature Review For "A Study Of The Retinal Vascular Pathology In The RCS Rat...".

1.1 Aims

The primary goal of this project was to investigate the dynamics of the retinal vasculature in the pigmented dystrophic Royal College of Surgeons (RCS) rat that develop in conjunction with the appearance of pigmented cells in the inner retina. Vascular anomalies were observed in our laboratory (Villegas-Perez et al., 1998; Villegas-Perez et al., 1996) during investigations of ganglion cell loss in advanced retinal degeneration in the dystrophic RCS rat model and later vascular pathology in the rd mouse and RCS rat (Wang et al., 2000) (Wang et al., 2003).

This work has three major aims: 1) To investigate the vascular events that accompany progressive photoreceptor loss and to develop computerised image analysis methodology to quantify changes, 2) To develop pharmaceutical treatments to modify the secondary vascular events, 3) To examine the effects of sub-retinal transplantation of human retinal pigmented epithelium (RPE) cells on the retinal vascular network in the RCS rat.

These three areas of study utilised the naturally occurring events in the RCS rat as a model of vascular pathology that is relevant to human retinal degenerative diseases. The RCS retina provided an assay system for assessing pharmaceutical and cell-based modifications to the retinal environment with minimal disturbance of the natural conditions. This contrasts with previous models, which have relied on creating retinal lesions to simulate conditions occurring in the diseased human retina (Campochiaro and Hackett, 2003) or have used inappropriate non-pigmented animals (Seaton et al., 1994).

The long-term objective of this work was to gain an understanding of the secondary vascular events in retinal degeneration and to enable manipulation of the retinal environment that could improve the outcome of potential therapies for human diseases of retinal degeneration.

1.2 Anatomy Of The Retina

Before any analysis of the vascular network of the retina can be undertaken a clear understanding of the basic structure of the retina is required.

1.2.1 Development Of The Retina

The retina is the light sensing part of the eye containing the visual pigments that absorb and process light into neural impulses in the process called photo-transduction. The retina develops out of the neural tube early in embryonic life as two optic vesicles forming in the region that will become the animal's head (Fig **1.1**). These optic vesicles invaginate to form proto-eye structures called optic cups. The cells on the inner surface of the optic cup divide and differentiate into the seven different layers of the retina (Marquardt and Gruss, 2002), while the outer layers develop into the retinal pigment epithelium.

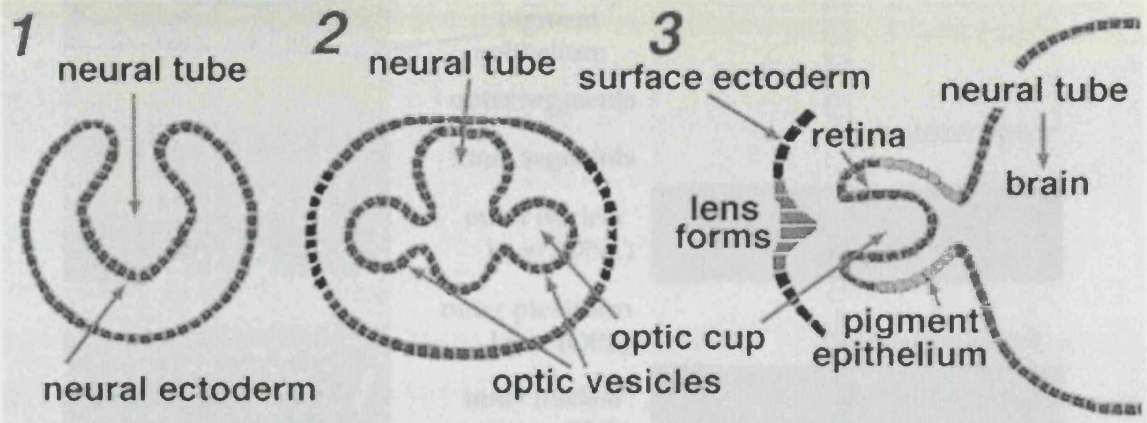

Figure 1.1 Eye Development, Three early stages of eye development, showing the origins of the retina. (picture courtesy of www.webvision.med.utah.edu).

Due to its origins in development the retina has many shared characteristics of neural tissue such as the blood-retinal barrier and the relative lack of extracellular matrix within the retina. Retinal progenitor cells have been found to produce a limited repertoire of cell types in an ordered sequence as the retina develops with ganglion cells generally being produced first. The order in which the retinal cells develop varies with different species but cones, horizontal cells and amacrine cells generally follow ganglion cells (development of different cells greatly overlap each other) with rods next and bipolar and Muller cells last (Cepko et al., 1996).

1.2.3 Retina Structure

The structure of the retina is complex and laminated in nature with alternating layers of cellular elements and interconnecting neural processes. These act to collect and process visual information before transmission to the visual centres of the brain via the optic nerve. Anatomically the retina forms seven major layers, bound between two membranes,

the inner limiting membrane on the inner surface of the retina and Bruch's membrane separating the RPE from the choroid.

As mentioned above there are seven major cell types within the retina of which there are numerous subtypes that vary from species to species. These cell types tend to populate distinct zones within the retina forming distinct anatomical layers of the retina as illustrated in figure **1.2** below.

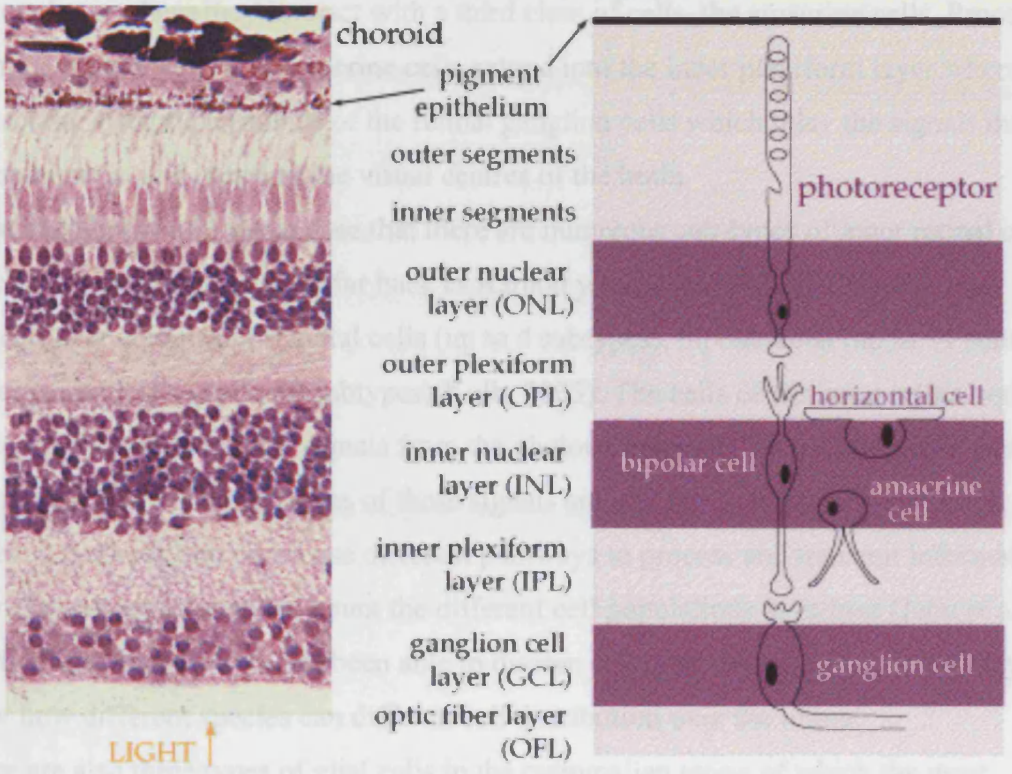

Figure 1.2 Mammalian Retina. Cross section of the retina (left) with associated diagram (right) showing important cell types in signal transduction of light from the photoreceptors back to the ganglion cells and optic fibre layer which sends the visual signals to the optic nerve.

The exception to this is the Müller cells which extend processes from the photoreceptors to the ganglion cells layer where its lateral processes form the inner limiting membrane with basement membrane molecules. A good basic overview of the structure of the retina can be obtained online at the WebVision web site (Kolb, 2002). The neural cells of the retina form the bulk of the cellular mass of the retina. Starting with the photoreceptors, of which there are two basic types called rods and cones. There may be several different subtypes of each depending on the wavelengths of light required by the evolutionary

niche of the animal studied (Bowmaker, 1998). The density of photoreceptors may also vary but much of that may be due to specialised adaptations such as the macula. The macula is a very densely packed cone rich region of the retina that is adapted for colour vision. Rat retinas may not require colour vision and have no macula but are rich in rod photoreceptors that detect monochromatic light levels and contrast. The photoreceptors extend from the RPE in to the outer plexiform layer where they connect via synaptic processes to the bipolar and horizontal cells. Both of these cells extend into the inner nuclear layer where they interact with a third class of cells, the amacrine cells. Processes from the bipolar cells and amacrine cells extend into the inner plexiform layer where they contact the synaptic terminals of the retinal ganglion cells which relay the signals through the optic nerve and hence to the visual centres of the brain

It has been known for some time that there are numerous sub-types of inner retinal cells which been described from as far back as Ramon y Cajal in 1892. The human inner nuclear layer contains horizontal cells (up to 4 subtypes), bipolar cells (up to 11 subtypes) and amacrine cells (up to 30 subtypes)(Kolb, 2003). The cells of the inner retina both process and transmit neural signals from the photoreceptors to the ganglion cells (up to 20 sub-types). The exact sequences of these signals are still not fully understood, but it is believed that rods and cones use different pathways to process and transmit information. There have been attempts to count the different cell populations in retinae (Jeon et al., 1998). These studies have not been able to discern cell type sub-populations but they show how different species can differ in cell distribution over the retina.

There are also three types of glial cells in the mammalian retina of which the most numerous are Müller cells. These cells have essential support functions to neural cells such as fuelling aerobic metabolism to nerve cells and removing waste end products from these cells. The other two types of glial cells are astrocytes and microglia, which are found in the optic fibre layer and alongside blood vessels.

The outermost layer of the retina is the RPE, a monolayer that is an essential regulatory component for the retina. The RPE and the photoreceptors interact within a glycosaminoglycan rich area called the inter photoreceptor matrix (IPM) The RPE is not directly involved in signal transduction but has an essential role in photopigment regeneration, nutrient transfer, maintaining the photoreceptors and the outer blood-retinal barrier. The RPE also maintains Bruch's membrane: a basal lamina to which it is attached and which separates the retina from the highly vascular choroid.

1.3 Rod And Cone Photoreceptors

The photoreceptors are the cells where phototransduction takes place in the retina and as such are the first step in the chain of information being relayed to the visual centres of the brain. There are two types of photoreceptors, called rods and cones due to the shape of their outer segments. Within those two types can be several sub-types which have evolved to detect different types of light depending on the evolutionary requirements of the species (Ahnelt and Kolb, 2000). To do this they have evolved different visual pigments, rods contain rhodopsin (Menon et al., 2001), which detect low intensity light. Cone photoreceptors contain opsins (Travis, 2005), which detect high intensity light of various wavelengths adapted for daylight conditions.

1.3.1 Photoreceptor Structure

The physical structure of these cells consists of long thin columns with two major segments and a synaptic terminal, as shown in figure **1.3**.

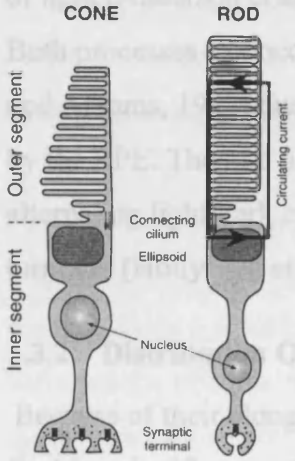

Figure 1.3 Photoreceptor structure (courtesy of The visual neurosciences by Chalupa & Werner)

Both rods and cones have their synaptic terminal in the OPL. The inner segment or cell body is located in the INL. It comprises of the nucleus and the cell organelles, such as the endoplasmic reticulum and Golgi apparatus, followed by a mitochondria rich area called the epsiloid. The epsiloid is responsible for delivering adenosine triphosphate (ATP) to the photoreceptor disks of the outer segments and for focusing photons onto the photoreceptor disks. The inner segments end with the photoreceptor cilium, a narrow constriction where proteins waiting to be formed into photoreceptor disks must pass before assembly into photopigment disks. The assembly of the photopigment

membranous disks occurs at the base of the outer segments (OS). The OS are formed of many membranous disks formed into stacks that reach into the interphotoreceptor matrix (IPM) and contact the apical process of the RPE. There are between 500-2000 disks in each rod photoreceptor (Brown et al., 1963) with membrane-bound visual pigment molecules (about10^9 molecules to each photoreceptor cell) studded along the disks.
The stacks of rods and cones have slightly different structures in that the rods are sealed off by the surrounding plasma membrane whereas the cone stacks are connected and continuous with the plasma membrane and therefore open to the extracellular environment. Early electron microscopy of radioactive pulse chase experiments showed rod outer segment assembly and casting (Young and Bok, 1969) but due to the open structure of cone photoreceptors this was not immediately apparent with cones (Anderson et al., 1978). More recent research showed that the radioactive tracer diffused through the cones due to the open structure of the cone stacks. Cones do shed OS but with peak activity immediately after dark as opposed to rods whose peak casting time is after onset of light (Anderson et al., 1978; Besharse et al., 1977; LaVail, 1976).
Both processes can occur very rapidly and require the interaction of healthy RPE (Hall and Abrams, 1987) due to the vast quantities of OS disks, which must be phagocytosed by the RPE. The rate of turnover is affected by light levels and temperature, with alternating light/dark cycles being optimal, increased body temperature resulting in faster turnover (Hollyfield et al., 1977);(Besharse et al., 1977).

1.3.2 Distribution Of Photoreceptors

Because of their elongated structure and the densely packed environment of the retina (lacking significant extracellular matrix) it is nearly impossible to grow intact photoreceptors *in vitro*, a fact that has greatly limited research on these cells.
Rods and cones are arranged in a mosaic with usually many rods surrounding each cone with exceptions such as the primate fovea, which is a very cone rich central region of the retina and another being the tree shrew (*Tupaia Belangeri*) retina that has 95% cones with 5% very small rods (Petry et al., 1993). In humans the composition is 95% rods to 5% cones, in rodents that are nocturnal animals it is 99% rods to 1% cones (Ahnelt and Kolb, 2000; Peichl, 2005). The distribution of cones and rods also changes from central to peripheral retina, with the majority of cones being situated in the central retina. It should be noted that the ratio of cones to rods in primates and rodents are roughly the same away from the macula.

1.3.3 Phototransduction

This study is not concerned with the metabolic pathways of phototransduction but a brief overview of the process helps explain the importance of the effect of the Mertk mutation in the RPE of the RCS rat that is central to this study.

The absorption of light by the photoreceptors of the retina is only the initial part of the cascade of reactions that comprise phototransduction. There are several steps, leading to the hyperpolarisation of the photoreceptor, which in turn triggers the synaptic release of the neurotransmitter, glutamate. This process, must be followed by recovery cascades before the photoreceptor can recover sensitivity (Jones et al., 1989). In cones, this process occurs very rapidly but requires many photons of light to be triggered whereas in rods, the process takes much longer but is up to 4 log units more sensitive requiring only several photons to be triggered.

The rods and cones have different photopigments responsible for absorption of light at differing wavelengths. Rods contain rhodopsin or porphoryin, corresponding to vitamin A_1 aldehyde and vitamin A_2 aldehyde based metabolisms respectively and cones contain iodopsin. Detailed structural analysis of rhodopsin, its binding sites and the transduction cycle can be found in several reviews (Burns and T., 2003; Menon et al., 2001).

Photoreceptor activation starts when sufficient photons are absorbed by rhodopsin, triggering biochemical changes that result in the separation of the retinal pigment from the rhodopsin (called bleaching). This in turn activates the G-protein, transducin which activates the effector protein, phosphodiesterase (PDE). The activated PDE hydrolyses cyclic guanosine monophosphate (cGMP), reducing cGMP levels in the cell, this closes the cGMP-gated Na^+ and $Ca2^+$ channels causing the photoreceptor cell to hyperpolarise and release glutamate from the terminal synapse.

Photoreceptor inactivation is still not entirely understood but its known to be an active process, critical for fast response in the visual system, especially in high light levels. To inactivate the photoreceptor, the molecules mentioned above have to be returned to their original state. Rhodopsin is shut off by phosphorylation of its COOH terminal domains by rhodopsin kinase, followed by arrestin binding to quench the catalytic effect of activated rhodopsin. Transducin and PDE must also be shut off. It is theorised that regulators of G protein signalling (RGS) proteins are responsible for shutting down both

of these molecules when transducin is bound to PDE. Transducin cannot be turned off until it has bound to PDE.

The exact trigger for the inactivation sequence is not fully understood, but cytoplasmic calcium ion levels are thought to be instrumental in feedback circuitry controlling phototransduction (Hwang et al., 2003).

1.4 The Interphotoreceptor Matrix (IPM)

Under normal light microscopy it appears that the photoreceptor OS are in direct contact with processes of the apical RPE. However this is not the case as at higher magnifications (electron microscopy), using selective immunocytochemistry with lectins (Mieziewska et al., 1991) or alcian blue histochemistry, a glycosaminoglycan-rich area can be seen separating the photoreceptor OS from the RPE (Chen et al., 2004). This is the interphotoreceptor matrix (IPM) which envelopes the OS and acts as a transition layer for transport of vitamin A (Adler and Evans, 1985). The IPM is important in the attachment of the retina to the RPE (Hageman et al., 1995). Electron microscopy has also shown Muller cell processes terminating in the IPM (Bernstein, 1985). It is known that there are rod and cone specific areas in the IPM, which may have different biochemical microenvironments due to transport of the different rod and cone retinols and processed by-products (Mieziewska et al., 1991).

The IPM is composed of proteoglycans and glycosaminoglycans, such as hyaluronic acid and relatively high levels of chondroitin sulphates. These proteoglycans are believed to bind to pigment epithelial derived factor (PEDF) in the IPM (Alberdi et al., 1998) and may be involved in growth factor interactions within the IPM. The IPM, through retinoid binding protein (IRBP) plays a role in the retinol/vitamin A exchange (Adler and Evans, 1985) between photoreceptors and the RPE, which makes it an extremely biochemically active site. Consequently any abnormalities in the IPM would have serious consequences. Mutations in interphotoreceptor matrix proteoglycan-1 have been implicated in several forms of Stargardt's disease but have been eliminated as a candidate for others (Gehrig et al., 1998). The RCS rat has been shown to have abnormal IPM staining due to the formation of the debris zone (LaVail et al., 1981).

1.5 The Retinal Pigmented Epithelium

The RPE has a role in all forms of photoreceptor degeneration either as the primary cause such as in the RCS rat (D'Cruz et al., 2000) or as a secondary consequence when the primary defect lies with the photoreceptors (Cideciyan et al., 1998). This is due to the fact that the RPE's role in reprocessing of used photoreceptor photo-pigment for transport back to the photoreceptors is essential for healthy retinal metabolism.

1.5.1 The Structure Of The RPE

The structure of the RPE appears as a monolayer of darkly pigmented cuboidal cells, sandwiched between the photoreceptor outer segments/IPM and Bruch's membrane to which they are anchored. The cells are not really cuboidal as they have many thin processes that reach out into the IPM where they interact with the photoreceptor's OS. Bruch's membrane is a basal lamina that forms the outer limits of the retina and separates the cells of the retina from the choroid but allows nutrients to pass from the highly vascular choroid to the retina (Bialek and Miller, 1994). Water and waste products flow back into the choroid to help maintain the correct physiological conditions in the outer retina. The intracellular structure of the RPE on the other hand is fairly complex due to the number of functions these cells accomplish.

The individual RPE cell structure can be separated into three functional areas, with the apical surface towards the photoreceptors having many long "end feet" which are intertwined with the rods, and reach into the inter-photoreceptor matrix to the shorter cone outer segments. The apical side contains the microtubules and microfilaments responsible for capturing and ingesting spent photoreceptor outer segments. It also contains most of the melanosomes, granules that contain the dark pigment melanin. The central portion contains the nucleus, Golgi apparatus and all of the organelles required for manufacturing, as well as phagocytic lysosomes for breaking down used OS disks (Bosch et al., 1993). The basal side adheres to Bruch's membrane and provides as much surface area as possible for transport of nutrients and metabolites to and from the choroids via Bruch's membrane. The RPE monolayer is maintained by tight junctions between adjacent RPE cells called zonula occludens that form near the apical surface.

1.5.2 Function Of The RPE In The Retina

The dark pigment of the RPE is melanin, found in granules called melanosomes throughout the apical surface of the cells, which may play a role in absorbing scattered

stray light. A second pigment called lipofuscin is also present in the RPE. Lipofuscin increases with age and it starts to bind to melanosomes eventually causing them to fade (Delori et al., 2001). Lipofuscin is found throughout the nervous system, where it accumulates with age.

In humans further macular pigments, Lutein and Zeaxanthin, are found in the macula where they accumulate with age according to dietary intake, and have been investigated for their anti-oxidant properties to protect the macula (Davies and Morland, 2004).

Although the RPE forms a monolayer, the density of RPE cells varies across the retina being more densely packed in the central retina than in peripheral retina where it tends to be broader and flatter. This follows the distribution of photoreceptors; roughly there are 45 photoreceptors (rods) in humans and 300 in rats for each RPE cell (Marmor, 1998). This along with knowledge of the rate of photoreceptor shedding allows calculations to be made of how much OS are ingested and processed each day by a single RPE cell. This is about $3.68x10^8$ opsins/RPE cell processed daily in humans and roughly ten times as much in rats and has been summarised for several species (Besharse and Defoe, 1998). The high metabolic turnover demonstrates just how essential the RPE is to healthy vision.

From the viewpoint of retinal degeneration, the most important role for the RPE in the retina is in the turnover of photoreceptor outer segments, as elegantly shown by Young and Bok's radioactive pulse chase experiments (Young and Bok, 1969). The RCS rat serves as a good example of what can happen if this process is impaired: the lack of OS metabolism results in the formation of the debris zone and rapid degeneration of the rod photoreceptors by apoptosis (Custer and Bok, 1975; Travis, 1998). The process of OS phagocytosis follows the sequence of OS detachment-RPE binding-internalisation-digestion-recycling of vitamin A/retinol back to the photoreceptors (Bosch et al., 1993; Flannery et al., 1990). This process allows the reprocessing of the vitamin A/retinol essential for healthy photoreceptor metabolism.

The RPE perform a host of functions outside of OS ingestion, such as maintaining the outer retinal environment by controlling the blood-retinal barrier, maintaining osmotic regulation in the retina, production of growth factors and pigments, and transport of nutrients/waste to and from the choroidal blood supply. The RPE also plays an essential role in repair of damaged retina, with immunological functions and scarring of the retina all associated with the RPE.

1.5.3 RPE And Retinal Degeneration

The RCS rat, Mertk (D'Cruz et al., 2000) mutation and its human orthologue MERTK (Gal et al., 2000) both present a photoreceptor degeneration due to a mutation in the receptor tyrosine kinase gene mer . In the RCS rat this causes a very specific fault, due to a deletion, producing a truncated protein, which halts the internalisation phase of rod OS phagocytosis by the RPE (Feng et al., 2002). In humans, mutations in MERTK, are found in a subset of RP patients (Gal et al., 2000). Antibody studies have shown binding of OS with Mertk (MERTK for human, Mertk for rat: tk refers to tyrosine kinase) to RCS RPE cells *in vitro*, but only when the Mertk fault was repaired by gene therapy could internalisation of OS take place at non-dystrophic levels(Vollrath et al., 2001). This is important, as it shows that the Mertk mutation does not disable the rest of the internalisation process, therefore correction of the human MERTK mutation is at least feasible. There is still some debate as to exactly how healthy RPE internalise OS but recent work has started to eliminate some of the possible candidates with two hypotheses being put forward. One group favours integrin $\alpha V\beta 5$ dependent binding of OS (Finnemann et al., 1997; Finnemann and Rodriguez-Boulan, 1999; Finnemann and Silverstein, 2001), resulting in focal adhesion kinase (FAK) signalling CD36 (scavenger receptor), and Mer (or Mertk blocked internalisation) mediated internalisation (Finnemann, 2003)(this step is blocked in the dystrophic RCS rat).

The second hypothesis is that OS phagocytosis is membrane-receptor mediated with RPE bound GAS6 (growth arrest specific gene6) being required for OS internalisation (Hall et al., 2001) as it is the cognate ligand for the tyrosine kinase family. This second hypothesis does not require the integrin $\alpha_V\beta_5$ (Hall et al., 2003) and is supported by experiments using primary cell cultures rather than passaged cells, as membrane changes due to passaging of cells give erroneous results in the first hypothesis. The exact mechanism is still unclear, and investigations continue.

The migration of the RPE, seen in later secondary events in the RCS dystrophy, may in part be due to oxidative stress (Bailey et al., 2004) due to the formation of the debris zone. This may partly explain why the RPE, eventually lifts off Bruch's membrane and migrates onto the vasculature of the inner retina (Wang et al., 2003). This phenomenon is very similar to the classic "bone spicule" formations seen around blood vessels in clinically defined RP (Li et al., 1995). The exact trigger for this migration is unknown but

may lie in the microenvironment around the tight junctions involved in RPE-RPE interactions, and/or the RPE basal surface attachments to Bruch's membrane.
The fact that RPE cells are so active raises the questions why these cells migrate into the inner retina under conditions of retinal degeneration? and what are these cells doing once they get there?

1.6 Human Diseases Of Retinal Degeneration

The majority of cases of human retinal degeneration occur in aged individuals (age>65), with the increasing average age in the occidental world, diseases of retinal degeneration have become leading cause of blindness, with the most common being Age Related Macular Degeneration (AMD, or ARMD) and retinitis pigmentosa (RP); Less common are Stargardt's disease, Usher's syndrome and Leber's Congenital Amaurosis. Both AMD and RP are in reality a complex group of diseases with related clinical pathologies, but different causal agents. RP is inherited and while some forms of AMD are clearly monogenic, there are also environmental factors that increase incidence, such as smoking and diet (Tomany et al., 2004). The incidence of these diseases has been studied extensively over time in large clinical studies (Bundey and Crews, 1984a; Bundey and Crews, 1984b; Bunker et al., 1984; van Leeuwen et al., 2003; Wang et al., 2004) and also in isolated communities where increased susceptibility/incidence has been recorded (Eichers et al., 2002). There are good reviews (Inglehearn, 1998) and resources such as RetNet (Daiger et al.) which list most of the inherited mutations currently known to cause human retinal degenerative diseases. It is clear that many of these disorders are closely related and patients may possess several sets of mutations complicate diagnosis, and future treatment.

1.6.1 Age Related Macular Degeneration

The most common group of retinal degenerative diseases is AMD, with an incidence of 1in 3 patients over age 65 (Sommer et al., 1991). AMD is characterised by RPE dysfunction, resulting in build up of extracellular material (called drusen) between the RPE and Bruch's membrane. Clinically AMD presents in two forms, dry and wet, both of which exhibit drusen. Dry AMD or geographic atrophy is characterised by an area of hypopigmentation, depigmentation or apparent lack of RPE usually round or oval in appearance allowing visualisation of the choroidal vessels. Wet AMD (also called disciform or exudative) is less common (10% of AMD cases) but much more serious; where patients may exhibit RPE detachments, major choroidal neovascularisation (CNV)

associated with extensive hard exudative drusen and characteristic breaches in Bruch's membrane (Bird et al., 1995). This leads to subretinal haemorrhaging with the potential total loss of vision (Bird et al., 1995). Dry AMD may not result in total blindness but loss of quality of life for elderly patients can be devastating. Changes in the retina due to AMD are preceded by gradual changes in the RPE and Bruch's membrane, which are notoriously difficult to detect prior to the insurgence of clinical symptoms. Over the past decade there have been some far reaching surveys of which the largest have been the Beaver Dam, Blue Mountain (Wang et al., 2004) and Rotterdam (van Leeuwen et al., 2003) studies, now collated (Tomany et al., 2004) which detail the incidence, onset and progression of AMD in large populations. Regular eye exams might allow earlier changes to be detected with the aid of fluorescein angiography and Amsler grids (Fink and Sadun, 2004) although recent attempts to computerise these tests have elicited mixed opinions (Zaidi et al., 2004).

There is no current cure for AMD, but some certain treatments such as radiation therapy, photodynamic therapy and removal of submacular CNV (Chong and Bird, 1998; Fine et al., 2000; Stokkermans, 2000)} have been shown to slow down its progression. High dose vitamins A & E, β-carotene and zinc (Sackett and Schenning, 2002) (age-related eye disease study - AREDS) have been shown to lower the risk of developing AMD by 25%. A problem with this approach has been getting patients to adhere to the required treatment (Chang et al., 2003). Surgical treatments such as laser photocoagulation (Abdelsalam et al., 1999) and photodynamic therapy (Regillo, 2000; Wenkstern and Stokes, 2003) have been tried with limited success to control the choroidal neovascularisation of wet AMD as they do not address the underlying pathology. In macular translocation, a treatment where the retina is detached, the damaged part of the retina is moved away from the centre of vision then reattached with a relatively undamaged area of retina placed where it is needed most (Abdel-Meguid et al., 2003). These treatments can at best slow down the progression of AMD and can actually damage the retina if unsuccessful. Currently there is a lot of interest in anti-angiogenic pharmaceuticals, gene-therapy (Bainbridge et al., 2003) and cell based therapy/transplantation (Lund et al., 1997; Semkova et al., 2002)as possible cures, with clinical trials under way with most of the major pharmaceutical companies interested in this field. Treatments for dry AMD are currently limited to prevention (AREDS, 2001) and containment as its slow progression does not warrant high-risk surgical intervention.

The genetics of AMD is still fairly under developed (Gorin et al., 1999; Guymer, 2001) but is of prime importance in understanding how this group of diseases develop. Currently there is a lot of effort focused on this area (Abecasis et al., 2004; Rivera et al., 2000) and genes such as ARMD1 (Schultz et al., 2003) have been mapped, showing how a mutation in the protein Hemicentin-1 is related to incidence of AMD in one family. Another group has shown that 1.7% of AMD patients have mutations in the fibulin 5 gene (Stone et al., 2004), fibulins being extracellular matrix proteins (ECM) found in the basement membranes (in this case Bruch's membrane) involved in cell-ECM interactions. Recently several large groups have published data that shows that a mutation in complement factor H designated Y402h can increase the incidence of AMD in aged patients by over 43% (Edwards et al., 2005; Haines et al., 2005; Klein et al., 2005).

1.6.2 Retinitis Pigmentosa

This condition has been known to be inherited for some time. The family of RP diseases have an incidence of roughly 1/3500 (Bowne et al., 1999; Bundey and Crews, 1984a; Bunker et al., 1984; Inglehearn, 1998; Kaplan et al., 1990) and have been grouped together based on common clinical symptoms, electroretinographic responses and genetics (Phelan and Bok, 2000). A characteristic observation of RP is the appearance of pigmented cells that have migrated into the retina from the RPE. The pigmented cells accumulate in perivascular clusters throughout the peripheral retina sometimes referred to as "bone-spicule" formations. These manifest as a speckled appearance to the retina early in the disease with pigment deposits overlying the fundus. In more advanced cases histopathological examinations (Kolb and Gouras, 1974; Milam et al., 1998) have shown the degeneration of the rods as the primary consequence of many forms of RP with cone photoreceptor failure (John et al., 2000) occurring once rod failure reaches roughly 75% (Cideciyan et al., 1998). Other secondary pathological events include vascular attenuation (shared by advanced AMD) and changes to the optic nerve head (Milam et al., 1998). This results in progressive night blindness and loss of peripheral vision for the patient due to loss of rod photoreceptors. RP is more commonly a slow progressive degeneration that can result in total blindness, but as it is familial, its onset can occur much earlier than AMD. Of interest to this study mutations in the MERTK gene appear to cause RP (Kumar, 2001), MERTK is the human orthologue of the Mertk mutation in the RCS rat. As with AMD there is currently no cure for RP but research into cell transplantation

coupled with ex-vivo gene therapy (Lund et al., 2001b) may offer the best hope for patients .

1.6.3 Stargardt's Disease

First described by Karl Stargardt in 1909 (sometimes called fundus flavimaculatus). It presents as an autosomal recessive macular degeneration that causes an early onset loss of central vision. Most common in Scandinavian and Germanic families, it is one of the more common causes of juvenile macular degeneration. Genetic analysis has isolated the defect to chromosome 1p21-22 and subsequently identified it as the ATP-binding cassette transporter (ABCR) gene (Arnell et al., 1998; Rivera et al., 2000) (Allikmets et al., 1997) The defect is expressed in rod photoreceptors and is characterised by loss of transporter function leading to photoreceptor degeneration in the macular region resulting in much reduced visual acuity and loss of central vision. Another gene that has been identified is ELOV4 (Karan et al., 2004), but as yet the mechanism of how mutations in this fatty acid elongase gene can cause early macular degeneration is not known (this gene may be a factor in AMD as well). There are no current cures, but individuals may benefit from the use of low vision aids and orientation and mobility training. The early onset of Stargardt's disease poses an additional challenge for potential treatments such as cell-based therapies, as the cells must survive for the rest of the patient's life, or at least a significant portion without repeated reapplication.

1.6.4 Usher's Syndrome

Usher's syndrome is an inherited combination of profound hearing disability and progressive RP; the hearing disorder is present from birth and the RP onset is usually in adolescence. Usher Syndrome is the leading cause of deaf-blindness in the US with 10-15,000 sufferers (FFB website). There are three classifications of Ushers Syndrome. Type 1, where there is profound deafness present from birth, followed by RP symptoms by 5-6 years of age. Type II (USH2), characterised by a milder hearing loss (present from birth) followed by a later RP-like retinal degeneration in adolescence. Type III is very similar to type II but has a much more rapid loss of hearing and seems to be most prevalent in families originating from Finland. Progress has been made in determining the genetic cause of Usher's type IIa with recent research (Bhattacharya et al., 2002) identifying a novel basement membrane protein that has been localised to retina and the inner ear, where it is believed to play a role in development. People with Usher's type IIa have

mutations in the gene encoding the basement membrane protein usherin found in the retina and cochlea. The prospects for a cure are pretty much the same as for RP; with the exception that whatever treatment is eventually tried it must be effective over a much longer time span.

1.6.5 Leber Congenital Amaurosis

Leber Congenital Amaurosis (LCA) is a condition whereby patients suffer severe loss of vision from birth, with children failing to develop eye movements to stimuli and characteristically a flat electroretinogram (ERG). Genetic analysis has located several genes involved in LCA with progressive cone dystrophy (CORD5) found on chromosome 17p12-p13 (Balciuniene et al., 1995) . Also the gene RPE65 (also implicated in RP) that encodes a membrane associated protein involved in retinoid metabolism. This condition also frequently involves damage to the central nervous system and kidney malfunction suggesting that *in utero* damage to the retina or central nervous system has multiple effects. Due to the extremely early onset of LCA, gene therapy (Bennett, 2004) currently offers the only viable strategy, having proven successful with the Briard dog model (Acland et al., 2001). One requirement for this is that the defective retina has not lost its structural integrity; otherwise it is unlikely that restoration would be possible.

1.6.6 Current State Of Clinical Trials

Clinical trials are currently under way for several retinal degenerative diseases, with AMD being the main target due to the much larger patient base. Retinitis pigmentosa has a couple of clinical trials active but unfortunately there are no clinical trials active for Stargardt's disease or Usher's syndrome. Less common retinal degenerations will have to utilise whatever medical technology comes out of research into AMD and RP. Clinical trials are graded I-III to denote their proximity to marketable cures. Phase I trial typically determine safety and maximum dosage typically in small numbers of healthy volunteers, phase II trials test the effectiveness of the treatment in its target group and may involve large numbers. Phase III trials allow fine-tuning of the treatment with various dosage levels or strategies to control side effects. A full listing of those currently underway can be found in Gateways to clinical trials (Bayes et al., 2004).

Treatment	Clinical trial	Strategy	Company
VEGF trap (Saishin et al., 2003)	Phase 1	Anti-angiogenesis	Regeneron
Aventis + advPEDF (Imai et al., 2005)	Phase 1	Anti-angiogenesis	GENVEC
Combrestatin (Stevenson et al., 2003)	Phase I/II	Microtubule polymerisation inhibitor	Oxigene
Celicoxib with PDT (Rao et al., 2000)	Phase I/II	Cox-2 inhibitor	Genara
Anacortave acetate (Augustin et al., 2004)	Phase III	Anti-angiogenic	Alcon
Lucentis + PDT (Husain et al., 2005)	Phase III	Anti-angiogenic	Genetech

Figure 1.4 Clinical trials currently under way for retinal degenerative diseases.

Figure **1.4** shows six examples of clinical trials for AMD currently underway, two phase three, two phase I/II and two phase I comprising of a number of different approaches to the clinical problems in AMD. The majority utilise anti-angiogenesis strategies, sometimes in combination with photodynamic therapy (PDT) (Regillo, 2000), therefore they will be used to treat the symptoms of AMD but not the underlying pathology of the disease. These trials offer potential treatments but not cures for AMD.

The current outlook for RP patients is interesting with two clinical trials in progress, one in phase 1 trials is encapsulated human RPE cells genetically modified to express ciliary neurotrophic factor (CNTF)(Tao et al., 2002). A new trial just commencing will follow up the docosahexaenoic acid (DHA) coupled with Vitamin A trial (Berson et al., 2004a) which to treat RP patients. The first trial was not favourable generally but on further analysis it was found to slow RP in its early stages (Berson et al., 2004b).

The most common cause of these retinal dystrophies appears to be defects within the photoreceptors, with defects in the RPE second. Although it should be noted that, due to their interdependent relationship, primary defects in one quickly lead to secondary defects

in the other. Later secondary effects commonly affect the retinal vasculature and neural connections of the retina. In many clinical cases these conditions will be moderately advanced and/or complicated by secondary events. Therefore, the ability to reduce some of those secondary effects, such as vascular damage, would be very useful in eventual treatments.

1.7 Animal Models Of Retinal Disease

An important first step in this study was to select an appropriate animal model. As a general rule, mammalian models are used to study human diseases due to underlying physiological similarities. Recently genetic analysis has made use of fish such as zebra fish to examine gene expression of important target genes (Li, 2001). This is possible due to the transparency of the larval stages of zebra fish growth allowing clear identification of gene expression during development.

1.7.1 General Considerations

There are many animal models of photoreceptor degeneration, in which photoreceptors degenerate at various rates due to intrinsic genetic defects usually in the photoreceptors themselves, but sometimes in ancillary cells such as the RPE.

The majority of retinal research utilises small animal models such as mice, rats, guinea pigs and zebra fish due to their inherent advantages of fast breeding cycles, ease of handling and animal husbandry as well as well defined genomes.

Rodent genomes are particularly well defined and this has enabled a rise in specifically designed mutations to remove specific genes (knock-outs), add-in specific genes (knock-ins) or change the levels of expression of certain gene products.

For retinal studies rats provide a good compromise between the advantages of a small rodent model while still exhibiting quantifiable visual function and supporting sophisticated surgical procedures.

Medium sized animal models such as rabbits, ferrets and cats have been used for anatomical studies due to historical precedent and also where a larger eye is required to practise more detailed surgical procedures (usually rabbits). Medium sized models generally do not have as well defined genomes severely limiting the opportunities for genetic manipulation; also the quantity and quality of available reagents are much reduced limiting cellular biology approaches to research on these models.

Large animal models such as dogs and pigs tend to be used in transitional research where proof of principle has been proven in small animal models but a large animal study is usually required before approval can be given for human trails. These large models allow for extensive surgical intervention and long term studies that cannot be carried out with short-lived small animals. Dogs have been particularly useful as the various kennel clubs keep exacting breeding records allowing identification of useful genetic mutants such as the Briard dog (Acland et al., 2001) where mutations in the gene RPE65 (which is similar to human LCA) cause severe early onset retinal degeneration, This was corrected by recombinant adeno-associated virus (AAV) carrying wild type RPE65 delivered intra-occularly and the animals retinal development followed. Electroretinographic assessment showed a marked improvement in retinal function over control animals. Other groups have produced genetically engineered pigs (Petters et al., 1997) for use in studying long term cone photoreceptor survival in RP. These animals express a known human RP mutation (Pro347Leu) that results in rapid rod loss followed by gradual cone loss. This animal has a higher cone density and allowed long term studies to be conducted (20+ months).

1.7.2 Advantages Of Rodents As Models Of Retinal Degeneration

Visual acuity in the rat is much lower than in humans. In comparison to a human 20/20 vision, a normal pigmented rat would have 20/600 vision, and albino rats around 20/1200 vision (Prusky et al., 2002). This could imply that the rat is unsuitable for visual studies whereas in fact current behavioural experiments have shown that very consistent recordings of visual acuity can be obtained in experimental rodent models (McGill et al., 2004) as well as electrophysiological data (Girman et al., 2003) and ERG (Sauve et al., 2004).

Rodents offer many advantages to research of retinal degenerations, primarily due to their extremely well studied genome, and the extensive anatomical studies of the CNS and retina. The range of genetic strains available is vastly superior to any other animal model and if mouse eyes are too small, rat eyes are much easier to work with being large enough for surgical procedures (Lund et al., 1997). The availability of rodent specific antibodies and genetic probes are another major consideration. The disadvantages of rodent models are, lack of a macula (where comparisons with human are necessary), nocturnal activity, small size and comparatively short lifespan which limits studies on aged individuals.

Albino strains should be investigated with special care, and avoided if comprehensive testing of visual function is to be attempted. This is due to two reasons: 1) the lack of pigment makes the animals susceptible to light damage to the retina and 2) albinos have been shown to have abnormal optic chiasma (Lund, 1975) which could further compromise interpretation of visual signals as well as underdeveloped central retina and reduced rod numbers (Jeffery, 1998).

Rodents have proven excellent for genetic knockouts (Reynolds et al., 2002), and growth factor efficacy experiments (LaVail et al., 1992; LaVail et al., 1998).

Three natural rodent models of retinal degeneration have been studied in some detail, each having relevance to human retinal degeneration. Two of these are mice in which the defect is intrinsic to the photoreceptor. The rd mouse, where degeneration results from a defect in the β2 sub-unit of cyclic GMP phosphodiesterase (Bowes et al., 1990) (Lem et al., 1992), and the rds mouse, where the defect lies in the peripherin/rds gene (Sidman and Green, 1965)(Connell et al., 1991). In both cases there is a resultant progressive degeneration of photoreceptor cells followed by secondary events such as vascular leakage and deformation of the vascular network (Wang et al., 2000), and eventually, loss of the ganglion cells.

1.7.3 The Royal College Of Surgeons Rat

The basis for these studies is the pigmented dystrophic RCS rat (rdy- P+)(Bourne et al., 1938)(LaVail et al., 1975). This naturally occurring mutation exhibits photoreceptor loss (Dowling and Sidman, 1962), due to a defect in the RPE cells (Chaitin and Hall, 1983).The defect is a deletion in the gene for the receptor tyrosine kinase designated Mertk (D'Cruz et al., 2000). The mutation in the Mertk gene has the effect of blocking normal circadian driven rod outer segment phagocytosis (Bosch et al., 1993). In the dystrophic RCS abnormalities can be seen in the rod outer segments starting at 15 days of age (Davidorf et al., 1991) this is before the photoreceptors have fully matured. By P20 both the inner and outer segments of the rods exhibit abnormal deformations and debris has started to build up between the outer segments and the RPE. The rods decrease in number, which can be detected by a concurrent reduction in the ERG, which becomes flat as the rat reaches maturity (Dowling and Sidman, 1962; Sauve et al., 2004) At first, changes to the RCS retina are only visible with electron microscopy (Davidorf et al., 1991), but by 45 days light microscopy is able to pick out the reduction in the photoreceptor layer (Dowling and Sidman, 1962). This mutation eventually results in

complete loss of photoreceptors (LaVail and Battelle, 1975). The lack of outer segment phagocytosis results in a build up in shed OS that are not metabolised by the RPE, which accumulate between the OLM and the RPE forming the characteristic RCS debris zone. One of the end products of normal OS metabolism is the return of pigment to the photoreceptor, which is essential for the assembly of new healthy OS. As the turnover of these cells is so rapid it does not take long for the photoreceptors to become stressed and descend down apoptotic pathways resulting in retinal degeneration (Travis, 1998). The reduction in rod photoreceptors has many secondary effects such as the debris zone and also gaps in the photoreceptor layer that allow cells that do not normally come into contact to interact. The photoreceptor cells are no longer supported by their neighbours, and cell-cell interactions are disrupted. Interestingly it is becoming apparent that the cones are more resistant to disruption at this level than the rods (Girman et al., 2005; Leveillard et al., 2004).

Viral gene transfer of the Mertk gene has been used to correct the RCS dystrophy (Vollrath et al., 2001) and *in vitro* studies have isolated the Mertk gene site of action to RPE phagocytosis (Feng et al., 2002) giving conclusive evidence that the Mertk gene is responsible for the dystrophy.

While the RCS rat dystrophy is not directly homologous to AMD, particularly as the rat has no macula, does not form drusen and only in very advanced cases exhibits choroidal neovascularisation. With these caveats, there are a number of similarities that make it a useful model for testing potential treatments, such as secondary vascular complications and neuronal cell death within the retina. Furthermore the RCS rat exhibits pigment migration into the retina with an occluded vascular network and associated changes possibly neovascular in nature. This close relationship between the RPE and vascular deformation was missed in early studies (Caldwell et al., 1989; Seaton and Turner, 1992) due to the use of RCS rats on albino backgrounds where the lack of pigment made anatomical examination more difficult. Later damage to the ganglion cells occur as blood vessels appear to be pulled into the retina after the integrity of the retina has been compromised (Villegas-Perez et al., 1998). Vascular leakage has been documented in the RCS rat making it one of the closest models to AMD currently available. The RCS rat also bears a close relation to RP in that both exhibit migration of pigmented cells into the inner retina (Li et al., 1995) and a gradual reduction in rod photoreceptors. There is a

reduced vascular supply due to occluded vessels and vascular remodelling. Furthermore, loss of RGCs has been reported in advanced cases in both RCS rats (Villegas-Perez et al., 1998) and RP patients (Santos et al., 1997), this is in excess of the natural reduction of RGCs seen in elderly patients (Gao and Hollyfield, 1992).

The pigment seen in the RCS inner retina during degeneration is very similar to that found in RP and is now known to be from the same source; aberrant RPE cells, that have migrated off Bruch's membrane into the inner retina where they attach around the retinal vasculature (Li et al., 1995; Wang et al., 2003), There is still some debate about the origin of these cells which will remain until a reliable RPE marker is found but so far all major anatomiocal studies have concluded that they are in fact RPE (Li et al., 1995; Milam et al., 1998; Santos et al., 1997).

The development of these vascular complexes in the RCS rat has never been fully shown but figure 1.5 below shows a diagram of how they develop anatomically as seen in this study

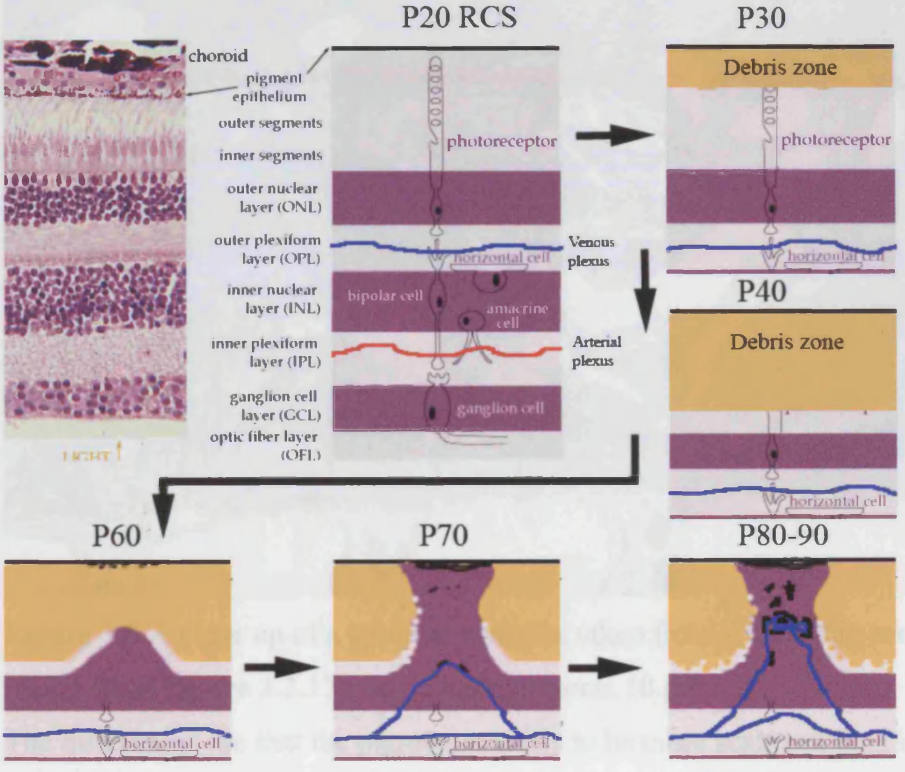

Figure 1.5 Showing the development of a VC in the RCS rat using figure 1.2 as a basis. The major changes in the RCS rat occur with the early death of the photoreceptors and the formation of the debris zone which may restrict the oxygen supply to the remaining photoreceptors and outer nuclear layer. CXells from the ONL are found to migrate into the debris zone in areas where the RPE looks disturbed eventually bridgeing the debris

zone. Between P60 and P80 blood vessels start tio sprout and enter the ONL in these areas Possibly in response to altered oxygen and nutritional requirements of the tissues. This forms a conduit that allows the RPE to migrate into the ONL onto blood vessels where they restrict flow, cause fenestrations and eventually leakage, forming vascular complexes and atrophy of the vessels (P150+)

Figure 1.5 shows a close up of an RCS vascular complex which is extremely close to the semi-thin pictures published By Li of human RP(Li et al., 1995), the black melanin granules (white arrows) can be clearly seen in the RPE surrounding the blood vessels and also the thickened ECM deposits around the vessel walls (black arrows).

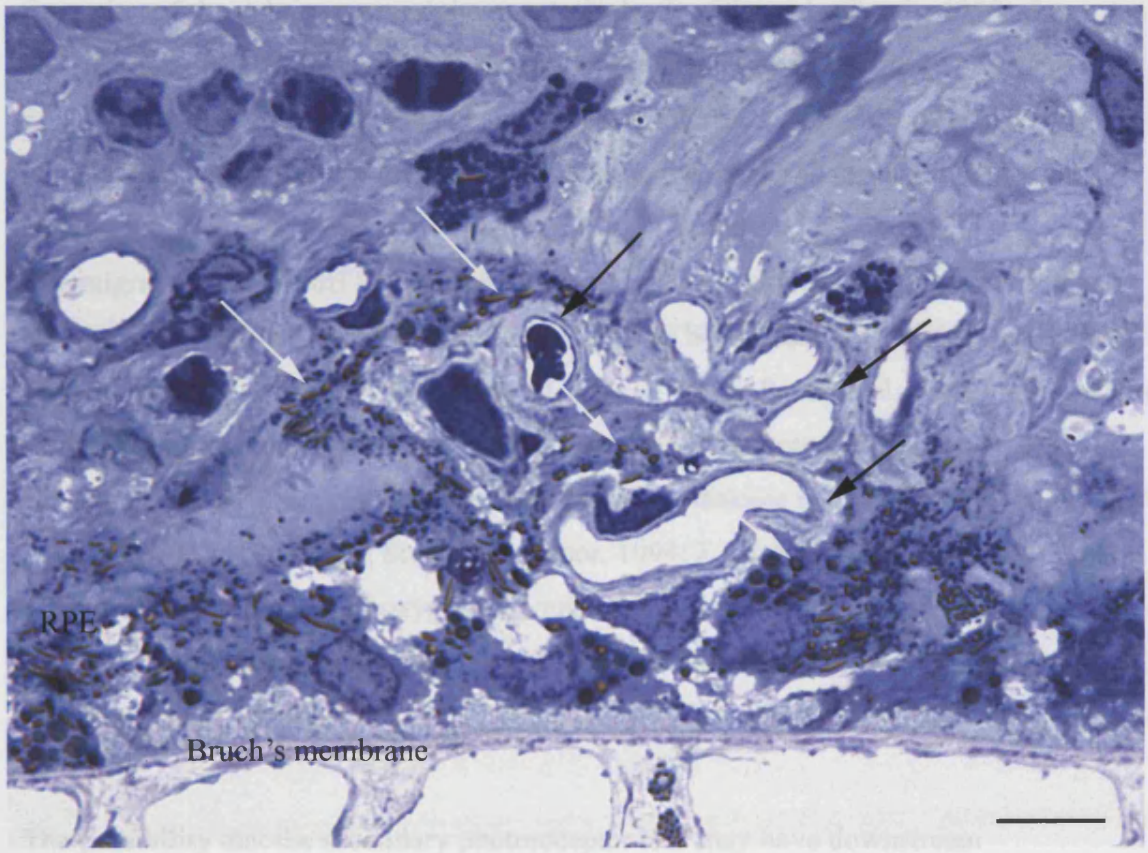

Figure 1.5 A close up of a vascular complex taken from a semi-thin section at x250 mag. (insert from **Figure 3.2.17**). Scale bar represents 10 μm.

The differences are that the pigment appears to be more scattered than in classical human RP and does not form "bone spicule" like deposits when RCS retinea are viewed as flat mounts (see **Figure 3.1.6**), This may be due to the presence of the debris zone blocking mass RPE migration in the RCS rat. The RCS dystrophy is now known to be a subset of RP (Kumar, 2001) and as such they share common features such as the attenuation of the retinal blood vessels seen first in the capilliaries and venus vessels of the mid-ventral

retina (Milam et al., 1998). At present there have been no fundus photographs published of the human orthologue of the RCS dystrophy so it is difficult to say exactly how its anatomical features differ from the RCS, although there has been an extensive cLSO study (Zambarakji et al., 2005) of the RCS rat, there has not been a difinative anatomical comparison carried out between the human and rat MERTK mutations.

The mechanism for the initiation of RPE migration is currently unknown but is thought to involve localized ischemia destabilizing the tight junctions between the RPE and the RPE and Bruch's membrane (refs). The differences between Classical RP and the RCS rats occur in the exact mechanism of how the disfunction develops, with the RCS rat the defect is in the RPE which fails to phagocytose used rod outer segments leading to the formation of the debris zone and the apoptotic death of the rods (Travis, 1998). In classical RP the defect is usually in the rod photoreceptor itself and there is no formation of a debris zone. Without a detailed anatomical examination it is currently unknown whether the human form of the MERTK mutation results in the formation of a debris zone.

The migration of RPE off Bruch's onto the venous vasculature and formation of thick layers of extracellular matrix around the vessels has been observed at the EM level in both human RP (Li et al., 1995)and the RCS rat (Villegas-Perez et al., 1998). This causes thickening of the vessel walls and resultant atrophy of the vessel. The vessel walls adjacent to the RPE develop fenestrations that allow leakage in both RP patients and in the RCS rat (Li et al., 1995; Stewart and Tuor, 1994; Zambarakji et al., 2005) While this may result in a reduction of oxygen and nutrient supply this may be offset by the reduction in photoreceptors (Milam) making detection of these events difficult to interpret.

The possibility that the secondary photoreceptor loss may have downstream consequences has been largely ignored or missed due to inappropriate animal models used, but they are the focus of the work reported here.

1.7.4 Transgenic Rat Models

Two more recent rodent models worth mentioning are the transgenic Pro23His (P23H) rat and the S334ter rat. The P23H transgenic rat has a mutant mouse opsin gene identical to that found in 12% of American autosomal dominant RP patients inserted into its genome(Lewin et al., 1998). The mutation results from a histidine substitution in the

rhodopsin gene giving an abnormal rhodopsin gene product that eventually kills the rod cells. ERG in these animals shows slow progressive rod dysfunction(Machida et al., 2001) while initially cones remain normal, once the rods have degenerated the cones are also lost. This can be a relatively slow degeneration model.

The S334ter rat has a dysfunctional rhodopsin gene which results in extremely rapid photoreceptor degeneration starting at P6-8 with fully 50% of photoreceptors lost between P11&12 (Liu et al., 1999) This model is useful for investigating late effects of photoreceptor degeneration but due to its rapid rate of degeneration it is difficult to conduct comprehensive testing of functional vision with this model. Both the P23H and S334ter mutations are on albino backgrounds that necessitate breeding with pigmented rats (such as Long Evans) to give heterozygote pigmented offspring. As noted earlier albino animals are not optimal for assessing vision.

1.7.5 Animal Models of AMD

There has been no good naturally occurring animal models of AMD, This has led to the selective use of inappropriate models and the modification of other models of retinal disease to give a more "AMD-Like" model through physical trauma (Campochiaro and Hackett, 2003; Semkova et al., 2003)

The use of genetic manipulation to produce models had to wait for breakthroughs in identifying the important genes involved in AMD. A model of AMD should have the following characteristics. It should present a progressive photoreceptor degeneration affecting first cones of the central retina, it should in advanced cases exhibit choroidal neovascularisation breaching Bruch's membrane into the subretinal space, it should develop drusen next to Bruch's membrane. Optimally it should be found in an animal that has a macula (no rodents or small mammals). Another major obstacle to developing an animal model is that diseases that affect aged individuals are extremely expensive to mimic due to the length of time that the animals must be kept and the resultant losses due to death by natural causes before completion of the experiment. Consequently researchers are always trying to find models that do not involve aged animals. The following are a brief overview of those models that have been used. The first genuine attempts to develop serious models of AMD were surgical in nature using primates (Ryan, 1982) with subretinal injections of enzymes to disrupt Bruch's membrane. Aged populations of Rhesus monkeys were discovered to exhibit AMD-like symptoms but their extreme cost and difficulty of handling has slowed research (Hope et al., 1992; Ulshafer et al., 1987).

Physical damage using either laser photocoagulation or surgical removal of RPE has also been attempted (Del Priore et al., 1996; Ryan, 1982) but without knowledge of the underlying processes research was slowed until the genetic of AMD was better understood. With the major breakthroughs in understanding the genetics of AMD, particularly with the recent complement factor H genes (Edwards et al., 2005; Haines et al., 2005; Klein et al., 2005) and the finding that inflammation may play a major role (Bok, 2005),there has been a lot of activity in designing transgenic models of AMD (Elizabeth Rakoczy et al., 2006; Marx, 2006) (sadly these came too late to influence this study).

Examples of these mice models are the ELOVL4 mutants (of which our laboratory has performed several studies – unpublished data) which are really models of Stargardt's disease but include lipofuschin accumulation much like AMD (Karan et al., 2004). Alos of interest are the APO B100 mice which can be induced with diet and blue/green light to exhibit basal deposits much like drusen by 2 months of age (Espinosa-Heidmann et al., 2004). Finally the $CCl2^{-/-}/Ccr2^{-/-}$ mice which display a near complete list of AMD-like features with photoreceptor degeneration, Bruch's membrane thickening and disruption, drusen, lipofuschin (Ambati et al., 2003)

These animals offer significant improvements on previous models and are all much more relevant to AMD than the RCS rat used in this study. That said this study is primarily concerned with producing a method of quantifying vascular damage and applying it in the RCS rat, this work could be modified to work in the mouse models listed above.

1.8 Retinal Blood Supply And Secondary Events Of Retinal Degeneration

The retina is highly vascular, as would be expected with the extremely high metabolism of its constituent cells, but due to the mobility of the eye as a whole all blood flow must enter the eye via the choke point of the optic artery alongside the optic nerve as shown below in Figure 1.7

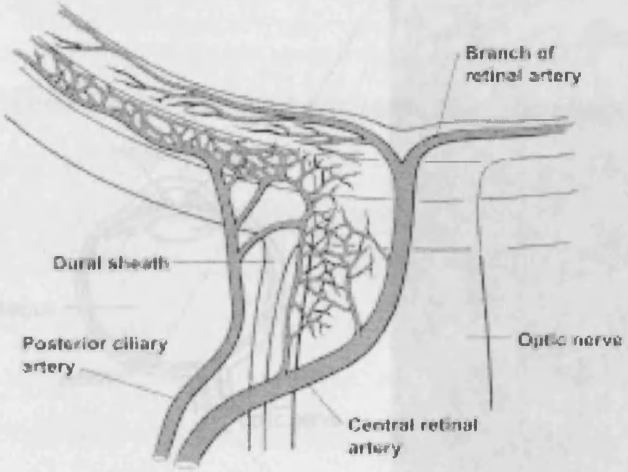

Figure 1.7 Diagram of the Ocular blood supply (courtesy of "Practical Viewing of the Optic Disk"

1.8.1 Anatomy of the Retinal Vasculature

There are two main routes whereby the vascular system supplies the retina in most animals including both rodents and humans: these are the capillaries of the choroid and the retinal vasculature.

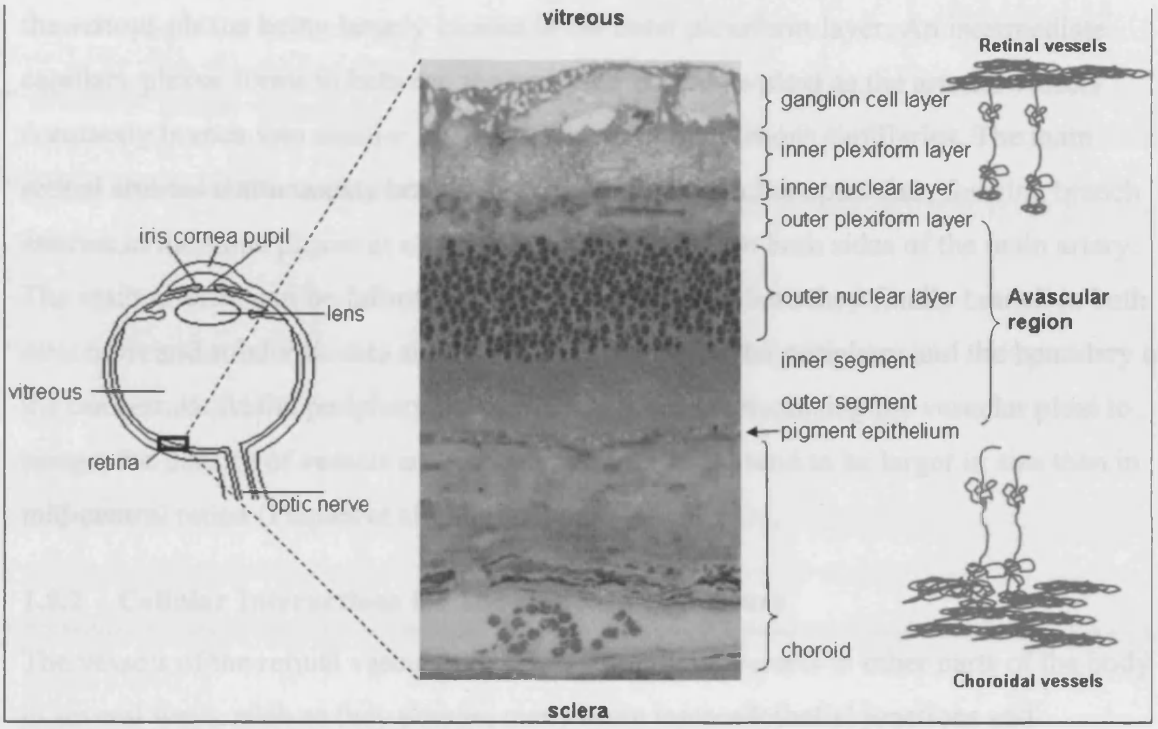

Figure 1.7 Retinal blood vessels (courtesy of Shen et al 2006

That said it is known that fluorescein angiograms fill the retina from the optic disk out and from the ciliary body in (Cunha-Vaz, 2004)simultaneously, therefore there must be some blood flow from the ciliary body into the peripheral retina. The vessels of the choroid are believed to supply the photoreceptors and RPE of the outer retina as shown in figure 1.7 above (Campochiaro, 2000). The retinal vascular network covers the entire retina from the optic disk to the furthest periphery. The vessels fan out from the optic disk in alternating main arteries matched with an equal number of returning veins. In humans there are four arteries originating from the central retinal artery whereas in RCS rat used in this study there are 5-6. Although there are minor differences between different species the general structure of the retinal vasculature remains very similar due to functional requirements. The only obvious anomaly is the human macula. This highly specialised region is largely avascular and is served by vessels around the fovea forming a ring like

(Zhang, 1994). Rats do not possess this structure that occupies a relatively small area of the retina.

The vascular network within most mammalian retinae, including rats is laminated with three distinct vascular plexi as (Paques et al., 2003).

An arterial plexus located in the inner plexiform layer and retinal ganglion cell layer with the venous plexus being largely located in the outer plexiform layer. An intermediate capillary plexus forms in between the arterial and venous plexi as the arterial vessels constantly branch into smaller arterioles and drain into venous capillaries. The main retinal arteries continuously branch after dispersing from the optic disk, forming branch arteries in the same plexus at either acute angles or 90^0 on both sides of the main artery. The main arteries can be followed out to the periphery where they finally branch in both directions and subdivide into smaller arteries that reach the periphery and the boundary of the ora serrata. At the periphery the retina is much thinner causing the vascular plexi to merge, the density of vessels are reduced and capillaries tend to be larger in size than in mid-central retina (Paques et al., 2003).

1.8.2 Cellular Interactions Of The Retinal Vasculature

The vessels of the retinal vasculature differ from blood vessels in other parts of the body in several ways, such as they possess many more interendothelial junctions and endothelial processes essential for fluid transport out of vessels. Retinal vessels are lined with approximately four times as many pericytes as normal vessels (Stewart and Tuor, 1994). These pericytes are embedded in the vessel walls instead of lining the out side and form part of the blood-retinal barrier (Leeson, 1979). In the retina Muller cells are also involved in the formation of barrier properties (Tout et al., 1993). Taken together these findings suggest adaptations to very high transport volumes and pressure.

The blood-retinal barrier (BRB) is a feature the retina shares with the brain, which confers immuno-privileged status to these tissues, in that the blood vessels are remarkably selective in what they will release into surrounding tissues. Retinal and choroidal blood vessels have more pores than normal blood vessels but retinal vessels also have more tight junctions allowing control over permeability, the choroidal vessels are outside of the BRB.

Another essential component of the blood retinal barrier is the RPE, which is responsible for active transport of nutrients from the choroid to the photoreceptors. From clinical observations it has been proposed that the endothelium of retinal blood vessels be

designated the inner BRB and the RPE as the outer BRB (Cunha-Vaz, 2004) as a way of simplifying clinical assessments for fluorescein angiograms.

The retinal vasculature may enter a proliferative phase due to disease or injury. This can occur from inside the retina (retinal neovascularisation) where retinal vessels can grow out into the vitreous or from the choroid (choroidal neovascularisation or CNV) where vessels sprout from the choroid forming thick bundles, which can breach Bruch's membrane. Retinal neovascularisation is usually preceded by excessive ischemia (Chan-Ling et al., 1995), which up-regulates growth factors such as VEGF, a potent angiogenic growth factor (Plate et al., 1992). There are other important factors involved such as PEDF and nitric oxide whose roles are presently under investigation. Choroidal neovascularisation differs from retinal neovascularisation in that the exact stimulus for retinal sprouting is unknown but in AMD patients it may involve the thickening of Bruch's membrane with lipophilic material decreasing oxygen supply to the outer retina (Campochiaro, 2000). A more popular theory is that CNV is associated with inflammation possibly triggered by the accumulation of drusen, this is backed up by the recent findings on the importance of the complement genes in susceptibility to AMD(Edwards et al., 2005; Haines et al., 2005; Kijlstra et al., 2005; Klein et al., 2005; Marx, 2006)

1.8.3 Tools To Investigate Retinal Vasculature

The anatomy and dynamics of retinal blood supply has been studied using both non-invasive methodology such as fluorescein angiography (FA), indocyanine green angiography (Aydin et al., 2000) and scanning laser ophthalmoscopy (SLO) (Paques et al., 2003; Schmidt-Erfurth et al., 2001)as well as more traditional anatomical studies using trypsin digestion, methacrylate methylester corrosion casting (Zhang, 1994), also India ink , horseradish peroxidase (HRP) (Villegas-Perez et al., 1998) and Nicotinamide adenine dinucleotide phosphate-diaphorase (NADPH-d) staining (Wang et al., 2000). All of the methods previously used in the literature have advantages and disadvantages. For example SLO and FA were valuable to follow and record changes i*n vivo* in animals or patients, but they both suffer disadvantages such as the inability to view peripheral retina and with SLO there is insufficient detail in the video images captured although this is improving with more advanced video technology (Bellmann et al., 2003; Zambarakji et al., 2005). In addition computerised image analysis is not yet integrated into the system making quantitative assessment difficult.

Delicate corrosion casts (Zhang, 1994) using refinements like methacrylate methylester casting can be dissected and viewed using scanning electron microscopy. But are incredibly time consuming and delicate procedures, which are not suitable for use as a model to assess retinal vascular changes. Horseradish peroxidase (HRP) staining has the advantage of that it fills very small vessels and is quick and easy to use but it is prone to obscuring detail when vascular leakage occurs (Villegas-Perez et al., 1998). This may be very useful if vascular leakage is what is being assessed but FA and SLO can perform the same function i*n vivo,* even in rodents. Fluorescein-labelled dextran has been used in a number of studies to assess the vasculature and while it binds to the vascular cell walls it requires fluorescent microscopy and fades, which in capturing and archiving high-resolution images can be problematic.

NADPH-d histochemical staining of whole mount retina preparations is useful for light microscopy studies of entire retinae. NADPH-d staining is quick, permanent and as the vessel walls are stained, rather than filled, leakage is not a problem. NADPH-d staining was originally used to stain brain tissue (Vincent and Kimura, 1992) but was found to be useful for retinal staining (Roufail et al., 1995). NADPH-D staining gives a permanent blue stain to the retinal vasculature, the reaction relies on the enzyme NADPH-diaphorase in the retinal endothelial cells where it catalyses inducible nitric oxide synthase (iNOS) production of Nitric Oxide, a potent vasodilator. The 'diaporases' are dehydrogenase enzymes that catalyze the dehydrogenation of the reduced forms of the co-enzyme NAD and NADP, i.e. they catalyze the reactions, NADPH--NADP+H. The hydrogen liberated then combines with the tetrazolium salt, in this case Nitro Blue Tetrazolium - (NBT) to form a formazan salt; which is visible at the site of enzyme reaction.

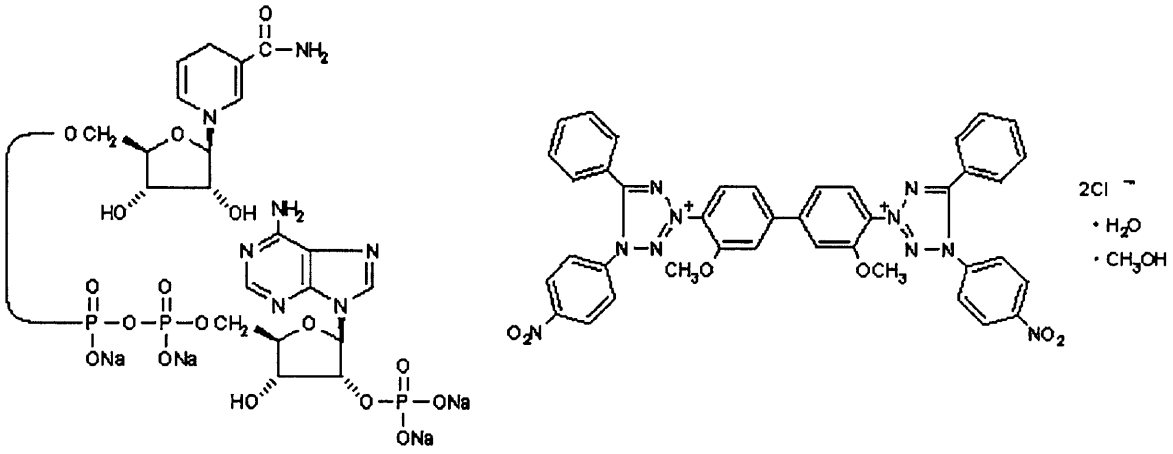

Figure 1.9 NADPH Nitro Blue Tetrazolium

Vascular endothelial cells are stained blue with minimal to zero background expression that proved ideal for this study. Amacrine cells stain positively and if the reaction is left running overnight light staining of the nerve fibre layer could be seen. After the stained retinae are flat-mounted, they are amenable to high-resolution computerised imaging. In human tissue the stain can also show up photoreceptors (Diaz-Araya et al., 1993) NADPH-d has been shown to co-localise with neuronal nitric oxide synthase (nNOS) and differential-staining patterns under certain conditions may be a result of differing levels of NOS in the vasculature.

1.8.4 Retinal Degeneration And Its Effect On Retinal Vasculature

The abnormal vascular phenotypes seen in advanced retinal degenerations are secondary consequences caused by physical changes in the retinal architecture, or ischemia. There are two areas of concern from a clinical standpoint, choroidal neovascularisation as seen in wet AMD, and the abnormal interaction between the RPE and retinal vasculature as described in the RCS rat and advanced cases of human retinal diseases.

The onset of vascular damage is determined by the rate of retinal degeneration in the disease/model studied. This is clearly illustrated in the C57Bl/6J-rd le (rd) mouse, in which the retinal degeneration is rapid and has a very early onset so that the vascular network never actually has a chance to fully develop and differences are seen between littermates as young as 14 days (Matthes and Bok, 1984). Comparisons are made with albino RCS dystrophic rats of 1 month of age where there are no vascular abnormalities due to the retinal degeneration being of a much slower nature (vascular abnormalities do

not occur in the pigmented dystrophic RCS rat until 2.5-3 months of age) (Wang et al., 2003).

Descriptions of phototoxic induced retinopathy in Long-Evans rats (Bellhorn et al., 1980) show vascular effects very similar to those found in the dystrophic RCS rat (Wang et al., 2003). By perfusing with higher weight fluorescein-labelled dextrans, size specific vascular leakage was demonstrated indicating failure of the BRB and fenestration of the retinal vessels.

The following vascular changes are characteristic of vascular damage due to retinal degeneration. Initial loss of photoreceptors leads to a general thinning of the retina; vessels are seen to form coil-like formations in the arterioles and some thickening of the deep draining vessels. As more photoreceptors are lost the deeper vessels start to approach the RPE, and RPE cells are seen to leave Bruch's membrane and move onto the deep vascular plexi. The trigger for this migration is currently unknown, but may involve changes to the RPE environment or chemotaxis of the RPE towards the vessels.(Wang et al., 2003)

Many areas of neovascularisation or vascular remodelling are seen as vessels are rerouted past obstructions. Finally once the photoreceptor layer has been lost the vascular network exhibits multiple sites of RPE cells enveloping vessels with large areas of non-perfusion of the deeper vessels, many shunt vessels are in evidence (Bellhorn et al., 1980) to reroute blood past constricted veins and the vascular network is now dangerously compromised.

1.8.5 Choroidal Neovascularisation

The choroid provides the photoreceptors, IPM, RPE and Bruch's membrane with essential nutrients. It is known that increased oxygen levels in the eye result in vascular regression and ischemia results in neovascularisation (Campochiaro and Hackett, 2003; Stone et al., 1995). Choroidal neovascularisation (CNV) from AMD is the commonest cause of severe blindness in elderly patients (study, 1991). This may involve lowered choroidal blood flow or thickening of Bruch's membrane from accumulation of abnormal ECM. The deposition of abnormal ECM is also seen in Sorsby's fundus dystrophy and appears to a preliminary to breaches in Bruch's membrane. The choroidal blood vessels enter into localised areas of neovascularisation forming tortuous bundles of new vessels, which can breach Bruch's membrane and enter the retina. Choroidal blood vessels are not part of the BRB and may be at a disadvantage in the biochemically active

microenvironment surrounding the RPE and IPM, this could cause damage to the vessels leading to retinal haemorrhaging and blindness.

1.9 Models For Investigating Proliferative Vascular Diseases

There are several possible models that can be used to study retinal vascular changes, that can be divided into *in vitro* or *in vivo* models. Secondly the correct investigative tools must be matched to the model. Large animal models tend to allow closer approximation to clinical studies, where fluorescein angiography, Indocyanine green angiography and more recently confocal scanning laser ophthalmoscopy (cSLO) are the main tools for investigating the retinal vasculature. For genetic manipulations or more extensive longer term *in vivo* studies, rodent models, such as the RCS rat, rd and rds mice are more useful. It is now more common to see transgenic rodents such as the P23H and S334ter rats being investigated (Lewin et al., 1998; Liu et al., 1999).

1.9.1 *In Vitro* Vs. *In Vivo* Models

In vitro models are very useful for determining the specific viability of pathways and in simplifying systems so that complex interactions can be isolated.

Common *in vitro* models comprise of retinal cells grown in culture either from transformed cells or primary culture and can include RPE cell cultures (Steuer et al., 2004) and retinal endothelial cells sometimes grown on collagen gels to simulate retinal vessel growth (Fan et al., 2002). While these models are useful they cannot reproduce the complex interactions that occur in an *in vivo* system.

In vivo systems such as the chick chorioallantoic membrane (CAM) assay (Ausprunk et al., 1975; Glaser et al., 1980), laser photocoagulation (Campochiaro and Hackett, 2003), transgenic knockout rodents (Lau et al., 2000) and retinal degenerative rodent mutants (Essner et al., 1980) have been used to investigate retinal vasoproliferative events. Rarely primate retinas have been investigated to model retinal vascular development (Provis, 2001) and diabetic retinopathy (Lebherz et al., 2005)

1.9.2 Laser Photocoagulation

Laser Photocoagulation utilising an argon laser to treat retinal neovascularisation or CNV has recently begun to be used as model of retinal angiogenesis (Campochiaro and Hackett, 2003; Ryan, 1982; Semkova et al., 2003). Laser Photocoagulation has been used in rabbits, primates and even mice to produce a model of CNV designed to approximate AMD by burning holes through Bruch's membrane resulting in CNV. Attempts can then

be made to modify this response using antiangiogenic compounds such as kinase inhibitors (Seo et al., 1999) which blocks several members of the protein kinase C family involved in VEGF signalling. This model is interesting in that it is one of the few that involves breaches in Bruch's membrane but it is also flawed in that it causes a relatively large full thickness retinal burn wound right at the site to be investigated. This contamination of the site by the resulting wound healing process complicates any assessment of treatments.

Some other *in vivo* models involve intravitreal injections through the retina but these micro-wounds appear to have very local effects and are usually sited away from the main site of study minimising contamination of the tissue. The laser photocoagulation model as been used to investigate various growth factors (Kwak et al., 2000) and potential drugs but unless more proof can be obtained that the lesions created mimic actual CNV lesions in AMD rather than unnatural retinal burn wounds its usefulness is in question. Finally the resulting scar at the site of the laser burn does not in any way mimic the CNV found in clinical AMD studies (Semkova et al., 2003).

1.9.3 Transgenic Rodents

Transgenic rodents have made it possible to engineer knockouts that either omit essential factors or express missing factors to correct defects in known mutations. Transgenic animals do not comprise a single model for investigating retinal vasculature as such but as they are becoming essential in determining the effects of removing parts of the retinal pathways such as integrin knockouts (Reynolds et al., 2002), Interleukin-18 knockouts (Qiao et al., 2004) and along with gene therapy in correcting known genetic retinal defects as with the RCS rat (Vollrath et al., 2001) they should be included here. Knockout mice are slowly giving way to the more elegant gene therapy route as it can be extremely difficult to determine just how "normal" a surviving phenotype is. Knockouts that are missing an essential factor may well be non-viable and the phenotype consequently lethal to the developing embryo. More subtle differences may go undetected unless comprehensive behavioural testing is carried out. More relevant to ophthalmic research is the SPARC/Osteonectin knockout, which appears phenotypically normal until six months of age when it develops severe cataracts and ruptures in the lens capsule due to aberrant ECM interactions (Gilmour et al., 1998).

1.9.4 The Vascular Secondary Effects Of The RCS Rat

The RCS rat has been known to develop abnormal vascular formations as a secondary consequence of retinal degeneration for some time (Essner et al., 1980) with several studies investigating the breakdown of the BRB as the retinal degeneration leads to progressively worse vascular damage (Essner et al., 1980). Sadly some early studies were compromised by being conducted with RCS rats on an albino background (Caldwell, 1989; Caldwell et al., 1989; May et al., 1996) which did not allow for clear visualisation of the formation of RPE/vascular complexes and also were handicapped by the short comings of albino animals for vision research. Albino animals have a point mutation in tyrosinase, an enzyme essential to melanin synthesis resulting in non-pigmented pigment epithelium and severe visual defects (Jeffery, 1998). These defects include a reduction in the amount of rod photoreceptors, underdeveloped central retina and defects in the optic chiasma leading to poor spatial awareness in vision, these animals are notoriously poor at visual behavioural tasks (Prusky et al., 2002). The pigmented RCS rat provides a naturally occurring example of slow onset progressive vascular damage that can be used as a model to investigate ocular angiogenesis.

1.9.5 Controlling Retinal Vascular Events

The models used in the preceding sections detail how retinal vascular abnormalities are investigated but not how they are controlled. There are many anti-angiogenic strategies of which the most common are surgical removal of CNV, anti-angiogenic drugs, growth factors and growth factor antagonists, low power photocoagulation and gene therapy. Surgical debridement of CNV membranes is commonly carried out for human retinal proliferative diseases and while it can be damaging if mistakes are made it is one of the few options available in the current clinical environment (Schmidt et al., 2003). Anti-angiogenic drugs are used to treat many disorders and research carried out in other fields such as cancer has recently been applied to the vascular problems inherent in retinal degenerative diseases with growth factors like PEDF and blocking peptides to VEGF as well as some potential therapies taken from cancer research such as angiostatin and endostatin (Hajitou et al., 2002). VEGF kinase inhibitors have been shown to block retinal neovascularisation (Seo et al., 1999)and are currently in phase II clinical trials for treatment of AMD CNV(2003). Another growth factor that receives a lot of attention is PEDF (details in section 1.10), which is a natural anti-angiogenic compound produces by

the RPE involved in protecting the eye from abnormal neovascularisation (Tombran-Tink et al., 1991).

Argon laser induced photocoagulation of CNV membranes as discussed earlier is currently used to cauterise and seal damaged blood vessels in the retina but it does not stop the underlying pathology.

Gene therapy is a relatively new development for ocular diseases and at present all proposed gene therapy treatments are experimental or awaiting approval for phase I clinical trials. Proof of principal has already been shown with correction of LCA in the Briard dog (Acland et al., 2001) and in numerous small animal models gene therapy has been shown to reverse well known retinal dystrophies (Vollrath et al., 2001) and models of retinal ischemia induced neovascularisation (Bainbridge et al., 2002). Another use of gene therapy is to introduce genes into cells that are then placed into the eye using transplantation techniques (Lawrence et al., 2004). These cell-based therapies combined with gene transfer technology (ex-vivo gene therapy) may reduce safety issues over classic gene therapy. By improving the retinal environment by reducing vascular problems, these treatments may be used as either a pre-treatment or in combination with further potential cures for retinal degeneration.

1.10 Pigment Epithelium Derived Factor

PEDF is a retinal peptide involved in angiostasis of the retina with neuroprotective properties making it an excellent candidate for pharmaceutical intervention in retinal degenerative diseases. PEDF is a 50-kDa non-inhibitory member of the serine protease inhibitor (serpin) family of proteins. It was first discovered during investigations into differentiation of neuroblastoma cells by RPE cell conditioned media (Tombran-Tink and Johnson, 1989) and later isolated and named PEDF after the cells it was extracted from (Tombran-Tink et al., 1991). PEDF is known to be secreted from the RPE into the interphotoreceptor matrix (Tombran-Tink et al., 1995) and it is also secreted by the cornea and ciliary body, which accounts for the high levels of PEDF found in the vitreous (Ortego et al., 1996). PEDF levels have been approximately calculated at 1-2 μg/ml in the vitreous with $1/5^{th}$ of that in the aqueous and 10 times that figure in the IPM (although in much less volume). There is evidence that PEDF extracted from several tissues and the vitreous differs from PEDF extracted from the IPM in that the N-terminus is blocked (Wu et al., 1995), this may be a control mechanism for activation. Interestingly it is difficult to

detect PEDF protein in the RPE (Karakousis et al., 2001), possibly due to the autofluorescence of the lipofuscin but mRNA can be detected suggesting that while it is produced by the RPE in the retina it is neither stored, nor active there.

PEDF is important in the retina because it is known to have neurotrophic, (Steele et al., 1993) neuroprotective (Cayouette et al., 1999; DeCoster et al., 1999; Houenou et al., 1999)and anti-angiogenic properties (Dawson et al., 1999; Ogata et al., 2002; Ohno-Matsui et al., 2001; Stellmach et al., 2001; Stitt et al., 2004) which allows it to protect the neural retina while also inhibiting neovascularisation, neither process is completely understood but both are of interest in retinal degenerative diseases such as AMD, RP and retinopathy of prematurity.

1.10.1 Neuroprotective Properties Of PEDF

One of the first experiments with PEDF showed how it was neurotrophic to cultured Y79 retinoblastoma cells where it induced a change in cell phenotype to neuron-like processes (Steele et al., 1993). This has been postulated to be due to PEDF inhibiting cell proliferation by influencing the mitotic cycle at key points, PEDF was also called early population doubling level cDNA-1 (EPC-1) as its expression is up regulated during cell cycle phase G_0, thereby driving some cells towards differentiation. Since then PEDF has also been shown to be able to influence the survival of various types of neural cells such as immature cerebellar granule cells (but not mature cells)(Araki et al., 1998), developing primary hippocampal neurons (DeCoster et al., 1999), mouse photoreceptors from retinal degeneration (Cayouette et al., 1999), developing spinal motor neurons (Houenou et al., 1999), cultured neurons from hydrogen peroxide induced apoptosis (Cao et al., 1999) and photoreceptors from light damage (Cao et al., 2001).

These cases share several similarities, in most cases the neuroprotective property requires pre-treatment or presence of PEDF for at least 1 hour in experimental systems (Cao et al., 1999). Only a single application of PEDF is required to show an effect (Cao et al., 2001; Cayouette et al., 1999). The PEDF appears to trigger a biochemical change but with the photoreceptor studies it is not clear if the effect is direct or on supporting cells. PEDF can also protect the neural retina from ischemia, which is important in nearly all retinal degenerative diseases, and also it has been found to be extremely effective against the resulting neovascularisation that follows retinal ischemia (Stellmach et al., 2001).

1.10.2 Anti-Angiogenic Properties Of PEDF

PEDF has been described as the most potent anti-angiogenic compound produced in mammals (Dawson et al., 1999). Under normal conditions the retinal vasculature is held quiescent by an equilibrium reached between pro-angiogenic factors like VEGF, fibroblast growth factor-2 (FGF-2) and anti-angiogenic factors like PEDF which can be triggered by changing oxygen levels in the retina. Retinal diseases can change this equilibrium, especially those that involve large scale cell death or vascular proliferation such as retinal degenerations and proliferative diabetic retinopathy. There is a lot of information suggesting that PEDF and VEGF act as antagonists, if one increases the other decreases, but no direct link has been proven (Gao et al., 2001; Ohno-Matsui et al., 2001).

PEDF expression is lowered under hypoxic conditions making it less effective at countering the pro-angiogenic effects of VEGF. Most vascular proliferative diseases involve at least localised ischemia, which in turn trigger growth factors, in the retinal environment the most important of these appears to be the PEDF/VEGF equilibrium (Ogata et al., 2002). The exact method for this interaction is currently unknown but clues are emerging that PEDF may induce apoptosis in new vessel endothelium thereby killing new vessel growth before it gets started (Volpert et al., 2002). This is presumably done by a cell surface receptor but to date no such receptor has been identified. In retinal transplantation studies the sham effect has been known to produce slightly improved retinal architecture over untreated retinae, recent evidence points to the action of PEDF up regulation at the site of penetrative ocular wounding (Stitt et al., 2004) which may account for this phenomena.

1.10.3 PEDF And Retinal Diseases

The PEDF gene has been linked to several retinal degenerative diseases and its location being associated with a known RP locus (RP13) on chromosome 17 (Goliath et al., 1996) and variations in the PEDF gene have been found in patients with Leber congenital amaurosis (Koenekoop et al., 1999). Mutations in the PEDF gene would have serious consequences for retinal angiostasis. PEDF is a prime candidate for pharmaceutical intervention in retinal degenerative diseases. PEDF levels have been shown to be lower in patients with proliferative diabetic retinopathy (Spranger et al., 2001), other retinal diseases with an angiogenic component may show similar findings.
Other properties of PEDF that may affect neuroretinal cells are its ability to directly affect microglia by increasing their metabolism and inhibiting proliferation (Sugita et al., 1997). In turn there was a secondary indirect effect on astrocytes, as PEDF-treated microglia release a soluble factor that reduces astrocyte proliferation. This was taken as evidence of a role for PEDF in regulating glial cells in the central nervous system. PEDF binds to the extracellular matrix by attaching directly to glycosaminoglycans (Alberdi et al., 1998), which is likely be essential for its role in the IPM as that is the main source of glycosaminoglycans in the retina.

1.10.4 Gene Therapy Delivery Of PEDF

Models of retinal proliferative vascular diseases or retinal degeneration with secondary CNV are excellent ways of testing gene therapy delivery of PEDF with a view to later

clinical trials. One such trial used transplantation of iris pigmented epithelium cells genetically engineered to deliver PEDF via high capacity adenovirus (HC-ad) to both laser photocoagulation in Long Evans rats and into dystrophic RCS rats(Semkova et al., 2002) . In the Long Evans photocoagulation experiment, the adPEDF inhibited the CNV produced by the laser burn although it is not clear what the effect of the laser burning through the IPE transplant was. The RCS rats with adPEDF did exhibit more photoreceptor layers than controls but unfortunately the animals were sacrificed two months after transplantation (20 days) and they did not investigate the secondary vascular complexes forming in the RCS retina. If they had waited another month they could have flat-mounted the retina and looked at the effects on the vasculature without the complication of the wound healing response from the laser photocoagulation model.

Several other groups are investigating gene therapy delivery systems for evaluating PEDF effectiveness in retinal diseases. GenVec (Galthersburg MD) has an exclusive licence from the Federal Drug Agency to conduct gene therapy phase I clinical trials using adPEDF which are currently underway run by Dr. L. Wei (Imai et al., 2005). PEDF was chosen as a potential antiangiogenic treatment for use in this study as it had known antiangiogenic properties in rodents and it was also neuroprotective which it was hoped would help maintain the cells of the retina. Some growth factors have shown conflicting responses with in vivo models as non-physiological concentrations resulting from inappropriate dosages can in fact be detrimental while more appropriate dosages can be beneficial. This is usually due to non-physiological dosages changing the equilibrium of growth factor profiles until the cellular environment deteriorates.

1.11 Integrins In The Eye

Integrins mediate many interactions in the eye such as cell migration and proliferation as well as RPE phagocytosis (Elner and Elner, 1996) and angiogenesis (Hodivala-Dilke et al., 2003). This makes them an attractive target for pharmaceutical intervention in order to control retinal degenerative diseases. Integrins are present in the cornea, retina and choroid. The cornea primarily requires integrin functionality in corneal wound healing where corneal epithelial cells need to interact with and migrate on basement membranes utilising $\alpha_2\beta_1$, $\alpha_3\beta_1$ and $\alpha_V\beta_1$ integrins

1.11.1 General Overview And Structure Of Integrins

There are four main groups of adhesion molecules; integrins, immunoglobulins, selectins and cadherins. Of these, this study is concerned with the integrins, as they are involved in cell migration, proliferation, differentiation and activation through cell-cell or cell-extracellular matrix (ECM) interactions. Integrins are heterodimeric molecules comprising one α sub-unit in conjunction with one β sub-unit; there are sixteen α sub-units and eight β sub-units combining to give 21 known integrin pairs. Each integrin has intracellular, transmembrane and extracellular domains with the α sub-unit being mainly responsible for specificity and the β sub-unit anchoring the assembly to the cell cytoskeleton (Cox et al., 1994). The α sub-units are generally involved in cell-ECM interactions with collagens laminins fibronectin and vitronectin whereas the β sub-units are found on many cell types such as endothelial cells, epithelial cells fibroblasts and leukocytes (Elner and Elner, 1996).

Many integrins share a common binding motif known as the RGD sequence (named after the three amino-acids that comprise it – arginine-glycine-aspartic acid) which is essential for binding to many ECM molecules such as fibronectin, vitronectin, collagens, laminins, fibrinogen and thrombospondin. There have been a number of reviews on the role and expression of integrins in the eye (Elner and Elner, 1996) and recently the retina (Clegg et al., 2000; Cox et al., 1994; Finnemann and Rodriguez-Boulan, 1999; Zhao et al., 1999). Integrin involvement in angiogenesis has been shown in β_3 and β_5 knockouts (Hodivala-Dilke et al., 1999) and blocking studies where they have been shown to enhance pathological angiogenesis (Reynolds et al., 2002).

1.11.2 Integrins In The Retina

The retina has a wider range of integrins but of most interest in this study are the integrins involved in RPE phagocytosis (section 1.7.3.) and in vascular cell interactions. The integrin $\alpha_V\beta_3$ has been implicated in both vascular cell migration (Rupp et al., 2004), endothelial cell sprouting (Soldi et al., 1999)and in angiogenesis by activation of the VEGF-2 receptor. The integrin $\alpha_V\beta_5$ is known to be involved in RPE binding prior to phagocytosis (Finnemann et al., 1997; Nandrot et al., 2004). These processes are extremely relevant to studies of retinal degeneration, but $\alpha_V\beta_3$ expression on RPE cells is known to be low (Anderson et al., 1995). Both of these integrins are also known to receptors for Vitronectin, a multifunctional protein involved in tissue remodelling, the immune system and neuronal development (Martinez-Morales et al., 1995).
$\alpha5\beta1$ has been shown to be essential for the internalisation phase of phagocytosis of ECM fragments by RPE cells (Zhao et al., 1999) which may well be important in those models where a significant wound healing component is present but it is unknown if this is true for OS phagocytosis. The findings of D'Cruz and colleagues have implicated the integrin pair $\alpha_V\beta_5$ in the RCS retinal dystrophy (D'Cruz et al., 2000) and this molecule is known to be involved in the binding of photoreceptor fragments to RPE (Lin and Clegg, 1998) making it a good candidate for blocking experiments.

1.11.3 Integrins In The RCS Rat

There have been very few studies investigating integrin expression in the RCS rat with one study on microglial cell invasion (Roque et al., 1996) and footnotes in the ongoing RPE phagocytosis debate (Hall et al., 2003; Nandrot et al., 2004).
The integrin pair $\alpha_V\beta_5$, is the only integrin receptor that localizes to the apical, phagocytic surface of RPE *in vitro* and *in vivo* (Finnemann et al., 1997) and therefore may have a role in the binding of photoreceptor outer segments to RPE and association with the Mertk gene for the RCS dystrophy. This is controversial (section 1.7.3) and it is unclear if the requirement for $\alpha_V\beta_5$ is limited to *in vitro* assays only (Feng et al., 2002). Hall et al found that in primary RPE cultures from dystrophic RCS rats that antibody blocking of $\alpha_V\beta_5$ reduced RPE binding by 30-40% but not internalisation (Hall et al., 2003). Until more thorough *in vivo* studies are done this will remain unknown. The integrin pair $\alpha_5\beta_1$ may be a interesting target in the RCS rat as it has been shown to mediate motility in and RPE cells (Jin et al., 2000) and in increased expression in retinal vascular proliferative

membranes (Robbins et al., 1994). Recent findings that dedifferentiated and proliferate RPE cells up regulate α_5 protein levels (Proulx et al., 2003) may also be relevant for RPE motility in the RCS pathology.

1.12 Integrin Antagonists; Disintegrins

Molecules capable of modulating integrin expression could be very important candidates for pharmaceutical intervention in many pathological conditions, integrin antagonists if controlled and specific may be invaluable tools (Curley et al., 1999). Integrin antagonists can be divided into two groups 1) Artificial integrin blockers such as antibodies and blocking peptides created specifically to block certain receptors. 2) Natural inhibitors of integrins such as the snake venom derived disintegrins (Kamiguti et al., 1998).
This study was particularly interested in disintegrins for their small size, stability and effectiveness at blocking integrins. Disintegrins are small non-enzymatic RGD containing cystine rich polypeptides, they share some homology with the ADAMs family of metalloprotease-disintegrins found in mammals (Schlondorff and Blobel, 1999).
The primary function of the snake venom disintegrins is to disable the clotting system and damage blood vessel walls thereby causing massive haemorrhaging in the victim, although differing disintegrins may elicit a wide range of effects.
Disintegrin specificity is currently being studied by several groups and the full range of responses to these potent integrin antagonists are not yet known (Belisario et al., 2000; Marcinkiewicz et al., 1996), particularly their specificity to blocking different integrin pairs via their RGD recognition site (Marcinkiewicz et al., 1997).

1.12.1 Echistatin

A suitable candidate for this study is echistatin; a 5-kDa disintegrin extracted from the venom of *Echis Carinatus* (Gan et al., 1988). This decision was based on echistatins reported ability to inhibit RPE detachment and migration *In vitro* in a bovine RPE adhesion assay (Yang et al., 1996). It was speculated that by inhibiting the migration of the RPE cells into the inner retina of the dystrophic RCS rat it might be possible to retard the secondary vascular problems associated with the RCS pathology.

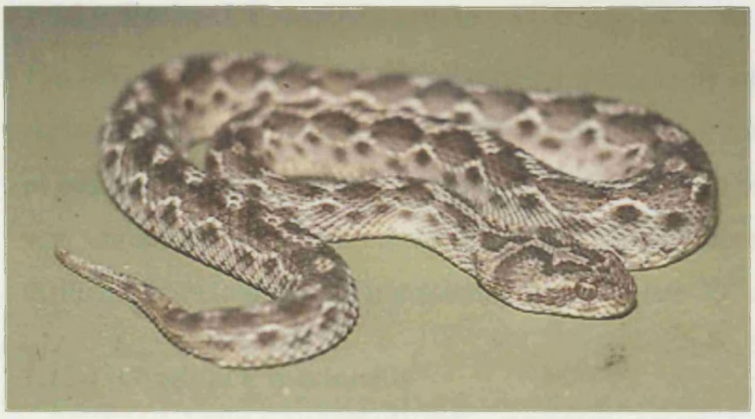

Figure 1.9 *Echis Carinatus* aka Saw Scaled viper

Echistatin binds to and inhibits the platelet receptor $\alpha_{IIb}\beta_3$ (Belisario et al., 2000) and the vitronectin receptor $\alpha_V\beta_3$ (Nakamura et al., 1998) which is involved in neovascularisation. Echistatin can also inhibit $\alpha_5\beta_1$ (Wierzbicka-Patynowski et al., 1999) which has been implicated in the internalisation phase of RPE phagocytosis. By studying echistatin and other disintegrins such as eriostatin (Wierzbicka-Patynowski et al., 1999) a new range of artificial disintegrin analogues are being constructed with much higher specificity to target individual integrin units (Kumar et al., 2001).

1.13 Retinal Transplantation History

The first attempts at retinal transplantation were purely surgical in nature with attempts to replace whole eyes. This coupled with the relatively primitive surgical facilities and lack of basic immunological knowledge available at the turn of the 19th century made success very unrealistic. Retinal transplantation was not considered feasible until successes were made in the field of neural transplantation in the late 20th century.

1.13.1 Original Experiments

The first recorded experimentation in retinal or rather whole eye transplantation took place in may of 1885 by a Dr M. Chibret, according to an account by Dr Charles May of New York who documented an unsuccessful case of human whole eye transplantation and four subsequent cases of which unsurprisingly all were failures, even though the last did survive for approximately 18 days (with no mention of functional vision). Not discouraged Dr May experimented on 24 rabbits of which the first 18 were total failures (which he put down to his inexperience with the technique and difficulties keeping bandages in place) but the last 6 he judged successful as the eyes became attached and reconnected blood vessels (May, 1887). He went on to describe the eyes surviving after 10 weeks, slightly smaller and with cloudy corneas. Dr May then felt suitably confident to take up a request to perform a similar operation on a human patient, transplanting an entire rabbit eye into a 29-year-old male recipient of sound health other than having lost sight in one eye. Dr May did not succeed with his ambitious experiment although the patient did express willingness to try again but as it took two weeks for the orbit to heal this was not considered.

Clearly what Dr May required for success was knowledge of modern immunology (xeno-grafting being unfavourable at best) and immuno-suppression (Cinader et al., 1971; Streilein et al., 2002); both of these pieces of information were a long time in arriving. Early transplants of foetal to maternal eyes were conducted by Royo and Quay in 1959 as a way around rejection before immuno-suppression was understood, but that was never going to be a viable treatment for human retinal diseases.

Modern retinal transplantation starts with the other immuno-privileged neural tissue: the brain. Transplantation of neural tissues in the late 1970's and early 1980s showed that developing neural tissue could survive transplantation (McLoon and Lund, 1980). Sadly a pattern started to emerge with neural and then retinal transplants that as soon as a researcher published the next break-though an ambitious clinician would try it on patients

(usually in countries with less active legal resources) claiming fantastic results that could not be reproduced (Molina et al., 1994)giving the field a less than respectable reputation. Transplantation techniques progressed through the 1980's until the first retinal transplants were performed (Turner et al., 1988), from then there have been many advances and a gradual move away from transplanting retinal tissues to cell based therapies such as stem and Schwann cell (Lawrence et al., 2000; Young et al., 2000) based treatments and now genetically engineered cell treatments to correct specific genetic disorders (Vollrath et al., 2001).

1.13.2 Clinical Problems

The clinical problems facing successful retinal transplantation are now well known although answers to many of them are not. This study is concerned with treatments towards human retinal degenerative diseases and as such the main questions are 1) Function - will the cells support or maintain visual function? 2) Availability of tissue/cells - can they be made available in sufficient numbers and be stored and applied easily? 3) Safety – will they cause side effects? will they invade other tissues and produce tumours? Due to the possibility of various human diseases like HIV/hepatitis, explanted donated tissue may not be advisable and it is always in short supply 4) Survival - how long will the cells survive? will they require continual reapplication? This is important because patients are often unwilling to undertake continual surgical treatments (even for minor treatments) Another less important consideration is whether the cells/procedure will provoke an inflammatory reaction – is immunosuppression required? which has its own side effects and considerable additional expense (Lund et al., 2001b).

Which cells to use and their source are very important, not just from the point of view of the recipient but also to the surgical team carrying out the surgery. Ideally the cells should be non-immunogenic to the host, stable and easy to grow and store and available in large numbers. Transformed cell lines such as ARPE19 human RPE cells have certain advantages in that they are stable and can be grown in vast numbers ready for patient use, they have been well characterised and are considered safe (Dunn et al., 1996; Kanuga et al., 2002) but they do suffer eventual rejection in animal models even under immunosuppression.

Allografts survive somewhat better, but humans are not inbred (generally) so this typically requires extensive immunosuppression in humans, in rats this in combination

with gene therapy has extended functional rescue further than previous experiments (Lawrence et al., 2004). Autografts of tissue extracted from the host, either of ancillary cells like Schwann cells (extracted in advance from peripheral nerves of the patient such as the perineal nerve grown in culture) may be a useful if controversial source. Autologous grafts such as iris pigmented epithelial cells suffer from the problems of harvesting sufficient cells from the patients which results in cells of suspect health with the same genetic disorder, Iris pigmented cell transplants have not shown long term efficacy(Semkova et al., 2002). Genetically modified retinal cells that produce natural chemicals such as PEDF and GDNF are another possibility (Lawrence et al., 2004).

Cell survival in the recipient may depend on several factors such as the anatomical site of delivery and timing of delivery of the transplant. Cells must be delivered into an anatomical site where they can integrate into the host retina without spreading into the vitreous or interfering with neural retinal function. The subretinal space is the only site that qualifies in the mammalian retina as it allows cells to be kept in place. The subretinal space is inside the BRB therefore it enjoys the immuno-protective benefits of the BRB as long as the delivery procedure does not damage the vascular network. The environment should be as healthy as possible, the studies discussed in this work have outlined the progressive degeneration of the entire retina set in motion by photoreceptor degeneration as modelled by the RCS rat (Caldwell et al., 1989; Davidorf et al., 1991; Essner et al., 1980; Wang et al., 2003). These studies highlight the importance of early detection of retinal disease as in advanced cases the retinal environment may well be hostile to any cells transplanted greatly reducing their effectiveness no matter how compatible they would be. Changes in the RPE cells due to aging are also a consideration both as a source of cells and for the environment into which transplanted cells are placed (Boulton et al., 2004).

The final end point for a successful procedure is not a healthy retina but functional vision and sadly any studies that do not follow transplants over long periods of time and do not use functional assays such as behavioural testing (McGill et al., 2004), Electroretinograms (ERG)(Cuenca et al., 2004), or electrophysiology (Lawrence et al., 2000) cannot claim complete success. Patients will not be impressed by doctors describing how healthy their retinas look if they cannot see the pictures themselves.

1.13.3 Reconstruction vs. Rescue

Retinal transplantation can be broadly divided into two strategies which can be termed reconstruction and rescue respectively. Reconstruction is the more traditional transplantation approach where transplanted tissue or cells are placed in or on the retina with the expectation that they will take the place of the damaged cells and function normally. This may be done with whole or partial thickness retinal sheets (Del Priore et al., 2004) or cell aggregates (Kwan et al., 1999). This requires the new tissue or cells to successfully integrate as a unit into the already damaged host retina.

Rescue is where the transplanted cells do not assume the role of the recipient tissue but provide aid in the form of growth factors or other diffusible agents that improve the recipient cells propects of survival (Lawrence et al., 2000).

Detection of the transplant after application is necessary to determine the degree of integration into the host, which with retinal sheets is fairly easy by basic anatomical means but with cell aggregates this is not always apparent as the cells disperse in the subretinal space making determining the fate of transplanted cells difficult. Specific antibodies are required to determine the fate of cell aggregate transplants as green fluorescent protein (GFP) labelling does not last for effective time periods. Retinal sheets (Del Priore et al., 2004; Ghosh et al., 2004) were technically more difficult to apply being very difficult to micro-dissect cleanly, clearly these would not be a viable option for mass human therapies as even cadaver allografts would not be sufficient for the number of patients.

Current transplants appear to rescue photoreceptors from apoptotic death (Travis, 1998) either by production of missing growth factors or by supplying excess factors that reduce the effects of the abnormal biochemistry found in retinal disorders. There is currently no evidence that full integration of host and recipient cells takes place and very little evidence for improved visual functionality over that, which existed at or prior to the transplant being administered. There is however a growing body of data showing that transplants can rescue or at least temporarily halt the functional decline of the visual system in models of retinal degeneration (Cuenca et al., 2004; Girman et al., 2003; Lawrence et al., 2004; McGill et al., 2004; Sauve et al., 2002; Sauve et al., 2004).

Transplants are generally viewed as explanted tissues/cells taken from a donor and placed into a recipient to replace non-functional tissues. In most retinal transplantation

experiments it now appears that the donor cells are not replacing but assisting failing cells, as such cell aggregate transplants should really be thought of as cell based therapies

1.13.4 Success So Far

At present the state of the art as far as retinal transplants go is genetically modified Schwann cells producing glial cell line-derived neurotrophic factor (GDNF)(Lawrence et al., 2004) and iris pigmented epithelial cell transplants modified to produce PEDF at the same stage (Semkova et al., 2002). These strategies offer the best chance of success for the greatest number of patients as they provide strategies for groups of diseases rather than cures for specific disorders. They can be modified to suit particular degenerative disorders and they may allow less radical interventions to treat vasoproliferative retinal diseases with anti-angiogenic peptides. Retinal sheet transplants while technically feasible have the disadvantages of difficult initial dissection protocol coupled with difficulties of supply and screening of suitable tissues, the insertion protocol is well within the skills of good surgeons but it is not without risk. The best retinal sheet transplants have not been demonstrated to fully integrate into the retina and no functional assessment has been undertaken to determine if the transplant had improved vision or even interfered with the healthy vision of the porcine recipient (Del Priore et al., 2004; Ghosh et al., 2004).

1.14 Image Analysis Of The Retina

Computerised image analysis of light microscopy is now a standard tool of cell biology with several key manufacturers supplying highly modular programs that can grow in complexity with the experience and knowledge of the user. Today nearly every manufacturer of microscopes offers their own image analysis program that is usually customisable to whatever configuration of microscope you might need such as Zeiss axiovision, Leica QWin quantitative software, and Olympus Microsuite, Nikon microscopes use Metamorph from Universal Imaging Corporation. These programs have the advantage of already being customised for their application. There are many other commonly used programs such as Image Pro Plus (media cybernetics) and ImageJ (a Java based cross platform application allowing users to run software on any computer system). The image analysis software used in this study has evolved out of tried and tested systems used to count retinal ganglion cells in whole mounted rodent retinae (Danias et al., 2002; Lafuente et al., 2002; Wang et al., 2003). Early image analysis took advantage of the mathematical algorithms in Adobe Photoshop to process captured images so that the target cells would stand out from the background allowing quantification (Danias et al., 2002) But over time this has been improved upon with dedicated image analysis programs such as Metamorph and Image pro plus (Wang et al., 2003)which can run multiple microscope accessories such as motorised stages, filter wheels and digital cameras. They also include a comprehensive suite of image manipulation algorithms to allow processing of raw images sufficient to increase signal to noise ratios allowing quantification beyond what was previously possible. These programs also include macro languages that allow grouping of processes to allow much greater automation of procedures. In quantifying cells or other biological features the main problem is usually in removing interfering background without altering the original target cells and in distinguishing individual cells in crowded populations. When trying to quantify vascular complexes in a flat-mounted retina the problems are slightly different. The main difference is that damage to the vascular network often results in a lack of vasculature and the computer systems are not very good at detecting a lack of target. Where vascular complexes occur there are a combination of features such as collapsed vessels, pigmented cells, aberrant shunt vessels avascular spaces and contorted vessels all of which comprise the vascular complex Which is why in this study it was necessary to use area of interest (AOI) analysis, whereby the operator traces an area of interest around the vascular

complex, Which encompasses all of the factors above. The image analysis software can then calculate the area of the total AOI for the retina and compare it against a similar trace taken of the entire retina. For retinal flat-mounts it was found that the NADPH-d staining method gave the best signal to noise ratio with complete staining of every vessel allowing a complete retinal map to be assembled. From this map the combined areas of all vascular complexes could be extracted and analysed very quickly (in under an hour for each prepared flat-mount). Analysis of the data was performed using Microsoft Excel spreadsheet software due to compatibility with the imaging software. 3d analysis was not possible during the timeframe of this study and indeed is not yet possible due to constraints on the confocal microscopy technology. This would require extremely accurate stepping stage technology to be built into the confocal microscope and also require a fluorescent marker that is not susceptible to fading to allow multiple zseries and XxY series of images to be captured. This is not a feasible undertaking with current technology

1.15 Summary

Research into human retinal degenerative diseases is currently at an exciting stage with several strategies such as gene therapy (Bainbridge et al., 2003) and cell-based therapies (including stem cells) (Lund et al., 2003; Semkova et al., 2002) maturing towards clinical trials. Progress in pharmaceutical enhancement of existing treatments has further refined their efficacy. Advances in understanding the genetics of the two main disease groups, AMD and RP has been invaluable in guiding research (Edwards et al., 2005; Guymer, 2001; Michaelides et al., 2003; Rivera et al., 2000). One area that is receiving special attention is angiogenesis within the retina. All retinal degenerative diseases have a vascular component that directly affects the health of the retina and indirectly the viability of any retinal treatment regime. This is reflected in four out of six current clinical trials mentioned earlier (figure **1.4**) being based on anti-angiogenic treatments (Augustin et al., 2004; Husain et al., 2005; Imai et al., 2005; Saishin et al., 2003) as well as anti-angiogenic treatments from . As many retinal treatments are invasive in nature, the treatments themselves may alter the vascular pathology. The present study points to the dynamics of vascular pathology and how they may be visualised.

2.0 Materials And Methods For "A Study Of The Retinal Vascular Pathology In The RCS Rat..."

2.1 Animal Model

Rodents were used due to the availability of suitable strains with analogy or homology to human retinal diseases. In addition, background experiments provided a foundation to the experiments conducted in this study, their short breeding time also allowed longer-term experiments necessary for this study. Most of this study utilises dystrophic and non-dystrophic (control animals) Royal College of Surgeons rats in which photoreceptor loss is due to RPE dysfunction. Long Evans rats were also used as a normal non-degenerative test animal.

2.2 Perfusion

Animals were given terminal anaesthesia of 25% Urethane (Sigma) at1ml/100g animal weight, before being perfused with PBS followed by 4% paraformaldehyde (EM Science). This involved:

1. Intraperitoneal injection for terminal anaesthesia.
2. Opening of the chest cavity, cutting though ribs to access the heart.
3. Clamping of the descending aorta (to prevent PBS/Fix being pumped around all the body).
4. Cutting the right atrium to release blood after it has been pumped to the brain.
5. Cutting the left ventricle, inserting and clamping in place a 20-gauge feeding/intubation needle into the incision.
6. Using a peristaltic pump (Masterflex. Cole Parmer), 80 ml PBS was pumped into the heart at rate of 10ml/minute to remove red blood cells from the head of the animal (to ensure none are left in the retina).
7. Pumping 80 ml of 4% paraformaldehyde through the upper body of the rat to ensure adequate fixation of the eyes.
8. Placing a 4/0 suture dorsally through the outer musculature of the eye to mark the eyes position before dissection.
9. Carefully remove the eye, cleaning off as much external musculature as possible form the orbit of the eye.

Some later experiments used immersion fixation where the animals were perfused with PBS and then the eyes dissected out, the sclera cut open and the eyeball immersed in 4% paraformaldehyde for 1 hour

2.3 Fixation

Light Microscopy Fixative

4% paraformaldehyde was used as a standard fixative for light microscopy as it was compatible with the histological procedures used in throughout this study. Paraformaldehyde was always used fresh. The following protocol was used to make up 1 litre of fixative

1. 40g of paraformaldehyde were added to 800ml of distilled water.
2. 10 drops of 1M NaOH (EM Science) were added.
3. The mixture was stirred constantly and heated until all of the paraformaldehyde dissolved (taking care not to heat above 60°C where the paraformaldehyde would be dissociated).
4. The pH was adjusted to between 7.2 and 7.4.
5. 100ml of 10x PBS concentrate (EM Science) was added and the resulting volume made up to 1litre by addition of distilled water.

Electron Microscopy Fixative

1. Modification of the standard paraformaldehyde protocol above to give 2.5% paraformaldehyde (25g in step 1)
2. 2.5% glutaraldehyde, (EM Science) 0.01% picric acid (Sigma) in 0.1M cacodylate buffer (Sigma) pH 7.4 was added.

2.4 Flat-Mounting The Retina

All manipulation of the retinae was carried out using very fine sable 000 size paint brushes to ensure as little damage as possible.

Animals were perfused with 4% paraformaldehyde.

1. The sclera was punctured with a sharp needle reducing ocular pressure and allowing the sclera to be gripped with forceps.
2. The sclera was cut from ciliary body to ciliary body to form an X with the dorsal suture at the top of the X.

3. The lens was carefully removed by applying pressure to the sides of the eye and cutting any zonular ligaments or iris, which impede the process.
4. The eye was fixed for a further ten minutes in 4% paraformaldehyde to allow the retina to stiffen prior to removal.
5. The eye was washed several times to remove the fixative and placed in a glass Petri disk lined with wax filled with PBS. The rest of this procedure was carried out under a Wild M3 dissecting microscope (Leica).
6. Using the X cut into the sclera as a guide the orbit of the eye is cut with fine scissors to within several millimetres of the optic nerve (figure **2.1**).
7. The eyeball was then flattened into a Maltese cross using the flaps of sclera, which were pinned to the wax using fine dissection pins.
8. The retina was carefully dissected away from the rest of the eye with special care being taken to remove excess vitreous and the zonular ligaments, which could prevent the retina from fully opening out.
9. The dorsal portion of the retina was marked by cutting a small notch in the outer edge of the periphery (figure **2.1**).
10. The optic nerve was cut after the entire retina has been detached, micro scissors were carefully placed under the retina and the optic nerve severed taking care not to damage the vasculature of the optic disk.
11. The detached retina was floated out into the PBS, any excess vitreous or debris can be carefully removed at this point using fine paintbrushes. The retina is then carefully manoeuvred onto a glass slide and flattened with the outer retina uppermost.
12. A square of very fine filter paper (Watmann, no. 50) was placed on top of the retina and the slide carefully blotted. The retina adhered slightly to the filter paper allowing it to be lifted off.
13. The retina (with filter paper backing) was placed in a glass vial (big enough for the paper to lie flat) with 4% paraformaldehyde and fixed once more for 1 hour.
14. The retinae were washed three times with PBS to remove the fixative.
15. The retinae were placed in a Petri dish full of PBS and the filter paper backing was carefully removed The retinae were then ready for staining.

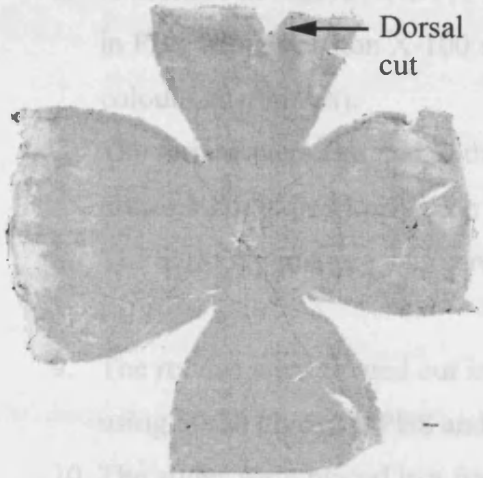

Fig 2.1 Flat-mount dissection showing a retina with four equal cuts made from the periphery into the mid to central retina. A notch was cut into the peripheral dorsal retina where the suture had been attached and the four cuts placed to allow designation of the four quadrants dorsal, nasal, ventral and temporal retina.

2.5 NADPH-Diaphorase Staining Of The Retina

The protocol used in this study utilised a histochemical reaction between the enzyme NADPH-diaphorase (Sigma, D-1630) and NADPH tetrasodium (Sigma,) salt to visualize the vascular network. Some retinae were stained with an antibody raised against high molecular weight neurofilaments (RT97; generous gift of Dr. Roger Morris, KCL, Guy's Hospital Campus, London).

Antibody pre-staining

1. RT97 antibody was prepared at a dilution of 1:1000 in PBS with 1% triton X100 (EM Science) detergent (to allow the antibody to penetrate the retina) and allowed to mix for 30 minutes.
2. 1 ml of antibody was added to each retina in a flat-bottomed glass vial and they were incubated at 4°C overnight (agitated if possible).
3. The secondary antibody, fluorescein-isothiocyanate (FITC) conjugated goat anti-mouse immunoglobulin (IgG) (Sigma) was prepared at a concentration of 1:50 in PBS taking care not to expose the antibody to light.
4. The antibody mixture was carefully drained off and the retinae washed 3x with PBS.
5. The retinae were incubated at room temperature with the secondary antibody for 1 hour, after which they were washed 3x as before.

6. A mixture of 0.02% NADPH-tetrasodium salt, and 0.04% nitroblue tetrazolium in PBS with 3% triton X-100 was prepared and mixed until it turned a purple colour (30 minutes).
7. The retinae were agitated in this solution for 90 minutes at 37°C until the vascular network could be clearly seen to the naked eye.
8. The antibody mixture was carefully drained off and the retinae washed 3x with PBS.
9. The retinae were floated out in PBS and carefully mounted on microscope slides using 50:50 glycerol: PBS and sealing the coverslips with nail varnish.
10. The slides were placed in a fridge until set and stored in slide boxes at 4°C.

2.6 Pigment Foci Quantification

The vascular complexes were easily visualized by the associated pigment deposition that occurred due to the pigment epithelium migrating onto blood vessels where the retina had lost photoreceptors completely. Flat-mounts were counted manually using a DMR research Microscope (Leica) utilising 10x objective with a 2.5x photomultiplier with a manual clicker counter.

The following criteria were used to quantify the VCs.

1. All distinct areas of pigment deposition in association with vascular damage (VCs) were counted manually including small peripheral single cell events, which we believe were indicative of precursors to vascular complexes.
2. Each retina was counted three times and the counts averaged. If the counts varied by more than 10% they were recounted.
3. Finally the counts for each group of retinae were averaged and standard errors of the mean (SEM) calculated using Microsoft Excel to show the data graphically followed by the F-test to give p values.

2.7 Intravitreal Injection Of Pharmaceutical Agents

1. A 30-gauge steel needle (Beckman Dickson) was glued into a fine glass capillary tube and attached to a 10 µl glass micro-syringe (Hamilton) Leur fitting using Tygon micro tubing (Masterflex, Cole-Palmer).
2. Animals were anaesthetized with tribromoethanol (Avertain 20 mg/100g animal weight, Sigma); their heads immobilized using a custom-made mouth bar to assist in positioning of the head.
3. The left eye was chosen for pharmaceutical intervention (see figure **3.1.9**) and the right eye was not treated in any way so that it could serve as an in animal control.
4. The injection was placed just behind the ciliary body taking care to angle the needle so that the injection site would be self-sealing. Care was taken to avoid any large blood vessels in the area.
5. The cornea was punctured with a 24-gauge steel needle (Beckton Dickson) to relieve the ocular pressure when the pharmaceutical agent was delivered and reduce reflux of said agent. Without puncturing the cornea the ocular pressure would result in reflux of a considerable amount of the preparation, slow delivery after relieving pressure resulted in minimal if any reflux.
6. 2 µl of pharmaceutical agent was delivered to the dorsal portion of the posterior chamber of the eye taking care not to damage the lens in any way (as damage to the lens capsule results in release of growth factors and potential scarring).
7. The animals were allowed to recover normally and the procedure repeated after two weeks (allowing plenty of time for the injection site micro injury to heal).
8. At 16 weeks of age the animals were harvested and perfused, the retinae were flat-mounted, stained and counted as detailed earlier.

2.8 Avertain Or Tribromoethanol Anaesthesia

1. A solution comprising of 4.67g of 2,2,2 tribromoethanol (Sigma) and 3.3ml of 100% ethanol was made up and sonicated until dissolved, should turn a light brown colour.
2. 250 ml of 70°C saline were added and mixed well.
3. The final solution was stored at room temp covered in foil.

2.9 Image Analysis

Originally the image analysis setup purchased from Scientific Imaging Management, comprised of several components, a research microscope (Leica DMRB) fitted with a 0.1 μm stepping stage (Prior H28) and a low light CCD Camera (Hamamatsu C5985). The image analysis comprised of a computer workstation (AST) with a frame grabber (data translation DT3155) running PC Image (Foster Finlay Associates) and Metamorph 3 (Universal Imaging Corp.). This system had been used to capture dark field fluorescent flat-mount images of neurofilaments and ganglion cells but unfortunately proved inadequate for transmitted light capture due to errors in capturing images and the manner in which they were assembled to produce large composite images. This involved producing three stages of 13x5 frames montaged then the three composite images assembled to produce a final 13x15 frame composite montage.

The system was upgraded to a custom built workstation running Image Pro Plus 3.5 (Media Cybernetics) on a more advanced frame grabber (Snapper 8, Datacell Ltd, UK), which enabled 13x15 frame montages of the entire flat-mounted retina to be produced. Images produced by this second generation system were 8-bit greyscale, which for this study did not exhibit enough contrast between areas of vascular damage and background debris/pigment to allow automated counting. Manual counting had to be used to allow focusing changes and to discern colour definition of associated pigment and whether vascular bundles were abnormal. Computer technology did not allow totally automated counting in this system due to the inability of the computer to discern patterns of vascular complexes or to choose which vascular plexus to focus on.

2.10 PEDF Preparation

PEDF was obtained from Pfizer Plc (originally sourced from Joyce Tombrand-Tink) along with an anti-PEDF rabbit polyclonal antibody. The PEDF was stored in Eppendorfs containing 10 mg PEDF in 1 ml PBS. As there were no certificates of purity with this delivery, prior processing was required to check purity and finally to reduce the volume down to 1 μg in 2 μl PBS. To reduce the volume down to a usable level, lyophilisation was attempted initially. Lyophilisation proved unsatisfactory as it resulted in dry PEDF mixed in with excessive salt residue.

Eventually the following method of reducing the volume was utilised: disposable PD-10 columns (Amersham Pharmacia) containing Sephadex G-25M were used to separate the buffer from the PEDF under centrifugation, which proved satisfactory.

1. 3 1 ml Eppendorfs were decanted into the upper chamber of 1 PD-10 column and the column spun at 10,000g for 2 hours until the volume in the upper chamber was reduced to roughly 50 μl (at least 3 PD-10s were used at any one time).
2. The residual PEDF solution was decanted out of the upper chamber into a locking Eppendorf, sealed with parafilm (SPI supplies) and stored at 4°C for short-term use.
3. 5 μl of concentrated PEDF was taken to check protein concentration

2.11 PEDF Protein Assay

In order to deliver a dose of 1 μg in 2 μl of PBS the concentration of the PEDF sample had to be determined to allow accurate dilution

To determine PEDF levels in sample after concentrating in PD-10 columns, the DC protein microplate assay was used (Biorad)

1. Preparation of working reagent. 20 μl of reagent S is added to each ml of reagent A (working reagent).
2. 3-5 dilutions of a protein standard (BSA) containing from 0.2 mg/ml to 1.5 mg/ml proteins were prepared; a standard curve was produced for each run of the assay.
3. 5 μl of standards and samples were added to a sterile 96 well plate.
4. 25 μl of reagent A (alkaline copper tartarate soln.) was added to each test tube.
5. 200 μl of reagent B (dilute Folin reagent) was added to each test tube and immediately agitated.

After 15 minutes absorbencies were read at 750 nm

In order to check the purity of the PEDF sample a western blot was performed using the anti-PEDF antibody to detect the protein from a SDS-page gel.

2.12 SDS-PAGE And Western Blot Of PEDF Sample

2.12.1 SDS-PAGE Of PEDF Samples

Equipment and reagents

- Mini-slab gel electrophoresis apparatus, giving 0.5–1.0 mm thick mini-gels (Biorad Mini Protean II system)
- 4 x lower gel buffer 1.5 M Tris–HCl (Sigma) pH 8.8, 0.4% SDS)
- 4 x upper gel buffer 0.5 M Tris–HCl pH 6.8, 0.4% SDS)
- 30% acrylamide gel mixture (30% acrylamide (Sigma) and 0.8% N,N'-methylenebisacrylamide (Sigma)

  10% ammonium persulphate (Sigma)
- TEMED (N,N,N',N'-tetramethylethylenediamine) (Sigma)
- 2-methyl-1-propanol (alternatively, water-saturated 2-butanol) (Sigma)
- 10x electrophoresis buffer stock (0.25 M Tris base, 1.92 M glycine).

Method

1. Two gel plates (8 x 10 cm) were assembled separated by 1 mm spacers.
2. Separating gel mixture of the correct concentration was made up as shown below.

Stacking gel mixture

Final % acrylamide	4	6	8	10	12	15
distilled water (ml)	3.0	2.75	2.42	2.09	1.75	1.25
4 x lower buffer (ml)	0	1.25	1.25	1.25	1.25	1.25
4 x upper buffer (ml)	1.25	0	0	0	0	0
30% acrylamide gel (ml)	0.7	1.00	1.33	1.66	2.00	2.50

3. To start polymerization, 11 ml TEMED and 30 ml 10% ammonium persulphate were added to the separating gel mixture, briefly swirled and then transferred to the gap between the glass plates using a Pasteur pipette, the meniscus should be approximately 1.5–2.0 cm from the top.
4. 0.5 ml of 2-methyl-1-propanol was layered on top of the acrylamide solution, and left to polymerize at room temperature for at least 30 min. The polymerized separating gel could be stored for a few hours at room temperature, or weeks at 4 °C if sealed in an airtight bag, before adding the stacking gel. Once the stacking

gel had been poured, however, the gel had to be run within 3 hours. The 2-methyl-1-propanol was washed out with distilled water and then any remaining drops of water were removed with tissue paper.

5. 11 ml TEMED and 30 ml 10% ammonium persulphate were added to the stacking gel mixture (see step 2 above), mixed and transferred to between the glass plates using a Pasteur pipette. A "well-forming" comb was placed between the glass plates taking care to avoid bubbles under the comb and left at room temperature for at least 20 min to polymerize.
6. The comb was carefully removed, then the gel was placed in an electrophoresis tank containing 1x electrophoresis buffer (made by diluting 10x electrophoresis buffer stock to 1x with distilled water, then adding SDS to a final concentration of 0.1%). sample wells were flushed with electrophoresis buffer using a Pasteur pipette.

Running Of SDS-Page

Equipment and reagents

- Power supply and apparatus for SDS-PAGE of proteins
- Vacuum gel drier
- prestained non-radioactive markers (Rainbow markers; Amersham)
- 2x SDS sample buffer (10% glycerol, 5% 2-mercaptoethanol, 3% SDS, 62.5 mM Tris–HCl pH 6.8, 0.2% Bromophenol Blue). Store in aliquots at -20 °C
- Fixing solution (25% 2-propanol, 10% acetic acid).

Method

1. The samples were transferred into 1.5 ml microcentrifuge tubes and combined with an equal volume of 2x SDS sample buffer. In order to estimate the size of any cross linked protein resolved in the gel, an additional sample containing prestained non-radioactive markers in SDS sample buffer has to be prepared.
2. Each microcentrifuge tube had its lid pierced with a needle, before the samples were placed in a boiling water bath for 5 min to denature the protein
3. The samples were loaded onto the SDS-polyacrylamide gel and electrophoresised at an appropriate voltage (check the manufacturer's guidelines; usually 100 V) until the sample reached the interface with the separating gel, then at 160 V until the dye reaches bottom of the gel. The total running time for a typical mini-gel was 1.5 h.

4. The gel was removed from the glass plates and fixed by incubating twice for 10 minutes in fixing solution at room temperature with gentle agitation.
5. The gel was placed on a piece of Watmann 3M paper and dried on a gel drier.

2.12.2 Western Blot Of PEDF Sample

Equipment and reagents

- Blocking buffer: 10 g gelatin, 8.77 g NaCl, 6.06 g Tris base in deionised, distilled water (heat until dissolved, adjust the pH to pH 7.4 with HCl, make up to 1 litre with double distilled (dd) H_2O)
- Rinsing buffer: 2.5 g gelatin, 1.86 g EDTA, 8.77 g NaCl, 6.06 g Tris base, dissolved in deionised distilled water (add 50 ml normal goat serum, adjust the pH to 7.4, and bring the volume to 1 litre with distilled water)
- Primary rabbit polyclonal antibody to PEDF (ab. 2520, Pfizer Plc)
- Secondary antibody conjugated to peroxidase (affinity-purified peroxidase-labelled goat anti-rabbit IgG (0.1 mg/ml; Dako.))
- Diaminobenzidine–hydrogen peroxide solution: 50 mg 3,3'-diaminobenzidine (Sigma.) in 100 ml of 50 mM Tris–HCl buffer, pH 7.5, containing 25ml of 30% hydrogen peroxide (filtered)
- Coomassie blue staining solution: 200 mg Coomassie Brilliant Blue(Sigma), 40 ml methanol, 10 ml glacial acetic acid(EM Science), 50 ml deionised distilled water (filter)
- Destaining solution: 2 ml glacial acetic acid, 90 ml methanol, 8 ml deionised distilled water
- Plastic bags and bag sealer
- 50 mM Tris–HCl, pH 7.5

Method

1. The membrane (blot) was soaked in a tray containing 500 ml of the blocking buffer for 2 h at room temperature with gentle agitation.
2. The membrane was rinsed in rinsing buffer three times at room temperature for 10 minutes with gentle agitation.
3. The blocked membrane was incubated with 40 ml of anti-PEDF (ab 2520, rabbit polyclonal used at 1:2000 dil.) primary antibody in a sealed plastic box at room temperature for 2 hours on a shaker.

4. The membrane was rinsed once more in rinsing buffer three times at room temperature for 10 minutes with gentle agitation.
5. The membrane was incubated with 40 ml of the anti-rabbit peroxidase conjugate (diluted at 1:200 with rinsing buffer) for 2 hours at room temperature.
6. The membrane was rinsed in rinsing buffer three times at room temperature for 10 minutes with gentle agitation followed by three rinses in 50 mM Tris–HCl buffer, pH 7.5.
7. For visualization of the antigen–antibody complexes, the membrane was incubated for 3–5 min in 100 ml of diaminobenzidine–hydrogen peroxide solution
8. The membrane was rinsed in deionised distilled water, and then air-dried.
9. Visualization of the protein size markers was accomplished by staining the membrane in Coomassie blue (0.2%) staining solution for 2 min, then destaining the membrane in the destaining solution followed by rinsing in deionised distilled water and finally drying between filter papers.

2.13 Preparation Of Immunocytochemistry Samples

1. Rats were cardially perfused with PBS to remove blood cells but not fixed.
2. Their eyes were dissected out carefully and placed in plastic moulds filled with OCT with the dorsal region clearly marked for orientation.
3. The moulds were placed on steel blocks partially submerged in liquid nitrogen to snap freeze the samples.
4. Samples were stored at –70°C prior to cutting.
5. Samples were cut at 5 μm sections with 3 sections/slide using a cryostat (Leica 3050CM) and stored at -70°C until needed.

2.14 **Immunostaining** - Using ABC Kit

1. Samples were removed from the freezer and allowed to warm to room temperature and placed in a humidified slide chamber.
2. A solution of 1% dried milk powder and distilled water was applied to the sections to block non-specific epitopes.
3. Sections were washed lightly in PBS.

4. 250 µl of primary antibody was applied to each section; a Dako hydrophobic pen was sometimes used to stop the solution spreading across the slide, which would result in sections drying.
5. Sections were incubated overnight at 4°C.
6. Appropriate secondary was antibody prepared; sections were washed 3x in PBS.
7. ABC solution was prepared according to Promega instructions, (40 µl soln. A, 40 µl soln. B in 2.5 mls PBS, left to stand 30 min.
8. Sections were covered with 250 µl ABC solution for 30 min.
9. Sections were washed 3x in PBS.
10. Sections were placed in filtered 1% nickel chloride (EM Science) in distilled water for 5 min.
11. The sections were transferred directly to Filtered DAB soln. (50Mg/100ml) in DAB buffer activated with 10µl of hydrogen peroxide and incubated for 3 min checking colour change.
12. The sections were washed 3x in PBS.
13. The sections were counter-stained (Cresol violet 0.5%) as required, dehydrated and mounted with DPX (Fluka Chemicals) mounting media.

Negative controls consisting of slides without the primary antibody and separate slides missing the secondary antibody were used with each staining run to determine if non-specific staining was occurring. Positive controls of either rat skin (for extracellular binding integrins) or rat spleen (for cellular binding integrins) were also run to prove that the antibodies did work correctly

2.15 Electron Microscopy

1. The eyes were perfused with EM fixative.
2. The Iris and ciliary body were dissected out allowing access to the lens.
3. The lens was removed.
4. A notch was cut into the nasal retina to allow positioning of eyeball for cutting dorsal-ventrally.
5. The eyes were post fixed in 1% Osmium tetroxide (Sigma) for 1 hour.
6. The eyes were dehydrated through successive concentrations of ethanol (50%, 75%, 90%, 95%, 100%X2).

7. The eyes were immersed in two washes of 100% acetone in alcohol for ten minutes. then 50% TAAB embedding resin (TAAB laboratories, Aldermaston, UK) in acetone for ten mins then overnight in 75% resin in acetone agitated.
8. The eyes were then transferred into 100% resin for 1 hour, agitated and then cured overnight in an oven at 65°C.
9. A bright light (LED torch) was used to visualise the notch cut into the nasal portion of the, allowing orientation for dorsal-ventral cutting
10. Semi-thin 500 nm sections were cut on an ultramicrotome (Leica Ultracut) and stained with 1% toluidine blue in 1% borate buffer (sigma) to determine areas of interest.
11. Ultra-thin 50 nm sections were cut (using the same ultramicrotome) of targeted areas placed on copper grids and contrasted using uranyl acetate (EM Science) and lead citrate (EM Science).
12. The grids were viewed on a transmission electron microscope (Jeol 1010 in London, Hitachi H600 in Utah).

2.16 The "VC Assay" Image Analysis

1. The stepping stage (Prior H28, Prior scientific) was initiated and calibrated by maximal movement to allow the computer to calculate distances. Care was taken to ensure that all optics were moved out of the way of stage travel so that they would not be damaged
2. The slide was placed on the stepping stage and the stage driven to the east edge (north being away from operator) of the retina and its position set to origin. The stage was then driven to the furthest southern edge and then driven east until the distance from origin becomes 0. At this point the stage would be ready to commence scanning the entire retina so the set origin function would be used again to record the start point.
3. Full retinal map was assembled using Image pro Plus 4.5 (Media Cybernetics) using the acquire function with a 9x12 grid capturing with a Digital Insight (diagnostic Instruments) camera at 1400 x 1000 pixels using 10x objective with 2.5x photomultiplier. After calibration this worked out as 9805.466 μm x 9338.52 μm for a total area of 9.1568×10^7 μm^2 of which a typical RCS rat retina at 4 months takes up approx. 4.5×10^7 μm^2.

4. The retinal map has a scale bar for 1000 μm overlaid using the measure-calibration-select spatial command.
5. Using the process-Trace objects command (pen Size 8) areas of interest were traced around individual vascular complexes. Care was taken to consistently draw the full extent of the vascular complex, with the area to be measured being inside the trace, not including the trace line itself.
6. A trace image was generated of all the AOI using the generate trace image command within trace objects; this produced a black and white image of the AOI without the background image.
7. The trace line was then thickened to allow the program to accurately measure the area within each AOI using the Process-Filters-Morphological-Erode command, set to 3x3 cross on two passes. This eroded the edges of the bright objects and thickened the dark objects resulting in the trace line being thickened; this slightly eroded the AOI within but was necessary and consistent with all counts.
8. The total area of the AOI were calculated using the measure-count/size function set to automatically count bright objects and ignore any bright objects in contact with the image edges. This meant that only the internal area of the traced AOI was counted.
9. The data were then transferred to a spreadsheet (Excel, Microsoft corp., Wa) using the direct data exchange (DDE to Excel) command within the Measure function window.
10. The area of the entire retina was counted by tracing a single AOI around the edge of the entire retina and following steps 6-9 above.

2.17 Semi-Thin Cutting Of Flat-Mounted Retinae

1. Coverslips were carefully removed from flat-mounted retinae under PBS.
2. The retinae were carefully detached from the slide using fine paintbrushes and transferred to a wide sample vial containing PBS.
3. The retinae were washed 2 more times in PBS to remove glycerol.
4. The retinae were dehydrated through successive alcohols, ten minutes for each concentration, 50%, 70%, 90%, 95%, 100%, and 100%.

5. The retinae were immersed in two washes of 100% Acetone in alcohol for ten minutes then 50% resin in acetone for ten minutes then overnight in 75% resin in acetone agitated.
6. The retinae were then transferred into 100% resin for 1 hour agitated.

7. The retinae were placed flat, ganglion cell side up between two sheets of plastic with mild weights on top to keep them flat and then cured overnight in an oven at 65°C.
8. The retinae were carefully peeled off their plastic backing and excess plastic cut away. The retinae were then trimmed with the nasal and temporal lobes removed, the remaining retina was divided into three separate zones of equal length, dorsal, central and ventral retina.
9. These three parts were stacked onto of each other with ventral on the bottom and dorsal on top, then placed in EM moulds with more resin and cured overnight at 65°C in an oven
10. Sections were cut from the retinae at 1μm on a microtome (Reichart Jung 2020) or ultramicrotome (Sorval MT 5000) and stained with 1% toluidine blue in 1% borate buffer.

2.18 Sub-retinal Transplantation

1. Dystrophic RCS rats at 22-24 days of age (post-weaning) were anaesthetised as in section 2.8 and positioned under a surgical microscope to allow full access to the target eye. The head was immobilised with a custom-made mouth bar clamped gently over the bridge of the nose.
2. A drop of Tropicamide ophthalmic solution 1% (Bausch & Lomb, Tampa, FL) was given to each eye to dilate the pupil allowing clear visualisation of the retina.
3. A rubber o-ring of diameter 1 cm was placed over the eye and Hypromellose HPMC 2% eye drops (Moorfields Eye Hospital) used to fill the o-ring allowing clear visualisation into the eye without drying out the cornea.
4. Slight pressure was applied to the sides to proptose the eye and a 4-0 silk suture was carefully tied around the eye to stop it from retracting back into the ocular orb.

5. Using the tip of a 24-gauge disposable needle (Beckman Dickson), a hole was scratched through the sclera and the choroid allowing access to the sub retinal space
6. A fire blunted ultra-fine glass pipette was prepared attached to a 10 μl micropipette.
7. A 30-gauge disposable needle was used to puncture the cornea allowing relief of pressure in the eye during transplant insertion.
8. The micropipette was used to administer 2 μl of cell suspension (10^5 cells approx) in DMEM F12 media subretinally into the eye. During insertion, care was taken to introduce the pipette at an angle to allow the layers of the sclera and choroid to seal during retraction.
9. Then the glass pipette was retracted with great care taken to reduce reflux of transplant suspension. The retina could then be viewed, checking for retinal puncture. A successful transplant would result in a localised detachment or bleb on the inside of the retina.

2.19 Human ARPE19 Cell Culture

1. Human ARPE19 cells (CRL-2302) were obtained from the American Type Culture Collection (Manasses, Va)
2. Cells were quickly defrosted from storage and transferred into T-10 flasks containing DMEM/F12 media with 10% Foetal Calf Serum (FCS)
3. Cells were grown in T-10 flask s at 37^0C in an incubator with 5% CO^2 until confluent.
4. Cells were harvested using Trypsin 1% with ETDA, resuspended in DMEM/F12 with 10% FCS to inactivate the trypsin.
5. Cell suspension is centrifuged at 1000rpm for 8 minutes and resuspended in DMEM/F12 without serum, and placed in an ice bath until transplantation.
6. Trypan blue cell viability assays were performed after each transplant session to check cell viability

2.20 Data Analysis & Statistics

As the sample numbers in these experiments were not even (due to the RCS litter size being the main constraint on experimental design) paired t-tests were used to determine

the p-values between two sets of data to show significance. This used MS Excel to determine if the variance in the data sets were equal using the F-Test. This was followed by paired t-tests for either equal or unequal variance as determined by the f-test.

All graphs were assembled using MS Excel and the error bars represent standard errors, data tables below the graphs show the data and number of retinas used.

3.0 Experiments For "A Study Of The Retinal Vascular Pathology In The RCS Rat..."

3.0 Introduction

The results from this study are presented as three chapters.

Key points

1. Rate of development of vascular complexes (DVCs) associated with photoreceptor loss in the RCS rat. This involved NADPH diaphorase (NADPH-d) staining and image analysis of second order vascular events.
   - NADPH-d staining was used to visualise the entire vascular network of the retina as well as pigmented cells, allowing evaluation of the relationship between the RPE and the vascular pathology.
   - Baseline studies exhibited a quantifiable increase in VCs over time allowing the procedure to be used as an assay (VC assay).
   - Manual image analysis of retinae was used to quantify either number of vascular complexes or absolute area of vascular complexes.
   - Image capture technology was developed, allowing more sophisticated quantification of vascular complexes.

2. Modification of rate of retinal degeneration using PEDF and echistatin
   - PEDF administered at three months slowed the rate of DVCs.
   - Echistatin administered at three months increased the rate of DVCs.
   - Echistatin did not cause DVCs in normal Long Evans rats.

3. Modification of rate of DVCs using human RPE cell line transplantation
   - Early sub-retinal transplantation of human RPE cells dramatically slowed down the rate of DVCs.
   - Transplantation at different time-points resulted in different effects on vascular pathology, with late transplantation increasing the DVCs.
   - The transplant affected large areas of the retina, not just the region where the transplanted cells were localised.

3.1 Calculation Of Rate Of Development Of Vascular Complexes Associated With Photoreceptor Loss In The RCS Rat

3.1.1 RCS Rat: Development Of Vascular Complexes

The aim of this part of the study was to investigate the progression of the naturally occurring vascular pathology of RCS rat retinae and determine whether quantification was feasible. The initial loss of rod photoreceptors caused by RPE dysfunction was followed by secondary vascular abnormalities and eventually damage to the retinal ganglion cell layer. RPE cells then migrated off Bruch's membrane into the retina and associated with abnormal vascular formations. These VCs take several forms from the typical VC found in the mid to central retina where pigmented cells have attached themselves onto the venous vasculature and caused contortions of the vessels to much smaller single cells exhibiting RPE pigment commonly found on the peripheral retina attached to the vasculature (where there should be no pigmented cells at all). Also there were in advanced cases huge VCs that had merged, forming large extended areas where the venous vascular system and capillary bed (later the arterial system) had totally broken down. This was usually found at later time-points in the RCS pathology after total photoreceptor loss had occurred. The early work in this study counted pigment foci, which were the pigmented cells that had migrated into the retina as the retinal maps were initially only available as greyscale images

While other studies have referred to the vascular complexes as neovascular formations (Caldwell et al., 1989), there is little evidence to support the implication of newly formed vessels as opposed to contortion of existing vessels. Hence the more conservative terminology above. There may well have been neovascularisation in this model but this study did not address that facet of the RCS pathology. The development of these VCs could be clearly visualised by flat-mounting the retina at different time-points and staining both the blood vessels and the neurofilaments of the RGC layer.
Second order events initiated by RPE cells migrating off Bruch's membrane onto the deep vascular plexus of the retina, were a consequence of overall thinning of the retina due to photoreceptor loss. Migrating RPE cells constricted vessels leading to loss of integrity in the blood/retinal barrier. These pigmented cells could be clearly seen in the RCS rat strain used here (Villegas-Perez et al., 1998). Many previous studies have failed

to show the close interaction of RPE cells (Caldwell et al., 1989; Seaton et al., 1994) and the vascular defects as they have utilised albino strains of RCS rats. Selective staining of the vasculature using NADPH-diaphorase made it possible to examine both RPE cells and vascular anomalies together (Wang et al., 2003). The optic axon bundles were visualised using RT 97; an antibody to large molecular weight neurofilaments.

3.1.2 Experiments

A baseline experiment was set up using RCS rats at 2, 3, 4 and 5 months of age in order to investigate the development of vascular complexes. The (Villegas-Perez et al., 1998)time-points were chosen based on preliminary experiments on a group on animals of different time-points. These showed that the first evidence of vascular pathology occurred at three months of age and by six months, the pattern of the vascular pathology was too complex for accurate pigment foci quantification. At least four animals were used for each time-point (minimum of 8 eyes).

The following techniques were utilised:

Flat-mounting of RCS rat retinae followed by NADPH-d staining of the vasculature.

Manual counting or image analysis of AOI counts followed by data analysis using Microsoft Excel to quantify the development of vascular complexes. RT 97 Immunostaining of the same flat-mounted retinae was used to determine the onset of damage to the optic fibre layer.

3.1.3 Two Months Baseline

The NADPH-d staining method exhibited very clear staining of the vascular network throughout the retina as shown in **figure 3.1.1**; a composite picture of a RCS rat retina at two months of age. The blood vessels show up blue with very little if any background staining. Whatever changes there may be going on at the cellular level within the retina there were no signs of vascular pathology at this time-point as shown in **figure 3.1.1**. The vascular network was undamaged and identical to that of a congenic (non-dystrophic) RCS rat seen in **figure 3.1.2**.

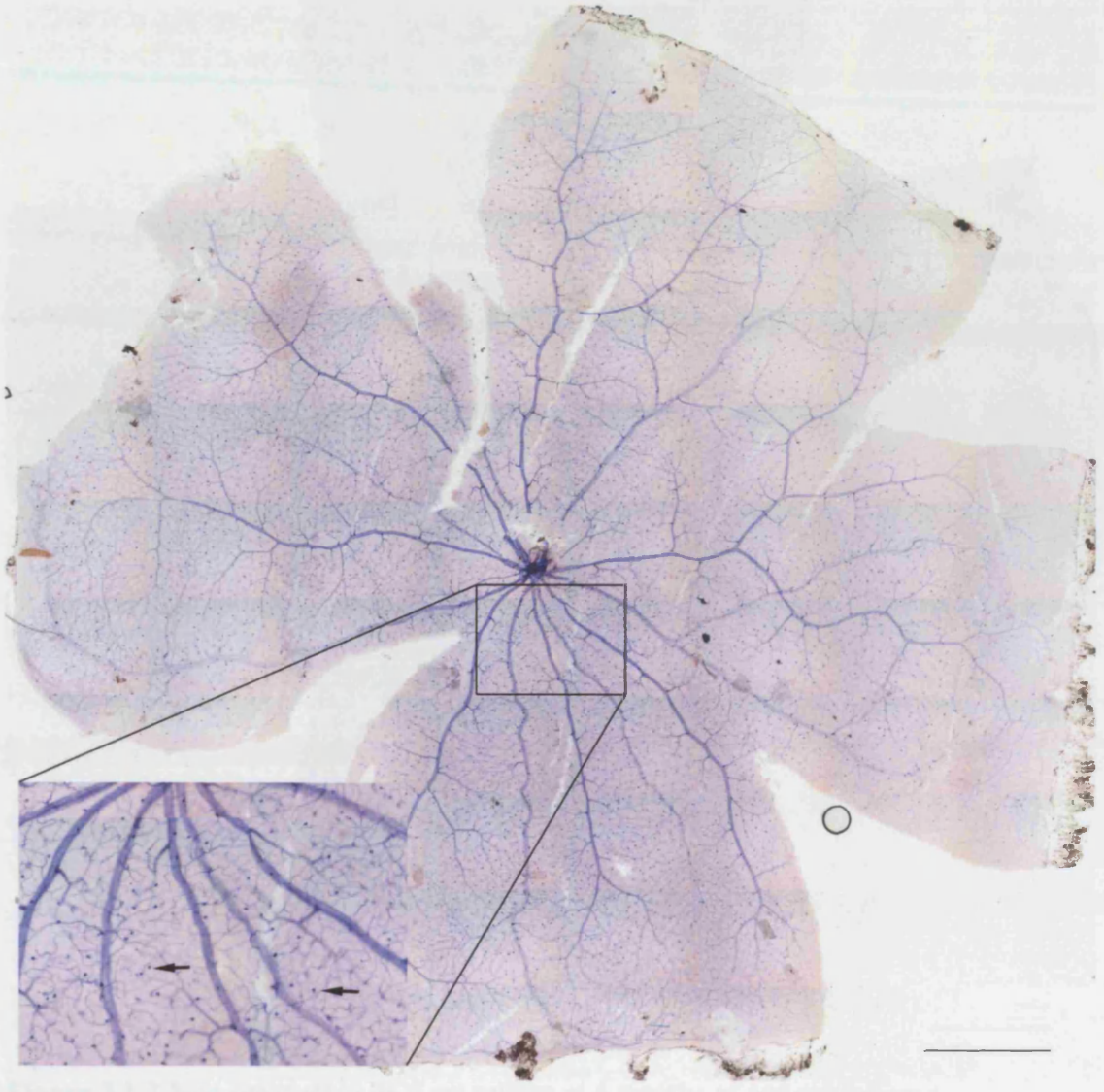

Figure 3.1.1 Dystrophic RCS retina at 2 months of age, The dorsal portion of the retina is uppermost in the picture; this convention was used throughout this study. Note the normal arrangement of darker staining arteries radiating out from the optic disc interspaced with the main draining veins. The small darkly staining cells scattered throughout the retina (see arrows in insert) are a subset of amacrine cells.
The insert shows the normal vascular network just ventral to the optic disc.
Scale bar represents 1000 μm.

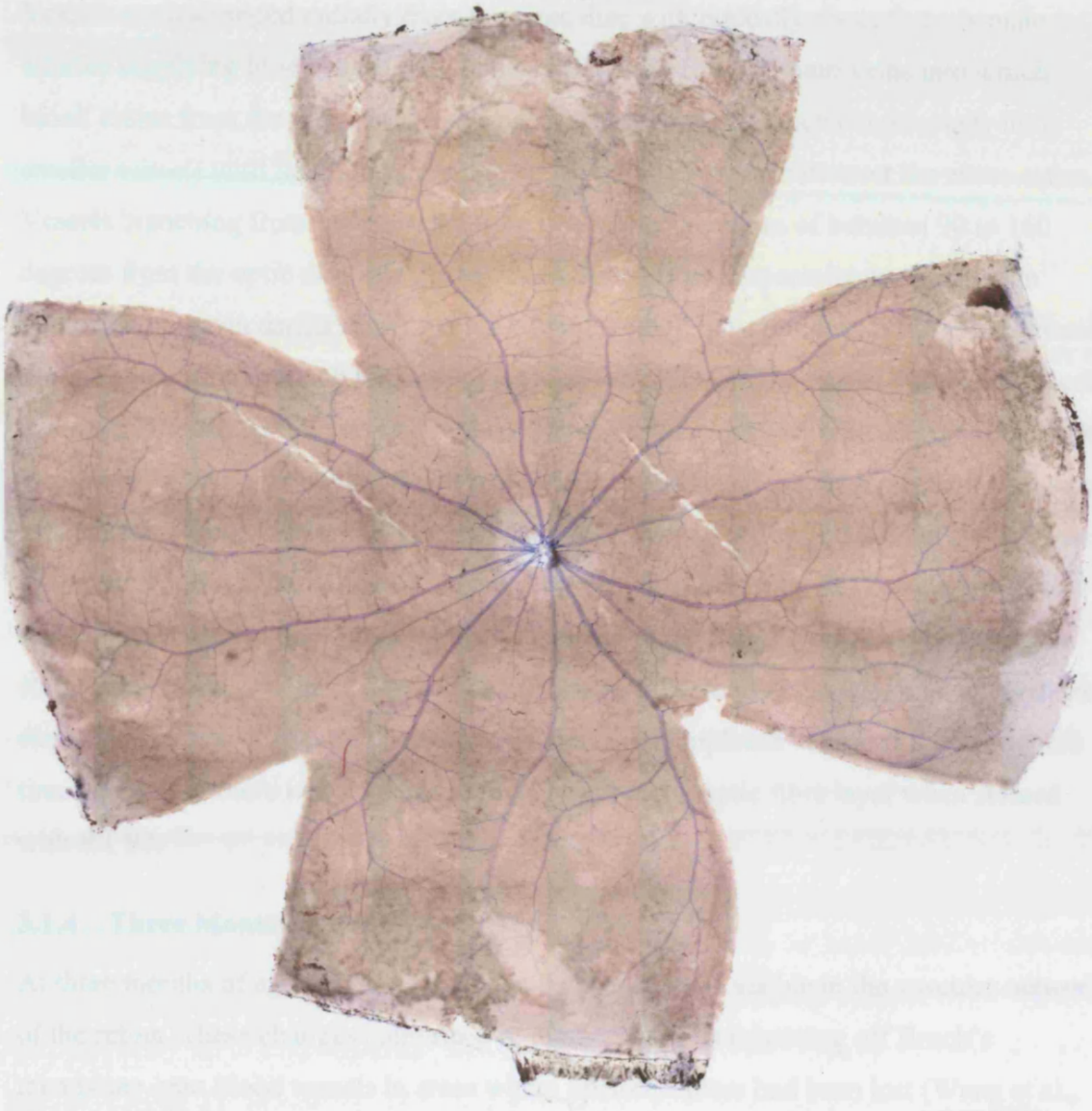

Figure 3.1.2 Non-dystrophic RCS rat retinae at 4 months of age exhibiting a normal vascular network devoid of any vascular complexes, very similar to **figure 3.1.1.** The retina has not stained as well as **figure 3.1.1** and has more background, hence the darker red colouration to the retina.
Scale bar represents 1000 μm

Vessels were arranged radially from the optic disc with typically about five-six main arteries supplying blood to the retina interspaced with five-six main veins into which blood drains from the retina to the optic disc. These vessels branch continuously into smaller vessels until they form interconnecting capillary beds that cover the entire retina. Vessels branching from the main draining veins do so at angles of between 90 to 160 degrees from the optic disc side of the vessel. Arteries and especially arterial branch points tend to stain darker under the NADPH-d method, possibly due to the greater blood pressure requiring more NO activity (Nagaoka et al., 2002). The retinal vascular network is normally separated into two main focal planes (or plexuses) with the superficial plexus located in the inner retina associated with arterial vessels and the deep plexus in the outer retina draining into the venous system via large vessels to the optic disc. For the purposes of this study all figures will focus on the deep venous plexus as vascular complexes are initiated there due to their physical location closer to the RPE layer. At no point in this study were vascular complexes seen on major arterial vessels (although at later advances stages this may well occur). There were no vascular complexes visible at the two month time-point; also there was no damage of any kind to the optic fibre layer when stained with RT 97.

3.1.4 Three Months Baseline

At three months of age the first pathological changes were visible in the vascular network of the retina. These changes comprised of pigmented cells migrating off Bruch's membrane onto blood vessels in areas where photoreceptors had been lost (Wang et al., 2003)). The RPE cells that migrated into the retina could be distinguished from RPE still attached to Bruch's membrane as they were on the same focal plain as the deep vascular plexus within the retina, whereas debris was limited to the surface of retina. These cells did not exhibit any of the morphological characteristics of macrophages in the flat mounts (compared with later flatmounts with transplants such as figure 3.3.9 insert a).Vascular complexes were seen to develop initially in the mid-ventral to central regions of the retina then throughout the ventral retina and finally spreading out over the entire retina with age.

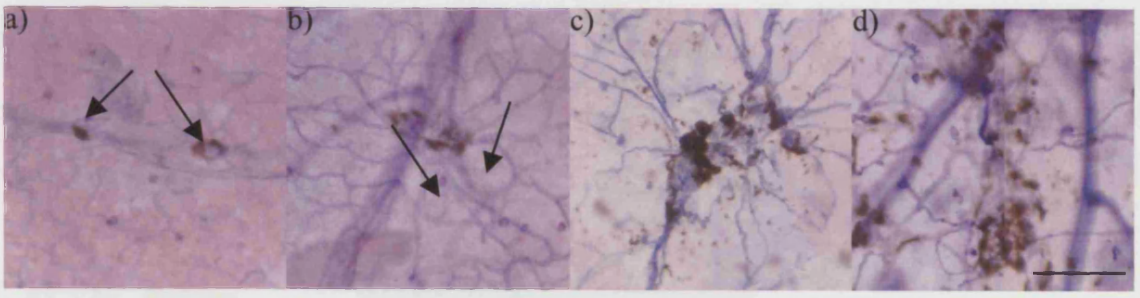

Figure 3.1.3 Development of vascular complexes. Illustrating the sequence of development of vascular complexes from initial single pigmented cells (arrows in a) through more involved multiple RPE involvement with the first signs of deformed vascular network in b), note the abnormal looping of the blood vessels around the vascular complex (arrows in b). Advanced vascular complexes such as c) and d) were rarely found until after 3 months and showed extensive damage to the normal vascular network in association with migrated RPE. Scale bar represents 100 μm.

The vascular complexes were formed by the attachment of pigmented cells (most likely RPE) to the venous vasculature where they appear to constrict and interfere with the blood flow and possibly with oxygen transport to the cells of the inner retina.

At three months of age dystrophic retinae such as **figure 3.1.4** displayed very small vascular complexes in the ventral retina. These vascular complexes were more advanced immediately ventral to the optic disc (50-100 μm across) as in insert **3.1.4a** (arrows) where the pigmented cells had affected the angles of the branching vessels: those vessels surrounded by RPE also appeared distended. The mid retinal vascular complexes were less developed as shown by insert **3.1.4b)** where individual pigmented cells had not caused significant vascular damage other than distending of the vessel walls in the immediate area. These vascular complexes were typically found on branches of a main ventral deep draining vein. This finding had been observed in previous studies(Wang et al., 2000) and may be an indication of early vascular complex formation. The optic fibre layer exhibited no visible damage with the RT 97 staining. The vascular complexes in each retina were counted manually using a research microscope (Leica DMR) at x25 magnification as described in section 2.6. Vascular complex counts were very low, typically around 20 / retina but consistent.

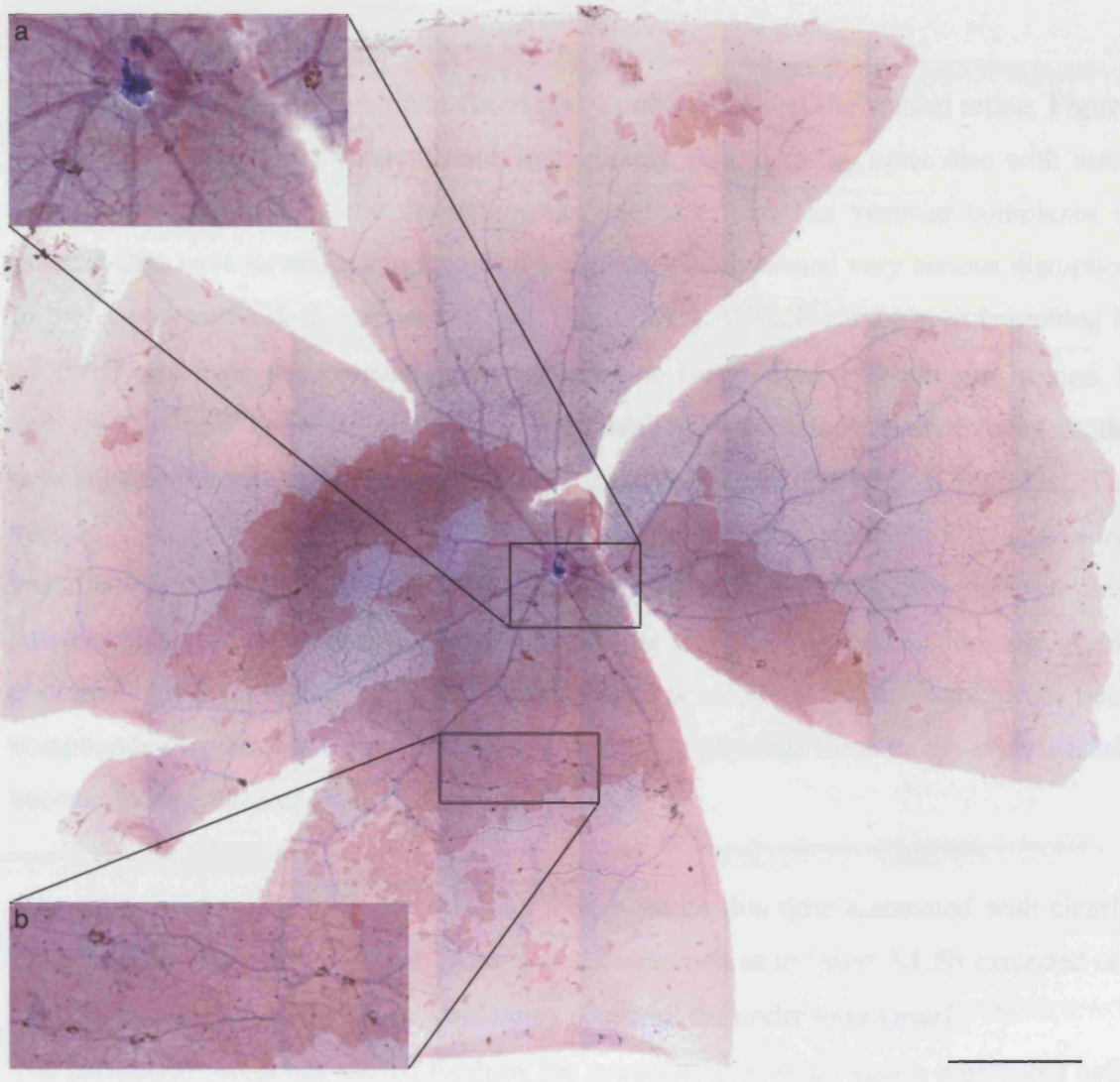

Figure 3.1.4 Dystrophic RCS retina at 3 months of age. The red discolouration was from the RPE layer not completely detaching during dissection and increasing background staining from the NADPH-d process. Insert a) shows new vascular complexes forming ventral to the optic disc with less developed complexes, characteristically smaller causing less vascular disruption shown further out in the mid-ventral retina in insert b). Scale bar represents 1000 μm

3.1.5 Four Months Baseline

By four months vascular complexes could be found throughout the ventral retina. **Figure 3.1.5a** shows an area of concentration immediately ventral to the optic disc with more vascular complexes scattered throughout the ventral retina. The vascular complexes in insert **3.1.5a** have developed to the point where they have caused very serious disruption to the venous network in comparison with **figure 3.1.4.** Vessels can be seen branching in all directions from the vascular complexes, which range from 100-300 μm in size. It appears that new connections have been formed between vascular complexes or the network has become so distorted physically that the original pattern has been lost. The vessels that have been affected are often distended and stain darkly suggesting vasodilatory stress. It is clear that many pigmented cells have migrated into the area: whether this is due to patchy photoreceptor loss or a more general thinning of the photoreceptor layer in the vicinity of blood vessels is unknown but the damage has been compounded by vessels being drawn into the area by physical force as the other vessels become more contorted.

The pigmented cells in the mid-ventral retina were by this time associated with clearly distorted vascular bundles, which in advanced cases such as in insert **3.1.5b** extended out along the vessel for 200-400 μm where they obscured the underlying vessel.

The peripheral retina has started to show the appearance of small single pigmented cells strung along the deep draining vessels as shown in insert **3.1.5c**. There were no visible abnormalities in the optic fibre layer. Pigment foci counts were more variable between animals at this time point averaging 40/ retina.

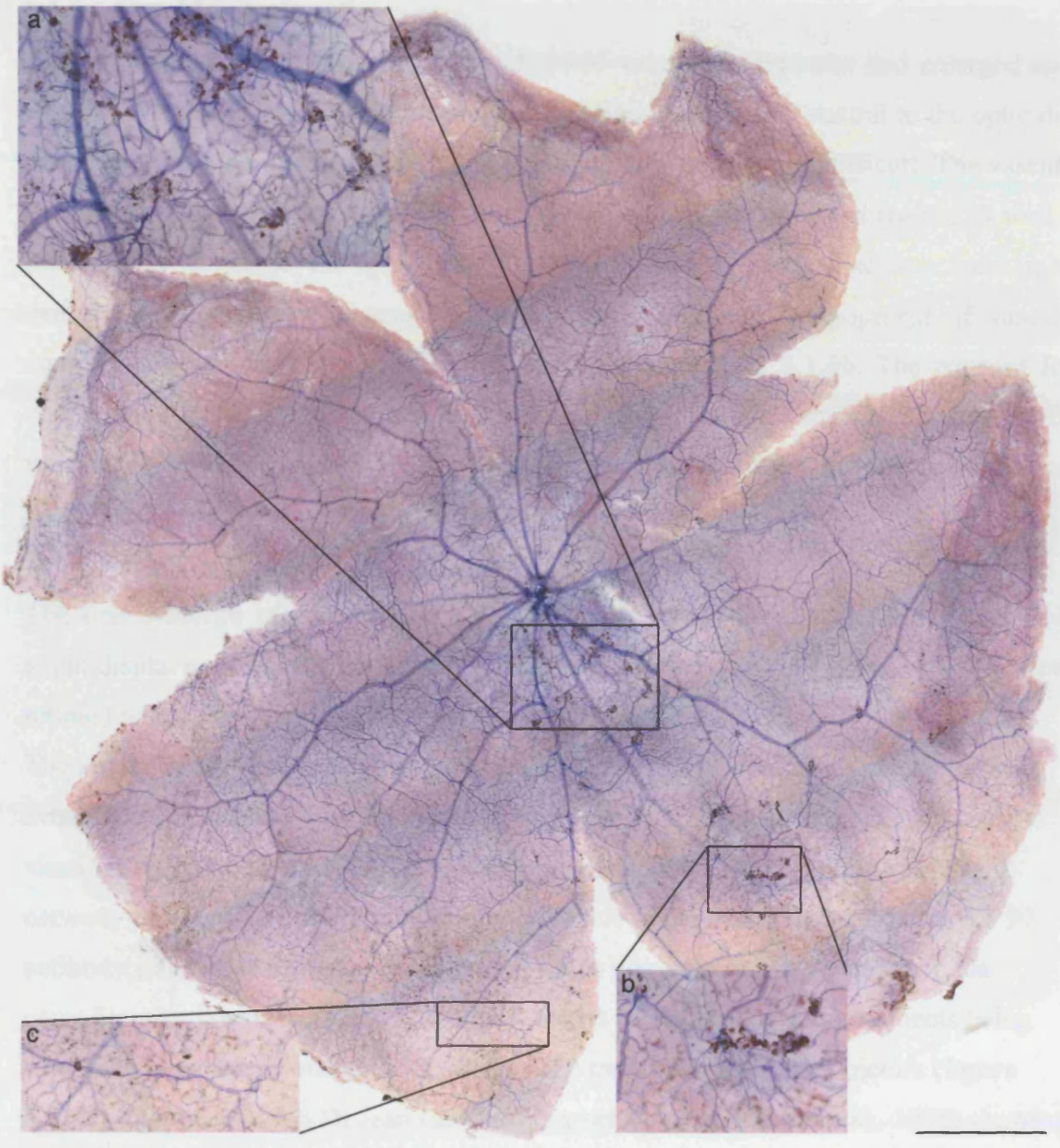

Figure 3.1.5 Dystrophic RCS retina at 4 months of age. The continued development of the vascular complexes was clearly evident with scattered vascular complexes found from the optic disc out to the periphery of the ventral retina. Insert a) illustrate how advanced the VCs have become ventral to the optic disc in contrast to insert **3.1.4a**. Insert b) shows how mid-ventral VCs have developed into much more extensive areas of damage. Insert C shows how more small single pigmented cell VCs spread further out from the ventral retina as time progresses. The Scale bar represents 1000 μm.

3.1.6 Five Months Baseline

At five months of age (**figure 3.1.6**) individual vascular complexes had enlarged such that they were starting to fuse together in the region immediately ventral to the optic disc as shown by **3.1.6a** making interpretation of manual quantification difficult. The vascular complexes had also started to spread into the temporal and nasal retinal regions as well as immediately dorsal to the optic disc. The area around the optic disc was much more densely populated than at previous time-points. Continued development of vascular complexes occurs near the periphery of the retina such as in **3.1.6b**. The pigment foci counts were higher at an average of 57 but at later time-points manual counting of the vascular complexes would become less accurate as a means of quantification and alternative methods would need to be employed.

The first evidence of damage to the optic fibre layer was in evidence at this time with slight displacement of the ganglion cell axon bundles being visible in two areas (different retinas) where large vascular complexes were also present.

The second order RGC events were caused by the deformation of the vascular network eventually constricting optic axons resulting in eventual death of the RGCs. In order to visualise this process the NADPH-d reaction was utilised to show up the vascular network within the retina and immunofluorescence of the neurofilaments using RT 97 antibody staining of the same flat-mounted retina was used to show damage to the neurofilament layer. **Figure 3.1.7a** clearly shows RT97 stained neurofilaments being constricted by a blood vessel (white arrow) at 5 months of age with a picture (**figure 3.1.7b)** reproduced from Dr Jean Lawrence's work (Villegas-Perez et al., 1998) showing a cross-sectional view of a nerve fibre stained with RT 97 visualised with DAB being pulled deep into the inner retina by a blood vessel (arrow).

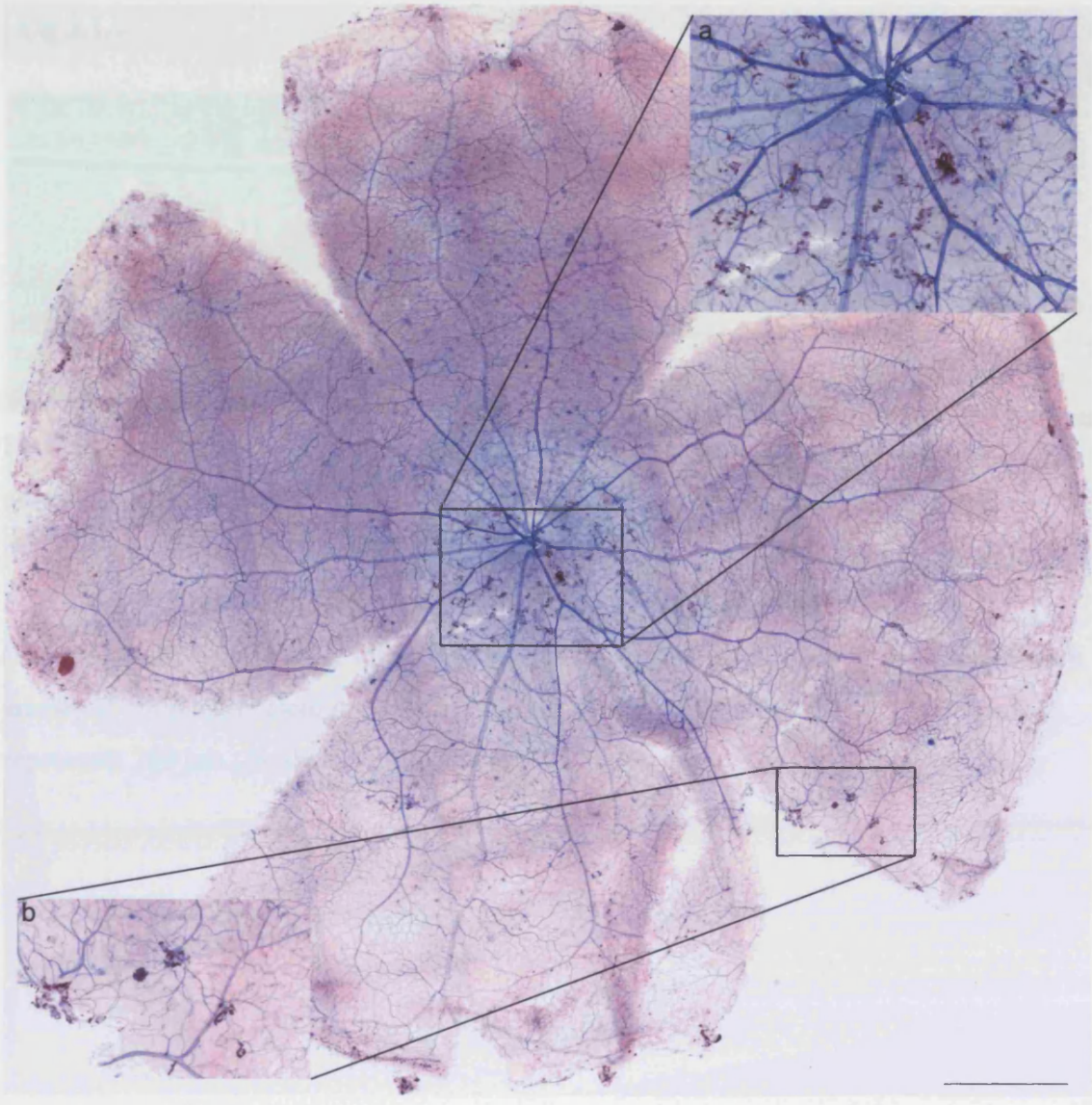

Figure 3.1.6 Dystrophic RCS retina at 5 months of age. The vascular complexes cover the area immediately ventral to the optic disc as shown in insert a) where the VCs have started to form a large area of interconnected VCs which will seriously disrupt blood flow in the ventral retina. Insert b) shows how the VCs have developed out in the peripheral retina. This time-point represents the limit of accurate manual counting of vascular complexes due to the merging of VCs especially near the optic disk. The light blue non-vascular staining pattern in the dorsal retina is due to pigment from the NADPH-d stain (blue formazan salt) adhering to residual vitreous.
Scale bar represents 1000 μm.

Fig 3.1.7

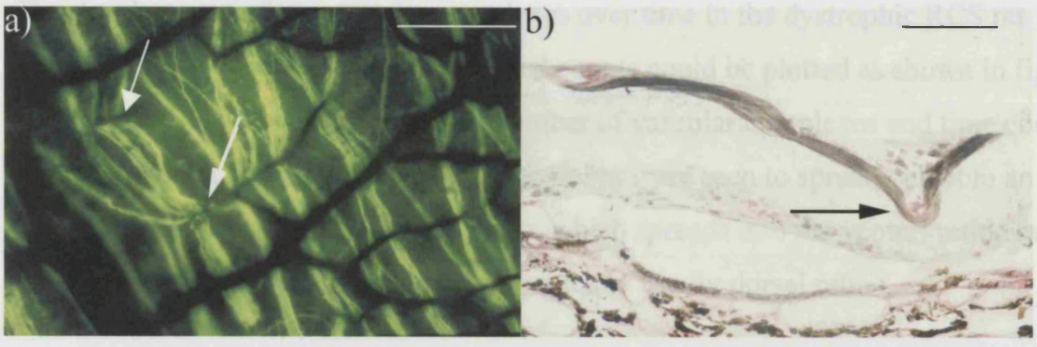

Figure 3.1.7 Damage to optic axons in the RGC layer caused by blood vessels constricting axons. White arrows in **3.1.7a** point to areas where optic axons on a flat-mounted five month old dystrophic RCS retina were displaced by blood vessels. Figure. **3.1.7b** shows a cross-sectional view where a blood vessel has pulled an optic axon (stained black) deep into the retina, there is a blood vessel in the centre of the loop (black arrow) of optic axon. Both pictures use the RT 97 ab at 1:1000 dilutions. Scale bar in A represents 200 μm , Scale bar in B represents 100 μm

3.1.7 Summary Of Baseline

The development of the vascular complexes over time in the dystrophic RCS rat progressed in a steady manner and manual counts could be plotted as shown in fig **3.1.8.** A very clear relationship between the number of vascular complexes and time could be seen in the chart below. The vascular complexes were seen to spread out from an epicentre slightly ventral to the optic disc, which spreads into the ventral retina before the leading edges spread into nasal and temporal and finally dorsal retina.

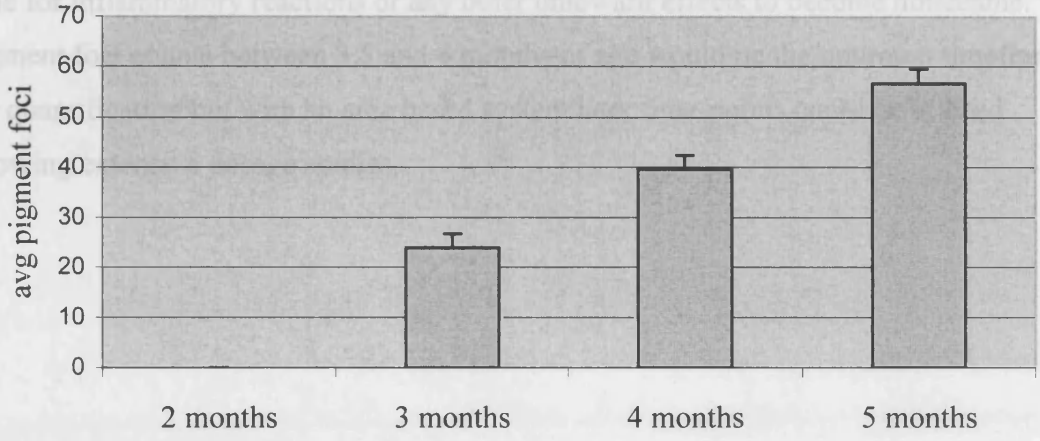

Figure 3.1.8 Baseline pigment foci count

Data Table

Time point	Average	Std Error	# retinas
2 months	0	0	8
3 months	23..92	2.72	8
4 months	39..67	2.82	15
5 months	56.63	2.88	8

Significance

P-values	2 months	3 months	4 months	5 months
2 months				
3 months			**0.00038**	**4.80E-07**
4 months		**0.00038**		**0.00047**
5 months		**4.80E-07**	**0.00047**	

The data above showed that VC development progressed in a manner that lent itself to quantification. Some retrospective retinas were added from later studies such as the

injection protocol exp (Figure 3.2.5) This experiment opened up the possibility of using the rate of development of vascular complexes as an assay to test out pharmaceutical agents and other interventional approaches for their effectiveness at preventing the appearance of second order vascular events.Each of the time points showed significant differences from over time From the data it was decided that 3 months would be the optimum time to commence pharmaceutical intervention, followed by flat-mounting the retinas at 4 months of age. This would allow sufficient time scale for the effects of the compound to be seen on the development of the vascular complexes and also sufficient time for inflammatory reactions or any other untoward effects to become noticeable. For pigment foci counts between 3.5 and 4 months of age would be the optimum timeframe for quantification but with an area based system later time-points could be utilised allowing extensive dosage studies.

Interestingly when the data was separated out for left and right eyes as shown in fig **3.1.9** below: a clear bias was found for left eyes having slightly less vascular complexes but the differences were not significant between eyes of the same timepoint except for at 3 months where the low numbers made differences more significant.

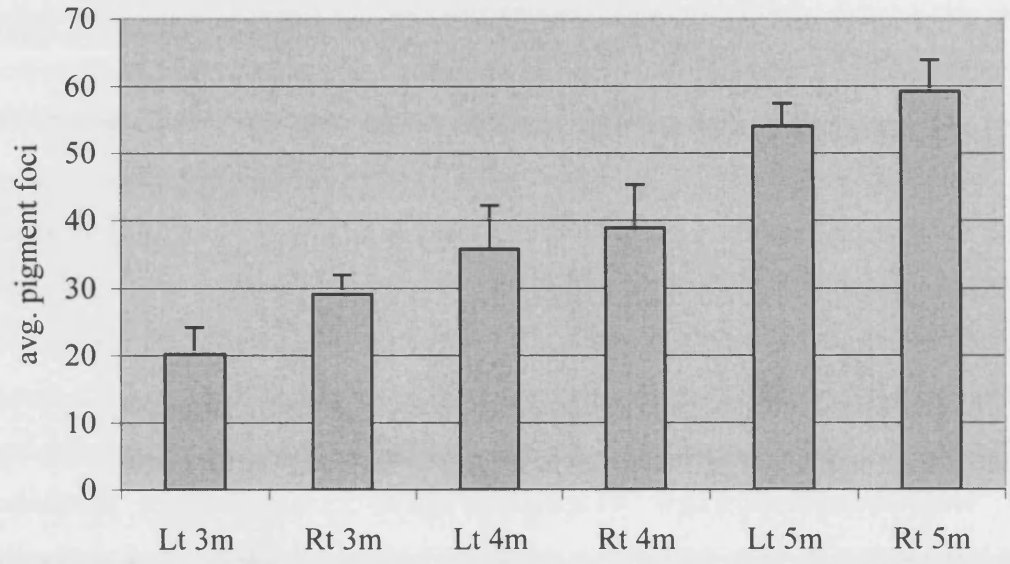

Figure 3.1.9 Baseline right vs. left eye counts

Data table

Age	Avg	Std Error	# retinas
Lt 3m	20.1666667	4.04717551	4
Rt 3m	29.0833333	2.89755644	4
Lt 4m	35.8333333	6.4125167	4
Rt 4m	38.9166667	6.40800281	4
Lt 5m	54	3.46410162	4
Rt 5m	59.25	4.69707356	4

Significance

P-values	Lt 3m	Rt 3m	Lt 4m	Rt 4m	Lt 5m	Rt 5m
Lt 3m		**0.062**	0.047	**0.028**	**0.00036**	**0.00037**
Rt 3m	**0.062**		0.195	0.117	**0.0007**	**0.0014**
Lt 4m	0.047	0.195		0.37	**0.023**	**0.013**
Rt 4m	**0.028**	0.117	0.37		**0.042**	**0.021**
Lt 5m	**0.00036**	**0.0007**	**0.023**	**0.042**		0.2
Rt 5m	**0.00037**	**0.0014**	**0.013**	**0.021**	0.2	

From this data it was decided that all further studies would use only left eyes to reduce data noise and possibly reduce the merging of complexes at the later time points.
As the damage to the RGC layer did not start until five months or later RT 97 staining was discontinued.

3.1.8 Image Analysis

In an attempt to simplify the process of counting the pigment foci and associated vascular complexes an image capture and analysis system was employed.
This originally consisted of PC-image (Foster Finlay Associates) in conjunction with a frame grabber (Data Translation DT3155) to capture images from a CCD camera (Hamamatsu 5098) attached to a research microscope (Leica DMR) using a 10x objective in conjunction with a 2.5x photomultiplier. The microscope used a stepping stage (Prior H28) to move the sample after each image was captured. Metamorph (universal imaging) was required to montage these images into an entire retina; this required a grid of 15 images by 13 giving a total of 295 images forming a single composite image of the entire retina. We found that that using the 10x objective with the 2.5x photomultiplier gave the best compromise of resolution adequate to view the vasculature of the retina while keeping the number of frames required to capture an entire flat-mounted retina within the capabilities of the computer technology. The computation was handled by a PC workstation (AST MS166). PC-image controlled the stage from which distance calibrations were obtained; therefore Metamorph could not measure a composite image. This system was originally setup to count fluorescently labelled retinal ganglion cells but was unsatisfactory for quantification of vascular complexes.

While this system could give very good high-resolution greyscale images it could not make any meaningful measurements (such as area) and it could not distinguish between pigment foci and debris as the resulting picture could only be resolved in 8 bit greyscale (256 levels of grey) that was insufficient for differentiating pigmented cells from debris. Even with the choroidal debris being in a different plane of focus from the RPE cells the final two-dimensional image was still confusing. It was found after comparisons that full manual counting gave a more accurate and reproducible result for the assay so image analysis was put on hold until a better system could be found.

Figure 3.1.10 an 8-bit image formed by the second generation image analysis system of a four-month-old RCS rat. The damage to the dorsal retina is from a two week old intravitreal injection; this approach was later modified to limit damage to the retina. VCs can be clearly seen in the nasal and ventral portions of the retina.

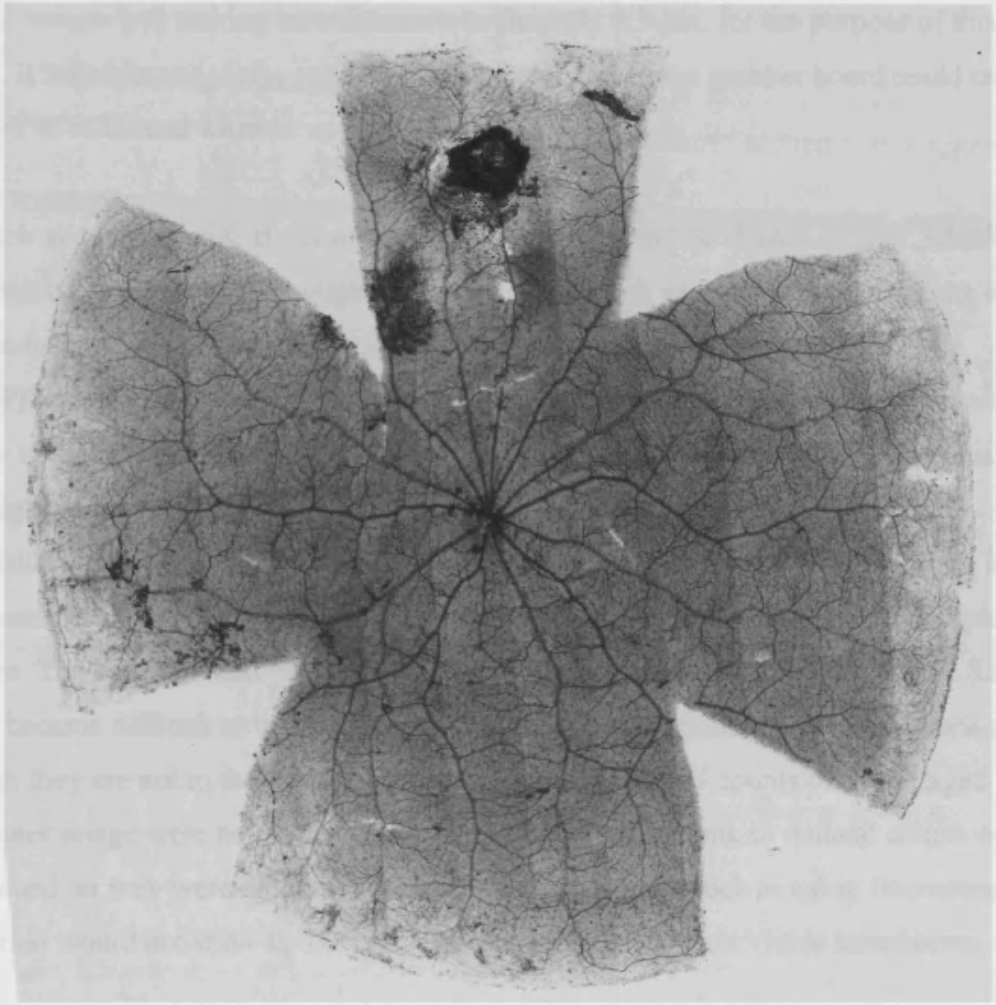

Due to the limitations of the image analysis setup a second generation system was commissioned; built around Media Cybernetics Image Pro Plus, a program that could control the stage, capture and analyse the images in one continuous process without resorting to other software. Improvements to the images captured were achieved by capturing less of the total image possible with the camera to reduce distortion caused by the curvature of the optics. Even with cropping, this resulted in a decrease in the number of images required to capture a complete retina but much greater detail. The more sophisticated computer equipment could cope with the increased memory requirements and produce images such as **figure 3.1.10**. Image Pro Plus was used to capture complete flat-mounted retinas and the feasibility of automating pigment foci counting tested.

3.1.9 Pigment Foci Counts Using Image Pro Plus 4.X

Image Pro Plus (Media Cybernetics) was selected as an all in one solution as it had a very comprehensive macro language and excellent software drivers for image capture and stepping stage control. While the system was very able at assembling high-resolution digital images and making measurements accurate to 0.1 μm, for the purpose of this assay, it failed in one single criterion. The camera and frame grabber board could only capture in black and white.

In black and white mode the computer could only discern 256 shades of grey, which unfortunately did not give enough contrast to distinguish vascular complexes from debris, inflammatory cells and amacrine cells of which a subset were also stained by the NADPH-d staining protocol. The retina was not of uniform thickness and that resulted in a very noticeable gradient as the centre of the retina was thicker than the edges causing the edges to be much lighter than the optic disc area. These factors made accurate thresholding of the composite image impossible under with this system. Therefore it was not possible to count vascular complexes automatically with a black and white capture system. The system could be used to manually tag complexes as shown in **figure 3.1.11** but it became difficult to distinguish complexes in the presence of choroidal debris even though they are not in the same focal plane. Manually tagged counts of a montaged computer image were no more accurate than full manual counts so manual counts were continued, as they were quicker. Different staining regimes such as using fluorescent detection would not show up the pigment deposits and were not viable alternatives.

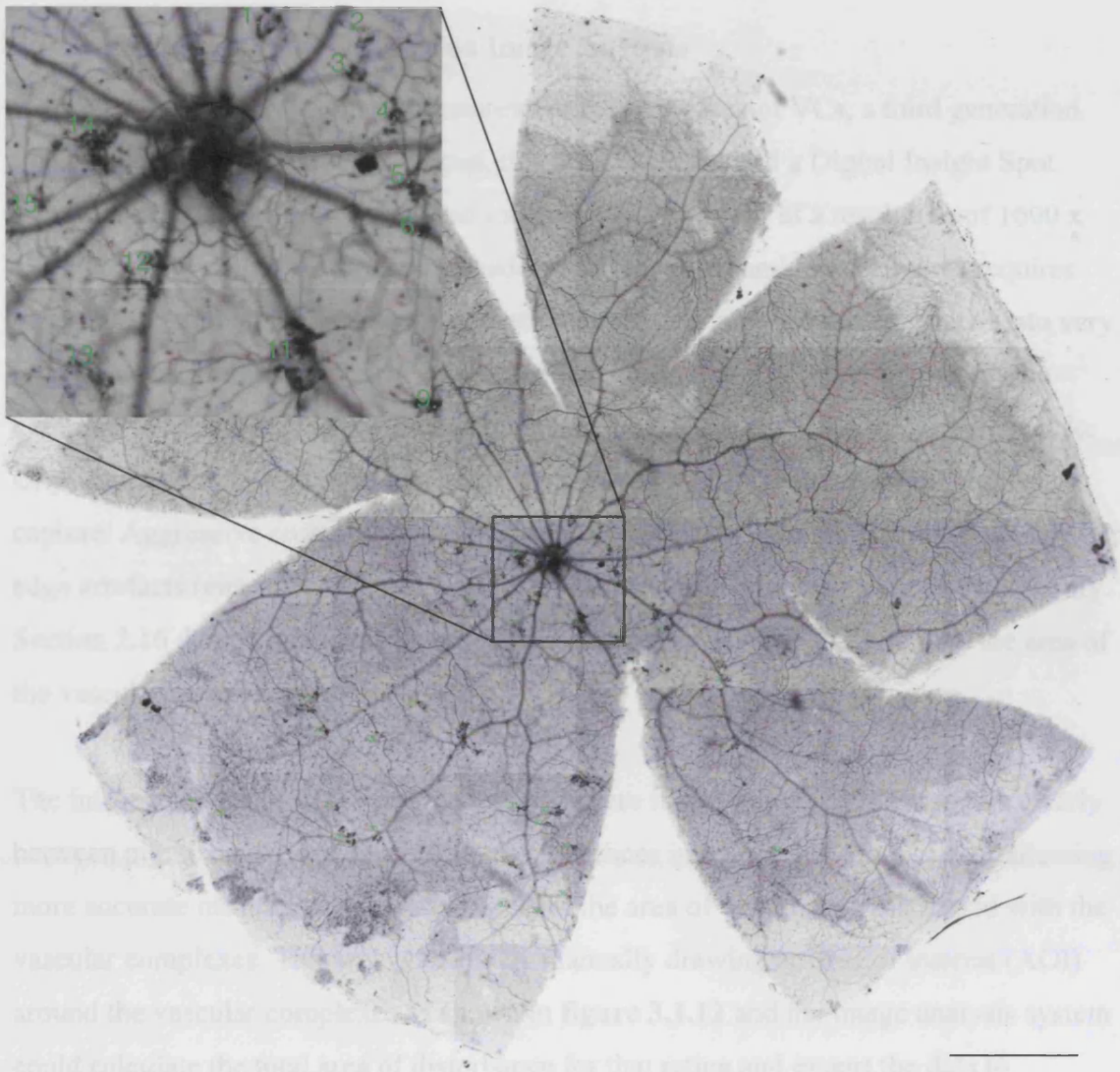

Figure 3.1.11 Dystrophic RCS retina at 4 months showing manually tagged vascular complexes. Clearly this method was limited in by its inability to resolve VCs that were very close together especially where large extended VCs were present. Even small VCs in close proximity such as numbers 2 & 3 (insert) could arguably be considered a single VC and conversely large VCs such as number 12 (insert) could be split into two VCs. Scale bar represents 1000 μm

3.1.10 Third and Final Generation Image Analysis

In order to provide a system of measurement based on area of VCs, a third generation image analysis system was developed, this time based around a Digital Insight Spot colour digital camera which captured images in 12 bit colour at a resolution of 1600 x 1200 pixels. A colour picture being made up of red, green and blue elements requires three times as much information as a black and white image and this translated into very large amounts of memory on a computer which necessitated another upgrade of the computer workstation to accommodate the new images. Starwest computers (Salt Lake City) supplied a computer with enough memory (2Gb of Ram) to allow full colour capture. Aggressive cropping of the images (100 pixels on each side) prior to capture kept edge artefacts (either from the camera or the optics) from compromising picture quality. Section 2.16 details the process used to generate colour images and calculate the area of the vascular complexes.

The image analysis system captured images where it was possible to distinguish clearly between pigment foci and debris (due to differences in colour and focal plane), allowing a more accurate measure of the assay based on the area of disturbance associated with the vascular complexes. This was possible by manually drawing an area of interest (AOI) around the vascular complexes as shown in **figure 3.1.12** and the image analysis system could calculate the total area of disturbance for that retina and export the data to Microsoft Excel. In the same way the area of the entire retina could be calculated. Total automation proved impossible as the system could not determine which vascular plexus to focus on, nor could it discern the extent of the vascular disturbance around pigment foci. This system of quantification was termed the VC assay.

All previous data were reanalysed using this system: all results from this point onwards refer to the VC assay rather then pigment foci counts. The archived NADPH-d stained retina from previous studies were still suitable for re-analysis using this more informative measure of vascular damage

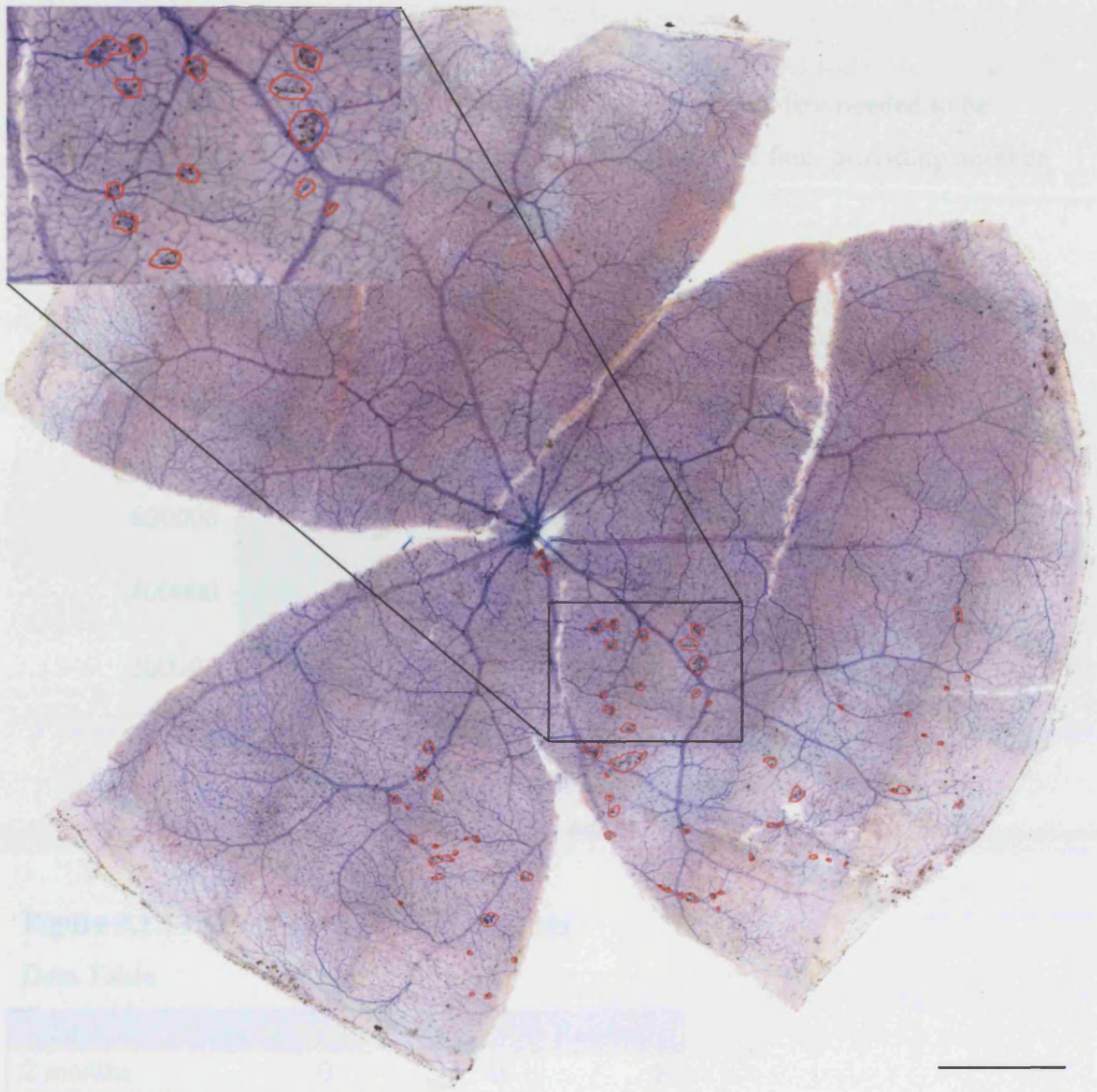

Figure 3.1.12 Dystrophic RCS retina at 4 months showing the VC assay method of quantification. This method was not limited by problems of resolution of VCs and was capable of capturing much more information in that by measuring area under VCs, accurate determination of VC size was possible. Scale bar represents 1000 µm

3.1.11 Baseline "VC Assay".

The original flat-mounts were still viable for analysis, while a few needed to be remounted due to PBS/glycerol leakage they were otherwise fine, providing another advantage of using the NADPH-d staining protocol.

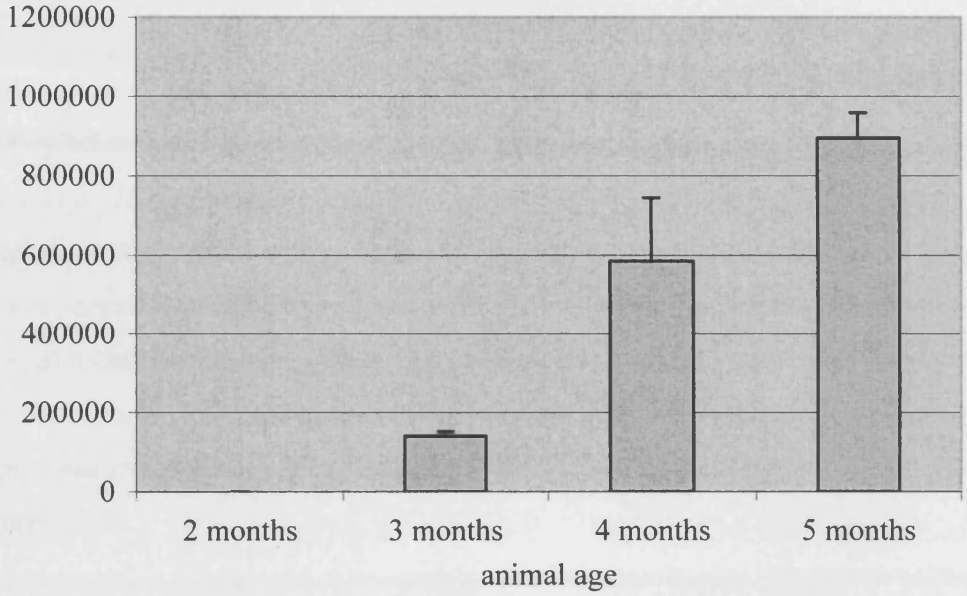

Figure 3.1.13 VC assay baseline AOI counts

Data Table

Time point	Area	Std. Error	# Retinas
2 months	0	0	8
3 months	140136.072	11363.4967	8
4 months	584990.334	160522.00	11
5 months	895430.937	63682.458	8

Significance

P-values	2 months	3 months	4 months	5 months
2 months				
3 months			**0.0038**	**0.0000038**
4 months		**0.0038**		**0.015**
5 months		**0.0000038**	**0.015**	

The figures above refer to area measured in μm^2 with a typical 4-month-old RCS rat retina measuring a total area of around $4.5x10^7$ μm^2.

Figure 3.1.13 shows that there was slightly more variation at 4 months than with pigment foci counts but the data was still solid enough to be used as the basis of an assay.

3.1.12 Discussion

The data obtained from this early study did indeed prove to be quantifiable and as the methods of quantification evolved it became clear that the data provided a suitable baseline for further studies. Using these methods it would be possible to investigate how different pharmaceutical agents or procedures would affect this progressive development of vascular complexes associated with the RCS dystrophic pathology. The use of NADPH-d staining in conjunction with RT 97 immunostaining allowed visualisation of the developing interaction between the vasculature and RPE cells and the further changes to optic axons. This interaction could only be seen using pigmented RCS rat and would have been missed in albino strains used in some previous studies. The range of vascular complexes seen in the later time-points made the VC assay much more informative as it gave a total measure of the progression of the vascular damage rather than the more abstract foci counts. The time course of the baseline data was dictated by the limitations of the pigment foci count as future advances in computer technology and software could not be predicted.

Had the technology been available earlier a more extensive timeline would have been possible using the VC assay, as this method was not affected by the merging of vascular complexes. The standard baseline experiment as it was still stretched over seven months (five month time course followed by analysis) making it a considerable investment in time, but nonetheless essential to determine the progression of the vascular complexes in the RCS pathology. Over the course of this study the image analysis system has evolved from being a basic tool to count cells into a powerful full colour-based system capable of taking multiple measurements throughout an entire flat-mounted rat retina. This evolution occurred over two years, fortunately allowing reassessment of archived flat-mount material using the VC assay procedure.

The use of the VC assay with the dystrophic RCS rat pathology presents itself as a unique tool in which it may be possible to assess drugs developed to help manage diseases where vascular proliferation causes problems within the retina. On a more basic level the VC assay could be used to quantify vascular effects of pharmaceutical agents *in vivo*. The image analysis system itself has many more capabilities that are not touched upon in this study, with a full suite of morphological filters and measuring tools many further

calculations such as vessel diameters during retinal degeneration could be measured as well as cell counts within the retina for cellular infiltrate or amacrine cells (NAPDH-d stains a subset of Amacrine cells (Rexer et al., 1998).

The retinal ganglion cell layer was relatively untouched during this timescale, with a few samples showing minor disturbance as early as four months but even at five months there were only several small areas of deformed neurofilaments (as seen in **figure 3.1.7**). Consequently the RT 97 staining was discontinued from further studies: had the progress with the image analysis occurred earlier an extended time-line could have shown further effects of the dystrophic RCS pathology on the optic axons by using the area based VC assay quantification.

3.2 Modification Of Rate Of Development Of Vascular Complexes

3.2.1 Aims

Chapter **3.1** showed that the development of vascular complexes in the dystrophic RCS rat proceeded in a linear fashion over a several month time window in manner that was amenable to quantification. A further aim of this study was to modify or eventually control formation of vascular complexes thereby improving the environment for treatments to correct the primary defect, the loss of photoreceptors. The data produced in the first chapter were robust and reproducible enough to provide the basis of the VC assay for comparison in testing pharmaceutical agents. It was hoped that the modification of the development of vascular complexes using specific probes might have two responses;

1. They could provide a potential treatment.
2. By using a probe of known function they could provide insight into the mechanisms that lead to formation of vascular complexes

3.2.2 Experiments

Based on the results of the previous chapter, the optimal timeline for pharmaceutical modification of the rate of development of vascular complexes in the RCS rat would be to administer treatments at 3 months of age and flat-mount the retina at 4 months. This allowed the RCS pathology to have advanced sufficiently that vascular complexes were present but had not developed to the stage where the original counting regimen would be unable to measure the result (the VC assay developed later did not have this limitation). Application too early may result in the compound being cleared from the system before there could be any visible effect. Experiments consisting of 8 animals were set up with three animals designated shams and five animal test subjects. The left eyes were injected with 1 μg of pharmaceutical agent in 2 μl of PBS, as described in methods. This protocol was based on previous studies (LaVail et al., 1992; LaVail et al., 1998) and was considered a reasonable starting point for this work. The right eye was not treated in any way to serve as an in animal control. Shams were injected with 2 μl of PBS in the left eye. Two pharmaceutical agents were tested, PEDF, a powerful natural anti-angiogenic compound produced in the RPE and ciliary epithelium. This was obtained from Pfizer but originally sourced from Dr Joyce Tombrand-Tink along with a rabbit polyclonal antibody to PEDF (Ab. 2520). The second candidate, echistatin (Bachem, San Carlos, Ca), an

integrin blocking peptide extracted from the venom of the saw-scaled viper (*Echis carinatus*), which had been shown to retard RPE migration *in vitro* (Yang et al., 1996). It was hoped that by using these two reagents with different targets, it might be possible to dissect out the relative roles of migration and new vessel formation in the development of vascular complexes in the outer retina.

3.2.3 Initial PEDF preparation

The samples we received were stored frozen in vials of 10 μg/ml of 500 μl PBS. For this to be used for intra-vitreal injections as carried out by La Vail's laboratory, a way had to be found to reduce the volume of the solution to give 1 μg/ 2μl. Secondly as no certificate of purity came with the samples, a way to verify the purity of the protein before *in vivo* use was attempted. Initially for the first PEDF experiment, freeze drying overnight was tried to reduce the volume of the PEDF followed by reconstitution in distilled water. This yielded the correct concentration of PEDF but with an excess of salts. It was hoped that the excess of salts would be immediately diluted on administering the PEDF into the vitreous and not cause a subsequent problem. Another technique that could have been used was micro-dialysis.

3.2.4 PEDF Pilot Experiment

The animals tested were healthy post-operatively and showed no signs of discomfort from the operations on their left eye or from the PEDF administered; their behaviour appeared normal throughout the experiment. Upon dissection of the eyes, it was found that some of the retinae were quite fragile and one sham retina was damaged beyond repair when flat-mounting.

The fragility of the retinae was most evident in the dorsal retina due to the injection protocol causing local vascular disruption and influx of inflammatory cells; very likely a basic wound healing response to the injection protocol. The untreated retinae were identical in appearance to those from the baseline experiments (**figure 3.2.1**) in that they exhibited the expected pattern of vascular complexes, moderately advanced in the epicentre just ventral to the optic disc (see insert) with smaller less advanced complexes sometimes spreading into the nasal, temporal as well as the ventral peripheral retina. The PEDF treated retinae (**figure 3.2.2**) exhibited slightly fewer vascular complexes and these were less well developed than the comparable sham (**figure 3.2.3**) operated. The injection site was clearly visible in the dorsal retina with inflammatory cells present and some local

vascular damage resembling VCs. These VCs were discounted from the assay, as they were likely to have been caused by the wound to the retina resulting from the injection and not the naturally occurring RCS pathology. It should be noted that the PEDF treated retinae were compared with the sham treatment as they had undergone identical operative procedures and the untreated retinae were used as an in-animal control to determine if deviation from the baseline occurred. The sham retina (**figure 3.2.3**) also exhibited damage around the injection site with associated pigment, most of which was on the surface of the retina not in the same focal plane as the venous vascular plexus. There was some cellular infiltrate in the area of the injection site showing evidence of a wound healing-type cascade in progress. The insert in **figure 3.2.2** shows typical VC development in mid-ventral retina.

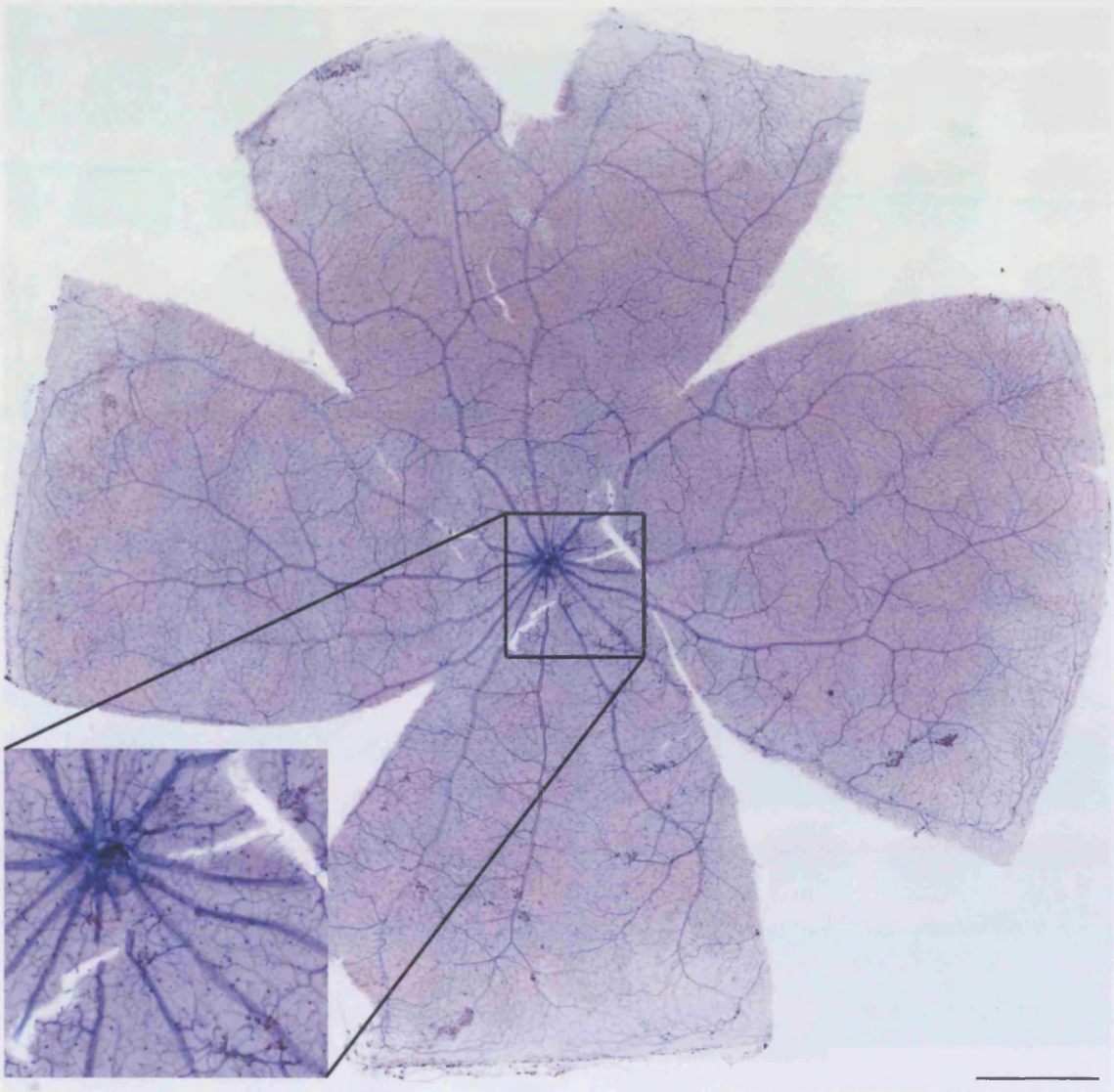

Figure 3.2.1 Untreated 4 month old dystrophic RCS rat exhibiting baseline vascular complex development concentrated ventral to optic disc as shown in the insert a). Further vascular complexes can be seen on branch vessel leading into the three ventral-most deep draining veins. Scale bar represents 1000 μm

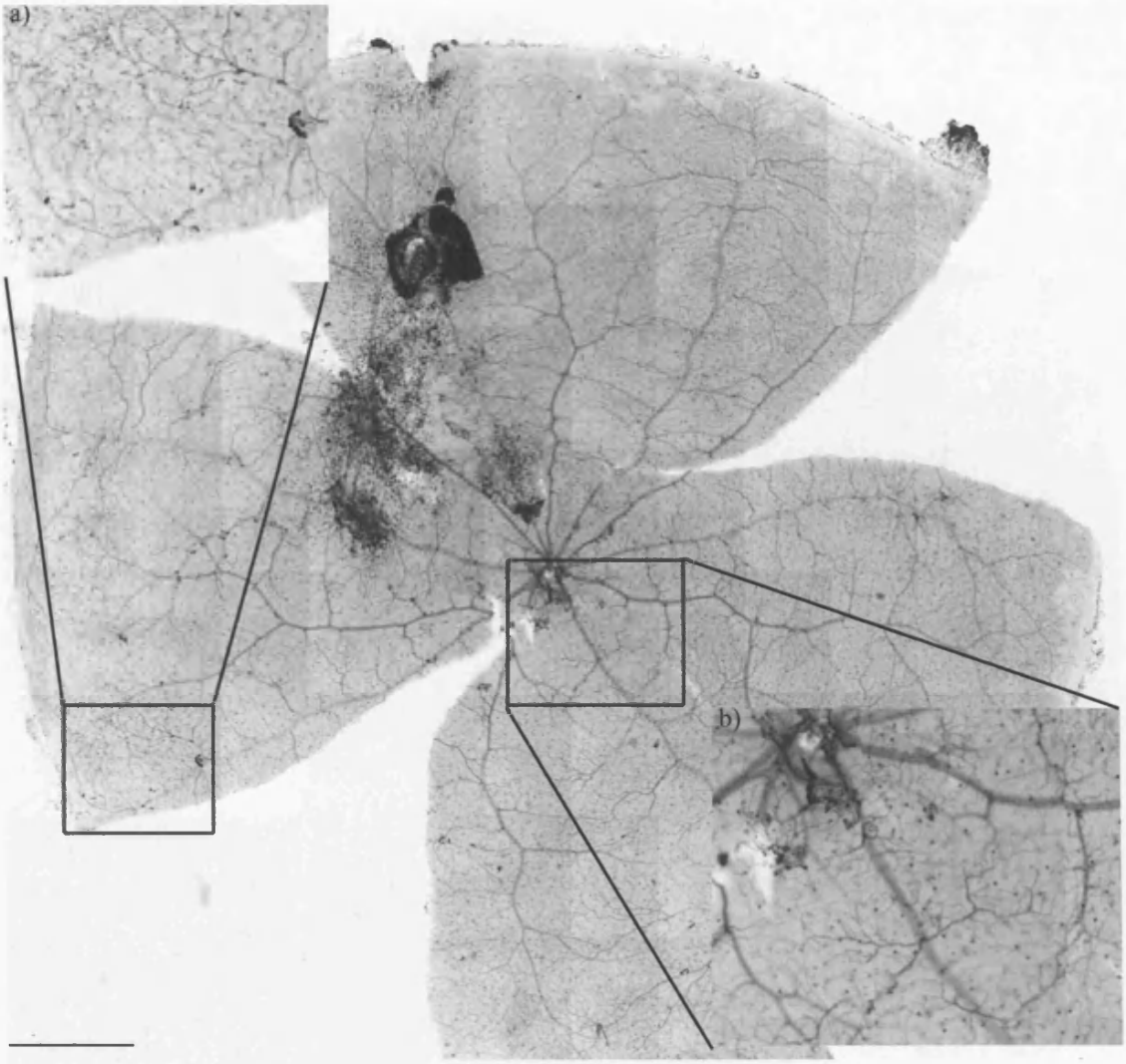

Figure 3.2.2 PEDF treated dystrophic RCS at 4 months from PEDF pilot experiment after treatment at 3 & 3.5 months. Injection site with associated damage is clearly seen in the dorsal retina. Insert a shows less developed peripheral VCs. Insert b shows the area ventral to the optic disc, normally this would be the epicentre of VC development but with PEDF treatment it is largely devoid of VCs. Image processed in black and white. Scale bar represents 1000 μm

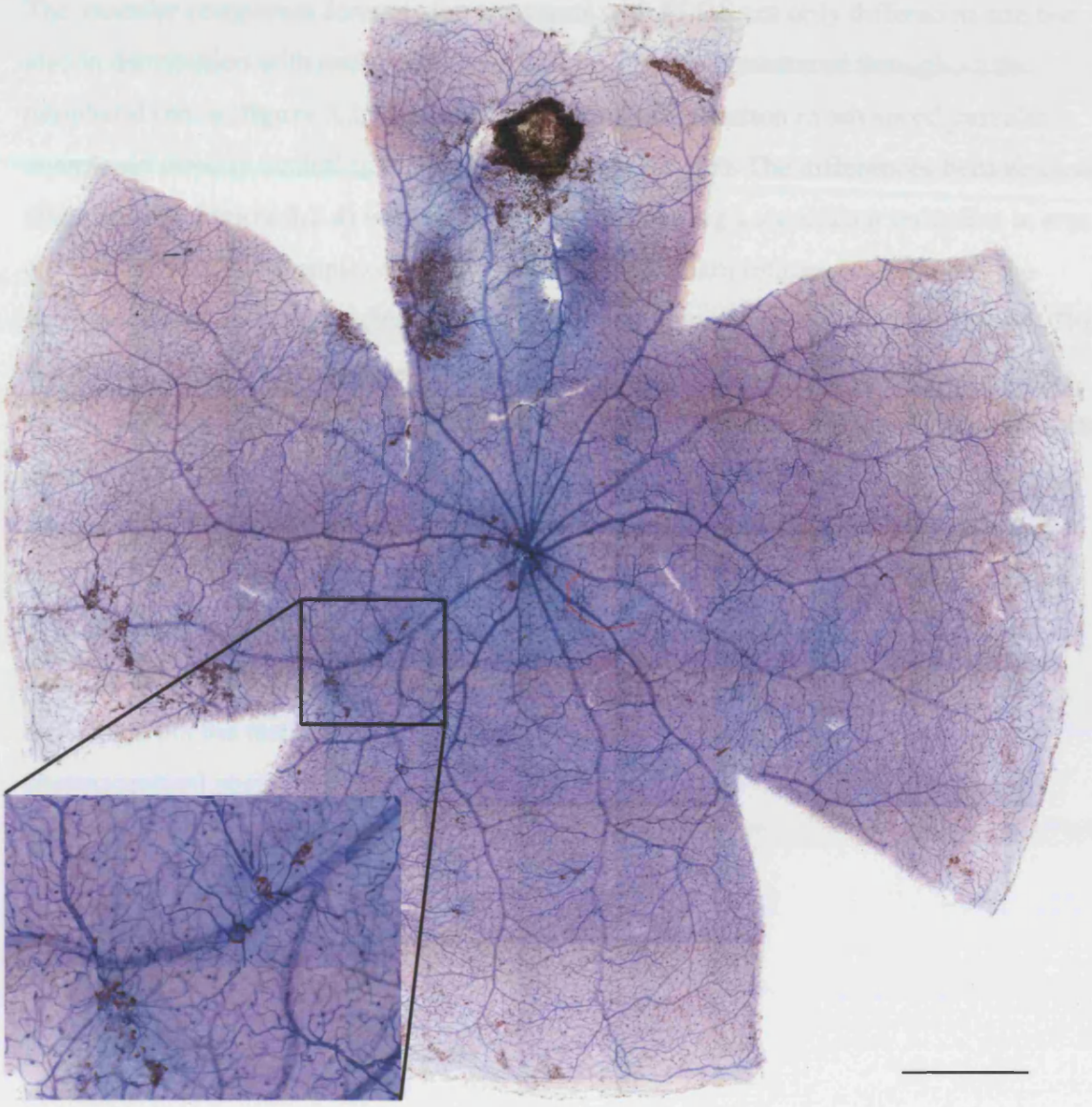

Figure 3.2.3 Sham 4 month old dystrophic RCS retina from PEDF pilot experiment showing extended VCs in mid-peripheral retina. The area around the optic disc also has some VCs. Injection site is clearly visible in dorsal retina. Scale bar represents 1000 μm.

The vascular complexes formed after treatment with PEDF not only differed in size but also in distribution with many small single pigmented cells scattered throughout the peripheral retina (**figure 3.2.2a** arrows) and a marked reduction in advanced vascular complexes directly ventral to the optic disc (**figure 3.2.2b**). The differences became clear after analysis (**figure 3.2.4**) with PEDF treatment showing a significant reduction in area covered by vascular complexes as compared with the sham retinae. Interestingly the sham-operated retinae exhibited more vascular complexes than the untreated retinae. This was an unexpected finding possibly attributable to secondary events associated with the wound inflicted on the retina by the delivery method. Previous work has shown that such injuries can cause release of a variety of growth factors (Cordeiro et al., 1999) and may also mobilise RPE cells. It should be noted that in the baseline data the left eyes (used here for PEDF & sham treatment) exhibited slightly fewer vascular complexes than the right eyes (untreated). The untreated retinae were included only for comparison with baseline data as a housekeeping control. The shams served as experimental controls differing from the test retinae only in that they lacked the application of the pharmaceutical agent.

Figure 3.2.4 shows the data after analysis using VC assay; PEDF clearly reduced the incidence of VCs compared to the sham controls. The untreated animals exhibited unusually low incidence of VCs compared to the four-month baseline data but not significantly lower than the PEDF treated animals. The pilot experiment showed that PEDF could affect VCs at a concentration of 1 μg/ 2μl PBS.

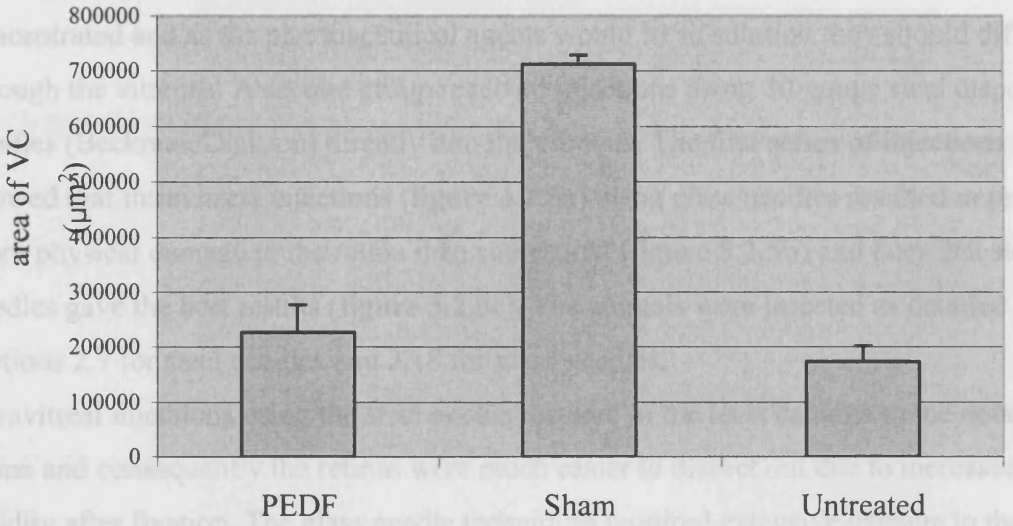

Figure 3.2.4 PEDF pilot experiment

Data table

Treatment	Average	Std Error	# Retinas
PEDF	227108.564	50150.0133	5
Sham	712392.479	16151.9531	2
Untreated	173992.903	28133.6517	7
avg entire retina	47918789.2		

Significance

P-values	PEDF	Sham	Untreated
PEDF		**0.00013**	0.172
Sham	**0.00013**		**0.0000015**
Untreated	0.172	**0.0000015**	

3.2.5 Delivery Of Pharmaceutical Agents

The fragility of the retinae in the PEDF pilot experiment was a result of too aggressive a delivery protocol. To improve on this a litter of RCS animals were allowed to grow to three months of age and the effects on the retina of intravitreal and sub-retinal delivery were compared.

Sub-retinal injections were given to half the animals to determine how they differed from intra-vitreal injection after flat-mounting and to explore the possibility of an alternative delivery method. The injections were placed dorsally just behind the ciliary body taking care to avoid any blood vessels or damage to the ciliary body, since this would result in release of growth factors, which might contaminate baseline conditions further. The dorsal position was chosen to avoid damaging the ventral retina where the VCs were concentrated and as the pharmaceutical agents would be in solution they should diffuse through the vitreous. A second group received injections using 30-gauge steel disposable needles (Beckman Dickson) directly into the vitreous. The first series of injections showed that intravitreal injections (**figure 3.2.5a**) using glass needles resulted in much more physical damage to the retina than sub-retinal (**figure 3.2.5b**) and later that steel needles gave the best results (**figure 3.2.5c**). The animals were injected as detailed in the sections 2.7 for steel needles and 2.18 for glass needles.

Intravitreal injections using the steel needle resulted in the least damage to the dorsal retina and consequently the retinas were much easier to dissect out due to increased rigidity after fixation. The glass needle techniques required extensive damage to the schlera using a micro-blade or steel needle to expose bruch's membrane and the RPE before insertion due to the fragility of the glass needle. An extensive wound healing response resulted in recruitment of inflammatory cells and damage to the retina with adhesions complicating dissection. Eventually it was possible to improve the injection protocol to cause minimal disturbance to the retina. This was important, as it would have been difficult to proceed with the VC assay if the delivery process caused excessive damage to the dorsal retina as the effects of this on the development of VCs could have complicated the normal RCS pathology. The release of growth factors during wound healing has been extensively studied in the eye (Cordeiro et al., 1999; Stitt et al., 2004) and in other tissues with large amounts of data suggesting that growth factor cascades are present in all wounding events (Ferguson and O'Kane, 2004). Nevertheless, such effects should be shown up by the shams, which would undergo identical procedures.

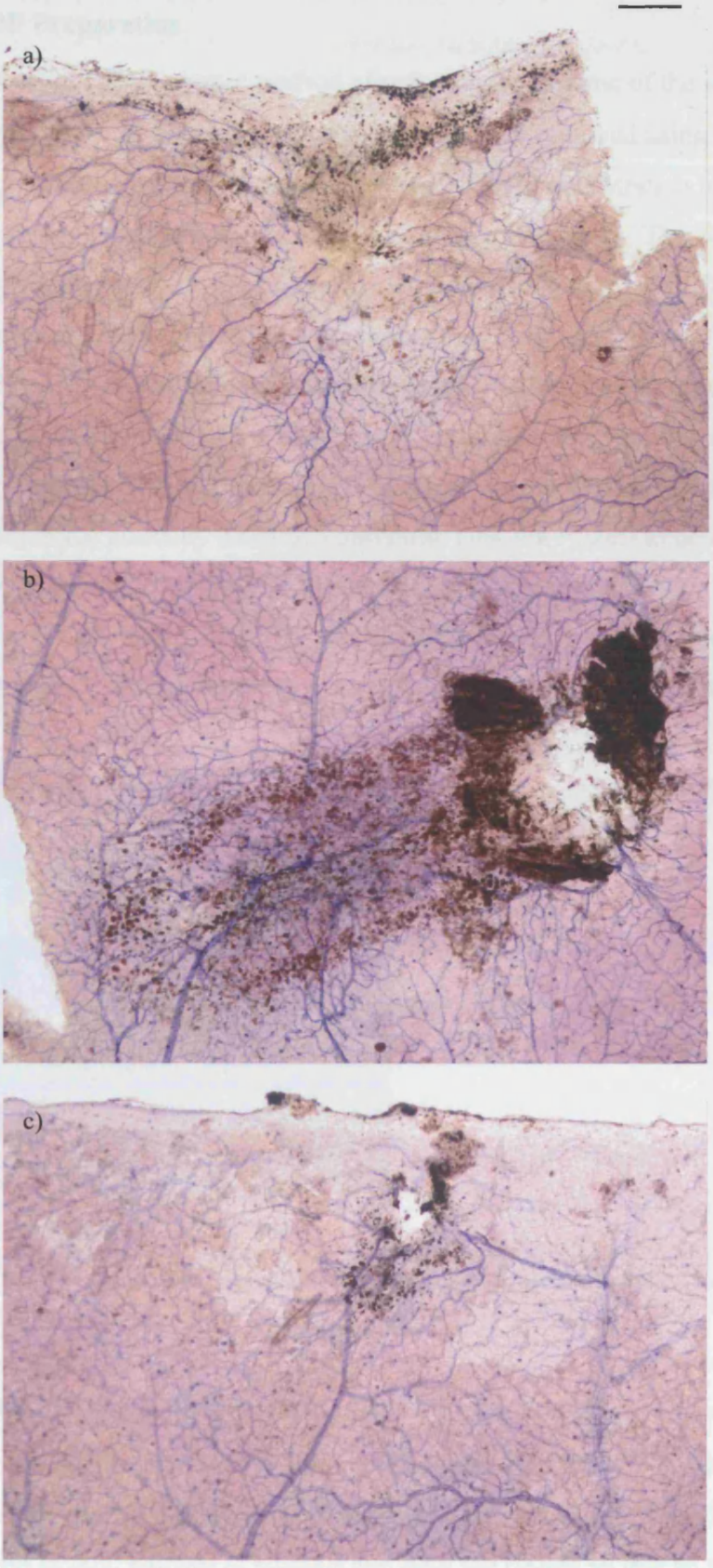

Figure 3.2.5 Modified injection protocols using PBS, a) subretinal injection using glass electrode type needle, b) trans-retinal injection using glass pipette, c) trans-retinal injection using 30 gauge steel needle. Scale bar represents 50 μm.

3.2.6 Final PEDF Preparation

For further studies using PEDF a better method of reducing the volume of the stock solution (10 μg in 500 μl) was found. The phosphate salts were removed using PD-10 desalting columns (Amersham Biosciences; UK), which utilised gel filtration to reduce the volume by allowing salts to pass through while retaining the protein. This was followed by a DC Protein Assay (Biorad Laboratories; USA) to determine PEDF yield after filtration. A typical volume reduction would result in a yield of around 80% as plotted against a series of concentrations of stock protein (BSA) in the DC Protein Assay. Protein yield could be as low as 36% if centrifugation continued too long. Secondly as we received the PEDF samples with no purity certification, a western blot was performed using the rabbit polyclonal antibody 2520 (J. Tombrand-Tink via Pfizer) to determine PEDF stock purity. The sample had no significant contaminants as can be seen in the western blot in **figure 3.2.6** where the PEDF was run against a set of known molecular weight standard proteins, (Promega) the only band present in the sample was at 50 kDa for PEDF.

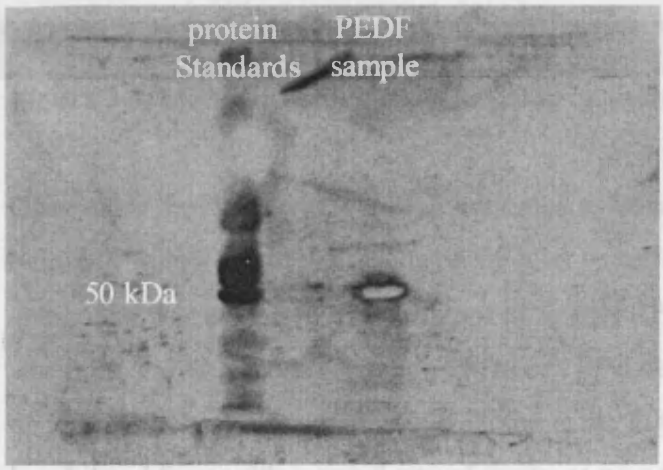

Figure 3.2.6 Western blot of PEDF sample

PEDF has a molecular weight of 46.3 kDa but has a carbohydrate side chain that increases its weight to 50 kDa in polyacrylamide gels (Wu et al., 1995).

3.2.7 Modification Of The Rate Of Development Of VCs

The flat-mounting protocol restricts the experiments to small batches of 7-8 animals (due to the time required for each preparation) from the same litter with similar survival times. It was decided to run several batches of animals and pool the results so that an adequate number of sham controls and tested animals could be obtained. In addition some animals

were processed for immunocytochemistry, wax histology and electron microscopy in order to obtain a clear picture of how the VCs develop. In total there were 42 additional animals, all three months old before commencement of procedures used for flat-mounts, Immunocytochemistry, wax histology and EM histology. The total numbers of animals for each protocol can be seen in **figure 3.2.7** and also included four of the injection practise animals as shams with untreated right eyes. Four of the PEDF animals were given a single injection of PEDF for regulatory reasons but the effects were indistinguishable from double injections two weeks apart. In later experiments bilateral injections were performed and the use of untreated eyes were dropped due to sufficient numbers having been recorded. **Figure 3.2.7** represents those eyes that survived the protocols in a usable state, hence the apparent loss of 10 eyes out of 84.

	Flat-mount	Immuno.	Wax histology	EM
PEDF	9	4	4	4
Echistatin	8	4	0	6
Sham	10	1	1	2
Untreated	17	1	1	2

Figure 3.2.7 Retinae used in six litters of animals to investigate VCs

Once more the right eyes were left untreated as housekeeping controls. PEDF was used as before to follow up on the results of the pilot experiment. Echistatin, an integrin antagonist was also used in an attempt to restrict RPE migration into the retina since prior work has shown a close correlation between RPE cells in the retina and the development of VCs (Villegas-Perez et al., 1998; Wang et al., 2003). Echistatin was obtained in lyophilised form with a certificate of purity so no prior preparation was necessary other than to reconstitute the protein in PBS at the required concentration (1 μg/ 2μl). All of the retinae were much less fragile than in the pilot experiment on flat-mounting with very little damage from the injection protocol visible but there were still the occasional retinae lost due to failure of the retina to detach. Of the 42 retinae flat-mounted, there was no correlation between treatment and failure of retina to detach and dissect out: untreated retinae were just as likely to be damaged.

PEDF

Retinae treated with PEDF (**figure 3.2.8**) were broadly in line with those seen in the pilot PEDF experiment with fewer VCs and a different distribution of those VCs throughout the ventral retina in comparison with the sham retinae. The area around the optic disc still exhibited a few VCs (**figure 3.2.8a**) but there were fewer and they were smaller in size than in comparable sham injected retinae (**figure 3.2.9a**). The largest difference could be seen in the mid-ventral retinae (**figure 3.2.8**) where there were very few VCs compared with the shams (**figure 3.2.9**). The peripheral retinae in PEDF treated retinas showed very few developed VCs (**figure 3.2.8b**), with some retinae exhibiting very small single pigmented cells situated on blood vessels of the peripheral (such as in **figure 3.1.3a**) venous supply. The untreated retinae (**figure 3.2.10**) were unremarkable and showed the expected pattern of VCs found in the RCS baseline experiments. The result was broadly in line with the PEDF pilot experiment and confirms that PEDF at a concentration of 1 μg/ 2μl could affect the development of VCs. It should be noted that the PEDF has not stopped the formation of vascular complexes, merely slowed down their development as compared with the baseline experiment and that this cannot be considered to be a "physiological dose". There is clearly a cascade of events associated with the breakdown of vision in retinal degeneration and it appears that the application of certain factors such as PEDF can slow down the progress of this progression towards retinal dysfunction.

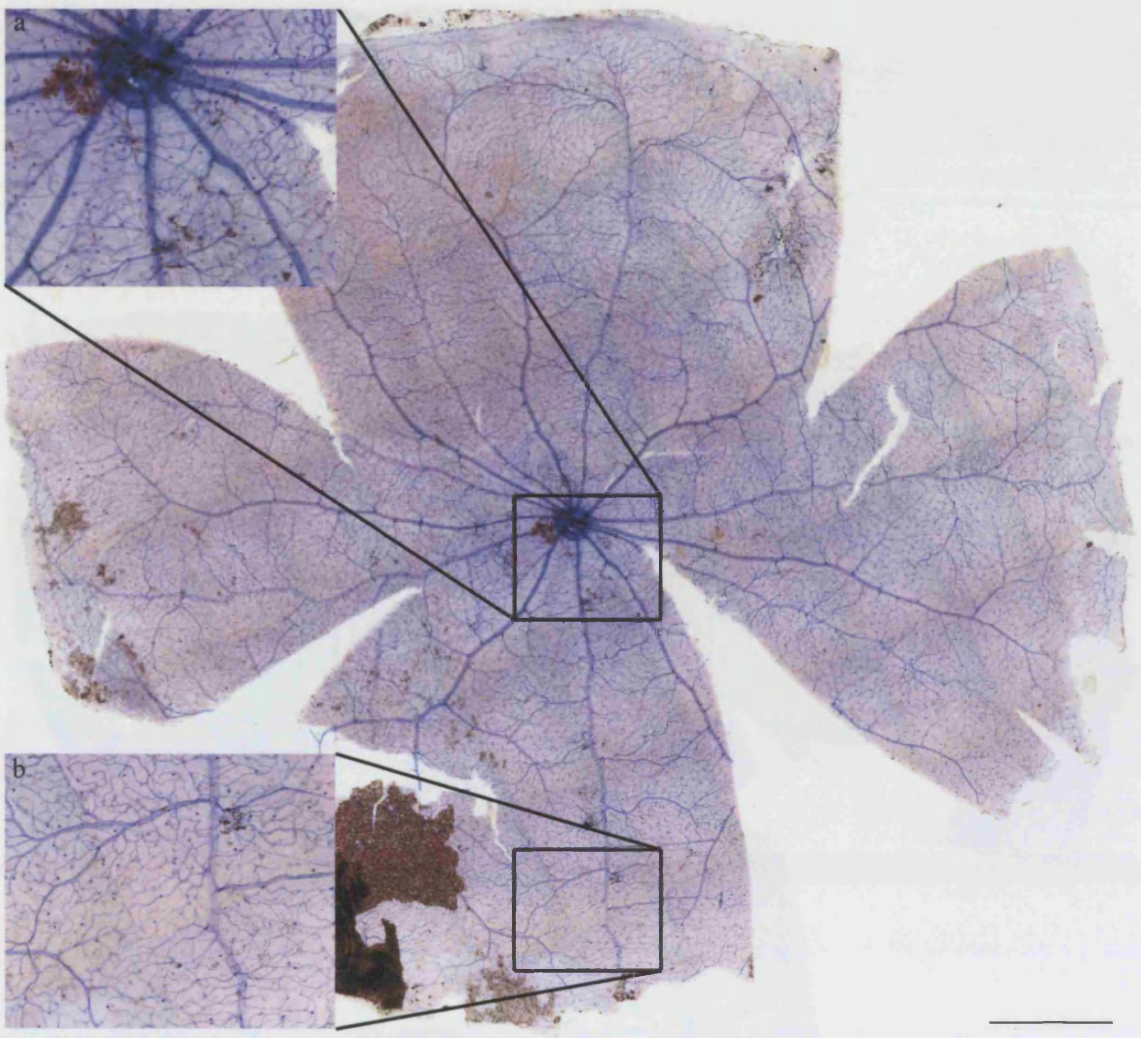

Figure 3.2.8 Dystrophic RCS at four months of age treated with PEDF. The injection site is visible in dorsal-temporal retina (all treatments were applied to left eyes). Insert a) shows normal VC epicentre containing a few underdeveloped VCs. Insert b) shows more peripheral retina with reduced VC content, arrow shows a single pigmented cell attached to a vein that we believe may be an early stage of VC formation. The dark pigment in the ventral- nasal retina is choroidal pigment that did not detach during dissection. There are several smaller patches of pigment in the mid retina where the choroid had to be carefully detached but none of this pigment is in the same focal plane as the vasculature. Scale bar represents 1000μm.

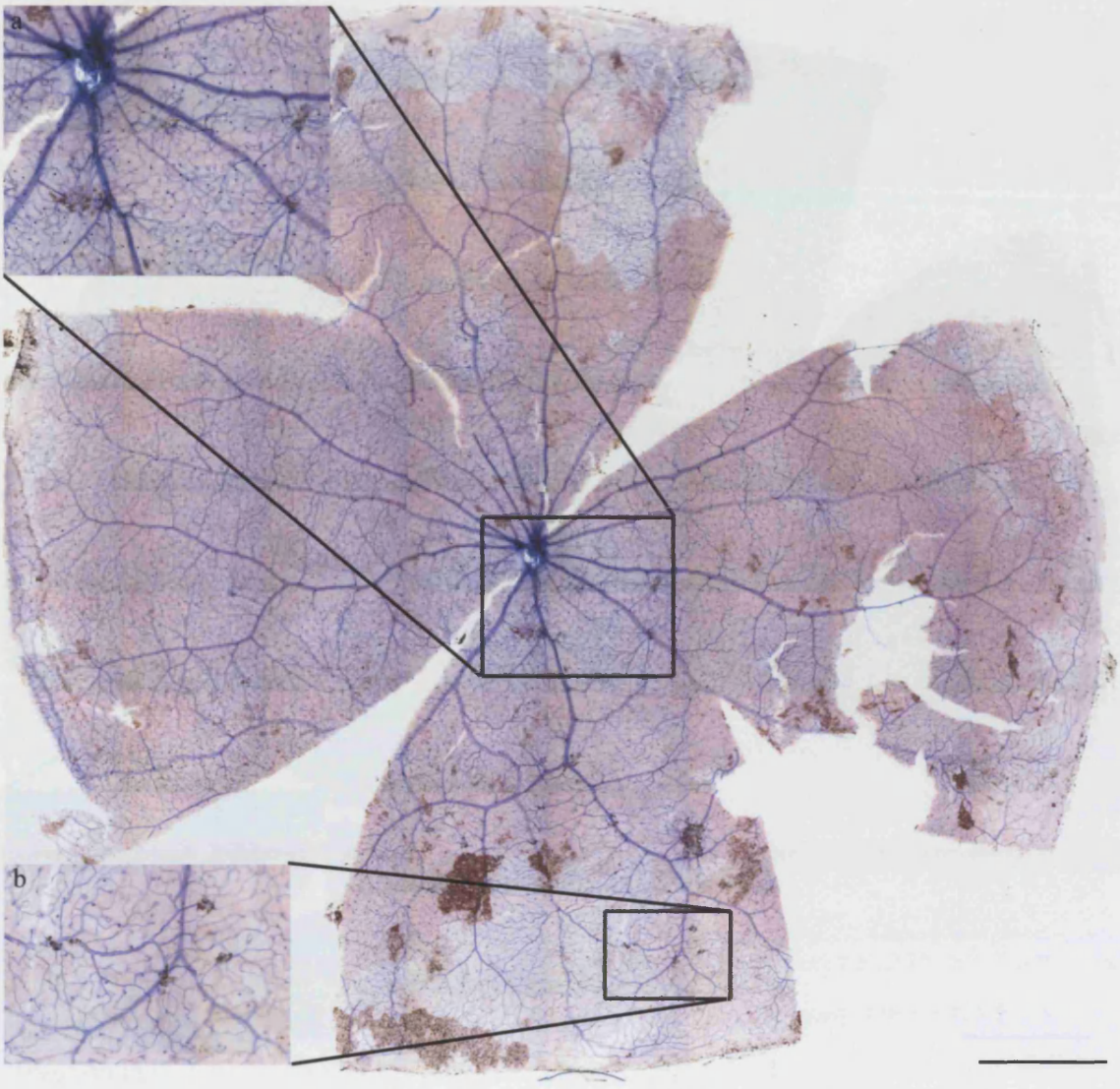

Figure 3.2.9 Dystrophic RCS at four months of age, sham treatment. Insert a) shows more advanced VC development around the optic disc than seen in **figure 3.2.8**. Insert b) shows more peripheral retina where VC development is once more increased from **figure 3.2.8**. There were numerous areas in this retina where choroidal pigment has failed to detach and also in the ventral-temporal retina where removal of debris resulted in damage to the retinal flat-mount. Scale bar represents 1000μm.

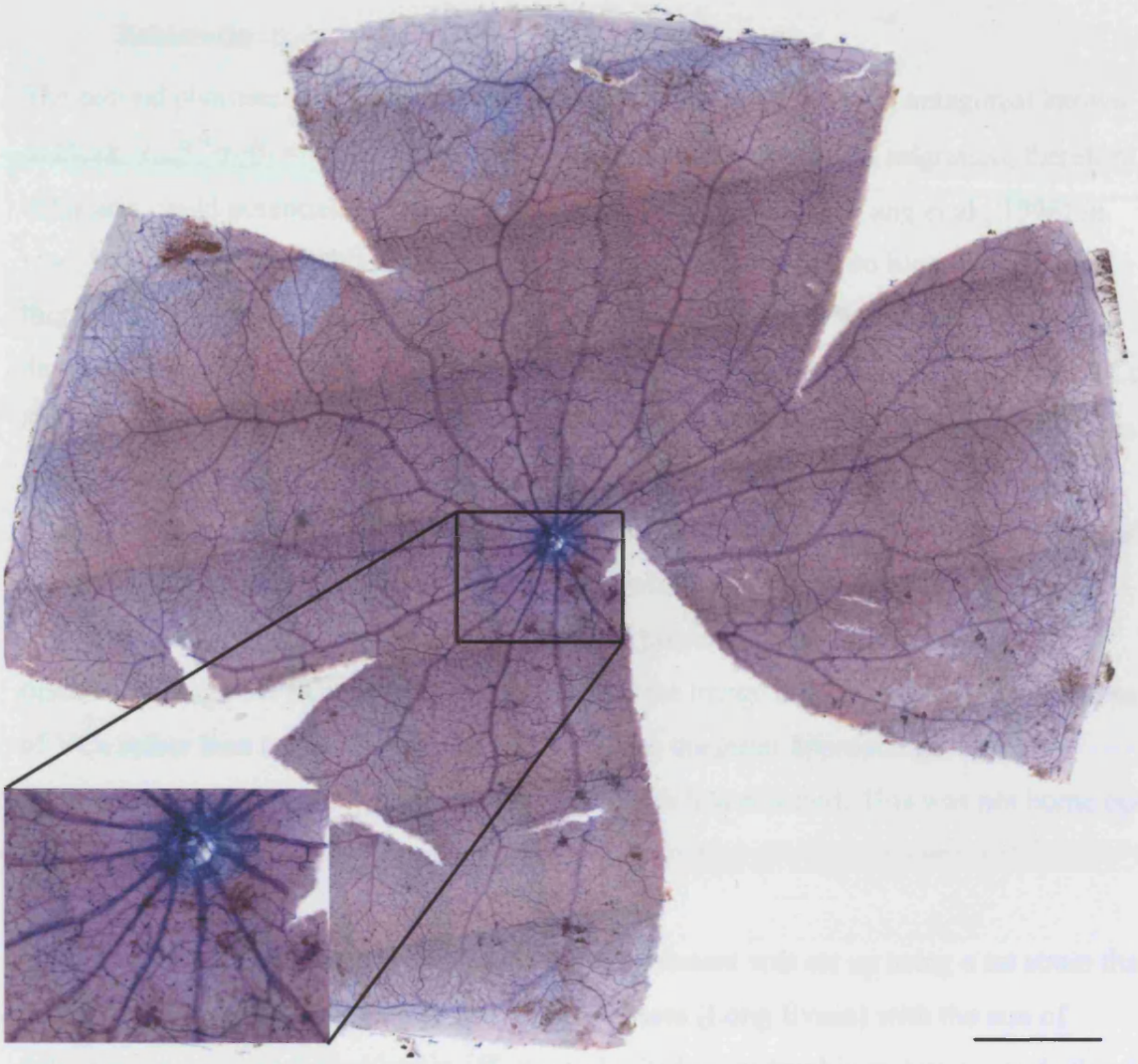

Figure 3.2.10 Dystrophic RCS at four months of age, untreated. Insert a) shows normal development of VCs at four months of age ventral to the optic disc. VCs can be seen in vessels branching from deep draining veins throughout the ventral retina and into the nasal retina (untreated retinae were always right eyes). Untreated retinae should not be compared directly with other treatments for two reasons 1) They have not received an injection piercing the retina and 2) they were all right eyes whereas treatments were applied to left eyes which have slightly reduced VC development as shown in **figure 3.1.9**. Scale bar represents 1000μm.

Echistatin

The second pharmaceutical candidate used was Echistatin, an integrin antagonist known to block $\alpha_{IIb}\beta_3$, $\alpha_V\beta_3$ and $\alpha_5\beta_1$. $\alpha_V\beta_3$ was known to play a role in cell migration, therefore echistatin could potentially block RPE migration as suggested by(Yang et al., 1996) *in vivo.* In the RCS model this could restrict the migration of RPE onto blood vessels and thereby disable one component of VCs. What actually happened was that the development of VCs was increased in retinas treated with Echistatin. The number of VCs did not actually increase dramatically but the overall size of some VCs was greatly enlarged (**figure 3.2.11**). The area around the optic disc (**figure 3.2.11a**) showed an increase in large well-developed VCs: this was not found with other treatments. The most obvious difference was in the mid ventral retina where large extensive VCs spread out over a relatively wide area (**figure 3.2.11b**) were present. These extensive areas of disturbance were the main impetus for upgrading the image analysis system to count area of VCs rather than counting numbers of VCs, since the latter approach gave the impression that Echistatin treated retinae were much less affected. This was not borne out by visual inspection.

With these results in mind a further echistatin experiment was set up using a rat strain that was not suffering from any degenerative eye diseases (Long Evans) with the aim of determining whether the echistatin effect was limited to dystrophic mutation or whether it could be used to create a retinal degenerative model in rats without a genetic defect. Exactly the same delivery method and concentrations of echistatin were delivered to a batch of eight Long Evans rats at 3 & 3.5 months of age and the retinas were dissected out and flat-mounted as before at 4 months.

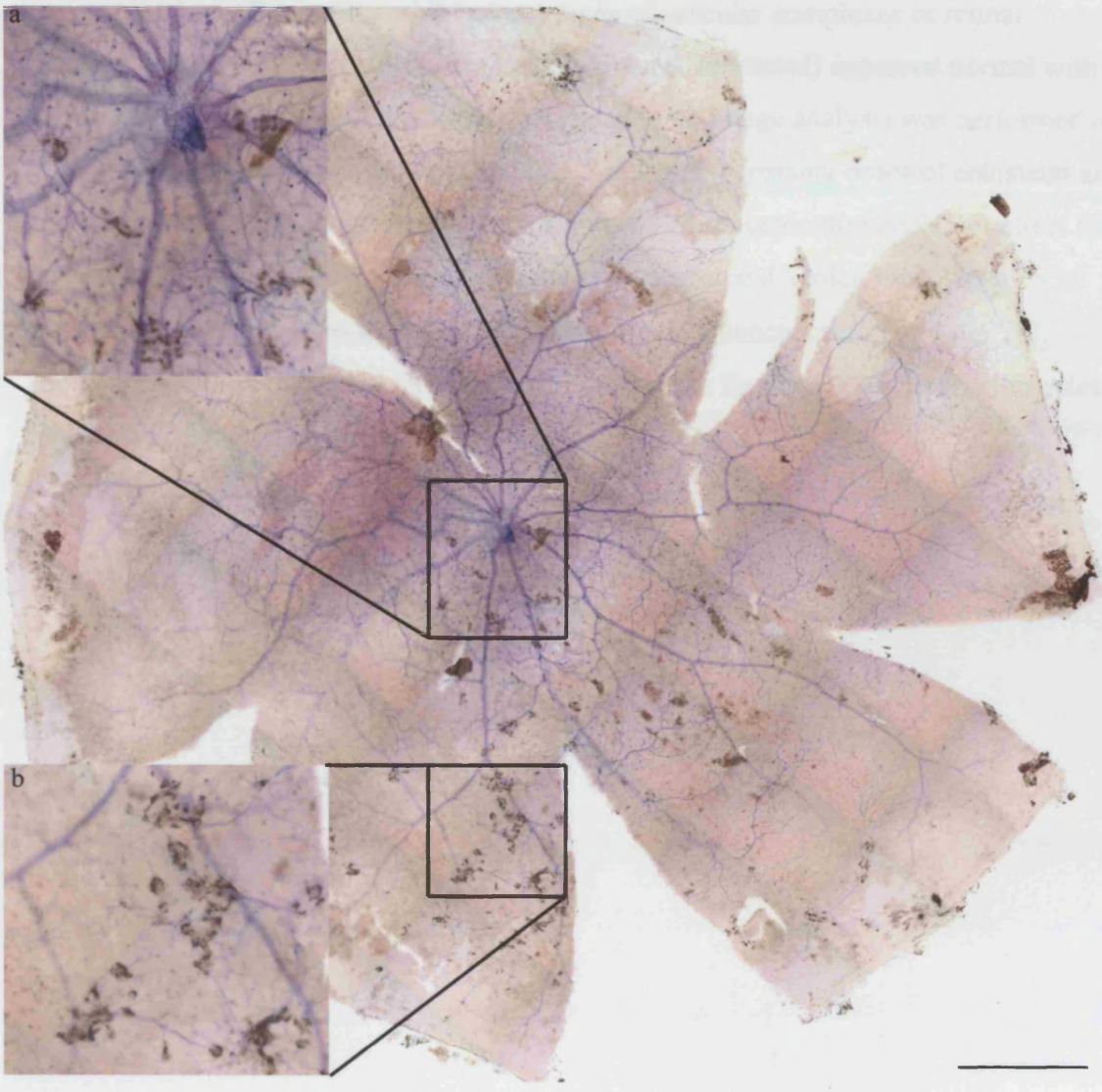

Figure 3.2.11 Dystrophic RCS at four months of age treated with echistatin.
The injection site is visible in the dorsal peripheral retina. Insert a) shows how advanced VCs in the optic disc have become after treatment with echistatin. Insert b) shows mid-ventral VCs far more developed than seen in previous retinae. The pinkish cast to the retina with clear patches is caused by some of the RPE layer remaining attached to the retina and picking up some staining from the NADPH-d staining protocol.
Scale bar represents 1000μm.

None of the Long Evans rats exhibited any signs of vascular complexes or retinal disruption (**figure 3.2.12**); all retinae (treated, sham & untreated) appeared normal with no vascular abnormalities of any kind, consequently no image analysis was performed on these animals. Later work using congenic RCS rats and increasing doses of echistatin also showed no effect. This suggested that echistatin at this concentration could not affect the vasculature of rats that do not have some underlying retinal disorder. Only the RCS rat has shown any affect from treatment with echistatin at a concentration of 1 μg/ 2μl. The image analysis date from these treatments shown in **figure 3.2.13** clearly illustrates the relative effects of these treatments.

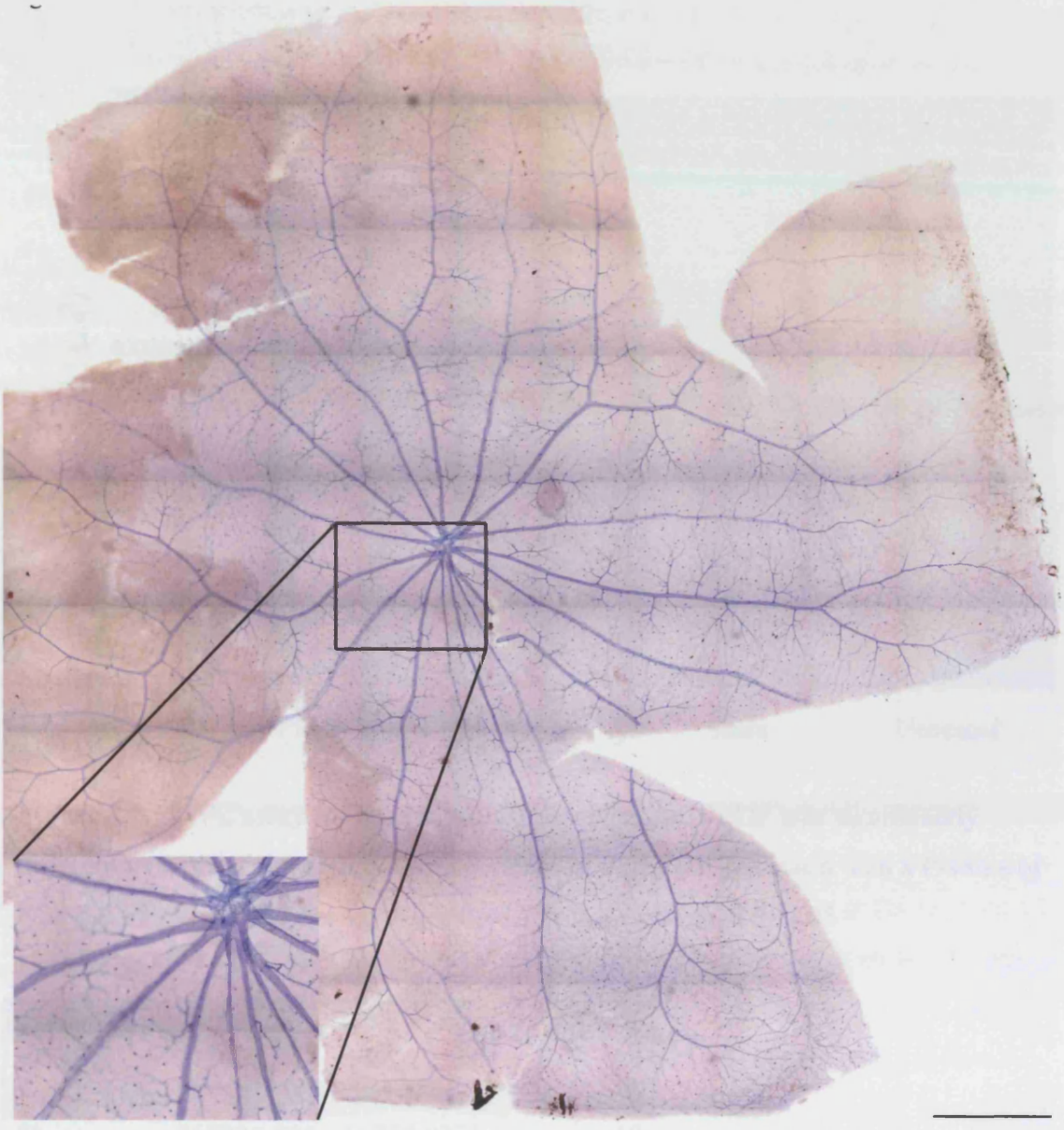

Figure 3.2.12 Long Evans rat at four months of age treated with echistatin,
There are no signs of VCs or pigmented cells anywhere in the retina. This retina has a normal vascular structure much like the congenic RCS in **figure 3.1.2**.
Scale bar represents 1000μm.

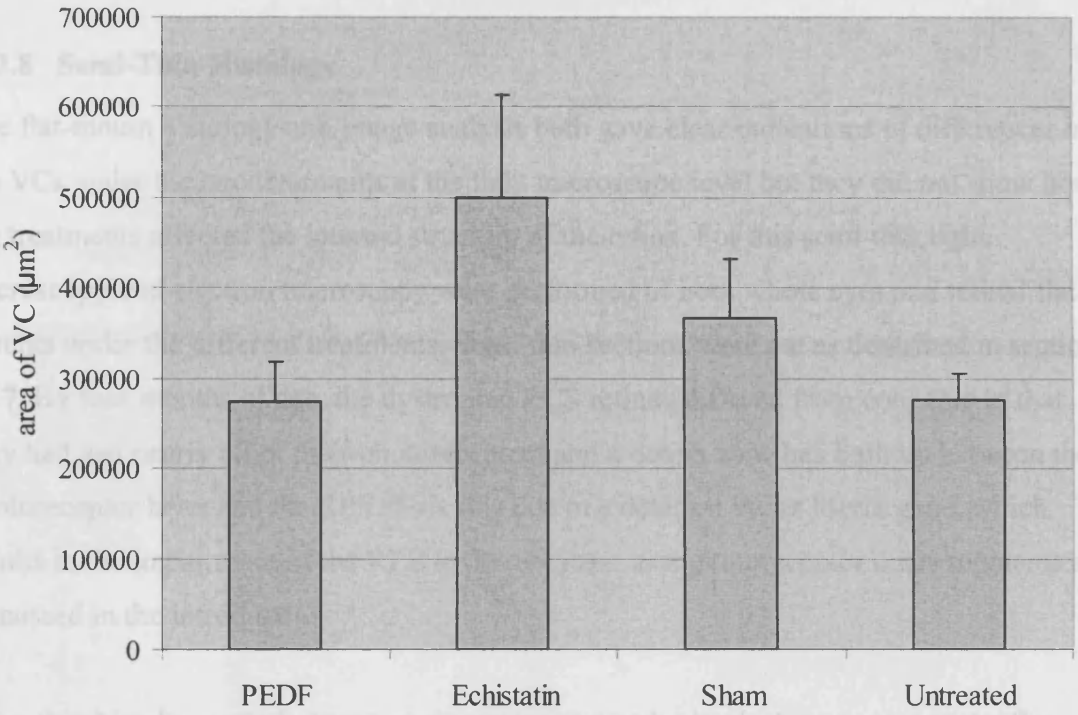

Figure 3.2.13 VC assay for pharmaceutical intervention. PEDF was significantly different from the sham controls with p values of 0.018 but echistatin with a P-value of 0.29 did not, PEDF did not significantly differ from untreated P<0.05

Data Table

Treatment	average	std Error	# retinas
PEDF	273492.973	44624.2131	14
Echistatin	498744.154	115061.213	8
Sham	367228.805	66054.0271	10
Untreated	276139.51	30412.0808	11

Significance

P-values	PEDF	Echistatin	Sham	Untreated
PEDF		**0.039**	**0.0186**	0.2363
Echistatin	**0.039**		0.2962	0.062
Sham	**0.0186**	0.2962		**0.05**
Untreated	0.2363	0.062	**0.05**	

One month after application, PEDF and echistatin had very different effects on the development of VC in the RCS rat. The sham retinae were the true controls for this experiment with both treatments exhibiting differences from the control although only

PEDF differing significantly. In the data set there was one outlier for the sham retina and error bars were standard error of the mean for total area of VCs in the retinae.

3.2.8 Semi-Thin Histology

The flat-mount histology and image analysis both gave clear indications of differences in the VCs under the two treatments at the light microscope level but they did not show how the treatments affected the internal structure of the retina. For this semi-thin light microscopy and electron microscopy were performed of both whole eyes and retinal flat-mounts under the different treatments. Semi-thin sections were cut as described in section **2.17.** By four months of age, the dystrophic RCS retinae differed from congenic in that they had lost nearly all of their photoreceptors and a debris zone has built up between the photoreceptor layer and the RPE. This was due to a deletion in the Mertk gene, which results in the impairment of the RPE to phagocytose cast photoreceptor outer segments as discussed in the introduction.

Semi-thin histology of whole eye cup preparations with identical treatments to the flat-mounts as shown in **figures 3.2.14** to **3.2.17** did not show any clear differences in anatomy. Of particular importance was the fact that none of the treatments resulted in rescue of photoreceptors. This is relevant as one possible explanation of the reduced VCs with PEDF (**figure 3.2.14**) could have been simply that PEDF through its neuroprotective properties allowed photoreceptors to survive forming a physical barrier to RPE migration. The larger vascular complexes which show up in echistatin treated retinae did show clearly in the ventral retina and were very easy to find when cutting through the eye cup but the depth of the debris zone and very sparse remaining photoreceptors were all characteristic of dystrophic RCS rats at 4 months of age. In all of the treatments there would occasionally be areas where the debris zone thinned out allowing the inner retina to come into contact with the RPE, which we believe may be indicative of an early stage leading to VCs formation (**figure 3.2.14** insert). The presence of photoreceptors in the semi-thin sections did not preclude the presence of vascular abnormalities (**figure 3.2.17** insert) but the photoreceptor layer was so badly depleted by 4 months of age that its influence may have been negligible.

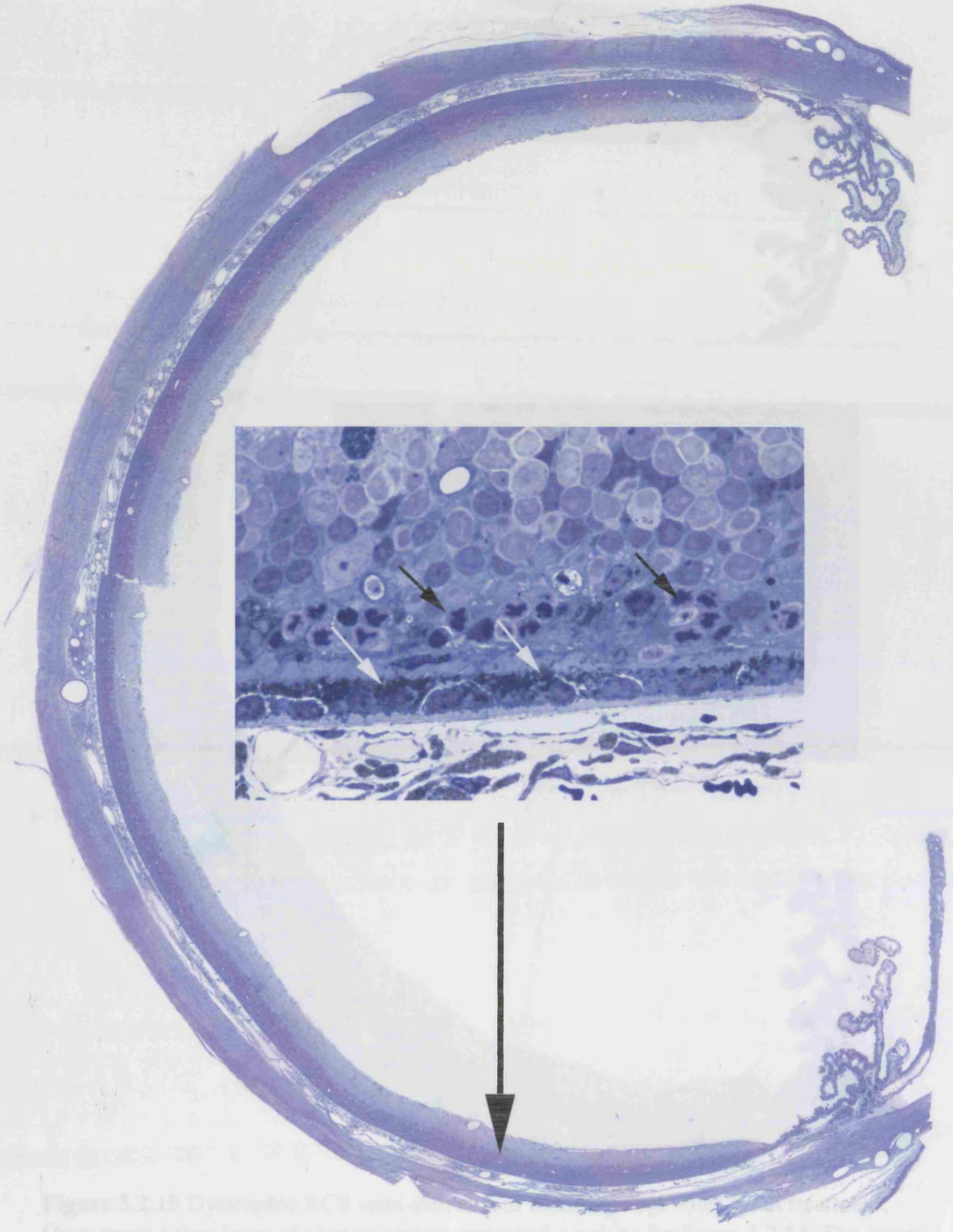

Figure 3.2.14 Dystrophic RCS retina semi-thin at four months of age after treatment with PEDF, stained with toluide blue. Insert shows ventral retina (x 158 mag.) with a thin broken layer of photoreceptors (black arrows) staining darkly, note the relatively thin debris zone separating the photoreceptors from the RPE layer (white arrows) in comparison with **Figures 3.2.15** & **3.2.16**. Scale bar represents 500μm.

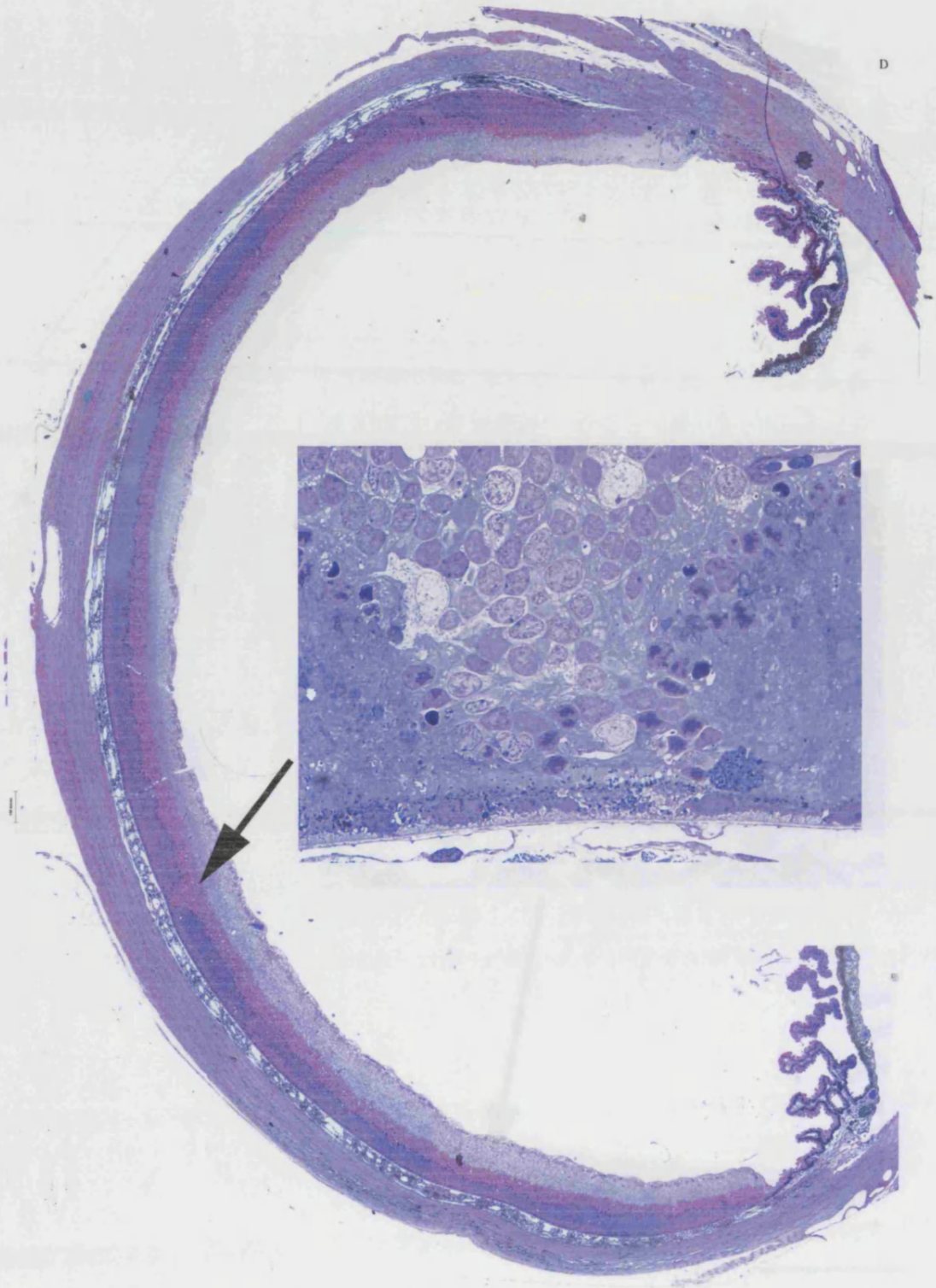

Figure 3.2.15 Dystrophic RCS semi-thin at four months of age after sham treatment. Once more a thin layer of photoreceptors remained much as for figure **3.2.14.** The insert shows an area (x 158 mag.) where the debris zone has been bridged by cells from the inner retina allowing the RPE layer has come into contact with cells of the inner retina, which we believe may result in the formation of VCs although the RPE has yet to migrate onto the venous vasculature in this instance. Scale bar represents 500 μm.

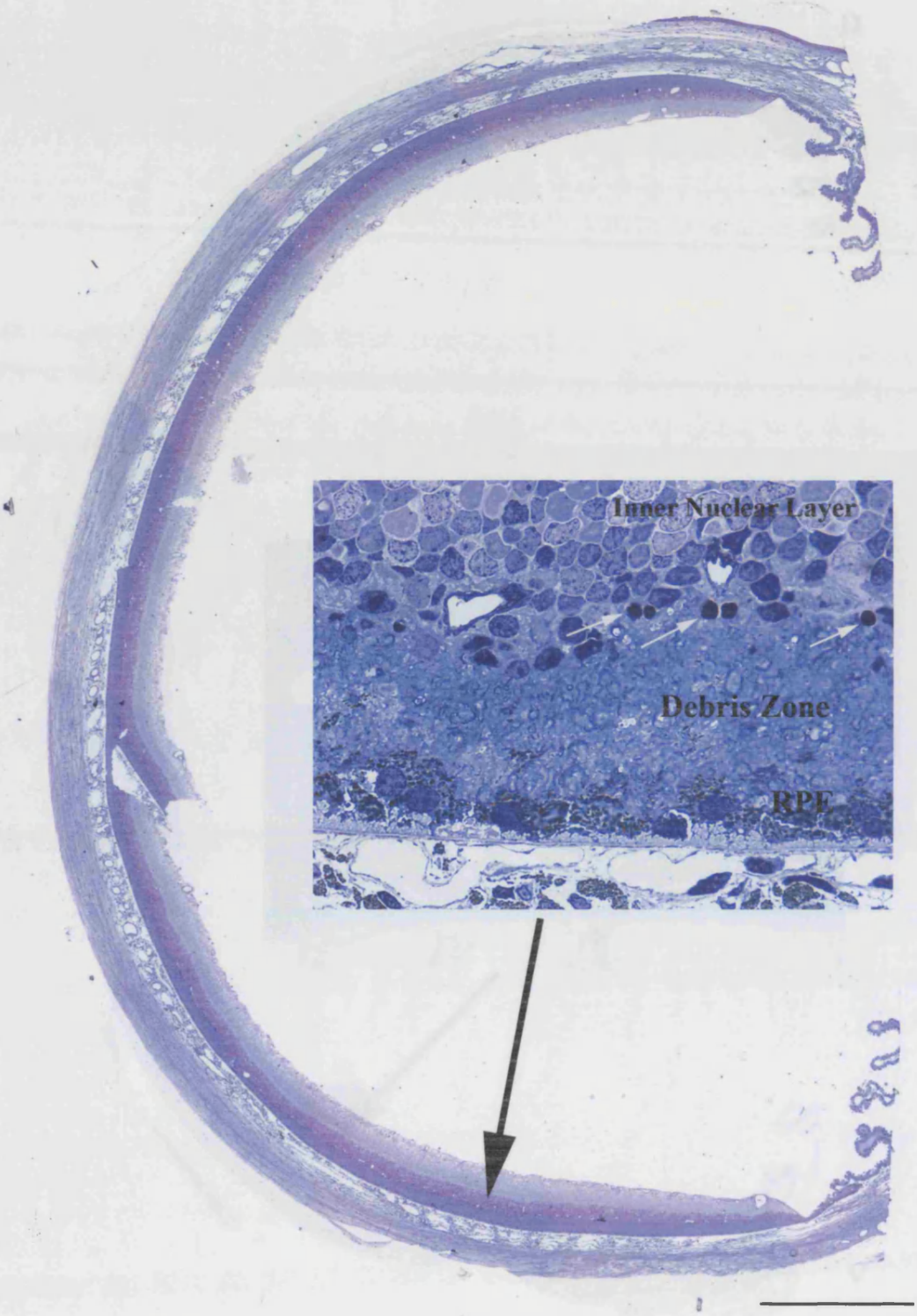

Figure 3.2.16 Dystrophic RCS at four months of age, untreated semi-thin.
Insert (x158 mag.)once more shows typical dystrophic RCS retinal structure of scattered remaining photoreceptors (white arrows) separated from RPE by the debris zone.
Scale bar represents 500 μm.

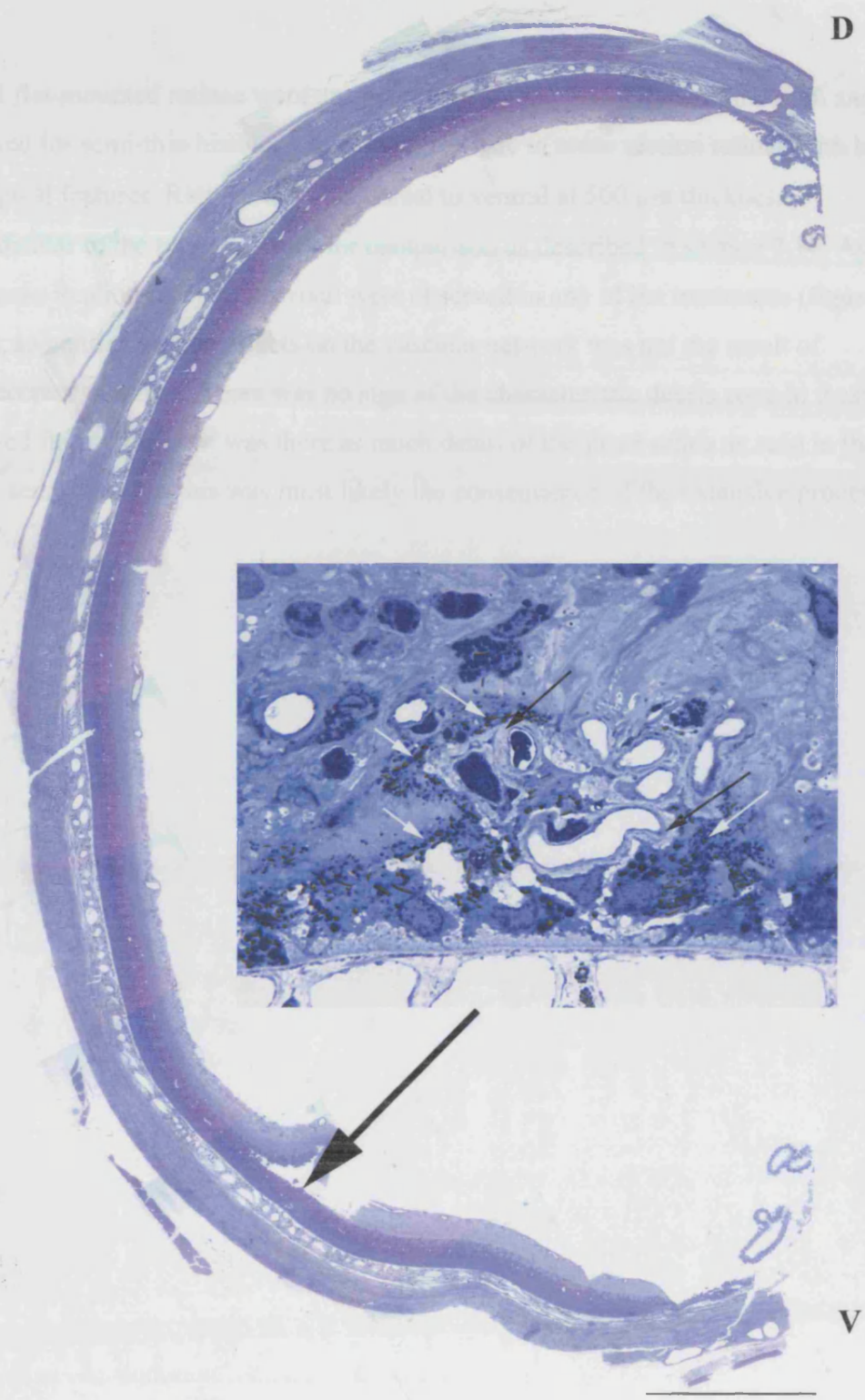

Figure 3.2.17 Dystrophic RCS at four months of age treated with echistatin, semi-thin. Insert shows a close up of a VC (x 250 mag.) where the sparse remaining photoreceptors were even less common. The black pigment granules (white arrows) from the migrated RPE can be clearly seen as can the thickened vessel walls with ECM deposits (black arrows) as described in the literature. The pigmentation surrounding the vessels very closely resembles that described in the RP literature due to coming from the same source. Scale bar represents 500 μm.

Several flat-mounted retinae were un-mounted from the PBS-Glycerol medium and processed for semi-thin histology to examine retinae in cross section retinae with known histological features. Retinae were cut dorsal to ventral at 500 μm thickness, perpendicular to the retinal surface for comparison as described in section **2.16**. Again no differences in photoreceptor survival were observed in any of the treatments (**figure 3.2.18**), so confirming the effects on the vascular network was not the result of photoreceptor numbers. There was no sign of the characteristic debris zone in these processed flat-mounts nor was there as much detail of the inner retina as seen in the normal semi-thins but this was most likely the consequence of the extensive processing.

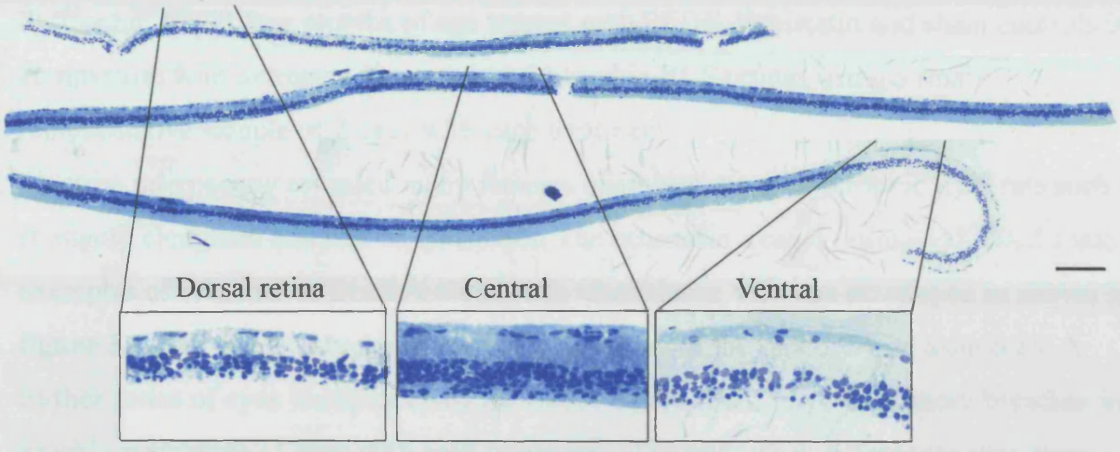

Figure 3.2.18 Dystrophic RCS at four months of age after treatment with PEDF. Semi-thin of flat-mounted retina treated showing cross-section of entire retina from dorsal to ventral. The three inserts show details of the retina in dorsal, central and ventral retinae after reconstruction using photomerge in Adobe Photoshop Elements 2.0. Scale bar represents 100 µm.

3.2.9 Electron Microscopy

Electron microscopy was used to determine if there were any major differences between dystrophic rats at four months of age treated with PEDF, Echistatin and sham controls in comparison with untreated 4 month old dystrophic RCS retinas using a small representative sample of 2 eyes with each treatment.

Electron microscopy revealed many features characteristic of dystrophic RCS rats such as strangely elongated end feet on RPE cells. The echistatin treated retinae exhibited some examples of breaches in Bruch's membrane where large VCs had developed as shown in **figure 3.2.19c.** These breaches were not seen in any of the other retinas axamined. A further series of eyes wereprocessed for EM to determine if there were more breaches in bruch's membrane (4 eyes with each treatment). The only clear differences seen were between the pigment granules found in PEDF (**figure 3.2.20a&b**) and echistatin (**figure 3.2.20c&d**) treated retinae. No further breaches in Bruch's membrane were seen probabl;y as breaches in bruch's membrane are only seen in very late timepoints with dystrophic RCS rats and 12-18 month duration experiments were not feasible within the timeframe of this study. PEDF treated retinae consistently exhibited more pigment granules, which were much darker in contrast than in Echistatin treated retinae. The differences in granule contrast were consistent with samples processed within a single batch and photographed in the same session. There were also more phagosomes containing outer segment fragments (arrow) in the PEDF treated retinae than in echistatin treated retinae. As the exact mode of action of PEDF and its receptor/s are at present unknown or at least not published it is very difficult to determine exactly what these results mean. One possibility is that the increased presence of PEDF may have aided RPE phagocytosis but there is no vidence in the literature to support this. In the case of the echistatin treatment one clue may come from a study which found that echistatin blocked integrin $\alpha_5\beta_1$ (Wierzbicka-Patynowski et al., 1999). Integrin $\alpha_5\beta_1$ is involved in RPE cell phagocytosis of ECM (Zhao et al., 1999) possibly the reduction in phagosomes in the echistatin treatment may be due to Echistatin further impeding the already impaired RPE cells in the dystrophic RCS rat.

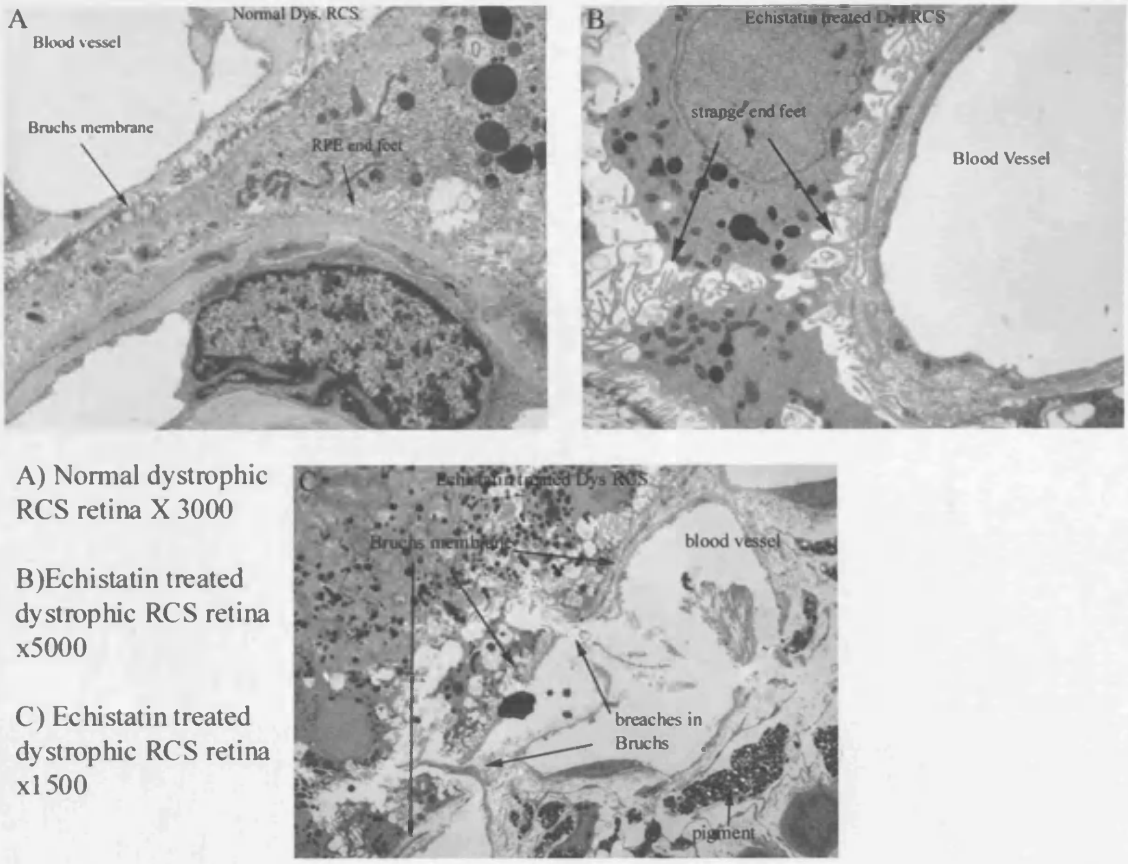

A) Normal dystrophic RCS retina X 3000

B)Echistatin treated dystrophic RCS retina x5000

C) Echistatin treated dystrophic RCS retina x1500

Figure 3.2.19 Sections from four month old dystrophic RCS retinae processed for electron microscopy as described in section 2.15 a) untreated b) treated with echistatin showing strange RPE end feet and c) echistatin showing breaches in Bruch's membrane.

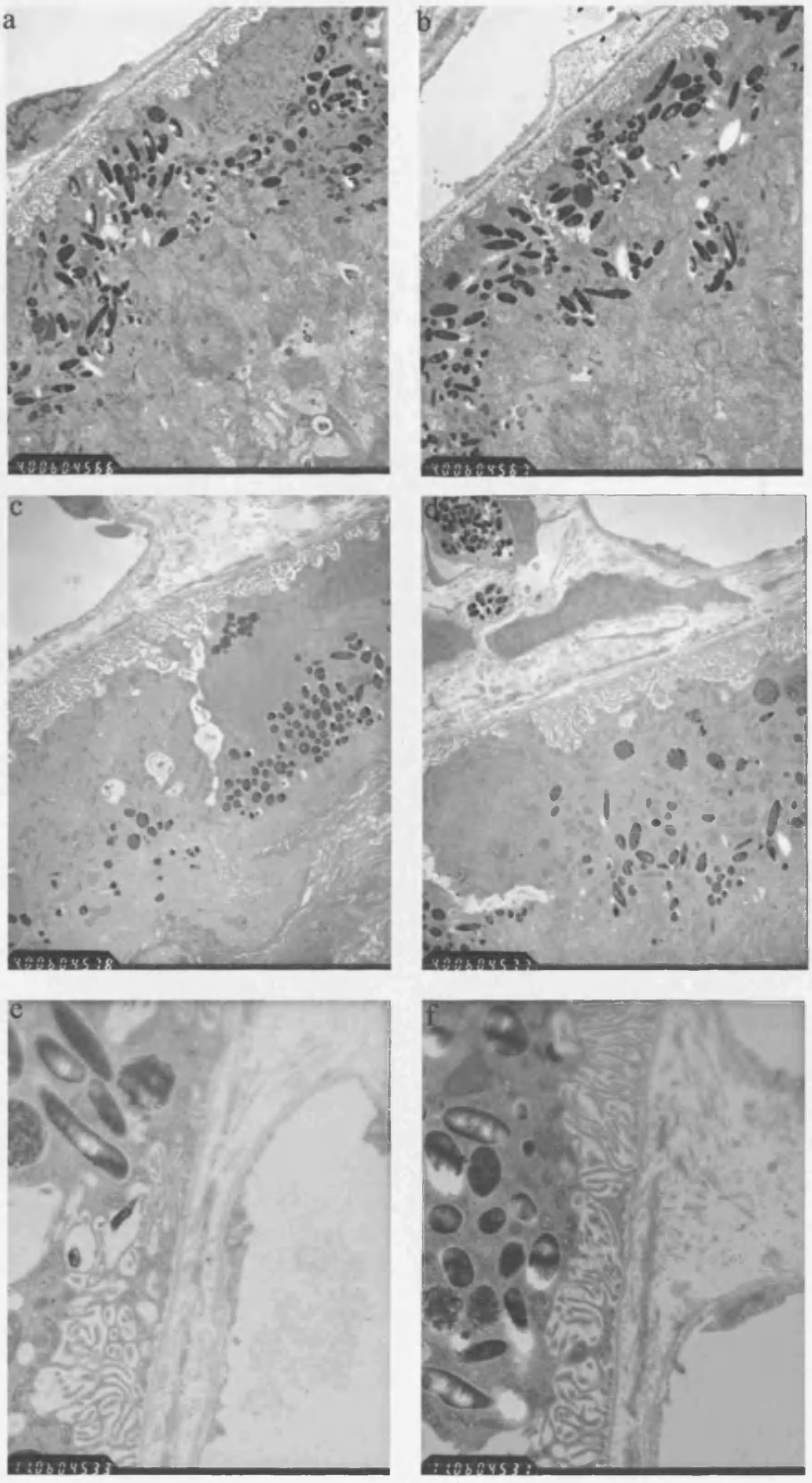

Figure 3.2.20 EM sections of four month old dystrophic RCS showing Bruch's membrane after treatments, a & b) PEDF treated at x8k mag., c & d) echistatin treated at x8k mag. and e & f) sham treated retinae at x 11k mag. Note the more numerous dark vesicles in the PEDF treated retinae in comparison with the relatively sparse echistatin treated retinae. The echistatin may be exhibiting an unforeseen interference with the RPE

3.2.10 Immunocytochemistry

Initial plans for analysing the effects of PEDF and echistatin treatments involved extensive immunocytochemistry of integrin sub-units, since such observations had not previously been made in the RCS rat. **Figure 3.2.21** shows the planned antibody regime with concentrations derived from test staining on cryosections. Cryosections were cut from retina as detailed in methods **2.12** and **2.13**, further sections were cut from skin and spleen for positive control controls. Antibodies were purchased from Santa Cruz Biotech chosen for its near complete range of integrin subunits available for use in the rat model and from Chemicon. Initial results for staining of α subunits were inconclusive. Serendipitously the staining coincided with a visit to the Institute of Ophthalmology by Dr Kairbaan Hodivala-Dilke who presented a talk on vascular changes in β3 & β5-Integrin knockout mice on the retina (Reynolds et al., 2002) where similarities in the vasculature were seen to those occurring in the RCS pathology. After comparison and discussion of results with Dr Hodivala-Dilke and showing her both NADPH flat-mounted and integrin immunocytochemical staining, she recommended that we discontinue the immunocytochemistry. The commercial antibodies were not suitable for the tissues as they were they not specific enough to allow dissection of the integrin components in the retina. Wax histology did not add anything to the study and was also discontinued leaving the semi-thin histology to show cross-sectional views through the retina.

Integrin	Cat ref	host	origin	Dilution
α1	sc-6584	gt poly	rat	1:50
α2	sc-6586	gt poly	hmn	1:100
α3	sc-7019	ms mono	rat	1:250
α4	sc-6591	gt poly	hmn	1:100
α5	sc-6593	gt poly	hmn	1:200
α6	sc-6597	gt poly	hmn	1:100
αL	sc-6611	gt poly	mus	1:50
αM	sc-6614	gt poly	mus	1:100
αV	sc-6617	gt poly	hmn	1:100
β1	sc-6622	gt poly	hmn	1:100
β2	sc-6624	gt poly	hmn	1:200
β3	sc-7311	ms mono		1:100
β4	sc-6628	gt poly	hmn	1:100
β5	AB1926	rbbt poly	hmn	1:100
β6	MAB2076Z	ms mono	hmn	1:250

Figure 3.2.21 Integrin Antibody Data

Note all antibodies with catalogue reference numbers starting with SC were sourced from Santa Cruz Biotechnology and β5 & β6 antibodies were sourced from Chemicon.

This clearly shows the differences in the anatomy of the two retinae where in the dystrophic animal there were very few photoreceptors left in contrast to the robust 10-12 cell thick photoreceptor layer in the congenic RCS rat. The α4 staining pattern was clearly positive in the photoreceptor inner segments near to the cell body of the congenic rats but in the dystrophic staining is diffused throughout the debris zone where only fragments of photoreceptor inner segments would remain.

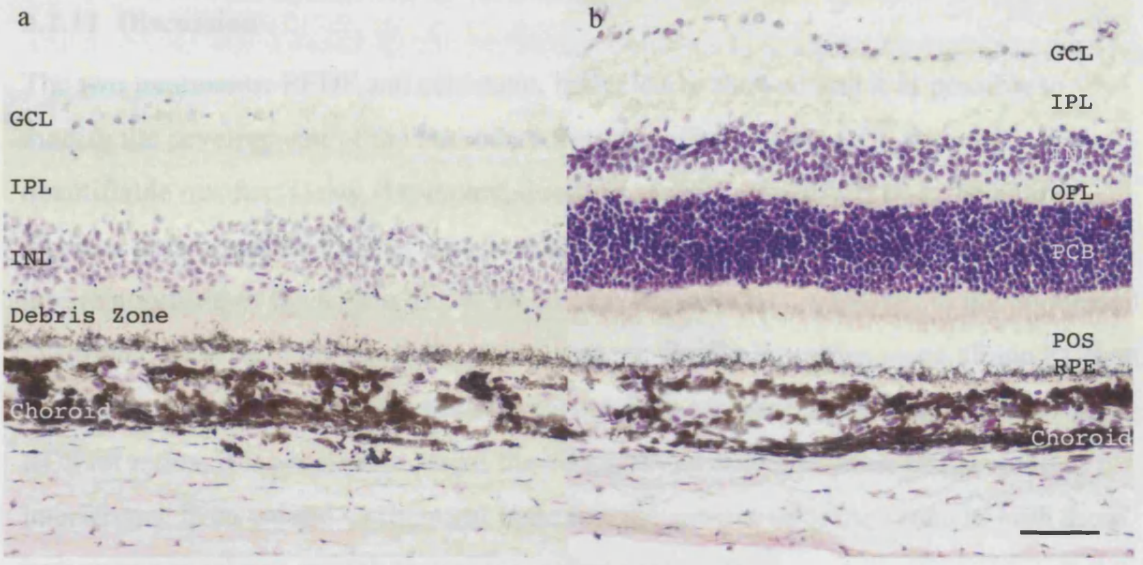

Figure 3.2.22 Immunocytochemistry of retinal cross-sections. Examples of 4 month old dystrophic (**figure 3.2.22a**) retina with dramatically reduced photoreceptor layer and below that the debris layer where the photoreceptor inner and out segments should be. The five month old congenic (**figure 3.2.22b**) RCS retina exhibited normal retinal lamination found in rats without the dystrophic pathology. Both sections were stained with antibody sc-6591 to the a4 integrin subunit and counterstained using cresol violet
GCL= ganglion cell layer, IPL= inner plexiform layer, INL= inner nuclear layer,
OPL= outer plexiform layer, PCB= photoreceptor cell bodies,
POS= photoreceptor outer segments, RPE= retinal pigmented epithelium.
Scale bar represents 100 μm

3.2.11 Discussion

The two treatments: PEDF and echistatin, both clearly showed that it as possible to modify the development of the secondary vascular effects of the RCS pathology in a quantifiable manner. Using flat-mounted retinae stained with NADPH-d, the entire vascular network of the retina could be displayed (Wang et al., 2000), revealing the interrelationship of the RPE with the vasculature in vascular complexes in the pigmented dystrophic RCS rat. This interrelationship was not visible in studies using albino RCS rats (Caldwell, 1989). By recording the area occupied by vascular complexes in a dystrophic RCS rat retina, it is possible to assess the efficiency of antiangiogenic drugs without interference from wound or chemical trauma to the same area of the retina as both these processes can release growth factors that affect angiogenesis.

This is important as there is currently a lack of models for *in vivo* assessment of angiogenic/antiangiogenic drugs that utilise naturally occurring retinal vascular changes rather than laser induced retinal damage (Campochiaro and Hackett, 2003). In the latter a hole is burned into the retina entirely through into the choroid, this is supposed to emulate the breaches in Bruch's membrane seen in AMD. This actually creates a large wound where the repair process not only relates to control of AMD-like vascular pathology, but also to wound healing of damaged tissue (Semkova et al., 2003). While it is true that administering pharmaceuticals into the eye trans-sclerally also involves making a wound through the retina, the wound was very small and in this case positioned as far from the area of effect (ventral retina) as possible. Possibly alternative delivery methods may in future remove the requirement for damaging the retina in any way, such as through the front of the eye in human surgery.

More traditional *in vitro* assays such as cell culture and the chicken chorioallantoic membrane (CAM) assay (Glaser et al., 1980) could be useful for answering questions such as whether or not certain molecular pathways were possible (i.e. can growth factor X reduce angiogenesis), but they could not prove whether the chemical would function identically *in vivo*. An example of this deficiency was the echistatin result where our original intention was to use echistatin to inhibit RPE migration (Nakamura et al., 1998; Yang et al., 1996): our actual result was the opposite. Crucially only *in vivo* assays could give any indication of how an animal with a competent immune system would react to

application of a pharmaceutical agent. That said there is still the caveat that while no animal model would guarantee the performance of a particular pharmaceutical agent in a human patient.

Neither treatment used in this study managed to halt the development of vascular complexes completely. This was thought to be due to the continual loss of photoreceptors and further work was added to cut sections from the flat mounted retinae although no changes were observed in photoreceptor numbers between treatments. This was possibly due to the treatment delivery after significant photoreceptor loss being too late to counter the effects of the RPE defect (which started immediately after photoreceptor development (Davidorf et al., 1991)). The dosage regime of one or two injections may not have allowed a long enough window of effectiveness for the drugs before they were cleared from the vitreous (Wu et al., 1995). It may be possible to assess photoreceptor survival using the VC assay by administering treatments earlier and following up the VC assay with processing the flat-mounts for semi-thin histology as in section 3.2.8 or by immunostaining flat mounts with rod or cone specific antibodies. Alternatively constant dosage regimes of injections every week for several months or using a constant slow release delivery mechanism may result in increased photoreceptor survival. None-the-less, the minimal dosage regime used yielded quantifiable changes to the area of vascular complexes.

The strength of the VC assay procedure lay in its ability to give a global assessment of the entire vascular network of the retina over a significant period of time. This could allow future treatment regimes to be optimized in areas such as concentration of dosage, periodicity of dosage and length of treatment. Also possible would be combinations of pharmaceutical treatments with physical surgical intervention such as those currently carried out on human patients such as retinal translocation or retinal transplantation/cell based therapy. The rat eye may not be suitable for certain procedures (such as retinal translocation) but the VCs assay could be scaled up to larger animal models to accommodate these (providing the animal model had similar retinal pathology).

Further technological advances in computer equipment should allow much larger images to be assembled. The Image Pro Plus software used could assemble and quantify images up 36 K^2 pixels which equates to a flat-mounted retina roughly $1cm^2$ (rat eyes used here

are 12.6K x 12K pixels for approx. 1 cm^2). Human eyes were roughly 4 cm^2 when flat-mounted but the staining protocol works exactly as for rat eyes, which would allow assessment of eye bank sourced eyes with known retinal disorders once this software limit is breached. Alternatively lower magnification optics could be used to produce a smaller global picture of lesser resolution or selected areas could have been examined rather than the entire retina.

The vascular complexes observed in the flat-mounts were centred on an area just ventral to the optic disc generally following the course of one or more deep draining vessels as described in chapter 3.1, with much smaller less well developed vascular complexes found in the peripheral retina. The vascular complexes not only differed in the total area but also in the distribution of vascular complexes within the retina between the two treatments and their controls.

PEDF

PEDF treated retinae typically exhibited smaller complexes in the mid-ventral retina with many small-pigmented cells attached to peripheral vessels. PEDF has been shown to have considerable neuroprotective (Houenou et al., 1999; Imai et al., 2005) as well as potent anti-angiogenic (Dawson et al., 1999) properties. What this study has shown is that even with limited dosage of PEDF the cascade that results in the development of VCs in the dystrophic RCS retina may be slowed. PEDF may have through its anti-angiogenic properties reduced the secondary vascular effects associated with retinal degeneration, but recent advances in PEDF research have uncovered a host of further properties and interactions that complicate this assessment such as (Gao et al., 2001; Kijlstra et al., 2005; Tombran-Tink, 2005).

Previous research has shown that in the rd and rds mice, PEDF has preserved photoreceptors (Cayouette et al., 1999; Imai et al., 2005) prolonging retinal function (Imai et al., 2005). The VCs assay measures vascular damage not photoreceptor survival therefore direct statements of PEDF function could not be deduced from this work. That said it is clear that from this work PEDF changed the profile of vascular complexes seen in the RCS rat by reducing their size. This study has not shown changes in photoreceptor survival (**figure 3.2.14-18**) but EM work did show increased numbers of pigment granules in the RPE (**figure 3.2.20**). These results suggest that the PEDF is affecting the

RPE. Further work would have to be done to specifically target the RPE with PEDF possibly for intensive electron microscopy after PEDF treatment or perhaps using proteomics.

Sham injections

An interesting and unforeseen result with the VC assay was that the sham injections resulted in enhanced VC development in comparison to untreated animals. There are several possible explanations for this in that the injection site, small as it was, may have resulted in the release of growth factors that trigger a wound-healing cascade increasing the development of VCs (Cordeiro et al., 1999; Silverman and Hughes, 1990). Another possibility is that the media used in the sham injection injected into the subretinal space physically disrupts the debris layer changing the environment in the dystrophic retinae in favour of VC development, although this happens only in sites already susceptible to VC development (ventral retina). The sham injections were the true controls for the VC assay as they underwent the same procedures as both PEDF and echistatin treated retinae. The VCs found in the sham injections conformed to the same distribution and general morphology of those seen in the baseline experiment, they were slightly more numerous than in untreated retinae suggesting that sham injections did alter the development of the VCs.

Echistatin

Echistatin treated retinae exhibited large extended complexes mainly in the mid-ventral retinae far in advance of those seen in the baseline experiments of similar time points. These results were initially perplexing as previous *in vitro* studies suggested that RPE motility would be decreased by echistatin (Yang et al., 1996) not increased as seen in this assay by comparing the relative area covered by VCs. The results may be explained by several works which showed that the binding specificity of echistatin was much wider than previously known in that it not only blocked RGD sites affecting $\alpha_v\beta_3$ but also blocked $\alpha_5\beta_1$ which is involved in RPE phagocytosis of ECM (Wierzbicka-Patynowski et al., 1999; Zhao et al., 1999). It was therefore quite likely that the application of echistatin resulted in further aggravating the genetic defect in the RPE of the dystrophic RCS rat thereby accelerating the formation of the vascular complexes.

Exactly why the RPE in the mid ventral retina should be affected more than other regions of the retina in RCS rats is currently unknown but as this is the area where the first VCs were found it is not surprising that this is where the effects of echistatin were most clear. The reduced numbers of pigment granules in the electron microscopy also points towards an effect on the RPE but the result showing a clear breach in Bruch's membrane (**figure 3.2.19c**) unlike mechanical damage was intriguing in that it suggested further effects on the extracellular matrix that may well exacerbate damage to the retina. The lack of any visible effects of echistatin on the Long Evans rat suggests that the concentration used was either not sufficient to impair RPE function (if that is how echistatin affects the retina) or the healthy retina possessed some mechanism of protection. The effects of Echistatin in this model were disappointing but there is a possible future role of inducing breaches in Bruch's mimicking AMD. There has recently been research into truncated echistatin analogues that specifically block single integrin pairs that would allow the experiment we originally envisaged to be carried out. Further, as more is learned about echistatins specificity/structure, it could be possible to block RPE phagocytosis entirely or target essential functions of other cell groups involved in retinal degeneration such as the vascular epithelium.

These results give hope that it may be possible to improve the underlying environment in more advanced cases of retinal degeneration thereby aiding therapeutic treatments that aim to correct or arrest the primary effects of human diseases of retinal degeneration.

3.3 The Effects Of ARPE19 Cells Transplanted Sub-Retinally In The RCS Rat On Vascular Complexes

3.3.1 Aims

The long term aim of creating the vascular complex assay system in the RCS model was to determine if it was possible to improve the chance of successful treatment in more advanced cases of retinal disease such as with a typical patient with progressive loss of vision where interventional treatment would likely be a late stage event. In the context of studies using retinal transplantation or cell-based therapies applied to the eye, the effects of introducing cells sub-retinally into the eye on the vascular complex assay had to be ascertained. The act of introducing cells sub-retinally substantially changes the environment of the retina and specifically in this study it was unclear how this would affect the vascular complexes exhibited in the RCS pathology.

By using a cell line of known characteristics (human RPE cells of the ARPE19 lineage) transplanted and then harvested at differing time points, we hoped to determine the following:

1.What would be the background effects of the xenotransplant procedure using the VC assay?

2.When would be the optimal time point for transplantation from the perspective of this assay?

3. When might be the optimal time to add therapeutic agents to the transplant?

3.3.2 Experiments

Our current research on retinal transplants has focused on the use of cell lines for the following reasons 1) for transplantation to be effective as a treatment, the cells must at least rescue visual function. 2) The cells must be safe to use, stable and extensively characterised. 3) It is impractical to screen primary cultures effectively for infectious pathogens (HIV, hepatitis) or potential pathogens (human variant BSE), the difficulty involved in preparing and purifying primary cultures limits their value for retinal transplantation. 4) The cells must be made easily available

A series of experiments was set up to determine how sub-retinal application of ARPE19 cells applied for differing time regimens would affect the development of vascular complexes in the RCS retina. The normal transplant regimen would be to administer

transplants at 21-25 days of age immediately after weaning as early as possible in the sequence of photoreceptor degeneration.

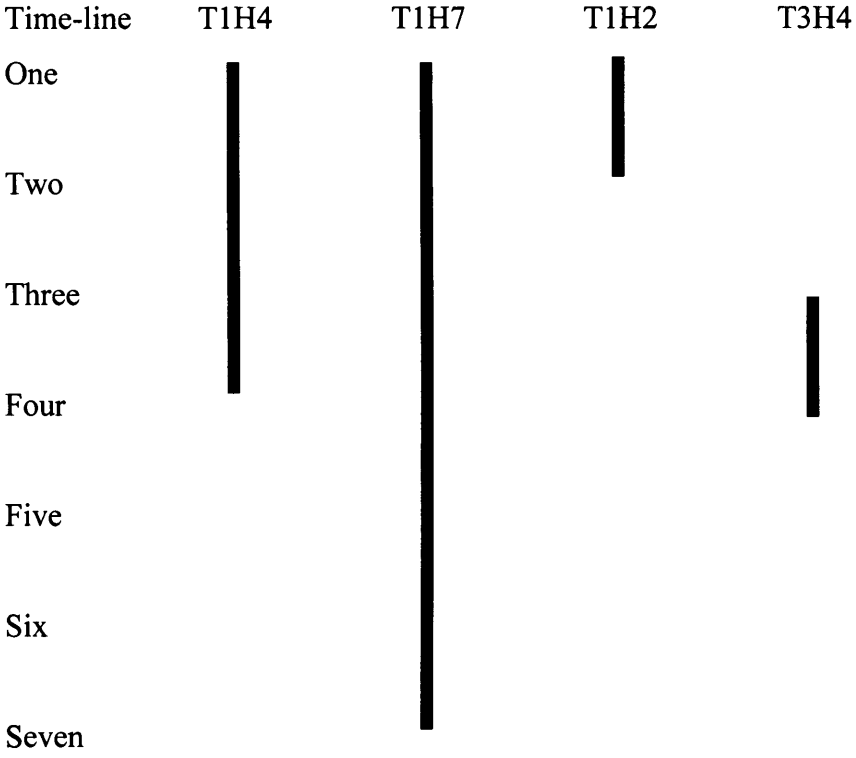

Figure 3.3.1 Time-line for original planned experiments (months) **Note** that early transplants actually occurred at 23-25 days not 1 month

T1H3 Transplantation at 1 month, harvested at 3 months.

Typical early transplantation before significant photoreceptor death and VC development. Flat mounting when VCs should be advanced and directly comparable with data from previous chapters.

T1H7 Transplantation at 1 month, harvested at 7 months.

Typical transplantation time with animals left for a much longer time point to determine long term effects of transplantation on VC development that would normally be very advanced.

T1H2 Transplantation at 1 month, harvested at 2 months.

Short term survival experiment to investigate how the transplanted RPE integrate into the retina and the effects of the transplant on the vascular system at a time-point where there should be no VCs present.

T3H4 Transplantation at 3 month, harvested at 4 months.

Late transplantation into the retina to determine effects on retina of introducing cells after significant vascular damage had occurred and the majority of photoreceptors had been lost.

All transplants were unilateral (left eye transplanted only) with the transplant placed in the ventral retina where it could provide local protection to the area most heavily damaged. The transplant procedure was carried out by the laboratory's resident eye surgeon, Dr Bin Lu as detailed in section **2.18**. All transplanted and sham animals were administered oral cyclosporine in their drinking water (210 mg/l) to minimise immune reactions to the transplants for the duration of the experiments under conditions identical to Coffey et al (Coffey et al., 2002).

3.3.3 Transplantation At 23 Days, Harvested At 4 Months

Initially as a trial, several litters of dystrophic RCS underwent the transplantation procedure. The animals were transplanted at P23 to introduce the transplant as early as possible before the dysfunctional RPE could cause major photoreceptor damage. These trial animals were left until they were four months old before harvesting and removal of their eyes to be processed for the VC assay. By four months there would normally be very few photoreceptors left in the dystrophic RCS rat retina but previous work in our laboratory had shown that sub-retinal transplants prolonged visual function past this time point (Coffey et al., 2002). This group consisted of 16 animals of which 4 were sham animals (injected with media only) and 12 were given human ARPE19 transplants of approx $2x10^5$ cells in 2 µl of media (DMEM F12, Invitrogen)
These animals were harvested and their retinae flat-mounted as discussed in section **2.4**.

Unfortunately the staining failed due to fluctuations in the temperature during the incubation phase of the NADPH-d reaction. But a clear initial result of this experiment was that in every retina that had a transplant there were no pigmented cells visible in areas where there would normally have been VCs (**figure 3.3.2**); however the vascular component of the VCs was not initially visible due to failure of the staining so the retinas were restained. The untreated right eyes exhibited normal pigmented cells in the central/mid ventral retina. This result was clear enough to warrant further investigation of flat-mounted transplants. Image analysis of this result was not performed due to there being nothing to quantify in the transplanted retinae. The shams from this pilot also exhibited pigmented cells signifying VCs. These retinae were later restained

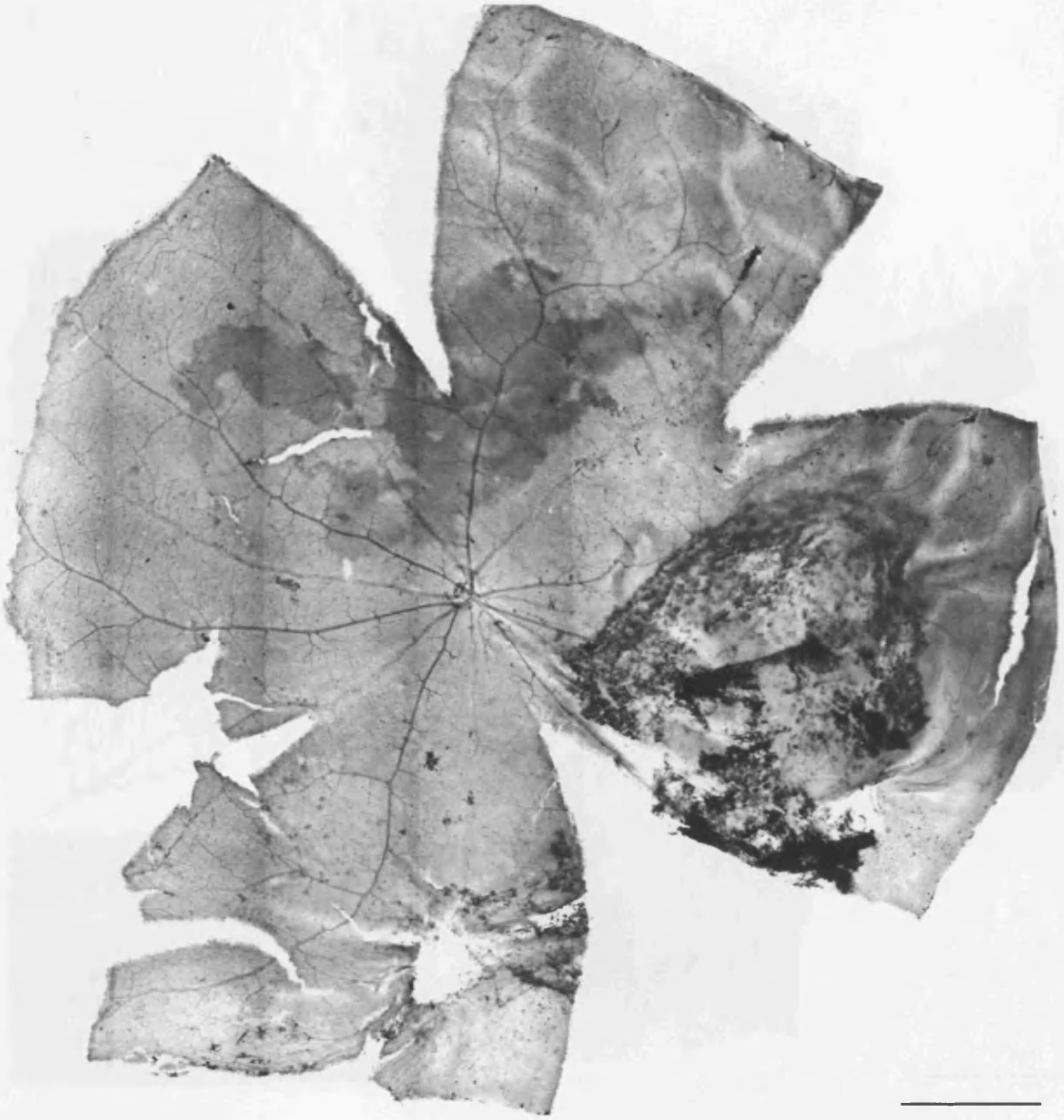

Figure 3.3.2 Pilot transplant experiment. A four month old dystrophic retina that has received a sub-retinal injection of ARPE19 cells at P23. This image has been restained with NADPH-d and consequently had much higher background colouration, which has been removed by converting to a greyscale image. The hole in the ventral retina is where the injection site formed attachments to the retina, which had to be dissected out on flat-mounting. The transplant site can be clearly seen in the temporal retina (this was a left eye) and the lack of vascular complexes noted even though the vascular staining is not optimal. Scale bar represents 1000μm

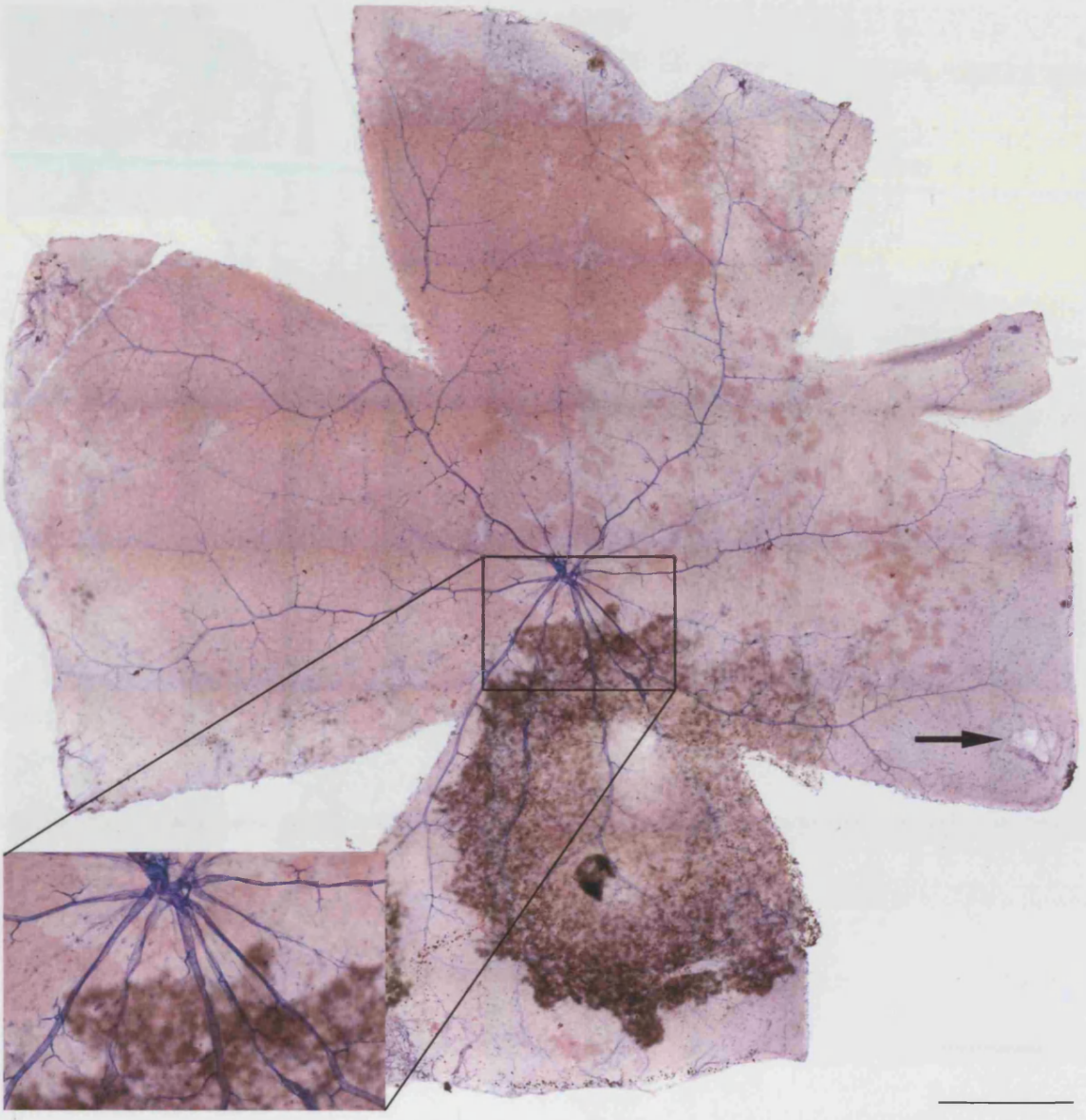

Figure 3.3.3 A four month old dystrophic retina showing an ARPE19 transplant injected at P23. Note the much smaller injection site in the temporal quadrant (arrow) that improved with practise from the first experiment. Also the lack of VCs and extent of the transplant are much clearer than in **figure 3.3.2.** Scale bar represents 1000μm.

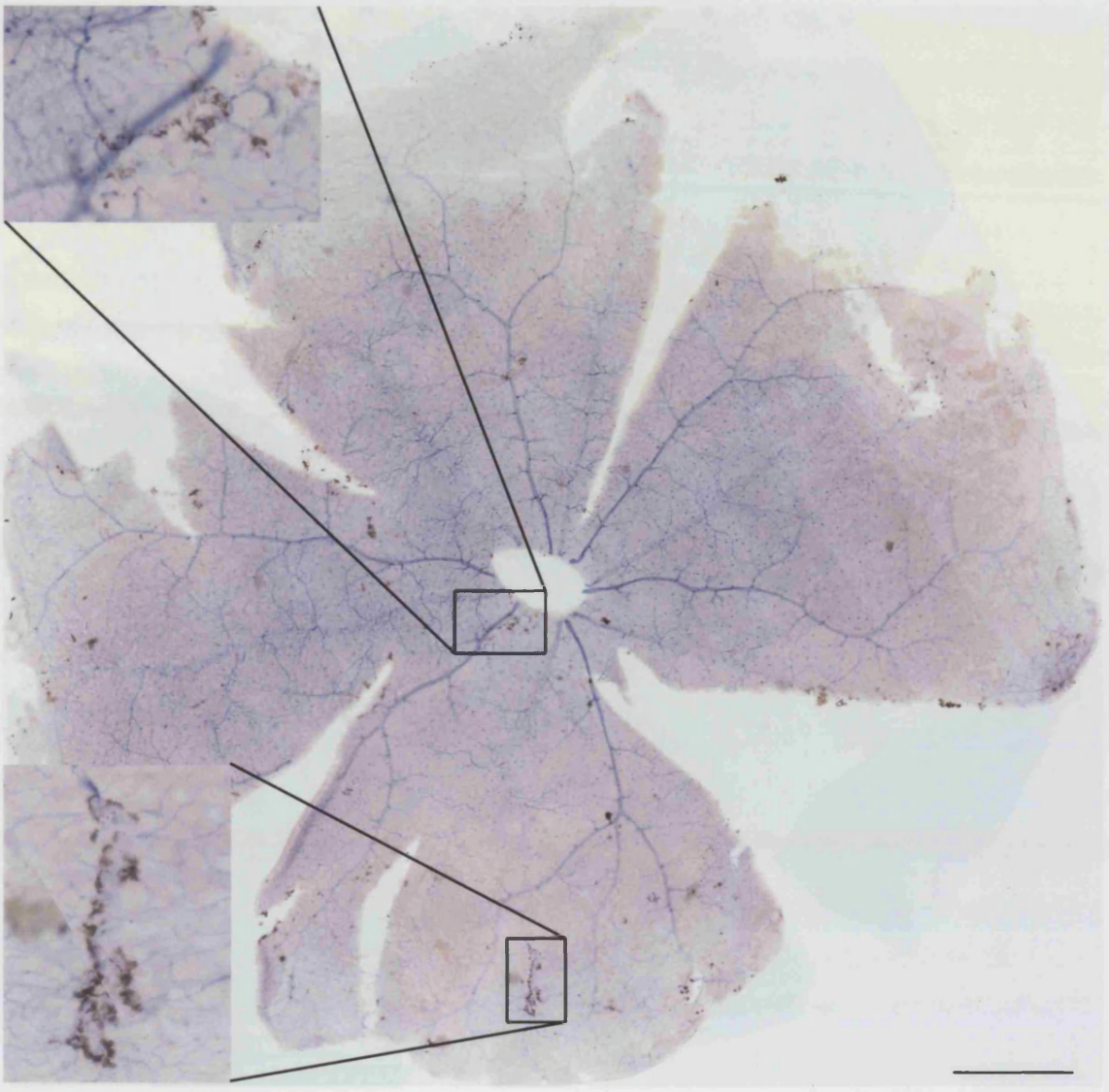

Figure 3.3.4 A four month old sham from the same experiment as **figure 3.3.3**. This retina has several extensive VCs (inserts a & b). Scale bar represents 1000μm

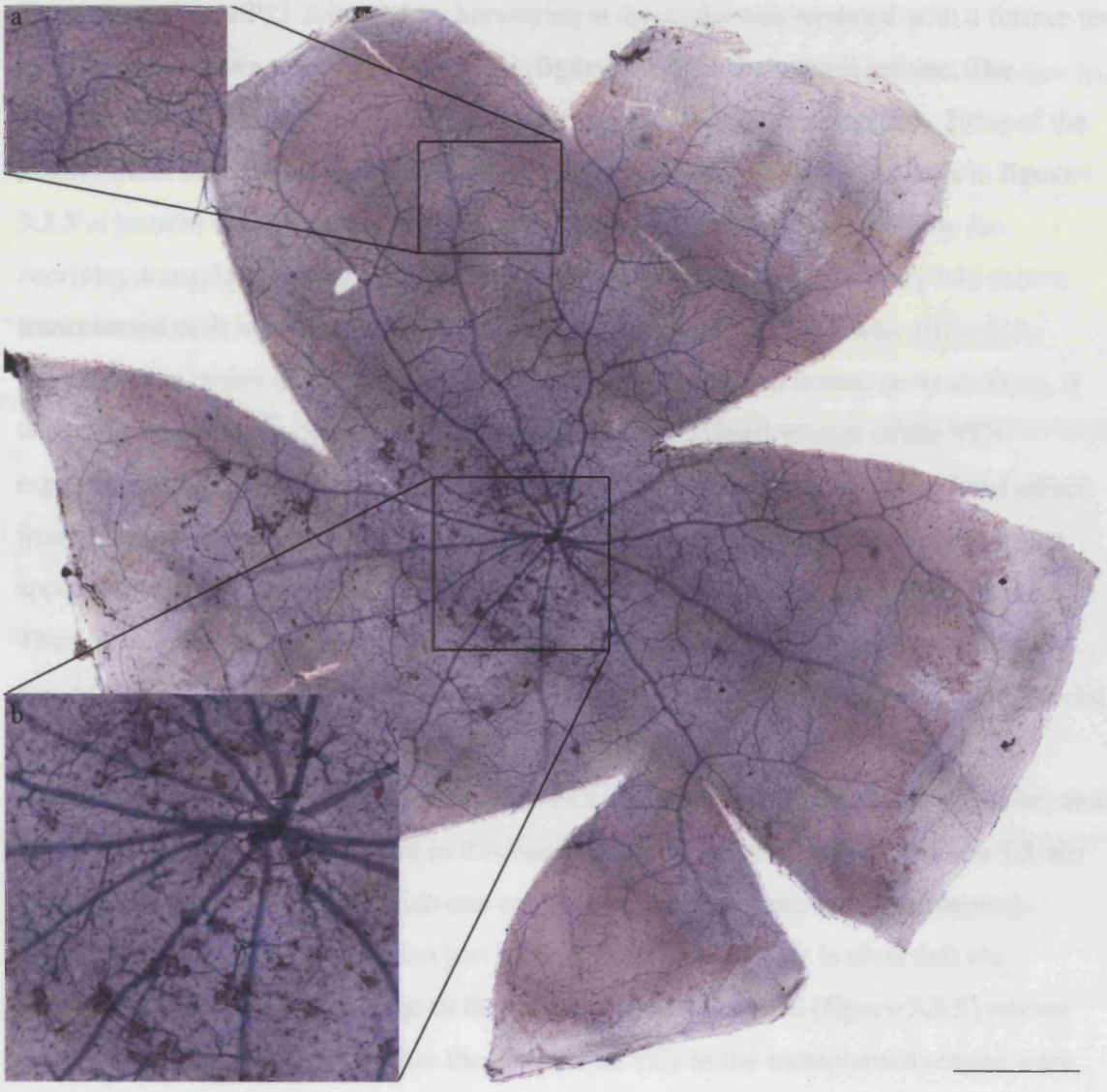

Figure 3.3.5 Untreated four month dystrophic control from the same experiment as **figure 3.3.3**. The vascular complexes are comparable to four month baseline RCS with the dorsal retina clear of VCs (insert a) and the optic disk to mid-ventral retina exhibiting clear VCs (insert b). Scale bar represents 1000μm.

Transplantation at P23 followed by harvesting at 4 months was repeated with a further ten animals, again there were no VCs visible (**figure 3.3.3**) in the ventral retinae. The transplant could be clearly seen and was attached over a wide area (approx. 20%) of the ventral/nasal retina. The transplant was robustly attached to the retina as seen in **figure 3.3.3** at present this provides the most complete picture we have seen on how far surviving transplant had spread. Recent histological work in out laboratory had shown transplanted cells significant distances from the transplant site but it was difficult to determine the extent of the transplant in the retina from stained frozen cross sections. It was clear from this study that the effect on retarding the development of the VCs, especially around the optic disc extended further than was accountable for a local effect from the transplanted cells. Therefore the transplants mode of protection for the retina appeared to involve protecting against VC formation at a distance from the transplant. There were a lot of pigmented cells in the transplant area (as expected as the transplant was of RPE cells) but they were not in the same focal plane as any VCs and therefore did cause any confusion with VC associated pigmented cells.

Sham (**figure 3.3.4**) retinae exhibited clear VCs around the optic disc (**figure 3.3.4a**) and out in the peripheral retina where in this case some unusually large VCs (**figure 3.3.4b**) had developed. The sham injection site could be seen in the ventral retina (arrows) positioned at the edge of the retina just behind the ciliary body, it is clear that the injection caused minimal damage to the retina. Untreated retinae (**figure 3.3.5**) retinae also exhibited clear VCs, therefore the absence of VCs in the transplanted retinae were due to the ARPE19 cells placed subretinally in the ventral quadrant of the eye. In total 70 animals received either ARPE19 transplants or sham injections in their left eyes as outlined below in **figure 3.3.6**: right eyes were used as unoperated controls.

Timing	ARPE19 trans.	Sham	Untreated
T1H4	26	10	39
T1H2	8	0	8
T1H7	11	6	16
T3H4	5	0	5

Figure 3.3.6 Retinae used. Once more there were a few retinae lost in dissection

3.3.4 Transplantation At 23 Days, Harvest Six Months Later

In order to assess the long-term effectiveness of the results seen in section **3.3.2** another batch of animals were transplanted and left until the animals were seven months old.

Retinae from these animals as shown in **figure 3.3.7** exhibited numerous small VCs that were comparable to some untreated four month old baseline retinae(**figure 3.1.6**), this indicated that the transplanted ARPE19 cells have had some effect in reducing the development of VCs. This also matches previous work by Seaton(Seaton et al., 1994) but shows that they used time-points too late to see the complete effect. The transplant site could be clearly seen in the ventral retina where it occupied roughly 10% of the retina. This was a reduction of roughly 50% from the transplant size at three-month survival and was expected as previous studies in our laboratory had shown that transplant effects declined over time (Lund et al., 2001a). The untreated retinae were as expected with large VCs present, especially around the optic disc as seen in **figure 3.3.8** insert. The sham retinae exhibited more VCs than the transplanted retinae and also than the untreated retinae but not by a significant margin. This may confirm data from section **3.2** where the sham controls were found to exhibit more area under VCs than untreated retinae The shams were not directly comparable with the pharmaceutical intervention shams as they used sub-retinal injections rather that the intravitreal route used in section **3.2**. The transplanted retinas were roughly comparable with four month old baseline material (**figure 3.1.5**), not as should be expected for a seven month old dystrophic RCS. The ARPE19 cells have managed to slow the development of VCs in the retinae six months after transplantation

Figure 3.3.7 Dystrophic RCS rat retina at 7 months of age having received ARPE19 transplant at P23 days of age. The insert shows the area around the optic disc, which was lightly populated with VCs. The transplant is clearly visible extending from the ventral periphery well into the mid-ventral retina. Scattered VCs were found throughout the mid-peripheral ventral retina spreading into the nasal retina. Scale bare represents 1000 μm.

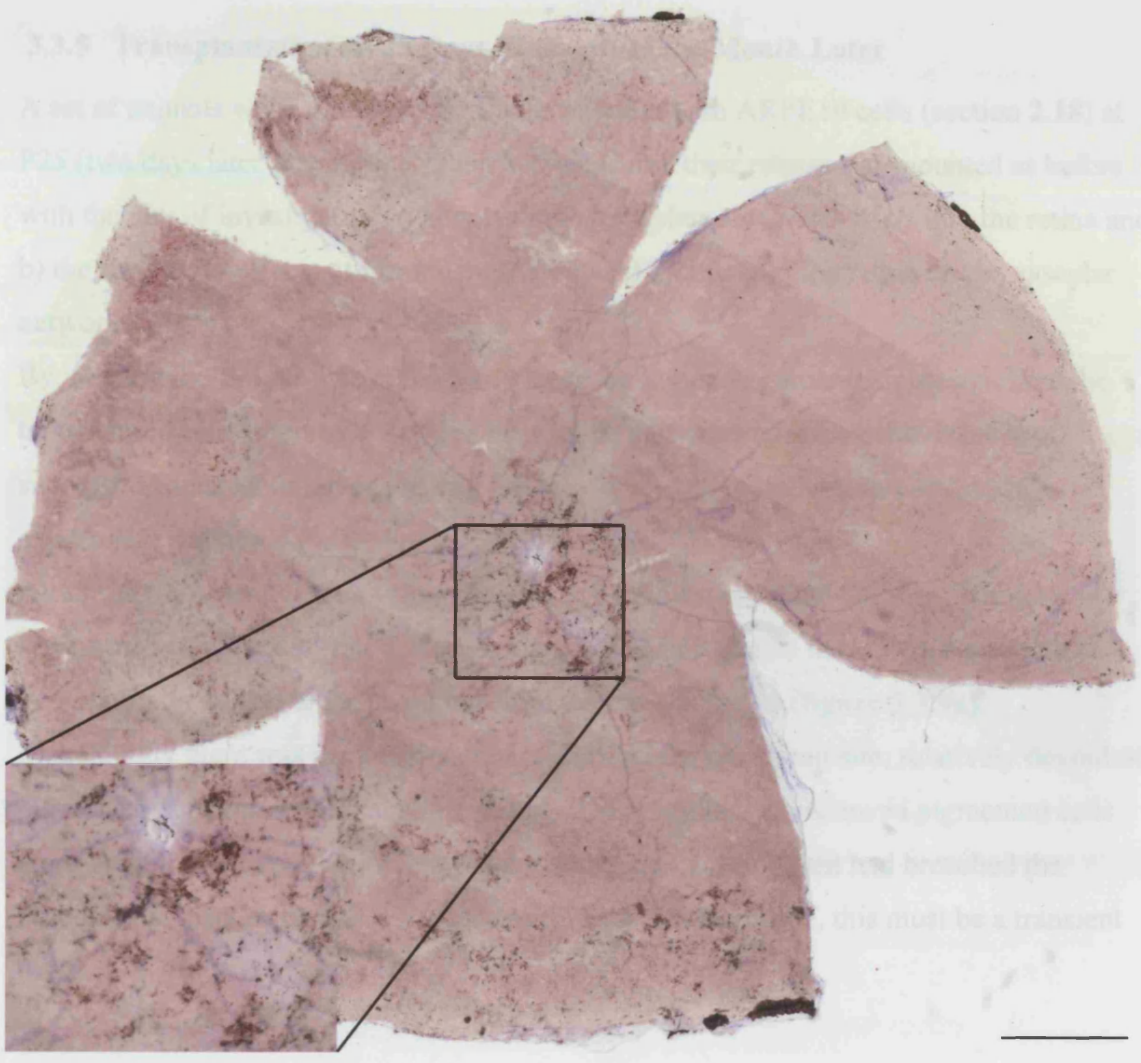

Figure 3.3.8 Untreated dystrophic RCS rat retina from same animal as **figure 3.3.7**. NADPH-d staining not as pronounced but pigmented cells were still visible. VCs were much more numerous than transplanted material especially around the optic disc (insert). Scale bar represents 1000 μm.

3.3.5 Transplantation At 25 Days, Harvested One Month Later

A set of animals were submitted for transplantation with ARPE19 cells (section **2.18**) at P25 (two days later than normal) then harvested and their retinas flat-mounted as before with the aim of investigating a) how well the transplant integrates itself into the retina and b) the short term effects of introducing foreign RPE cells into the retina on the vascular network.

By viewing the flat-mounts at this early stage we hoped to gather insights into how the transplanted cells interacted with the host retina in order to improve the chances of successful transplantation or prolong the effects seen in the pilot transplantation experiment (section **3.3.2**).

All of the transplanted retinae harvested at two months exhibited the same startling appearance (**figure 3.3.9**) in that these appeared at first glance to be VCs attached to vasculature in a large area spread out from the transplant site (**figure 3.3.9a**).

Interestingly there was a zone immediately around the transplant site, relatively devoid of pigmented cells but with intact vasculature. The transplant site showed pigmented cells along with limited cellular infiltrate suggesting that the transplant had breached the blood/retinal barrier, as this was not seen in the 4 month retinae, this must be a transient event.

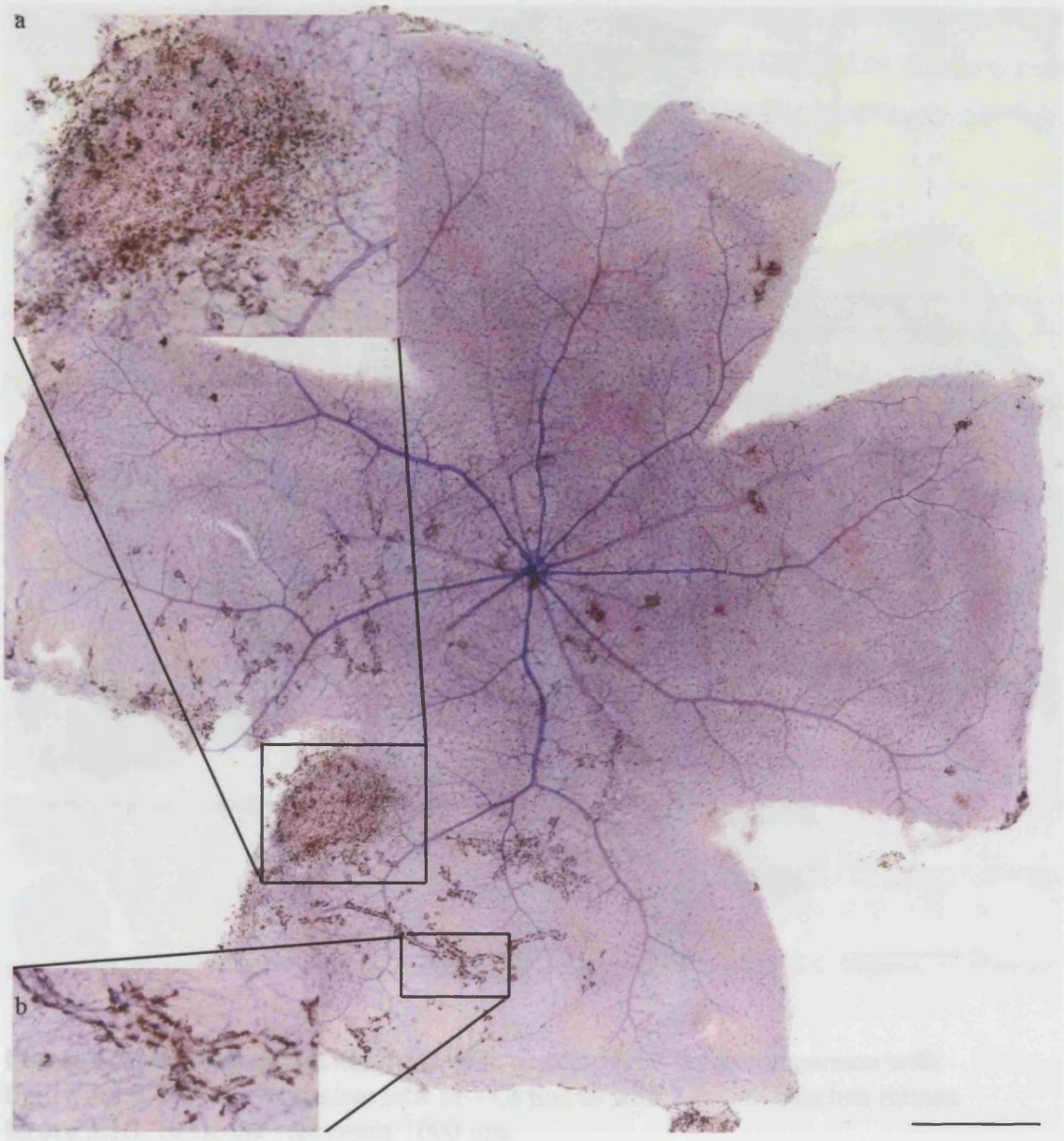

Figure 3.3.9 A two month old dystrophic retina after ARPE19 transplantation at p23. The transplant area can be clearly seen (insert a). Note the abnormal VCs seen along vessels but without apparently damaging them (insert b). Scale bar represents 1000 μm.

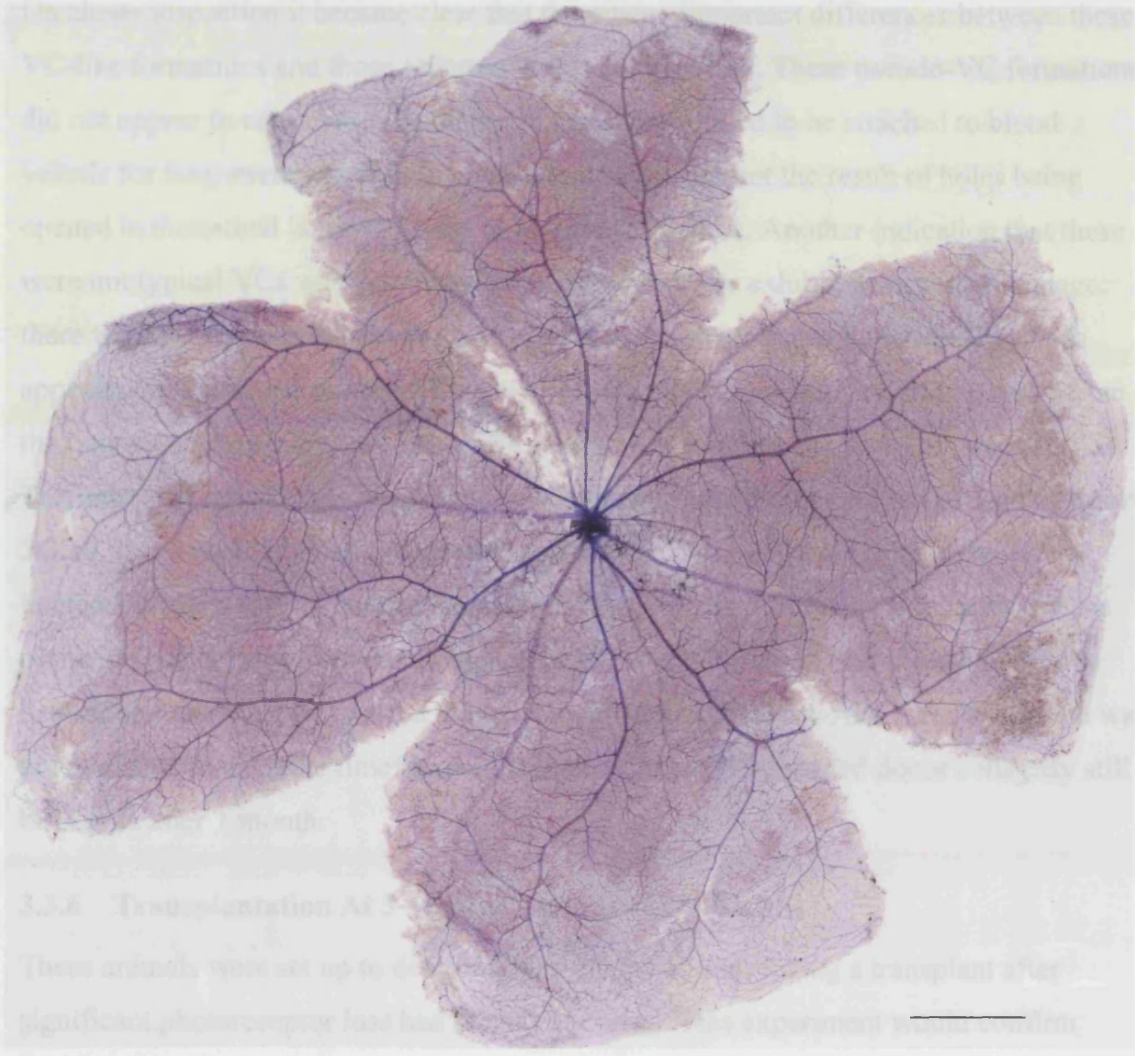

Figure 3.3.10 A two month old dystrophic untreated retina for comparison with **figure 3.3.9**. Note the complete lack of VCs just as with 2 month baseline retinae **figure 3.1.1**. Scale bar represents 1000 μm.

On closer inspection it became clear that there were important differences between these VC-like formations and those reported in this study earlier. These pseudo-VC formations did not appear to cause vascular disruption and they tended to be attached to blood vessels for long stretches. This suggested that they were not the result of holes being opened in the retinal lamination due to photoreceptor loss. Another indication that these were not typical VCs was that the underlying vasculature exhibited very little damage: there were no abnormal loops or signs of new vascular growth and the capillary beds appeared intact. These pseudo-VCs were possibly pigmented cells migrating away from the transplant site by the only basement membrane available, the vascular network. The untreated retinae at two months showed the normal vascular pattern as seen in **figure 3.3.10**. It is very likely that the transplant procedure temporarily disrupted the retinal lamination allowing RPE to migrate onto the vasculature. It remains to be seen if these pigmented cells were from the transplant or the host RPE layer. The easiest method to determine this would be to use a human specific antibody to the ARPE19 cells which was not available to us in the timeframe of this study, also GFP labelled donor cells may still be visible after 1 month.

3.3.6 Transplantation At 3 Months, Harvest At 4 Months

These animals were set up to determine the effects of introducing a transplant after significant photoreceptor loss had already occurred. This experiment would confirm whether the effects seen in section **3.3.2** were caused by the interaction of the transplanted RPE with the naturally degenerating photoreceptors or independent of the presence of photoreceptors as our previous hypothesis required photoreceptors to be absent for VCs to develop; therefore late transplantation when photoreceptors had been greatly reduced should result in development of VCs.

Retinae that received transplants at three months of age (**figure 3.3.11**) exhibited advanced VCs for their time point with a few examples of the pseudo VCs found in section **3.3.4** but the majority were composed of the more typical dystrophic RCS VCs found after photoreceptors had been lost. These VCs had all of the characteristics that had been described earlier in this study with abnormal vascular loops, distended deep draining veins and destruction of the capillary bed especially around the optic disc (insert).

The transplant site was visible just as with the one-month survival transplants in section **3.3.5** with associated cellular infiltrate but the VCs were if anything worse that expected for a four-month-old dystrophic RCS retinae. The insert in **figure 3.3.11** shows advanced VCs that had started to combine into an extended network of VCs. These VCs were destroying the capillary bed and would eventually limit the blood supply to the peripheral retina. The peripheral retina had numerous examples of the smaller single pigmented cells attached to the venous system indicative of VC formation. The transplant in this experiment provided no protection to the retina; in fact late placement of the transplant appeared to be detrimental to the retinal vasculature in the dystrophic RCS rat model of retinal degeneration. This suggested that the effects seen in section **3.3.2** were dependent on photoreceptor survival and that the transplanted ARPE19 cells may have been responsible for rescuing the host photoreceptors.

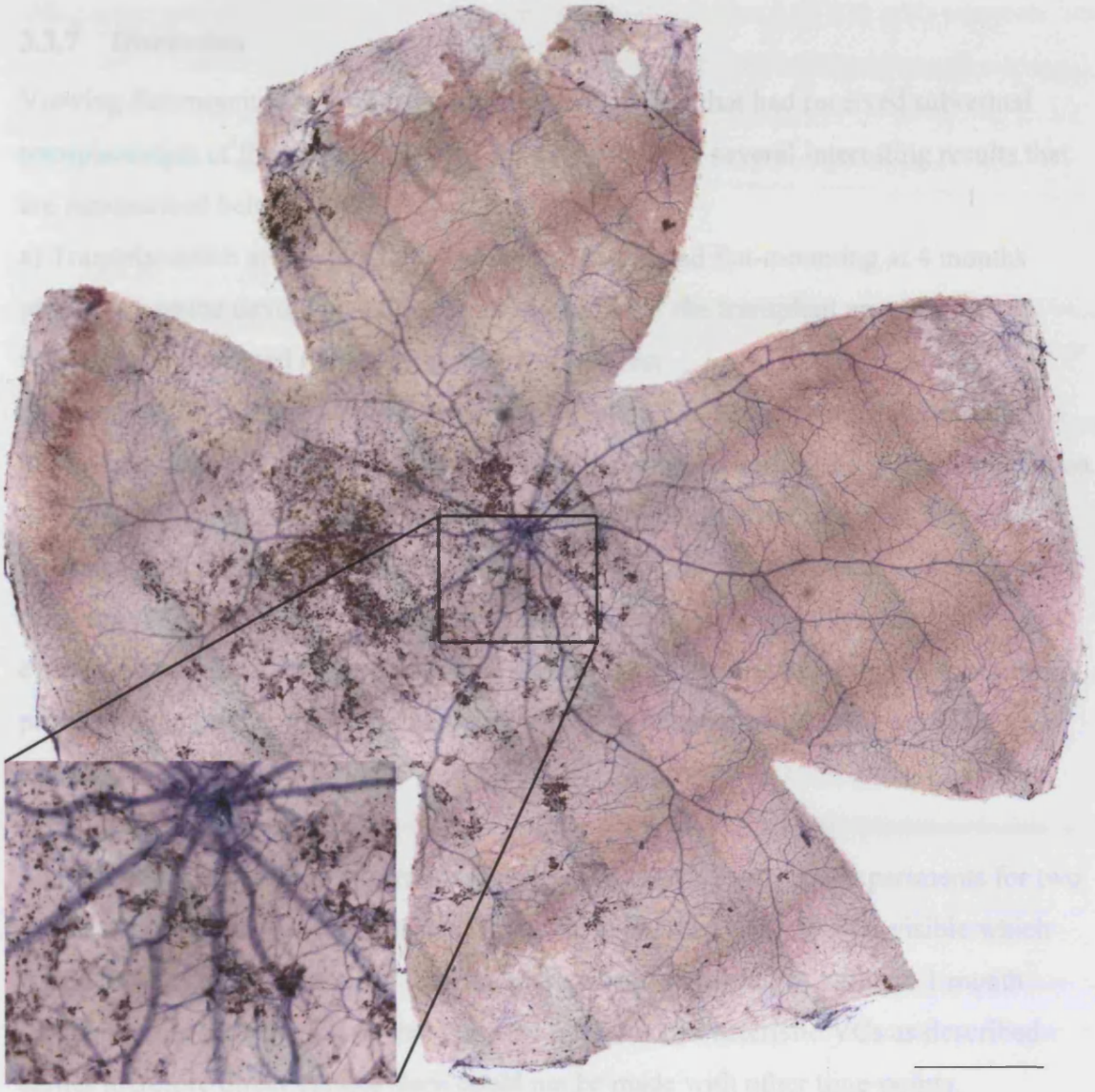

Figure 3.3.11 A four month old dystrophic retina after ARPE19 transplantation at P90. The extensive VCs are clearly visible especially around the optic disk (insert). The transplant area is not as clearly defined as in other experiments. Scale bar represents 1000 μm.

3.3.7 Discussion

Viewing flat-mounted retinae from dystrophic RCS rats that had received subretinal transplantation of the human ARPE19 cell line produced several interesting results that are summarised below:

a) Transplantation at 23 days followed by harvesting and flat-mounting at 4 months produces a retina devoid of VCs with an indication of the transplant area.

b) Sham and untreated retinae do not show this effect

c) Transplantation at 23 days followed by harvesting and flat-mounting at 7 months produced a reduced number of VCs relative to the controls with a smaller transplant area.

d) Transplantation at 25 days followed by harvesting and flat-mounting at 2 months produced an extreme amount of pigmented cells without vascular damage, presumably this eventually develops into situation a) above.

e) Transplantation at 3 months followed by harvesting and flat-mounting at 4 months produces many more VCs than untreated with significant damage to the vascular network.

The VC assay with image analysis was not used on these transplant experiments for two reasons: a) with the three month survival transplants there were no VCs visible which would have made the sham and untreated assay data irrelevant, b) with the 1 month survival transplants the pigmented cells did not form characteristic VCs as described earlier therefore direct comparisons could not be made with other time-points.

We know from previous lab work (Coffey et al., 2002; Girman et al., 2003; Lund et al., 2001a; Wang et al., 2005b) and current studies that the ARPE19 transplants provided some protection to the photoreceptors in the dystrophic RCS model. Depending on which parameters were tested, these transplants have been shown to rescue some vision as late as nine months of age in the RCS rat, which is effectively blind at three to four months (Girman et al., 2003). This appeared to work by protecting rod photoreceptors, which in this model were largely non-functional from an early age but they in turn ensured that the cone photoreceptors survived to provide the limited vision(Girman et al., 2005) (Leveillard et al., 2004). For these transplants to be effective we believe that they must be performed at as young an age as possible (immediately after weaning), before significant photoreceptor loss. We did not expect that the transplants would totally negate the formation of VCs at four months.

What these experiments have shown is a snapshot of how the ARPE19 cells integrate into the retina (1 month survival), protect the retina from vascular damage (3 month survival) and finally as the transplant effect reduces over time the cascade of events leading to VC formation once more continues (6 month survival).

Early One Month Survival

These transplants were at first glance confusing in that they showed an abundance of VCs that were not present in the later survival time-point at 4 months. Closer examination of the flat-mounts showed that there were several important differences to these supposed VCs in that they appeared to be encasing deep draining veins for long distances but were not associated with abnormal loops or serious constrictions of the vessels, also the capillary bed appeared undamaged. These factors indicated that these pseudo-VCs were not typical VCs seen in previous experiments in this study. There was an area clear of these pseudo-VCs around the transplant site. It appears that the transplant procedure disrupted the normal retinal environment (it would have resulted in a significant retinal detachment) sufficient to displace some of the RPE onto the vasculature even though there was still a significant photoreceptor layer in place. These errant pigmented cells must at some point after one month have then migrated back to the RPE layer or been cleared from the retina as they are not present two months later. This could be a phase involved in the integration of the transplant into the retina. A full investigation of these cells, using immunocytochemistry and electron microscopy to trace migration of these cells, was beyond the scope and time frame of this study.

The clear area around the transplant could be a result of the cellular infiltrate seen at the transplant site or be due to the RPE having migrated back to the RPE layer on Bruch's membrane more quickly local to the transplant. It is interesting that the transplant has attached at all to the retina as normally the RPE layer and Bruch's membrane would be removed by the flat-mounting protocol.

Three Month Survival

The three month survival transplants consistently produced retinae devoid of any VCs. Previous transplant experiments from our laboratory have demonstrated that ARPE19 cell transplants could rescue portions of the photoreceptor layer (Lund et al., 2001a; Wang et al., 2005a) in the vicinity of the transplant. One possible explanation of the lack of VCs in ARPE19 transplants at four months could be that the transplants rescue photoreceptors;

thereby blocking the RPE from coming into contact with the vasculature in the inner retina and forming VCs.

The transplant could be clearly seen and provided a useful indication of transplant extent in the retinae that could be useful to quantify transplant survival using image analysis. The effects of the transplant on VCs were clearly visible quite far from the closest margin of transplant suggesting that is effect was not limited to the location of the transplanted cells themselves. Recent work has shown photoreceptor rescue well beyond donor cell location (Wang et al., 2005b). Possibly a better test of this would be to place the transplant further from the epicentre of VC activity (dorsal to the optic disc). That said, in some retinae the closest extent of the transplant was as much as 2500 μm from the optic disc which in a retina averaging 9500 μm across was a significant distance. Therefore whatever the mode of action used to retard VC development in these experiments, it was effective over a distance. The sham and untreated retinae served as controls for the experiment and the animals respectively. Whatever the source of the pigmented cells along vessels in the one month survival retinae, none were in evidence two months later.

Six Month Survival

These retinae had VCs in evidence in a pattern that was seen for 4 month baseline dystrophic RCS flat-mounts, which as the animals were three months older suggested that the transplants were losing their effectiveness. Recent work in our laboratory has shown a reduction in donor cells over time (Wang et al., 2005b). Possibly the VC development was able to overcome the protection afforded by the transplant. The smaller transplant area suggests that the transplant may indicate a reduced effectiveness of the transplant over time. In each of these time points there has been a certain amount of cellular infiltrate visible around the transplant site that may also indicate that the protection provided by the oral cyclosporine-A was not adequate (Del Priore et al., 2003).

Late One Month Survival

From the stand-point of improving the chances of transplantation this experiment was not successful but it did provide interesting data in that it was clear that placing a transplant with its consequent retinal disruption into a retina which is already far down the cascade of degeneration results in a retina with enhanced damage to its vascular network. **Figure 3.3.11** clearly shows much more VCs than **figure 3.3.7** which was 3 months older. This result while not totally contradicting Seaton's work (Seaton et al., 1994) as it

did show reduced VCs, it highlights differences in models (pink vs. pigmented eyed RCS) and confirm that early intervention is better.

Summary

The original aims of this chapter were to determine the effects of the ARPE19 cell line transplants on the VC assay. This had interesting results in that at the correct application time and survival time-point of the procedure had been so successful that quantification using the assay was no longer relevant as there were no VCs present. It was clear that if the transplants were performed early enough in the cascade of events leading to VC formation, VC formation could be prevented from occurring for an extended period of time. Also it appeared that the mode of protection did not act directly but most likely through protection of the photoreceptor layer and that this protection was not limited to a local effect of the transplant.

To determine the optimal time-point for transplantation, further studies introducing transplants at possibly 1, 1.5 and 2 months of age would have to be performed but from the results of these experiments early transplantation would have the greatest chance of success. The optimal time point to add therapeutic agents would depend on the mode of action and target of the pharmaceutical in question, if photoreceptors for instance are the target then delivery should predate photoreceptor degeneration. The human ARPE19 cell line may in time prove not to be the best cell line to use but it was the best available for this study in that it had been extensively characterised and proven to be safe (Dunn et al., 1996; Kanuga et al., 2002). There is an established body of literature and experience from our laboratory and others in using ARPE19 cells(Girman et al., 2003; Lund et al., 2001a; Wang et al., 2005b) and they were proven to be effective in preserving vision as tested by electrophysiology and behavioural (Coffey et al., 2002; McGill et al., 2004) methods.

4.0 Discussion and Summary for "A study of the retinal vascular pathology in the RCS Rat..."

4.1 General Overview

4.1.1 Original Aims

The original aims of this study were to quantify the vascular abnormalities resulting from the retinal degeneration in the RCS rat and to modify those changes (Seaton and Turner, 1992; Villegas-Perez et al., 1998; Wang et al., 2003). After obtaining baseline data we proposed altering the dystrophic pathology with pharmaceutical intervention (LaVail et al., 1992; LaVail et al., 1998) and then with cell-based therapy intervention (Lund et al., 1997; Lund et al., 2003). While this study has largely achieved those initial aims, it has not been without some surprising results that have altered the original plan of investigation. 1) A reproducible method of quantifying the vascular changes seen in the dystrophic RCS rat has been achieved (Wang et al., 2003). 2) The normal vascular pathology has been modified by pharmaceutical intervention both for the better and for worse. 3) The effects of a cell based therapy using ARPE19 transplantation has been investigated with the conclusion that it too can affect vascular patterns and that early application appears to be important for efficacy. These results have also opened up further questions such as how does this model compare with other work (Seaton and Turner, 1992) and methods such as FA (Zambarakji et al., 2005), that lay outside the scope of this study.

Quantification of VCs has been attempted in the past using horseradish peroxidase-stained flat-mounts but HRP has the disadvantage of obscuring vasculature as soon as vessel leakage occurs and the animals used did not have pigmented retinas making VC counts difficult (Seaton et al., 1994; Seaton and Turner, 1992).

4.1.2 What Has This Study Achieved?

This study has provided a means of quantifying the vascular changes in the dystrophic RCS rat and in doing so has provided a novel assay system capable of testing anti-angiogenic pharmaceuticals *in vivo,* something that has been lacking in retinal anti-angiogenic research. The combination of flat-mounted NADPH-d staining with Image Pro Plus imaging software has allowed the development of the vascular complexes to be

visualised and quantified in a reproducible manner. This assay system could be used to test various pharmaceuticals and in addition, therapeutic strategies such as cell based therapies. The startling differences between the ARPE19 cells at three months after application compared with one month and six months after application clearly show that while the ARPE19 cells are not in themselves a long term solution, the cell based therapy strategy shows promise. The later application of ARPE 19 cells at three months showed that timing is critical for success.

4.1.3 Where Did It Deviate From The Original Plans?

There were several potential areas of study that were eventually abandoned for various reasons as the study progressed. The intention to study the damage to the axons of the retinal ganglion cells visualised with the RT97 antibody (Villegas-Perez et al., 1998; Wang et al., 2000) was the first casualty. It was found with the baseline study that only very light damage to the RGC axons occurred by 5 months in the RCS rat, therefore investigating RT97 staining patterns was outside of the range employed here. One of the goals of this study was to try to automate the quantification of the VCs as much as possible to remove user bias. This was one area that did not prove possible due to the nature of the VCs. As the VCs are a complex of migrated RPE, blood vessels and surrounding avascular space (Wang et al., 2003), it proved impossible to manipulate the images sufficiently using the program to allow accurate thresholding (the image target could not be differentiated from the retina background). It was decided that the most meaningful measure of the VCs was the area of retina that they occupied and the only accurate method of determining this was to trace AOI around the VCs. Possibly further advances in imaging technology could allow full automation of this assay.

It was originally intended that a full analysis of integrin antibody staining patterns would be accomplished using a time course of frozen dystrophic and non-dystrophic RCS tissues collected for comparison with the flat-mounted baseline. After commencing this part of the study it quickly became apparent that interpreting these patterns was not trivial and consultation with Dr Hodivala-Dilke (Barts and The London, Queen Mary's School of Medicine and Dentistry) resulted in her advising us that commercial integrin antibodies available at that time were not sufficient to the task. At this point the emphasis of the study centred more thoroughly on testing the assay system. In 2001 my host laboratory moved from the Institute of Ophthalmology, London to the Moran Eye Centre, Utah with

the result that we lost contact with Pfizer who were supplying us with PEDF. This had the effect of changing from our original plans to conduct pharmaceutical dosage experiments to investigating cell based therapies based on the ARPE19 cell line (Lund et al., 2001a). These studies were an update and improvement on the earlier attempts at quantification (Seaton and Turner, 1992). Echistatin experiments did continue in Utah using Long Evans and congenic RCS. Vitreous collected from baseline retinae were also frozen and stored potentially to investigate PEDF levels but after moving they were sent to another lab for proteomics analysis that unfortunately was not fruitful.

4.1.4 Problems Overcome

The largest problem that had to be overcome with this study was in finding a meaningful way of quantifying the VCs. The initial pigment foci count was adequate to show differences between different treatments but it produced very arbitrary results that were open to criticism of excessive operator bias (especially in resolving merged VCs) (Wang et al., 2003). It took advances in both imaging (colour digital cameras) and computer technology (personal computers with at least 2 Gb of RAM) to allow sufficiently large colour images to be assembled to form complete retinal maps of the entire retina. In total over 200 flat-mounts were imaged for this project which in turn presented problems in the volume of data to be stored: fortunately technology kept pace with development of the imaging equipment evolving from zip disks to optical disks to CDs to DVDs.

The NADPH-d staining methods proved to be excellent at producing low background permanently stained vascular networks but it did prove to be fairly demanding in its sensitivity to temperature. The NADPH-d reaction is enzyme based and therefore will not work if the reaction temperature fluctuates more than a few degrees centigrade off 37^0C. If the temperature is too low during the reaction, inadequate staining results with minor vessels being too faint to image. This could be remedied by carefully restaining with new reaction mixture but the result is rarely as good as freshly stained tissue. If the reaction temperature is too high excessive formazan salt is produced which adheres to the surface of the retina resulting in a dark blue retina which cannot be imaged in any way: entire experiments were lost to this problem.

4.2 Biological Mechanisms Of Retinal Disease

4.2.1 Relevance Of The RCS Model

The relevance of the RCS rat as a model of retinal degeneration was confirmed with the discovery of the Mertk (D'Cruz et al., 2000) gene and its human orthologue MERTK as form of RP (Gal et al., 2000), and later with the reversal of the phenotype by gene therapy (Vollrath et al., 2001). The present work has shown that the pigmented RCS rat could also be used as a valuable *in vivo* assay system to test antiangiogenic compounds. Controls were provided by using the congenic rats along with untreated dystrophics and sham controls (media or delivery vehicle only) for comparison with the treatment. Previous studies have noted that the delivery protocol can have effects on the retina (possibly due to growth factor release by the wound healing process) but these tend to be short lived (Lawrence et al., 2004; Sauve et al., 2002; Silverman and Hughes, 1990). This study makes no claims as to the status of photoreceptors or the inner retina, as it is solely concerned with visualising the vascular network and comparing the development of the characteristic vascular complexes. PEDF in particular could reduce vascular complexes by preserving photoreceptors (Cao et al., 2001; Cayouette et al., 1999) and therefore slowing the migration of RPE into the retina but semi-thin sections (**figure 3.2.14**) did not show significant differences even though Cayouette reported photoreceptor protection after nine days in the rd/rds mouse models (Cayouette et al., 1999). It is quite possible that the slower degeneration of the RCS (Davidorf et al., 1991) coupled with time-points chosen to focus on vascular damage rather than photoreceptor loss have masked this effect in this study.

4.2.2 RPE Phagocytosis

The debate about exactly how RPE phagocytose shed rod outer segments continues as different groups refine their arguments and experiments to determine whether integrins are essential or not (Finnemann, 2003; Finnemann and Rodriguez-Boulan, 1999; Finnemann and Silverstein, 2001; Hall and Abrams, 1987; Hall et al., 2003; Hall et al., 2001). The RCS rat is involved in this debate by virtue of its mutation being a tyrosine kinase involved in phagocytosing the rod outer segments (D'Cruz et al., 2000). This assay may have some relevance to this argument as the vascular complexes are intimately linked to the RPE, which detach from Bruch's membrane and migrate onto the retinal vasculature (Wang et al., 2003). The trigger for this appears to be localised ischemia

destabilising or activating the RPE cells (Bailey et al., 2004; Kijlstra et al., 2005) possibly encouraging neovascularisation. The migration is presumably in search of favourable basement laminae to attach to. It could be argued that the development of the vascular complexes is not a secondary anatomical event following photoreceptor loss but due to disruptions in RPE interactions with each other or Bruch's membrane. The exact trigger will require the underlying mechanism of RPE phagocytosis to have been elucidated.

4.2.3 Relevance To Human Diseases

This study has shown several key points that are of interest to research into human retinal diseases: 1) The RCS rat can be used as a novel tool for assessing anti-angiogenic drugs *in vivo*. 2) The cell-based therapy strategy has been shown to temporarily reduce VC formation without the addition of anti-angiogenic drugs. Previous studies have used less accurate HRP staining with albino retinas which are not as accurate (Seaton et al., 1994) and similar techniques have been used to map neurons (Palanza et al., 2005). The fact that the treatment regime may alter the underlying vascular pathology is interesting and suggests that further modifying the cells may produce even greater results (Kanuga et al., 2002; Lawrence et al., 2004; Semkova et al., 2002). The effects of PEDF treatment described here are broadly in line with other published work suggesting effective anti-angiogenic activity even at very low concentrations (Cao et al., 2001).

4.3 Initial Baseline And Quantification Of Vascular Complexes

4.3.1 Development Of The Assay

The initial baseline experiments in which the flat-mount technology was developed to quantify the vascular complexes has proven to be a very effective guide for assessing how badly damaged the retinal vasculature was to the retinal changes. The use of NADPH-d staining on flat-mounted retinae produced a stable, clear representation of the entire vascular network that could be viewed by transmitted light microscopy (Diaz-Araya et al., 1993; Palanza et al., 2005; Vincent and Kimura, 1992; Wang et al., 2003; Wang et al., 2000; Zambarakji et al., 2005). Quantification of the vascular complexes was made possible by adapting image analysis techniques developed in our own laboratory (Villegas-Perez et al., 1998) and elsewhere (Danias et al., 2003; Danias et al., 2002) to count retinal ganglion cells back-labelled with Fluoro-gold. The original software consisted of three programs used serially to capture, assemble and then count the cells,

that was upgraded to a single program (Image Pro Plus 4.0, Media Cybernetics) capable of driving and calibrating the motorised stage and to capture/assemble the retinal maps. These first retinal maps, captured in greyscale images, very clearly displayed the changes in the RCS retina as the dystrophic pathology advanced but were only useful to provide pigment foci counts (Wang et al., 2003). It is interesting that the VCs develop in a fairly linear progression radiating out from a specific geographic area; the mid-ventral retina. This phenomenon has parallels in human RP (Milam et al., 1998).

4.3.2 Progression Of VCs Over Time

A decision was made very early on that five months would be the end point for initial study as previous work (Caldwell et al., 1989; Villegas-Perez et al., 1998) had shown that by 5 months vascular damage was relatively wide-spread in the dystrophic RCS retina and this study was targeting the development of VCs. The initial baseline studies confirmed that the first VCs appeared between two and three months of age with very small vascular complexes found in the mid-ventral retina (Wang et al., 2003). The pigment foci quantification was in accord with previous descriptive works and allowed the progression to experiments changing the profile of VC development (Caldwell et al., 1989; Essner et al., 1980; Villegas-Perez et al., 1998; Wang et al., 2003).

Correlation with vascular leakage using FA with cSLO technology was performed in a complementary study that showed leakage preceding and correlating with sites of VC formation (Zambarakji et al., 2005) For this study to be of value to designing treatment strategies for retinal degenerative diseases it had to show that the retinal vascular changes could at least be delayed or slowed. One unexpected result for which there was no obvious explanation was that the left eyes gave slightly lower readings than right. The differences between right and left affected the future work in that treatments were given to the left eye and the right was used as a control. This reduced the chance of VCs merging and to reduced variance in the VC assay data.

The initial pigment foci counts showed a clear progression of VC development but did not yet allow a very accurate means of quantification. Later improvements with the capture technology allowed the VC assay to reassess the flat-mounts producing a more meaningful data set. This method of using a histological stain to map the entire retina had the advantage of giving a global view of the retina whereas other techniques such as investigating vascular leakage with FA images could not cover the entire retina (Bellmann et al., 2003; Rosolen et al., 2002; Zambarakji et al., 2005).

4.3.3 Distribution of VCs

The quantification approach used here provided data on the overall development of VCs across the retina but it did not address their distribution although the digital retinal map could be manipulated to record positional data of each VC if required A peculiarity of the RCS pathology is that VC formation occurs first in the mid-ventral retina at branch points along one of the deep veins. The exact mechanism of this is not fully understood but it is possible that these vessels being closest to the photoreceptors are the first to come into contact with the aberrant RPE. Current data suggests that RPE are destabilised or activated by localised ischemia (Bailey et al., 2004; Kijlstra et al., 2005) and data from our lab has shown correlation with vessel wall fenestrations (Stewart and Tuor, 1994; Villegas-Perez et al., 1998) resulting in leakage preceding VC formation (Zambarakji et al., 2005). These may be related to the loss of photoreceptors and formation of the debris zone, destabilising the RPE. The aberrant RPE then migrate off Bruch's onto blood vessels causing further damage by interacting with the cells of the vessel wall causing fenestrations and breakdown of the BRB (Caldwell, 1989; Essner et al., 1980). Further studies investigating the microenvironment of the debris zone using laser microdisection combined with early detection of sites vascular leakage using FA and cSLO (Zambarakji et al., 2005) could confirm this hypothesis.

VCs spread outwards along smaller vessels throughout the ventral retina into nasal and temporal quadrants and in very advanced cases finally into the dorsal retina (Villegas-Perez et al., 1998; Wang et al., 2003; Wang et al., 2000). The distribution of VCs in the peripheral retina tends to be slightly different as where the retina thins towards the far periphery the three vascular plexus gradually merge into a single more sparse network without capillaries (Zhang, 1994). Individual pigmented cells could be found attached to the venous vasculature of the outer periphery suggesting less developed VCs. It is possible that they could be partially protected by growth factors such as basic fibroblast growth factor from the ciliary body (Li et al., 1997)

4.4 Changing The Pattern Of VC Progression

Both of the candidate molecules picked for this study significantly altered the progression of the VCs in the VC assay system, although it has to be said that echistatin did not show the effects that were predicted by previous literature (Yang et al., 1996).

The application of pharmaceuticals into the eye by trans-scleral injection caused a slight sham effect, perhaps due to growth factor release from the micro-wound through the retina (Silverman and Hughes, 1990) but this could be controlled for.

4.4.1 Effects of PEDF Treatment

PEDF was particularly effective in reducing the size of the VCs and generally seemed to slow down the development of VCs. It did not stop the development of VCs altogether but considering only two doses of 1 μg/2μl were administered this was encouraging. With more time, combinations of differing doses and longer treatment regimens, it may have been possible to provide longer lasting and more complete protection.
Treatment with PEDF also modified the distribution of VCs with fewer VCs forming near the optic disk. That PEDF was able to have such an effect was interesting considering other studies had shown that PEDF could be cleared within 24 hours (Wu and Becerra, 1996) of introduction to the vitreous suggesting that PEDF may have a trigger effect. Also of note is the finding that PEDF levels decrease with oxidative stress (Ohno-Matsui et al., 2001) therefore PEDF levels may be decreased around VCs. The recent finding that PEDF only inhibits new vessel formation (Tombran-Tink, 2005) is interesting as it may explain how PEDF slowed the formation of VCs. That it did not totally stop VC formation could also be due to vascular remodelling (Villegas-Perez et al., 1998).

Unlike other studies (Cayouette et al., 1999) PEDF did not show significant differences in photoreceptor survival with semi-thin histology. Although it is possible that there was transient protection to the photoreceptors that would not show up due to the longer time-points used in this study. As the highest concentration of PEDF is normally found in the IPM (Karakousis et al., 2001), the formation of the debris zone may well change this in the RCS rat affecting the survival of photoreceptors. PEDF is one of several factors regulating angiogenic events factors within the eye with vascular endothelial growth factors and fibroblast growth factor-2 stimulating angiogenesis and PEDF and thrombospondin-1 inhibiting angiogenesis (Aparicio et al., 2005), these factors tend to interact by altering the oxygen levels within tissues. Recent advances have greatly expanded the available knowledge of PEDF interactions within the retina (Barnstable and Tombran-Tink, 2004) as well as its structure and genetics (Tombran-Tink et al., 2005).

4.4.2 Effects Of Echistatin Treatment

Echistatin was a candidate molecule for this study as it had been proven to be an effective blocker of RGD integrins and it was hoped might block RPE migration as it had *in vitro* (Yang et al., 1996). This is not what happened while using the *in vivo* VC assay system. Instead echistatin actually advanced the development of VCs, producing very large complexes especially in the mid-ventral retina. Further experiments with Long Evans rats and later with congenic RCS (unpublished work) rats showed that echistatin is unlikely to induce VCs on animals that do not have an underlying retinal pathology such as the dystrophic RCS. It has been shown that echistatin can block a range of integrins; $\alpha_{IIb}\beta_3$, $\alpha_V\beta_3$, (Marcinkiewicz et al., 1996; Marcinkiewicz et al., 1997) and $\alpha_5\beta_1$ (Wierzbicka-Patynowski et al., 1999). Blocking of the integrin $\alpha_V\beta_3$ has been shown to affect RPE migration but in this study echistatin did not block migration, in fact it made it worse.

The electron microscopy data showed that there were differences in the RPE between PEDF and echistatin treatments with what appeared to be breaches in Bruch's membrane after echistatin treatment. These results opened up the possibility of inducing a more AMD like model in the RCS rat but closer examination of Bruch's membrane at the electron microscopic level did not show more breaches. The reason for these results may be peculiar to the RCS rat as attempts to induce VCs or retinal dysfunction with echistatin in both Long Evans and congenic RCS rats failed, even at higher doses, this was in accord with previous studies in rabbits with histology and ERG (Yang et al., 1996). The difference may lie in echistatin blocking $\alpha_5\beta_1$ which has been implicated in RPE phagocytosis of ECM fragments (Clegg et al., 2000). It is possible that by further interfering in the already compromised phagocytic capabilities of the dystrophic RCS RPE, echistatin may have destabilise the RPE in excess of the RCS pathology alone. This would explain why echistatin had no effect on non-dystrophic rats in this study.

4.4.3 Relevance Of Results To Human Diseases

The PEDF results are broadly in line with other studies in suggesting that PEDF may well be a possible treatment for human retinal diseases as this study has shown that it can be used to help control the vascular complexes found in the RCS pathology. PEDF is currently under FDA licence to GENVEC (Imai et al., 2005; Takita et al., 2003) to assess adenoviral vector expressing PEDF for human use. The echistatin result is more difficult

to assess even with the possibility of damage to Bruch's as there is a chance that it may be peculiar to the RCS model. Truncated echistatin analogues with greater specificity to specific integrins (Wierzbicka-Patynowski et al., 1999) may yet show promise with *in vivo* assay systems. Previous growth factor delivery studies have postulated that multiple factors would be required to protect retinas from retinal degeneration (LaVail et al., 1998).

4.5 Cell Based Therapies

The injection of cell aggregates into the sub-retinal space within the retina offers a promising stratagem to treat retinal degenerative diseases. In this study the VC assay was applied to current cell based therapy technology in our laboratory (Coffey et al., 2002; Girman et al., 2003; Lund et al., 2001a; Sauve et al., 2002). It had been noted previously that sub-retinal application of cells could change the vascular network in the RCS rat (Seaton et al., 1994; Seaton and Turner, 1992) but advances in technology and a better knowledge of the underlying problems (Lund et al., 2003; Wang et al., 2003) made this study necessary to quantify the vascular-changes inherent in cell based therapy.

4.5.1 The ARPE19 Cell Line

One of the most important aspects of cell-based therapies would be to use a cell source that is safe, easily obtainable and well defined in how it works. For these studies the human ARPE19 cell line was used (Kanuga et al., 2002) as they had been extensively characterised and had the advantages of being safe and easily available. ARPE19 cells had formed the basis of several previous studies with known efficacy (Coffey et al., 2002; Lund et al., 2001a; Wang et al., 2005b). As these cells constituted xenografts, immunosuppressant cyclosporine A (Novartis, Basel) was required to ensure that the cells were not rejected. The initial results of this part of the study were very startling in that there were no vascular complexes present at all at four months, at first this was thought to be an error but repetition of the experiment gave the same result. The presence of the ARPE19 cells had totally stopped the development of vascular complexes, throughout the entire retina while untreated controls and sham retinae were identical to the baseline studies (with identical immunosupression). This protection may be due to preservation of photoreceptors, which are known to be preserved by ARPE19 transplantation (Lund et al., 2001a) or production of growth factors (Kanuga et al., 2002; Wang et al., 2005b).

4.5.2 Timing Of Transplantation

The three other experiments explored the issue of timing of application and the duration of the ARPE19 efficacy. These comprised short duration (5 weeks) post application, long duration (6 months post application) and a short duration but late application (applied at 3 months with 4 week duration).

These experiments showed that the cell based therapy with ARPE19 cells had a transient beneficial effect, which very much depended on early application, probably before significant photoreceptor loss had occurred. These findings were very much in accord with previous findings from our laboratory (Coffey et al., 2002; Lawrence et al., 2000; Lund et al., 2001a; Lund et al., 1997) and others (Bressler, 2002). One month after application, pigmented cells were visible on the vasculature without apparently causing lasting damage These cells were clearly caused by the tranasplant as both untreated and shams at this time-point did not exhibit pigmented cells. This was unexpected as we had assumed that pigmented cells attached to vessels formed VCs but that may be specific to the extracellular environment. As cell-specific antibodies were not available in this study we could not distinguish between donor or recipient cells. This did show that introducing cells into the subretinal space will result in abnormal cellular migration of pigmented cells, which are not necessarily detrimental to the retinal anatomy as two months later they were not present. The late treatment-short timescale experiment showed that by providing the cell-based therapy too late, it is possible to make the situation even worse than if no treatment was given. This result is important for consideration with human patients as it shows that even if cell-based therapies provide an effective treatment, incorrect application could be detrimental to patient vision.

4.5.3 Integration Of The Cells?

The short duration experiment was particularly interesting in that it appeared to show pigmented cells migrating along blood vessels without causing permanent damage as that would have shown up in the standard VC assay of three month survival retinae. There were no signs of inflammatory cells in the ventral retina so it is unlikely that there was significant clearance by inflammatory cells. While the subretinal space is known to be an immune privileged site (Streilein et al., 2002) this depends on the maintenance of the BRB (Essner et al., 1980; Saishin et al., 2003), which cannot be guaranteed in cases of retinal degeneration (Bok, 2005) where vascular leakage is an early occurrence (Villegas-Perez et al., 1998; Zambarakji et al., 2005). The long term experiments showed that the

RCS pathology eventually overcame the treatment (probably due to rejection of the xenograft (Del Priore et al., 2003)) but the progress of VC development had been slowed. This treatment also gave an indication of the area of the transplant as is clearly seen in figure **3.3.3**.

4.5.4 Implications For Treatments

These experiments have several implications for treatment of human retinal diseases, firstly that cell-based therapy is promising strategy for these diseases but it is key that treatment take place as early as possible. Introducing cells into cases of advanced retinal degenerations would appear to have the effect of placing cells into an environment that is too hostile to support their survival let alone integration. The cells would be confronted with too many extracellular signals directing cells towards apoptotic cell death and be at best ineffective (Travis, 1998). Another consideration should be the age of donor cells as aged RPE cells may not be healthy (Boulton et al., 2004), secondly consideration should be given to the health of aged recipient retinas.

The effects of a transplant can be expected to extend out beyond its area of distribution, but much work remains to be done to extend the therapeutic time-scale of the effects. The ARPE19 cell line in its present form is unlikely to be used for human trials but modification of the cell line (Kanuga et al., 2002; Lund et al., 2001a; Turowski et al., 2004; Wang et al., 2005b) or the use of different cell types may well take this strategy further (Lawrence et al., 2004; Lawrence et al., 2000; Lund et al., 2003).

4.6 Future Directions

There are several areas covered in this study that could be taken further with the aim of improving the retinal vasculature in a photoreceptor degeneration model. The RCS rat is a good model for testing proof of principle in treating retinal diseases but it should be supplemented with additional models before moving forward to human trials.

4.6.1 Pharmaceutical Intervention

The VC assay was designed to test candidate anti-angiogenic molecules *in vivo* and to quantify the results. This system could be used for dosage and long-term survival studies allowing assessment of a large range of data on candidate molecules. Testing of candidate molecules for pharmaceutical intervention requires a model that has as few extraneous complications or contaminations as possible. A problem that occurs in models involving

tissue damage is that the treatment may be modulating wound healing and not be working on vascular changes alone (Semkova et al., 2003; Stitt et al., 2004).

4.6.2 Cell-Based Therapies

This system has shown that it is flexible enough to show the effects of cell-based therapies. Different cell types such as stem cells and Schwann cells (Lawrence et al., 2004; Lawrence et al., 2000) could be tested. Dosage studies could be conducted to determine fully the effects of this strategy on controlling the retinal vasculature. This should also include methods of differentiating the host cells from the donor cells so that the extent of the donor cell coverage could be determined. Immunocytological analysis of sectioned retinae could be used in conjunction with the VC assay to identify changes in the inner retina for comparison with the flat-mounted retinal maps. This could be done in addition to FA to determine vascular leakage (Zambarakji et al., 2005). Recent advances in this technology include moves to assess visual function (Del Priore et al., 2004; Lund et al., 2003; McGill et al., 2004; Sauve et al., 2004) and dissection of relative cone and rod contributions to functional vision (Girman et al., 2005) after application as well as a greater understanding of immunological factors affecting retinal diseases (Kijlstra et al., 2005; Streilein et al., 2002). Cell based therapies are more suited to growth factor delivery as gene therapy is limited by the payload of the constructs currently used making cell based therapy the only strategy capable of delivering multiple growth factors from a single application.

4.6.3 Gene Therapy

Gene therapy has the potential to correct retinal degenerative disorders with a defined genetic component, making it one of the most exciting future strategies available to combat human retinal diseases (Imai et al., 2005). Animal models have already provided proof of principle for correction of models with known human orthologues (Acland et al., 2001; Vollrath et al., 2001). Retinal vascular disorders are also being targeted (Akiyama et al., 2004; Bainbridge et al., 2002; Bainbridge et al., 2003) with the aim of reducing the vascular components of retinal diseases. As the number of genes identified in retinal degenerations grows the possibilities for gene therapy improve, online databases such as RetNet (Daiger et al.) keep track of the latest advances. Gene therapy is not without its disadvantages as concerns about safety and controlling dosage delivered still need to be worked out. Recent advances in AMD research may offer hope to the widest range of

patients with complement H polymorphism identified in nearly half of all AMD patients (Edwards et al., 2005; Haines et al., 2005; Klein et al., 2005), by far the most significant grouping of genes yet discovered.

4.7 Conclusions

Vascular pathology accompanies photoreceptor degeneration in the RCS rat. It progresses in a manner that is amenable to quantification and can be modified by pharmaceutical intervention and other strategies such as cell-based therapies. In any treatment designed to modify the course of retinal degeneration the changes occurring in the vascular complexes need to be addressed.

5.0 Bibliography for " A Study of the retinal vascular pathology of the RCS rat"

Abdel-Meguid, A., Lappas, A., Hartmann, K., Auer, F., Schrage, N., Thumann, G., and Kirchhof, B. (2003). One year follow up of macular translocation with 360 degree retinotomy in patients with age related macular degeneration. Br J Ophthalmol *87*, 615-621.

Abdelsalam, A., Del Priore, L., and Zarbin, M. A. (1999). Drusen in age-related macular degeneration: pathogenesis, natural course, and laser photocoagulation-induced regression. Surv Ophthalmol *44*, 1-29.

Abecasis, G. R., Yashar, B. M., Zhao, Y., Ghiasvand, N. M., Zareparsi, S., Branham, K. E., Reddick, A. C., Trager, E. H., Yoshida, S., Bahling, J., *et al.* (2004). Age-related macular degeneration: a high-resolution genome scan for susceptibility loci in a population enriched for late-stage disease. Am J Hum Genet *74*, 482-494.

Acland, G. M., Aguirre, G. D., Ray, J., Zhang, Q., Aleman, T. S., Cideciyan, A. V., Pearce-Kelling, S. E., Anand, V., Zeng, Y., Maguire, A. M., *et al.* (2001). Gene therapy restores vision in a canine model of childhood blindness. Nat Genet *28*, 92-95.

Adler, A. J., and Evans, C. D. (1985). Proteins of the bovine interphotoreceptor matrix: retinoid binding and other functions. Prog Clin Biol Res *190*, 65-88.

Ahnelt, P. K., and Kolb, H. (2000). The mammalian photoreceptor mosaic-adaptive design. Prog Retin Eye Res *19*, 711-777.

Akiyama, H., Tanaka, T., Itakura, H., Kanai, H., Maeno, T., Doi, H., Yamazaki, M., Takahashi, K., Kimura, Y., Kishi, S., and Kurabayashi, M. (2004). Inhibition of ocular angiogenesis by an adenovirus carrying the human von Hippel-Lindau tumor-suppressor gene in vivo. Invest Ophthalmol Vis Sci *45*, 1289-1296.

Alberdi, E., Hyde, C. C., and Becerra, S. P. (1998). Pigment epithelium-derived factor (PEDF) binds to glycosaminoglycans: analysis of the binding site. Biochemistry *37*, 10643-10652.

Allikmets, R., Singh, N., Sun, H., Shroyer, N. F., Hutchinson, A., Chidambaram, A., Gerrard, B., Baird, L., Stauffer, D., Peiffer, A., *et al.* (1997). A photoreceptor cell-specific ATP-binding transporter gene (ABCR) is mutated in recessive Stargardt macular dystrophy. Nat Genet *15*, 236-246.

Ambati, J., Anand, A., Fernandez, S., Sakurai, E., Lynn, B. C., Kuziel, W. A., Rollins, B. J., and Ambati, B. K. (2003). An animal model of age-related macular degeneration in senescent Ccl-2- or Ccr-2-deficient mice. Nat Med *9*, 1390-1397.

Anderson, D. H., Fisher, S. K., and Steinberg, R. H. (1978). Mammalian cones: disc shedding, phagocytosis, and renewal. Invest Ophthalmol Vis Sci *17*, 117-133.

Anderson, D. H., Johnson, L. V., and Hageman, G. S. (1995). Vitronectin receptor expression and distribution at the photoreceptor-retinal pigment epithelial interface. J Comp Neurol *360*, 1-16.

Aparicio, S., Sawant, S., Lara, N., Barnstable, C. J., and Tombran-Tink, J. (2005). Expression of angiogenesis factors in human umbilical vein endothelial cells and their regulation by PEDF. Biochem Biophys Res Commun *326*, 387-394.

Araki, T., Taniwaki, T., Becerra, S. P., Chader, G. J., and Schwartz, J. P. (1998). Pigment epithelium-derived factor (PEDF) differentially protects immature but not mature cerebellar granule cells against apoptotic cell death. J Neurosci Res *53*, 7-15.

AREDS (2001). A randomized, placebo-controlled, clinical trial of high-dose supplementation with vitamins C and E, beta carotene, and zinc for age-related macular degeneration and vision loss: AREDS report no. 8. Arch Ophthalmol *119*, 1417-1436.

Arnell, H., Mantyjarvi, M., Tuppurainen, K., Andreasson, S., and Dahl, N. (1998). Stargardt disease: linkage to the ABCR gene region on 1p21-p22 in Scandinavian families. Acta Ophthalmol Scand *76*, 649-652.

Augustin, A. J., D'Amico, D. J., Mieler, W. F., Schneebaum, C., and Beasley, C. (2004). Safety of posterior juxtascleral depot administration of the angiostatic cortisene anecortave acetate for treatment of subfoveal choroidal neovascularization in patients with age-related macular degeneration. Graefes Arch Clin Exp Ophthalmol.

Ausprunk, D. H., Knighton, D. R., and Folkman, J. (1975). Vascularization of normal and neoplastic tissues grafted to the chick chorioallantois. Role of host and preexisting graft blood vessels. Am J Pathol *79*, 597-628.

Aydin, P., Akova, Y. A., and Kadayifcilar, S. (2000). Anterior segment indocyanine green angiography in scleral inflammation. Eye *14 (Pt 2)*, 211-215.

Bailey, T. A., Kanuga, N., Romero, I. A., Greenwood, J., Luthert, P. J., and Cheetham, M. E. (2004). Oxidative stress affects the junctional integrity of retinal pigment epithelial cells. Invest Ophthalmol Vis Sci *45*, 675-684.

Bainbridge, J. W., Mistry, A., De Alwis, M., Paleolog, E., Baker, A., Thrasher, A. J., and Ali, R. R. (2002). Inhibition of retinal neovascularisation by gene transfer of soluble VEGF receptor sFlt-1. Gene Ther *9*, 320-326.

Bainbridge, J. W., Mistry, A. R., Thrasher, A. J., and Ali, R. R. (2003). Gene therapy for ocular angiogenesis. Clin Sci (Lond) *104*, 561-575.

Balciuniene, J., Johansson, K., Sandgren, O., Wachtmeister, L., Holmgren, G., and Forsman, K. (1995). A gene for autosomal dominant progressive cone dystrophy (CORD5) maps to chromosome 17p12-p13. Genomics *30*, 281-286.

Barnstable, C. J., and Tombran-Tink, J. (2004). Neuroprotective and antiangiogenic actions of PEDF in the eye: molecular targets and therapeutic potential. Prog Retin Eye Res *23*, 561-577.

Bayes, M., Rabasseda, X., and Prous, J. R. (2004). Gateways to clinical trials. Methods Find Exp Clin Pharmacol *26*, 587-612.

Belisario, M. A., Tafuri, S., Di Domenico, C., Della Morte, R., Squillacioti, C., Lucisano, A., and Staiano, N. (2000). Immobilised echistatin promotes platelet adhesion and protein tyrosine phosphorylation. Biochim Biophys Acta *1497*, 227-236.

Bellhorn, R. W., Burns, M. S., and Benjamin, J. V. (1980). Retinal vessel abnormalities of phototoxic retinopathy in rats. Invest Ophthalmol Vis Sci *19*, 584-595.

Bellmann, C., Rubin, G. S., Kabanarou, S. A., Bird, A. C., and Fitzke, F. W. (2003). Fundus autofluorescence imaging compared with different confocal scanning laser ophthalmoscopes. Br J Ophthalmol *87*, 1381-1386.

Bennett, J. (2004). Gene therapy for Leber congenital amaurosis. Novartis Found Symp *255*, 195-202; discussion 202-197.

Bernstein, M. H. (1985). The interphotoreceptor matrix and the interphotoreceptor space of the vertebrate retina. Scan Electron Microsc, 859-868.

Berson, E. L., Rosner, B., Sandberg, M. A., Weigel-DiFranco, C., Moser, A., Brockhurst, R. J., Hayes, K. C., Johnson, C. A., Anderson, E. J., Gaudio, A. R., *et al.* (2004a). Clinical trial of docosahexaenoic acid in patients with retinitis pigmentosa receiving vitamin A treatment. Arch Ophthalmol *122*, 1297-1305.

Berson, E. L., Rosner, B., Sandberg, M. A., Weigel-DiFranco, C., Moser, A., Brockhurst, R. J., Hayes, K. C., Johnson, C. A., Anderson, E. J., Gaudio, A. R., *et al.* (2004b). Further evaluation of docosahexaenoic acid in patients with retinitis pigmentosa receiving vitamin A treatment: subgroup analyses. Arch Ophthalmol *122*, 1306-1314.

Besharse, J., and Defoe, D. (1998). Role of the retinal pigment epithelium in photoreceptor turnover, In The Retinal Pigment Epithelium, M. Marmor, and T. Wolfensberger, eds. (New York: Oxford University Press).

Besharse, J. C., Hollyfield, J. G., and Rayborn, M. E. (1977). Turnover of rod photoreceptor outer segments. II. Membrane addition and loss in relationship to light. J Cell Biol *75*, 507-527.

Bhattacharya, G., Miller, C., Kimberling, W. J., Jablonski, M. M., and Cosgrove, D. (2002). Localization and expression of usherin: a novel basement membrane protein defective in people with Usher's syndrome type IIa. Hear Res *163*, 1-11.

Bialek, S., and Miller, S. S. (1994). K+ and Cl- transport mechanisms in bovine pigment epithelium that could modulate subretinal space volume and composition. J Physiol *475*, 401-417.

Bird, A. C., Bressler, N. M., Bressler, S. B., Chisholm, I. H., Coscas, G., Davis, M. D., de Jong, P. T., Klaver, C. C., Klein, B. E., Klein, R., and et al. (1995). An international classification and grading system for age-related maculopathy and age-related macular degeneration. The International ARM Epidemiological Study Group. Surv Ophthalmol *39*, 367-374.

Bok, D. (2005). Evidence for an inflammatory process in age-related macular degeneration gains new support. Proc Natl Acad Sci U S A *102*, 7053-7054.

Bosch, E., Horwitz, J., and Bok, D. (1993). Phagocytosis of outer segments by retinal pigment epithelium: phagosome-lysosome interaction. J Histochem Cytochem *41*, 253-263.

Boulton, M., Roanowska, M., and Wess, T. (2004). Ageing of the retinal pigment epithelium: implications for transplantation. Graefes Arch Clin Exp Ophthalmol *242*, 76-84.

Bowes, C., Li, T., Danciger, M., Baxter, L. C., Applebury, M. L., and Farber, D. B. (1990). Retinal degeneration in the rd mouse is caused by a defect in the beta subunit of rod cGMP-phosphodiesterase. Nature *347*, 677-680.

Bowmaker, J. K. (1998). Evolution of colour vision in vertebrates. Eye *12 (Pt 3b)*, 541-547.

Bowne, S. J., Daiger, S. P., Hims, M. M., Sohocki, M. M., Malone, K. A., McKie, A. B., Heckenlively, J. R., Birch, D. G., Inglehearn, C. F., Bhattacharya, S. S., *et al.* (1999). Mutations in the RP1 gene causing autosomal dominant retinitis pigmentosa. Hum Mol Genet *8*, 2121-2128.

Bressler, N. M. (2002). Early detection and treatment of neovascular age-related macular degeneration. J Am Board Fam Pract *15*, 142-152.

Brown, P. K., Gibbons, I. R., and Wald, G. (1963). The Visual Cells And Visual Pigment Of The Mudpuppy, Necturus. J Cell Biol *19*, 79-106.

Bundey, S., and Crews, S. J. (1984a). A study of retinitis pigmentosa in the City of Birmingham. I Prevalence. J Med Genet *21*, 417-420.

Bundey, S., and Crews, S. J. (1984b). A study of retinitis pigmentosa in the City of Birmingham. II Clinical and genetic heterogeneity. J Med Genet *21*, 421-428.

Bunker, C. H., Berson, E. L., Bromley, W. C., Hayes, R. P., and Roderick, T. H. (1984). Prevalence of retinitis pigmentosa in Maine. Am J Ophthalmol *97*, 357-365.

Burns, M., and T., L. (2003). Visual Transduction by Rod and Cone Photoreceptors, In The Visual Neurosciences, L. Chalupa, and J. Werner, eds. (Cambridge, Massachusetts: MIT Press), pp. 215-234.

Caldwell, R. B. (1989). Extracellular matrix alterations precede vascularization of the retinal pigment epithelium in dystrophic rats. Curr Eye Res *8*, 907-921.

Caldwell, R. B., Roque, R. S., and Solomon, S. W. (1989). Increased vascular density and vitreo-retinal membranes accompany vascularization of the pigment epithelium in the dystrophic rat retina. Curr Eye Res *8*, 923-937.

Campochiaro, P. A. (2000). Retinal and choroidal neovascularization. J Cell Physiol *184*, 301-310.

Campochiaro, P. A., and Hackett, S. F. (2003). Ocular neovascularization: a valuable model system. Oncogene *22*, 6537-6548.

Cao, W., Tombran-Tink, J., Chen, W., Mrazek, D., Elias, R., and McGinnis, J. F. (1999). Pigment epithelium-derived factor protects cultured retinal neurons against hydrogen peroxide-induced cell death. J Neurosci Res *57*, 789-800.

Cao, W., Tombran-Tink, J., Elias, R., Sezate, S., Mrazek, D., and McGinnis, J. F. (2001). In vivo protection of photoreceptors from light damage by pigment epithelium-derived factor. Invest Ophthalmol Vis Sci *42*, 1646-1652.

Cayouette, M., Smith, S. B., Becerra, S. P., and Gravel, C. (1999). Pigment epithelium-derived factor delays the death of photoreceptors in mouse models of inherited retinal degenerations. Neurobiol Dis *6*, 523-532.

Cepko, C. L., Austin, C. P., Yang, X., Alexiades, M., and Ezzeddine, D. (1996). Cell fate determination in the vertebrate retina. Proc Natl Acad Sci U S A *93*, 589-595.

Chaitin, M. H., and Hall, M. O. (1983). The distribution of actin in cultured normal and dystrophic rat pigment epithelial cells during the phagocytosis of rod outer segments. Invest Ophthalmol Vis Sci *24*, 821-831.

Chan-Ling, T., Gock, B., and Stone, J. (1995). The effect of oxygen on vasoformative cell division. Evidence that 'physiological hypoxia' is the stimulus for normal retinal vasculogenesis. Invest Ophthalmol Vis Sci *36*, 1201-1214.

Chang, C. W., Chu, G., Hinz, B. J., and Greve, M. D. (2003). Current use of dietary supplementation in patients with age-related macular degeneration. Can J Ophthalmol *38*, 27-32.

Chen, Q., Cai, S., Shadrach, K. G., Prestwich, G. D., and Hollyfield, J. G. (2004). Spacrcan binding to hyaluronan and other glycosaminoglycans. Molecular and biochemical studies. J Biol Chem *279*, 23142-23150.

Chong, N. H., and Bird, A. C. (1998). Alternative therapies in exudative age related macular degeneration. Br J Ophthalmol *82*, 1441-1443.

Cideciyan, A. V., Hood, D. C., Huang, Y., Banin, E., Li, Z. Y., Stone, E. M., Milam, A. H., and Jacobson, S. G. (1998). Disease sequence from mutant rhodopsin allele to rod and cone photoreceptor degeneration in man. Proc Natl Acad Sci U S A *95*, 7103-7108.

Cinader, B., Jeejeebhoy, H. F., Koh, S. W., and Rabbat, A. G. (1971). Immunosuppressive and graft-rejecting anti--bodies in heterologous anti-lymphocytic serum. J Exp Med *133*, 81-99.

Clegg, D. O., Mullick, L. H., Wingerd, K. L., Lin, H., Atienza, J. W., Bradshaw, A. D., Gervin, D. B., and Cann, G. M. (2000). Adhesive events in retinal development and function: the role of integrin receptors. Results Probl Cell Differ *31*, 141-156.

Coffey, P. J., Girman, S., Wang, S. M., Hetherington, L., Keegan, D. J., Adamson, P., Greenwood, J., and Lund, R. D. (2002). Long-term preservation of cortically dependent visual function in RCS rats by transplantation. Nat Neurosci *5*, 53-56.

Connell, G., Bascom, R., Molday, L., Reid, D., McInnes, R. R., and Molday, R. S. (1991). Photoreceptor peripherin is the normal product of the gene responsible for retinal degeneration in the rds mouse. Proc Natl Acad Sci U S A *88*, 723-726.

Cordeiro, M. F., Schultz, G. S., Ali, R. R., Bhattacharya, S. S., and Khaw, P. T. (1999). Molecular therapy in ocular wound healing. Br J Ophthalmol *83*, 1219-1224.

Cox, D., Aoki, T., Seki, J., Motoyama, Y., and Yoshida, K. (1994). The pharmacology of the integrins. Med Res Rev *14*, 195-228.

Cuenca, N., Pinilla, I., Sauve, Y., Lu, B., Wang, S., and Lund, R. D. (2004). Regressive and reactive changes in the connectivity patterns of rod and cone pathways of P23H transgenic rat retina. Neuroscience *127*, 301-317.

Cunha-Vaz, J. G. (2004). The blood-retinal barriers system. Basic concepts and clinical evaluation. Exp Eye Res *78*, 715-721.

Curley, G. P., Blum, H., and Humphries, M. J. (1999). Integrin antagonists. Cell Mol Life Sci *56*, 427-441.

Custer, N. V., and Bok, D. (1975). Pigment epithelium-photoreceptor interactions in the normal and dystrophic rat retina. Exp Eye Res *21*, 153-166.

D'Cruz, P. M., Yasumura, D., Weir, J., Matthes, M. T., Abderrahim, H., LaVail, M. M., and Vollrath, D. (2000). Mutation of the receptor tyrosine kinase gene Mertk in the retinal dystrophic RCS rat. Hum Mol Genet *9*, 645-651.

Daiger, S., Sullivan, L., and Bowne, S. RetNet, http://www.sph.uth.tmc.edu/RetNet/ (University of Texas Houston Health Science Center).

Danias, J., Lee, K. C., Zamora, M. F., Chen, B., Shen, F., Filippopoulos, T., Su, Y., Goldblum, D., Podos, S. M., and Mittag, T. (2003). Quantitative analysis of retinal ganglion cell (RGC) loss in aging DBA/2NNia glaucomatous mice: comparison with RGC loss in aging C57/BL6 mice. Invest Ophthalmol Vis Sci *44*, 5151-5162.

Danias, J., Shen, F., Goldblum, D., Chen, B., Ramos-Esteban, J., Podos, S. M., and Mittag, T. (2002). Cytoarchitecture of the retinal ganglion cells in the rat. Invest Ophthalmol Vis Sci *43*, 587-594.

Davidorf, F. H., Mendlovic, D. B., Bowyer, D. W., Gresak, P. M., Foreman, B. C., Werling, K. T., and Chambers, R. B. (1991). Pathogenesis of retinal dystrophy in the Royal College of Surgeons rat. Ann Ophthalmol *23*, 87-94.

Davies, N. P., and Morland, A. B. (2004). Macular pigments: their characteristics and putative role. Prog Retin Eye Res *23*, 533-559.

Dawson, D. W., Volpert, O. V., Gillis, P., Crawford, S. E., Xu, H., Benedict, W., and Bouck, N. P. (1999). Pigment epithelium-derived factor: a potent inhibitor of angiogenesis. Science *285*, 245-248.

DeCoster, M. A., Schabelman, E., Tombran-Tink, J., and Bazan, N. G. (1999). Neuroprotection by pigment epithelial-derived factor against glutamate toxicity in developing primary hippocampal neurons. J Neurosci Res *56*, 604-610.

Del Priore, L. V., Ishida, O., Johnson, E. W., Sheng, Y., Jacoby, D. B., Geng, L., Tezel, T. H., and Kaplan, H. J. (2003). Triple immune suppression increases short-term survival of porcine fetal retinal pigment epithelium xenografts. Invest Ophthalmol Vis Sci *44*, 4044-4053.

Del Priore, L. V., Kaplan, H. J., Hornbeck, R., Jones, Z., and Swinn, M. (1996). Retinal pigment epithelial debridement as a model for the pathogenesis and treatment of macular degeneration. Am J Ophthalmol *122*, 629-643.

Del Priore, L. V., Tezel, T. H., and Kaplan, H. J. (2004). Survival of allogeneic porcine retinal pigment epithelial sheets after subretinal transplantation. Invest Ophthalmol Vis Sci *45*, 985-992.

Delori, F. C., Goger, D. G., and Dorey, C. K. (2001). Age-related accumulation and spatial distribution of lipofuscin in RPE of normal subjects. Invest Ophthalmol Vis Sci *42*, 1855-1866.

Diaz-Araya, C. M., Provis, J. M., and Billson, F. A. (1993). NADPH-diaphorase histochemistry reveals cone distributions in adult human retinae. Aust N Z J Ophthalmol *21*, 171-179.

Dowling, J. E., and Sidman, R. L. (1962). Inherited retinal dystrophy in the rat. J Cell Biol *14*, 73-109.

Dunn, K. C., Aotaki-Keen, A. E., Putkey, F. R., and Hjelmeland, L. M. (1996). ARPE-19, a human retinal pigment epithelial cell line with differentiated properties. Exp Eye Res *62*, 155-169.

Edwards, A. O., Ritter, R., 3rd, Abel, K. J., Manning, A., Panhuysen, C., and Farrer, L. A. (2005). Complement factor H polymorphism and age-related macular degeneration. Science *308*, 421-424.

Eichers, E. R., Green, J. S., Stockton, D. W., Jackman, C. S., Whelan, J., McNamara, J. A., Johnson, G. J., Lupski, J. R., and Katsanis, N. (2002). Newfoundland rod-cone dystrophy, an early-onset retinal dystrophy, is caused by splice-junction mutations in RLBP1. Am J Hum Genet *70*, 955-964.

Elizabeth Rakoczy, P., Yu, M. J., Nusinowitz, S., Chang, B., and Heckenlively, J. R. (2006). Mouse models of age-related macular degeneration. Exp Eye Res *82*, 741-752.

Elner, S. G., and Elner, V. M. (1996). The integrin superfamily and the eye. Invest Ophthalmol Vis Sci *37*, 696-701.

Espinosa-Heidmann, D. G., Sall, J., Hernandez, E. P., and Cousins, S. W. (2004). Basal laminar deposit formation in APO B100 transgenic mice: complex interactions between dietary fat, blue light, and vitamin E. Invest Ophthalmol Vis Sci *45*, 260-266.

Essner, E., Pino, R. M., and Griewski, R. A. (1980). Breakdown of blood. Retinal barrier in RCS rats with inherited retinal degeneration. Lab Invest *43*, 418-426.

Eyetech-study-group (2003). Anti-vascular endothelial growth factor therapy for subfoveal choroidal neovascularization secondary to age-related macular degeneration: phase II study results. Ophthalmology *110*, 979-986.

Fan, W., Zheng, J. J., and McLaughlin, B. J. (2002). An in vitro model of the back of the eye for studying retinal pigment epithelial-choroidal endothelial interactions. In Vitro Cell Dev Biol Anim *38*, 228-234.

Feng, W., Yasumura, D., Matthes, M. T., LaVail, M. M., and Vollrath, D. (2002). Mertk triggers uptake of photoreceptor outer segments during phagocytosis by cultured retinal pigment epithelial cells. J Biol Chem *277*, 17016-17022.

Ferguson, M. W., and O'Kane, S. (2004). Scar-free healing: from embryonic mechanisms to adult therapeutic intervention. Philos Trans R Soc Lond B Biol Sci *359*, 839-850.

Fine, S. L., Berger, J. W., Maguire, M. G., and Ho, A. C. (2000). Age-related macular degeneration. N Engl J Med *342*, 483-492.

Fink, W., and Sadun, A. A. (2004). Three-dimensional computer-automated threshold Amsler grid test. J Biomed Opt *9*, 149-153.

Finnemann, S. C. (2003). Focal adhesion kinase signaling promotes phagocytosis of integrin-bound photoreceptors. Embo J *22*, 4143-4154.

Finnemann, S. C., Bonilha, V. L., Marmorstein, A. D., and Rodriguez-Boulan, E. (1997). Phagocytosis of rod outer segments by retinal pigment epithelial cells requires alpha(v)beta5 integrin for binding but not for internalization. Proc Natl Acad Sci U S A *94*, 12932-12937.

Finnemann, S. C., and Rodriguez-Boulan, E. (1999). Macrophage and retinal pigment epithelium phagocytosis: apoptotic cells and photoreceptors compete for alphavbeta3 and alphavbeta5 integrins, and protein kinase C regulates alphavbeta5 binding and cytoskeletal linkage. J Exp Med *190*, 861-874.

Finnemann, S. C., and Silverstein, R. L. (2001). Differential roles of CD36 and alphavbeta5 integrin in photoreceptor phagocytosis by the retinal pigment epithelium. J Exp Med *194*, 1289-1298.

Flannery, J. G., O'Day, W., Pfeffer, B. A., Horwitz, J., and Bok, D. (1990). Uptake, processing and release of retinoids by cultured human retinal pigment epithelium. Exp Eye Res *51*, 717-728.

Gal, A., Li, Y., Thompson, D. A., Weir, J., Orth, U., Jacobson, S. G., Apfelstedt-Sylla, E., and Vollrath, D. (2000). Mutations in MERTK, the human orthologue of the RCS rat retinal dystrophy gene, cause retinitis pigmentosa. Nat Genet *26*, 270-271.

Gan, Z. R., Gould, R. J., Jacobs, J. W., Friedman, P. A., and Polokoff, M. A. (1988). Echistatin. A potent platelet aggregation inhibitor from the venom of the viper, Echis carinatus. J Biol Chem *263*, 19827-19832.

Gao, G., Li, Y., Zhang, D., Gee, S., Crosson, C., and Ma, J. (2001). Unbalanced expression of VEGF and PEDF in ischemia-induced retinal neovascularization. FEBS Lett *489*, 270-276.

Gao, H., and Hollyfield, J. G. (1992). Aging of the human retina. Differential loss of neurons and retinal pigment epithelial cells. Invest Ophthalmol Vis Sci *33*, 1-17.

Gehrig, A., Felbor, U., Kelsell, R. E., Hunt, D. M., Maumenee, I. H., and Weber, B. H. (1998). Assessment of the interphotoreceptor matrix proteoglycan-1 (IMPG1) gene localised to 6q13-q15 in autosomal dominant Stargardt-like disease (ADSTGD), progressive bifocal chorioretinal atrophy (PBCRA), and North Carolina macular dystrophy (MCDR1). J Med Genet *35*, 641-645.

Ghosh, F., Wong, F., Johansson, K., Bruun, A., and Petters, R. M. (2004). Transplantation of full-thickness retina in the rhodopsin transgenic pig. Retina *24*, 98-109.

Gilmour, D. T., Lyon, G. J., Carlton, M. B., Sanes, J. R., Cunningham, J. M., Anderson, J. R., Hogan, B. L., Evans, M. J., and Colledge, W. H. (1998). Mice deficient for the secreted glycoprotein SPARC/osteonectin/BM40 develop normally but show severe age-onset cataract formation and disruption of the lens. Embo J *17*, 1860-1870.

Girman, S. V., Wang, S., and Lund, R. D. (2003). Cortical visual functions can be preserved by subretinal RPE cell grafting in RCS rats. Vision Res *43*, 1817-1827.

Girman, S. V., Wang, S., and Lund, R. D. (2005). Time course of deterioration of rod and cone function in RCS rat and the effects of subretinal cell grafting: a light- and dark-adaptation study. Vision Res *45*, 343-354.

Glaser, B. M., D'Amore, P. A., Michels, R. G., Brunson, S. K., Fenselau, A. H., Rice, T., and Patz, A. (1980). The demonstration of angiogenic activity from ocular tissues. Preliminary report. Ophthalmology *87*, 440-446.

Goliath, R., Tombran-Tink, J., Rodriquez, I. R., Chader, G., Ramesar, R., and Greenberg, J. (1996). The gene for PEDF, a retinal growth factor is a prime candidate for retinitis pigmentosa and is tightly linked to the RP13 locus on chromosome 17p13.3. Mol Vis *2*, 5.

Gorin, M. B., Breitner, J. C., De Jong, P. T., Hageman, G. S., Klaver, C. C., Kuehn, M. H., and Seddon, J. M. (1999). The genetics of age-related macular degeneration. Mol Vis *5*, 29.

Guymer, R. (2001). The genetics of age-related macular degeneration. Clin Exp Optom *84*, 182-189.

Hageman, G. S., Marmor, M. F., Yao, X. Y., and Johnson, L. V. (1995). The interphotoreceptor matrix mediates primate retinal adhesion. Arch Ophthalmol *113*, 655-660.

Haines, J. L., Hauser, M. A., Schmidt, S., Scott, W. K., Olson, L. M., Gallins, P., Spencer, K. L., Kwan, S. Y., Noureddine, M., Gilbert, J. R., *et al.* (2005). Complement factor H variant increases the risk of age-related macular degeneration. Science *308*, 419-421.

Hajitou, A., Grignet, C., Devy, L., Berndt, S., Blacher, S., Deroanne, C. F., Bajou, K., Fong, T., Chiang, Y., Foidart, J. M., and Noel, A. (2002). The antitumoral effect of endostatin and angiostatin is associated with a down-regulation of vascular endothelial growth factor expression in tumor cells. Faseb J *16*, 1802-1804.

Hall, M. O., and Abrams, T. (1987). Kinetic studies of rod outer segment binding and ingestion by cultured rat RPE cells. Exp Eye Res *45*, 907-922.

Hall, M. O., Abrams, T. A., and Burgess, B. L. (2003). Integrin alphavbeta5 is not required for the phagocytosis of photoreceptor outer segments by cultured retinal pigment epithelial cells. Exp Eye Res *77*, 281-286.

Hall, M. O., Prieto, A. L., Obin, M. S., Abrams, T. A., Burgess, B. L., Heeb, M. J., and Agnew, B. J. (2001). Outer segment phagocytosis by cultured retinal pigment epithelial cells requires Gas6. Exp Eye Res *73*, 509-520.

Hodivala-Dilke, K. M., McHugh, K. P., Tsakiris, D. A., Rayburn, H., Crowley, D., Ullman-Cullere, M., Ross, F. P., Coller, B. S., Teitelbaum, S., and Hynes, R. O. (1999). Beta3-integrin-deficient mice are a model for Glanzmann thrombasthenia showing placental defects and reduced survival. J Clin Invest *103*, 229-238.

Hodivala-Dilke, K. M., Reynolds, A. R., and Reynolds, L. E. (2003). Integrins in angiogenesis: multitalented molecules in a balancing act. Cell Tissue Res *314*, 131-144.

Hollyfield, J. G., Besharse, J. C., and Rayborn, M. E. (1977). Turnover of rod photoreceptor outer segments. I. Membrane addition and loss in relationship to temperature. J Cell Biol *75*, 490-506.

Hope, G. M., Dawson, W. W., Engel, H. M., Ulshafer, R. J., Kessler, M. J., and Sherwood, M. B. (1992). A primate model for age related macular drusen. Br J Ophthalmol *76*, 11-16.

Houenou, L. J., D'Costa, A. P., Li, L., Turgeon, V. L., Enyadike, C., Alberdi, E., and Becerra, S. P. (1999). Pigment epithelium-derived factor promotes the survival and differentiation of developing spinal motor neurons. J Comp Neurol *412*, 506-514.

Husain, D., Kim, I., Gauthier, D., Lane, A. M., Tsilimbaris, M. K., Ezra, E., Connolly, E. J., Michaud, N., Gragoudas, E. S., O'Neill, C. A., *et al.* (2005). Safety and efficacy of intravitreal injection of ranibizumab in combination with verteporfin PDT on experimental choroidal neovascularization in the monkey. Arch Ophthalmol *123*, 509-516.

Hwang, J. Y., Lange, C., Helten, A., Hoppner-Heitmann, D., Duda, T., Sharma, R. K., and Koch, K. W. (2003). Regulatory modes of rod outer segment membrane guanylate cyclase differ in catalytic efficiency and Ca(2+)-sensitivity. Eur J Biochem *270*, 3814-3821.

Imai, D., Yoneya, S., Gehlbach, P. L., Wei, L. L., and Mori, K. (2005). Intraocular gene transfer of pigment epithelium-derived factor rescues photoreceptors from light-induced cell death. J Cell Physiol *202*, 570-578.

Inglehearn, C. F. (1998). Molecular genetics of human retinal dystrophies. Eye *12 (Pt 3b)*, 571-579.

Jeffery, G. (1998). The retinal pigment epithelium as a developmental regulator of the neural retina. Eye *12 (Pt 3b)*, 499-503.

Jeon, C. J., Strettoi, E., and Masland, R. H. (1998). The major cell populations of the mouse retina. J Neurosci *18*, 8936-8946.

Jin, M., He, S., Worpel, V., Ryan, S. J., and Hinton, D. R. (2000). Promotion of adhesion and migration of RPE cells to provisional extracellular matrices by TNF-alpha. Invest Ophthalmol Vis Sci *41*, 4324-4332.

John, S. K., Smith, J. E., Aguirre, G. D., and Milam, A. H. (2000). Loss of cone molecular markers in rhodopsin-mutant human retinas with retinitis pigmentosa. Mol Vis *6*, 204-215.

Jones, G. J., Crouch, R. K., Wiggert, B., Cornwall, M. C., and Chader, G. J. (1989). Retinoid requirements for recovery of sensitivity after visual-pigment bleaching in isolated photoreceptors. Proc Natl Acad Sci U S A *86*, 9606-9610.

Kamiguti, A. S., Zuzel, M., and Theakston, R. D. (1998). Snake venom metalloproteinases and disintegrins: interactions with cells. Braz J Med Biol Res *31*, 853-862.

Kanuga, N., Winton, H. L., Beauchene, L., Koman, A., Zerbib, A., Halford, S., Couraud, P. O., Keegan, D., Coffey, P., Lund, R. D., *et al.* (2002). Characterization of genetically modified human retinal pigment epithelial cells developed for in vitro and transplantation studies. Invest Ophthalmol Vis Sci *43*, 546-555.

Kaplan, J., Bonneau, D., Frezal, J., Munnich, A., and Dufier, J. L. (1990). Clinical and genetic heterogeneity in retinitis pigmentosa. Hum Genet *85*, 635-642.

Karakousis, P. C., John, S. K., Behling, K. C., Surace, E. M., Smith, J. E., Hendrickson, A., Tang, W. X., Bennett, J., and Milam, A. H. (2001). Localization of pigment epithelium derived factor (PEDF) in developing and adult human ocular tissues. Mol Vis *7*, 154-163.

Karan, G., Yang, Z., and Zhang, K. (2004). Expression of wild type and mutant ELOVL4 in cell culture: subcellular localization and cell viability. Mol Vis *10*, 248-253.

Kijlstra, A., La Heij, E., and Hendrikse, F. (2005). Immunological factors in the pathogenesis and treatment of age-related macular degeneration. Ocul Immunol Inflamm *13*, 3-11.

Klein, R. J., Zeiss, C., Chew, E. Y., Tsai, J. Y., Sackler, R. S., Haynes, C., Henning, A. K., SanGiovanni, J. P., Mane, S. M., Mayne, S. T., *et al.* (2005). Complement factor H polymorphism in age-related macular degeneration. Science *308*, 385-389.

Koenekoop, R., Pina, A. L., Loyer, M., Davidson, J., Robitaille, J., Maumenee, I., and Tombran-Tink, J. (1999). Four polymorphic variations in the PEDF gene identified during the mutation screening of patients with Leber congenital amaurosis. Mol Vis *5*, 10.

Kolb, H. (2003). How the retina works. American Scientist *91 (1)*, 28-35.

Kolb, H., and Gouras, P. (1974). Electron microscopic observations of human retinitis pigmentosa, dominantly inherited. Invest Ophthalmol *13*, 487-498.

Kolb, H. F., E. Nelson, R. (2002). WebVision: The Organisation of the Retina and Visual System, http://webvision.med.utah.edu/.

Kumar, A. (2001). Retinitis pigmentosa: mutations in a receptor tyrosine kinase gene, MERTK. J Biosci *26*, 3-5.

Kumar, C. C., Malkowski, M., Yin, Z., Tanghetti, E., Yaremko, B., Nechuta, T., Varner, J., Liu, M., Smith, E. M., Neustadt, B., *et al.* (2001). Inhibition of angiogenesis and tumor growth by SCH221153, a dual alpha(v)beta3 and alpha(v)beta5 integrin receptor antagonist. Cancer Res *61*, 2232-2238.

Kwak, N., Okamoto, N., Wood, J. M., and Campochiaro, P. A. (2000). VEGF is major stimulator in model of choroidal neovascularization. Invest Ophthalmol Vis Sci *41*, 3158-3164.

Kwan, A. S., Wang, S., and Lund, R. D. (1999). Photoreceptor layer reconstruction in a rodent model of retinal degeneration. Exp Neurol *159*, 21-33.

Lafuente, M. P., Villegas-Perez, M. P., Selles-Navarro, I., Mayor-Torroglosa, S., Miralles de Imperial, J., and Vidal-Sanz, M. (2002). Retinal ganglion cell death after acute retinal ischemia is an ongoing process whose severity and duration depends on the duration of the insult. Neuroscience *109*, 157-168.

Lau, D., McGee, L. H., Zhou, S., Rendahl, K. G., Manning, W. C., Escobedo, J. A., and Flannery, J. G. (2000). Retinal degeneration is slowed in transgenic rats by AAV-mediated delivery of FGF-2. Invest Ophthalmol Vis Sci *41*, 3622-3633.

LaVail, M. M. (1976). Rod outer segment disk shedding in rat retina: relationship to cyclic lighting. Science *194*, 1071-1074.

LaVail, M. M., and Battelle, B. A. (1975). Influence of eye pigmentation and light deprivation on inherited retinal dystrophy in the rat. Exp Eye Res *21*, 167-192.

LaVail, M. M., Pinto, L. H., and Yasumura, D. (1981). The interphotoreceptor matrix in rats with inherited retinal dystrophy. Invest Ophthalmol Vis Sci *21*, 658-668.

LaVail, M. M., Sidman, R. L., and Gerhardt, C. O. (1975). Congenic strains of RCS rats with inherited retinal dystrophy. J Hered *66*, 242-244.

LaVail, M. M., Unoki, K., Yasumura, D., Matthes, M. T., Yancopoulos, G. D., and Steinberg, R. H. (1992). Multiple growth factors, cytokines, and neurotrophins rescue photoreceptors from the damaging effects of constant light. Proc Natl Acad Sci U S A *89*, 11249-11253.

LaVail, M. M., Yasumura, D., Matthes, M. T., Lau-Villacorta, C., Unoki, K., Sung, C. H., and Steinberg, R. H. (1998). Protection of mouse photoreceptors by survival factors in retinal degenerations. Invest Ophthalmol Vis Sci *39*, 592-602.

Lawrence, J. M., Keegan, D. J., Muir, E. M., Coffey, P. J., Rogers, J. H., Wilby, M. J., Fawcett, J. W., and Lund, R. D. (2004). Transplantation of Schwann cell line clones secreting GDNF or BDNF into the retinas of dystrophic Royal College of Surgeons rats. Invest Ophthalmol Vis Sci *45*, 267-274.

Lawrence, J. M., Sauve, Y., Keegan, D. J., Coffey, P. J., Hetherington, L., Girman, S., Whiteley, S. J., Kwan, A. S., Pheby, T., and Lund, R. D. (2000). Schwann cell grafting into the retina of the dystrophic RCS rat limits functional deterioration. Royal College of Surgeons. Invest Ophthalmol Vis Sci *41*, 518-528.

Lebherz, C., Maguire, A. M., Auricchio, A., Tang, W., Aleman, T. S., Wei, Z., Grant, R., Cideciyan, A. V., Jacobson, S. G., Wilson, J. M., and Bennett, J. (2005). Nonhuman primate models for diabetic ocular neovascularization using AAV2-mediated overexpression of vascular endothelial growth factor. Diabetes *54*, 1141-1149.

Leeson, T. S. (1979). Rat retinal blood vessels. Can J Ophthalmol *14*, 21-28.

Leveillard, T., Mohand-Said, S., Lorentz, O., Hicks, D., Fintz, A. C., Clerin, E., Simonutti, M., Forster, V., Cavusoglu, N., Chalmel, F., *et al.* (2004). Identification and characterization of rod-derived cone viability factor. Nat Genet *36*, 755-759.

Lewin, A. S., Drenser, K. A., Hauswirth, W. W., Nishikawa, S., Yasumura, D., Flannery, J. G., and LaVail, M. M. (1998). Ribozyme rescue of photoreceptor cells in a transgenic rat model of autosomal dominant retinitis pigmentosa. Nat Med *4*, 967-971.

Li, L. (2001). Zebrafish mutants: behavioral genetic studies of visual system defects. Dev Dyn *221*, 365-372.

Li, Z. Y., Chang, J. H., and Milam, A. H. (1997). Distribution of basic fibroblast growth factor in human retinas with retinitis pigmentosa. Exp Eye Res *65*, 855-859.

Li, Z. Y., Possin, D. E., and Milam, A. H. (1995). Histopathology of bone spicule pigmentation in retinitis pigmentosa. Ophthalmology *102*, 805-816.

Lin, H., and Clegg, D. O. (1998). Integrin alphavbeta5 participates in the binding of photoreceptor rod outer segments during phagocytosis by cultured human retinal pigment epithelium. Invest Ophthalmol Vis Sci *39*, 1703-1712.

Liu, C., Li, Y., Peng, M., Laties, A. M., and Wen, R. (1999). Activation of caspase-3 in the retina of transgenic rats with the rhodopsin mutation s334ter during photoreceptor degeneration. J Neurosci *19*, 4778-4785.

Lund, R. D. (1975). Variations in the laterality of the central projections of retinal ganglion cells. Exp Eye Res *21*, 193-203.

Lund, R. D., Adamson, P., Sauve, Y., Keegan, D. J., Girman, S. V., Wang, S., Winton, H., Kanuga, N., Kwan, A. S., Beauchene, L., *et al.* (2001a). Subretinal transplantation of genetically modified human cell lines attenuates loss of visual function in dystrophic rats. Proc Natl Acad Sci U S A *98*, 9942-9947.

Lund, R. D., Coffey, P. J., Sauve, Y., and Lawrence, J. M. (1997). Intraretinal transplantation to prevent photoreceptor degeneration. Ophthalmic Res *29*, 305-319.

Lund, R. D., Kwan, A. S., Keegan, D. J., Sauve, Y., Coffey, P. J., and Lawrence, J. M. (2001b). Cell transplantation as a treatment for retinal disease. Prog Retin Eye Res *20*, 415-449.

Lund, R. D., Ono, S. J., Keegan, D. J., and Lawrence, J. M. (2003). Retinal transplantation: progress and problems in clinical application. J Leukoc Biol *74*, 151-160.

Machida, S., Chaudhry, P., Shinohara, T., Singh, D. P., Reddy, V. N., Chylack, L. T., Jr., Sieving, P. A., and Bush, R. A. (2001). Lens epithelium-derived growth factor promotes photoreceptor survival in light-damaged and RCS rats. Invest Ophthalmol Vis Sci *42*, 1087-1095.

Marcinkiewicz, C., Rosenthal, L. A., Mosser, D. M., Kunicki, T. J., and Niewiarowski, S. (1996). Immunological characterization of eristostatin and echistatin binding sites on alpha IIb beta 3 and alpha V beta 3 integrins. Biochem J *317 (Pt 3)*, 817-825.

Marcinkiewicz, C., Vijay-Kumar, S., McLane, M. A., and Niewiarowski, S. (1997). Significance of RGD loop and C-terminal domain of echistatin for recognition of alphaIIb beta3 and alpha(v) beta3 integrins and expression of ligand-induced binding site. Blood *90*, 1565-1575.

Marmor, M. (1998). Structure, function and disease of the retinal pigment epithelium, In The Retinal Pigment Epithelium, M. a. W. Marmor, TJ, ed. (New York: Oxford University press).

Marquardt, T., and Gruss, P. (2002). Generating neuronal diversity in the retina: one for nearly all. Trends Neurosci *25*, 32-38.

Martinez-Morales, J. R., Marti, E., Frade, J. M., and Rodriguez-Tebar, A. (1995). Developmentally regulated vitronectin influences cell differentiation, neuron survival and process outgrowth in the developing chicken retina. Neuroscience *68*, 245-253.

Marx, J. (2006). Genetics. A clearer view of macular degeneration. Science *311*, 1704-1705.

Matthes, M. T., and Bok, D. (1984). Blood vascular abnormalities in the degenerative mouse retina (C57BL/6J-rd le). Invest Ophthalmol Vis Sci *25*, 364-369.

May, C. (1887). Transplantation of a Rabbit'e Eye into the Human Orbit. Archives of Ophthalmology *1*, 47-53.

May, C. A., Horneber, M., and Lutjen-Drecoll, E. (1996). Quantitative and morphological changes of the choroid vasculature in RCS rats and their congenic controls. Exp Eye Res *63*, 75-84.

McGill, T. J., Douglas, R. M., Lund, R. D., and Prusky, G. T. (2004). Quantification of spatial vision in the Royal College of Surgeons rat. Invest Ophthalmol Vis Sci *45*, 932-936.

McLoon, S. C., and Lund, R. D. (1980). Identification of cells in retinal transplants which project to host visual centers: a horseradish peroxidase study in rats. Brain Res *197*, 491-495.

Menon, S. T., Han, M., and Sakmar, T. P. (2001). Rhodopsin: structural basis of molecular physiology. Physiol Rev *81*, 1659-1688.

Michaelides, M., Hunt, D. M., and Moore, A. T. (2003). The genetics of inherited macular dystrophies. J Med Genet *40*, 641-650.

Mieziewska, K. E., van Veen, T., Murray, J. M., and Aguirre, G. D. (1991). Rod and cone specific domains in the interphotoreceptor matrix. J Comp Neurol *308*, 371-380.

Milam, A. H., Li, Z. Y., and Fariss, R. N. (1998). Histopathology of the human retina in retinitis pigmentosa. Prog Retin Eye Res *17*, 175-205.

Molina, H., Quinones-Molina, R., Munoz, J., Alvarez, L., Alaminos, A., Ortega, I., Ohye, C., Macias, R., Piedra, J., and Gonzalez, C. (1994). Neurotransplantation in Parkinson's disease: from open microsurgery to bilateral stereotactic approach: first clinical trial using microelectrode recording technique. Stereotact Funct Neurosurg *62*, 204-208.

Nagaoka, T., Sakamoto, T., Mori, F., Sato, E., and Yoshida, A. (2002). The effect of nitric oxide on retinal blood flow during hypoxia in cats. Invest Ophthalmol Vis Sci *43*, 3037-3044.

Nakamura, I., Tanaka, H., Rodan, G. A., and Duong, L. T. (1998). Echistatin inhibits the migration of murine prefusion osteoclasts and the formation of multinucleated osteoclast-like cells. Endocrinology *139*, 5182-5193.

Nandrot, E. F., Kim, Y., Brodie, S. E., Huang, X., Sheppard, D., and Finnemann, S. C. (2004). Loss of synchronized retinal phagocytosis and age-related blindness in mice lacking alphavbeta5 integrin. J Exp Med *200*, 1539-1545.

Ogata, N., Wada, M., Otsuji, T., Jo, N., Tombran-Tink, J., and Matsumura, M. (2002). Expression of pigment epithelium-derived factor in normal adult rat eye and experimental choroidal neovascularization. Invest Ophthalmol Vis Sci *43*, 1168-1175.

Ohno-Matsui, K., Morita, I., Tombran-Tink, J., Mrazek, D., Onodera, M., Uetama, T., Hayano, M., Murota, S. I., and Mochizuki, M. (2001). Novel mechanism for age-related macular degeneration: an equilibrium shift between the angiogenesis factors VEGF and PEDF. J Cell Physiol *189*, 323-333.

Ortego, J., Escribano, J., Becerra, S. P., and Coca-Prados, M. (1996). Gene expression of the neurotrophic pigment epithelium-derived factor in the human ciliary epithelium. Synthesis and secretion into the aqueous humor. Invest Ophthalmol Vis Sci *37*, 2759-2767.

Palanza, L., Jhaveri, S., Donati, S., Nuzzi, R., and Vercelli, A. (2005). Quantitative spatial analysis of the distribution of NADPH-diaphorase-positive neurons in the developing and mature rat retina. Brain Res Bull *65*, 349-360.

Paques, M., Tadayoni, R., Sercombe, R., Laurent, P., Genevois, O., Gaudric, A., and Vicaut, E. (2003). Structural and hemodynamic analysis of the mouse retinal microcirculation. Invest Ophthalmol Vis Sci *44*, 4960-4967.

Peichl, L. (2005). Diversity of mammalian photoreceptor properties: Adaptations to habitat and lifestyle? Anat Rec A Discov Mol Cell Evol Biol.

Petry, H. M., Erichsen, J. T., and Szel, A. (1993). Immunocytochemical identification of photoreceptor populations in the tree shrew retina. Brain Res *616*, 344-350.

Petters, R. M., Alexander, C. A., Wells, K. D., Collins, E. B., Sommer, J. R., Blanton, M. R., Rojas, G., Hao, Y., Flowers, W. L., Banin, E., *et al.* (1997). Genetically engineered large animal model for studying cone photoreceptor survival and degeneration in retinitis pigmentosa. Nat Biotechnol *15*, 965-970.

Phelan, J. K., and Bok, D. (2000). A brief review of retinitis pigmentosa and the identified retinitis pigmentosa genes. Mol Vis *6*, 116-124.

Plate, K. H., Breier, G., Weich, H. A., and Risau, W. (1992). Vascular endothelial growth factor is a potential tumour angiogenesis factor in human gliomas in vivo. Nature *359*, 845-848.

Proulx, S., Guerin, S. L., and Salesse, C. (2003). Effect of quiescence on integrin alpha5beta1 expression in human retinal pigment epithelium. Mol Vis *9*, 473-481.

Provis, J. M. (2001). Development of the primate retinal vasculature. Prog Retin Eye Res *20*, 799-821.

Prusky, G. T., Harker, K. T., Douglas, R. M., and Whishaw, I. Q. (2002). Variation in visual acuity within pigmented, and between pigmented and albino rat strains. Behav Brain Res *136*, 339-348.

Qiao, H., Sonoda, K. H., Sassa, Y., Hisatomi, T., Yoshikawa, H., Ikeda, Y., Murata, T., Akira, S., and Ishibashi, T. (2004). Abnormal retinal vascular development in IL-18 knockout mice. Lab Invest *84*, 973-980.

Rao, M. N., Shinnar, A. E., Noecker, L. A., Chao, T. L., Feibush, B., Snyder, B., Sharkansky, I., Sarkahian, A., Zhang, X., Jones, S. R., *et al.* (2000). Aminosterols from the dogfish shark Squalus acanthias. J Nat Prod *63*, 631-635.

Regillo, C. D. (2000). Update on photodynamic therapy. Curr Opin Ophthalmol *11*, 166-170.

Rexer, M., May, C. A., and Lutjen-Drecoll, E. (1998). Changes in choroidal innervation in Royal College of Surgeons rats with hereditary retinal degeneration. Acta Anat (Basel) *162*, 112-118.

Reynolds, L. E., Wyder, L., Lively, J. C., Taverna, D., Robinson, S. D., Huang, X., Sheppard, D., Hynes, R. O., and Hodivala-Dilke, K. M. (2002). Enhanced pathological angiogenesis in mice lacking beta3 integrin or beta3 and beta5 integrins. Nat Med *8*, 27-34.

Rivera, A., White, K., Stohr, H., Steiner, K., Hemmrich, N., Grimm, T., Jurklies, B., Lorenz, B., Scholl, H. P., Apfelstedt-Sylla, E., and Weber, B. H. (2000). A comprehensive survey of sequence variation in the ABCA4 (ABCR) gene in Stargardt disease and age-related macular degeneration. Am J Hum Genet *67*, 800-813.

Robbins, S. G., Brem, R. B., Wilson, D. J., O'Rourke, L. M., Robertson, J. E., Westra, I., Planck, S. R., and Rosenbaum, J. T. (1994). Immunolocalization of integrins in proliferative retinal membranes. Invest Ophthalmol Vis Sci *35*, 3475-3485.

Roque, R. S., Imperial, C. J., and Caldwell, R. B. (1996). Microglial cells invade the outer retina as photoreceptors degenerate in Royal College of Surgeons rats. Invest Ophthalmol Vis Sci *37*, 196-203.

Rosolen, S. G., Saint-Macary, G., Gautier, V., and Le Gargasson, J. F. (2002). SLO angiography: arterio-venous filling times in monkey and minipig. Vet Ophthalmol *5*, 19-22.

Roufail, E., Stringer, M., and Rees, S. (1995). Nitric oxide synthase immunoreactivity and NADPH diaphorase staining are co-localised in neurons closely associated with the vasculature in rat and human retina. Brain Res *684*, 36-46.

Rupp, P. A., Czirok, A., and Little, C. D. (2004). alphavbeta3 integrin-dependent endothelial cell dynamics in vivo. Development *131*, 2887-2897.

Ryan, S. J. (1982). Subretinal neovascularization. Natural history of an experimental model. Arch Ophthalmol *100*, 1804-1809.

Sackett, C. S., and Schenning, S. (2002). The age-related eye disease study: the results of the clinical trial. Insight *27*, 5-7.

Saishin, Y., Takahashi, K., Lima e Silva, R., Hylton, D., Rudge, J. S., Wiegand, S. J., and Campochiaro, P. A. (2003). VEGF-TRAP(R1R2) suppresses choroidal neovascularization and VEGF-induced breakdown of the blood-retinal barrier. J Cell Physiol *195*, 241-248.

Santos, A., Humayun, M. S., de Juan, E., Jr., Greenburg, R. J., Marsh, M. J., Klock, I. B., and Milam, A. H. (1997). Preservation of the inner retina in retinitis pigmentosa. A morphometric analysis. Arch Ophthalmol *115*, 511-515.

Sauve, Y., Girman, S. V., Wang, S., Keegan, D. J., and Lund, R. D. (2002). Preservation of visual responsiveness in the superior colliculus of RCS rats after retinal pigment epithelium cell transplantation. Neuroscience *114*, 389-401.

Sauve, Y., Lu, B., and Lund, R. D. (2004). The relationship between full field electroretinogram and perimetry-like visual thresholds in RCS rats during photoreceptor degeneration and rescue by cell transplants. Vision Res *44*, 9-18.

Schlondorff, J., and Blobel, C. P. (1999). Metalloprotease-disintegrins: modular proteins capable of promoting cell-cell interactions and triggering signals by protein-ectodomain shedding. J Cell Sci *112 (Pt 21)*, 3603-3617.

Schmidt-Erfurth, U., Teschner, S., Noack, J., and Birngruber, R. (2001). Three-dimensional topographic angiography in chorioretinal vascular disease. Invest Ophthalmol Vis Sci *42*, 2386-2394.

Schmidt, J. C., Rodrigues, E. B., Meyer, C. H., and Kroll, P. (2003). Is membrane extraction in cases of exudative age-related macular degeneration still up-to-date? A 4-year resume. Ophthalmologica *217*, 401-407.

Schultz, D. W., Klein, M. L., Humpert, A. J., Luzier, C. W., Persun, V., Schain, M., Mahan, A., Runckel, C., Cassera, M., Vittal, V., *et al.* (2003). Analysis of the ARMD1 locus: evidence that a mutation in HEMICENTIN-1 is associated with age-related macular degeneration in a large family. Hum Mol Genet *12*, 3315-3323.

Seaton, A. D., Sheedlo, H. J., and Turner, J. E. (1994). A primary role for RPE transplants in the inhibition and regression of neovascularization in the RCS rat. Invest Ophthalmol Vis Sci *35*, 162-169.

Seaton, A. D., and Turner, J. E. (1992). RPE transplants stabilize retinal vasculature and prevent neovascularization in the RCS rat. Invest Ophthalmol Vis Sci *33*, 83-91.

Semkova, I., Kreppel, F., Welsandt, G., Luther, T., Kozlowski, J., Janicki, H., Kochanek, S., and Schraermeyer, U. (2002). Autologous transplantation of genetically modified iris pigment epithelial cells: a promising concept for the treatment of age-related macular degeneration and other disorders of the eye. Proc Natl Acad Sci U S A *99*, 13090-13095.

Semkova, I., Peters, S., Welsandt, G., Janicki, H., Jordan, J., and Schraermeyer, U. (2003). Investigation of laser-induced choroidal neovascularization in the rat. Invest Ophthalmol Vis Sci *44*, 5349-5354.

Seo, M. S., Kwak, N., Ozaki, H., Yamada, H., Okamoto, N., Yamada, E., Fabbro, D., Hofmann, F., Wood, J. M., and Campochiaro, P. A. (1999). Dramatic inhibition of retinal and choroidal neovascularization by oral administration of a kinase inhibitor. Am J Pathol *154*, 1743-1753.

Silverman, M. S., and Hughes, S. E. (1990). Photoreceptor rescue in the RCS rat without pigment epithelium transplantation. Curr Eye Res *9*, 183-191.

Soldi, R., Mitola, S., Strasly, M., Defilippi, P., Tarone, G., and Bussolino, F. (1999). Role of alphavbeta3 integrin in the activation of vascular endothelial growth factor receptor-2. Embo J *18*, 882-892.

Sommer, A., Tielsch, J. M., Katz, J., Quigley, H. A., Gottsch, J. D., Javitt, J. C., Martone, J. F., Royall, R. M., Witt, K. A., and Ezrine, S. (1991). Racial differences in the cause-specific prevalence of blindness in east Baltimore. N Engl J Med *325*, 1412-1417.

Spranger, J., Osterhoff, M., Reimann, M., Mohlig, M., Ristow, M., Francis, M. K., Cristofalo, V., Hammes, H. P., Smith, G., Boulton, M., and Pfeiffer, A. F. (2001). Loss of the antiangiogenic pigment epithelium-derived factor in patients with angiogenic eye disease. Diabetes *50*, 2641-2645.

Steele, F. R., Chader, G. J., Johnson, L. V., and Tombran-Tink, J. (1993). Pigment epithelium-derived factor: neurotrophic activity and identification as a member of the serine protease inhibitor gene family. Proc Natl Acad Sci U S A *90*, 1526-1530.

Stellmach, V., Crawford, S. E., Zhou, W., and Bouck, N. (2001). Prevention of ischemia-induced retinopathy by the natural ocular antiangiogenic agent pigment epithelium-derived factor. Proc Natl Acad Sci U S A *98*, 2593-2597.

Steuer, H., Jaworski, A., Stoll, D., and Schlosshauer, B. (2004). In vitro model of the outer blood-retina barrier. Brain Res Brain Res Protoc *13*, 26-36.

Stevenson, J. P., Rosen, M., Sun, W., Gallagher, M., Haller, D. G., Vaughn, D., Giantonio, B., Zimmer, R., Petros, W. P., Stratford, M., *et al.* (2003). Phase I trial of the antivascular agent combretastatin A4 phosphate on a 5-day schedule to patients with cancer: magnetic resonance imaging evidence for altered tumor blood flow. J Clin Oncol *21*, 4428-4438.

Stewart, P. A., and Tuor, U. I. (1994). Blood-eye barriers in the rat: correlation of ultrastructure with function. J Comp Neurol *340*, 566-576.

Stitt, A. W., Graham, D., and Gardiner, T. A. (2004). Ocular wounding prevents pre-retinal neovascularization and upregulates PEDF expression in the inner retina. Mol Vis *10*, 432-438.

Stokkermans, T. J. (2000). Treatment of age-related macular degeneration. Clin Eye Vis Care *12*, 15-35.

Stone, E. M., Braun, T. A., Russell, S. R., Kuehn, M. H., Lotery, A. J., Moore, P. A., Eastman, C. G., Casavant, T. L., and Sheffield, V. C. (2004). Missense variations in the fibulin 5 gene and age-related macular degeneration. N Engl J Med *351*, 346-353.

Stone, J., Itin, A., Alon, T., Pe'er, J., Gnessin, H., Chan-Ling, T., and Keshet, E. (1995). Development of retinal vasculature is mediated by hypoxia-induced vascular endothelial growth factor (VEGF) expression by neuroglia. J Neurosci *15*, 4738-4747.

Streilein, J. W., Ma, N., Wenkel, H., Ng, T. F., and Zamiri, P. (2002). Immunobiology and privilege of neuronal retina and pigment epithelium transplants. Vision Res *42*, 487-495.

study, M. P. (1991). Subfoveal neovascular lesions in age-related macular degeneration. Guidelines for evaluation and treatment in the macular photocoagulation study. Macular Photocoagulation Study Group. Arch Ophthalmol *109*, 1242-1257.

Sugita, Y., Becerra, S. P., Chader, G. J., and Schwartz, J. P. (1997). Pigment epithelium-derived factor (PEDF) has direct effects on the metabolism and proliferation of microglia and indirect effects on astrocytes. J Neurosci Res *49*, 710-718.

Takita, H., Yoneya, S., Gehlbach, P. L., Duh, E. J., Wei, L. L., and Mori, K. (2003). Retinal neuroprotection against ischemic injury mediated by intraocular gene transfer of pigment epithelium-derived factor. Invest Ophthalmol Vis Sci *44*, 4497-4504.

Tao, W., Wen, R., Goddard, M. B., Sherman, S. D., O'Rourke, P. J., Stabila, P. F., Bell, W. J., Dean, B. J., Kauper, K. A., Budz, V. A., *et al.* (2002). Encapsulated cell-based delivery of CNTF reduces photoreceptor degeneration in animal models of retinitis pigmentosa. Invest Ophthalmol Vis Sci *43*, 3292-3298.

Tomany, S. C., Wang, J. J., Van Leeuwen, R., Klein, R., Mitchell, P., Vingerling, J. R., Klein, B. E., Smith, W., and De Jong, P. T. (2004). Risk factors for incident age-related macular degeneration: pooled findings from 3 continents. Ophthalmology *111*, 1280-1287.

Tombran-Tink, J. (2005). The neuroprotective and angiogenesis inhibitory serpin, PEDF: new insights into phylogeny, function, and signaling. Front Biosci *10*, 2131-2149.

Tombran-Tink, J., Aparicio, S., Xu, X., Tink, A. R., Lara, N., Sawant, S., Barnstable, C. J., and Zhang, S. S. (2005). PEDF and the serpins: phylogeny, sequence conservation, and functional domains. J Struct Biol *151*, 130-150.

Tombran-Tink, J., Chader, G. G., and Johnson, L. V. (1991). PEDF: a pigment epithelium-derived factor with potent neuronal differentiative activity. Exp Eye Res *53*, 411-414.

Tombran-Tink, J., and Johnson, L. V. (1989). Neuronal differentiation of retinoblastoma cells induced by medium conditioned by human RPE cells. Invest Ophthalmol Vis Sci *30*, 1700-1707.

Tombran-Tink, J., Shivaram, S. M., Chader, G. J., Johnson, L. V., and Bok, D. (1995). Expression, secretion, and age-related downregulation of pigment epithelium-derived factor, a serpin with neurotrophic activity. J Neurosci *15*, 4992-5003.

Tout, S., Chan-Ling, T., Hollander, H., and Stone, J. (1993). The role of Muller cells in the formation of the blood-retinal barrier. Neuroscience *55*, 291-301.

Travis, G. H. (1998). Mechanisms of cell death in the inherited retinal degenerations. Am J Hum Genet *62*, 503-508.

Travis, G. H. (2005). DISCO! Dissociation of cone opsins: the fast and noisy life of cones explained. Neuron *46*, 840-842.

Turner, J. E., Seiler, M., Aramant, R., and Blair, J. R. (1988). Embryonic retinal grafts transplanted into the lesioned adult rat retina. Prog Brain Res *78*, 131-139.

Turowski, P., Adamson, P., Sathia, J., Zhang, J. J., Moss, S. E., Aylward, G. W., Hayes, M. J., Kanuga, N., and Greenwood, J. (2004). Basement membrane-dependent modification of phenotype and gene expression in human retinal pigment epithelial ARPE-19 cells. Invest Ophthalmol Vis Sci *45*, 2786-2794.

Ulshafer, R. J., Engel, H. M., Dawson, W. W., Allen, C. B., and Kessler, M. J. (1987). Macular degeneration in a community of rhesus monkeys. Ultrastructural observations. Retina *7*, 198-203.

van Leeuwen, R., Klaver, C. C., Vingerling, J. R., Hofman, A., and de Jong, P. T. (2003). The risk and natural course of age-related maculopathy: follow-up at 6 1/2 years in the Rotterdam study. Arch Ophthalmol *121*, 519-526.

Villegas-Perez, M. P., Lawrence, J. M., Vidal-Sanz, M., Lavail, M. M., and Lund, R. D. (1998). Ganglion cell loss in RCS rat retina: a result of compression of axons by contracting intraretinal vessels linked to the pigment epithelium. J Comp Neurol *392*, 58-77.

Villegas-Perez, M. P., Vidal-Sanz, M., and Lund, R. D. (1996). Mechanism of retinal ganglion cell loss in inherited retinal dystrophy. Neuroreport *7*, 1995-1999.

Vincent, S. R., and Kimura, H. (1992). Histochemical mapping of nitric oxide synthase in the rat brain. Neuroscience *46*, 755-784.

Vollrath, D., Feng, W., Duncan, J. L., Yasumura, D., D'Cruz, P. M., Chappelow, A., Matthes, M. T., Kay, M. A., and LaVail, M. M. (2001). Correction of the retinal dystrophy phenotype of the RCS rat by viral gene transfer of Mertk. Proc Natl Acad Sci U S A *98*, 12584-12589.

Volpert, O. V., Zaichuk, T., Zhou, W., Reiher, F., Ferguson, T. A., Stuart, P. M., Amin, M., and Bouck, N. P. (2002). Inducer-stimulated Fas targets activated endothelium for destruction by anti-angiogenic thrombospondin-1 and pigment epithelium-derived factor. Nat Med *8*, 349-357.

Wang, J. J., Jakobsen, K. B., Smith, W., and Mitchell, P. (2004). Refractive status and the 5-year incidence of age-related maculopathy: the Blue Mountains Eye Study. Clin Experiment Ophthalmol *32*, 255-258.

Wang, S., Lu, B., and Lund, R. D. (2005a). Morphological changes in the Royal College of Surgeons rat retina during photoreceptor degeneration and after cell-based therapy. J Comp Neurol *491*, 400-417.

Wang, S., Lu, B., Wood, P., and Lund, R. D. (2005b). Grafting of ARPE-19 and Schwann cells to the subretinal space in RCS rats. Invest Ophthalmol Vis Sci *46*, 2552-2560.

Wang, S., Villegas-Perez, M. P., Holmes, T., Lawrence, J. M., Vidal-Sanz, M., Hurtado-Montalban, N., and Lund, R. D. (2003). Evolving neurovascular relationships in the RCS rat with age. Curr Eye Res *27*, 183-196.

Wang, S., Villegas-Perez, M. P., Vidal-Sanz, M., and Lund, R. D. (2000). Progressive optic axon dystrophy and vacuslar changes in rd mice. Invest Ophthalmol Vis Sci *41*, 537-545.

Wenkstern, A., and Stokes, J. (2003). Photodynamic therapy in age-related macular degeneration: missing information. Age Ageing *32*, 357-359.

Wierzbicka-Patynowski, I., Niewiarowski, S., Marcinkiewicz, C., Calvete, J. J., Marcinkiewicz, M. M., and McLane, M. A. (1999). Structural requirements of echistatin for the recognition of alpha(v)beta(3) and alpha(5)beta(1) integrins. J Biol Chem *274*, 37809-37814.

Wu, Y. Q., and Becerra, S. P. (1996). Proteolytic activity directed toward pigment epithelium-derived factor in vitreous of bovine eyes. Implications of proteolytic processing. Invest Ophthalmol Vis Sci *37*, 1984-1993.

Wu, Y. Q., Notario, V., Chader, G. J., and Becerra, S. P. (1995). Identification of pigment epithelium-derived factor in the interphotoreceptor matrix of bovine eyes. Protein Expr Purif *6*, 447-456.

Yang, C. H., Huang, T. F., Liu, K. R., Chen, M. S., and Hung, P. T. (1996). Inhibition of retinal pigment epithelial cell-induced tractional retinal detachment by disintegrins, a group of Arg-Gly-Asp-containing peptides from viper venom. Invest Ophthalmol Vis Sci *37*, 843-854.

Young, M. J., Ray, J., Whiteley, S. J., Klassen, H., and Gage, F. H. (2000). Neuronal differentiation and morphological integration of hippocampal progenitor cells transplanted to the retina of immature and mature dystrophic rats. Mol Cell Neurosci *16*, 197-205.

Young, R. W., and Bok, D. (1969). Participation of the retinal pigment epithelium in the rod outer segment renewal process. J Cell Biol *42*, 392-403.

Zaidi, F. H., Cheong-Leen, R., Gair, E. J., Weir, R., Sharkawi, E., Lee, N., and Gregory-Evans, K. (2004). The Amsler chart is of doubtful value in retinal screening for early laser therapy of subretinal membranes. The West London Survey. Eye *18*, 503-508.

Zambarakji, H. J., Keegan, D. J., Holmes, T. M., Halfyard, A. S., Villegas-Perez, M. P., Charteris, D. G., Fitzke, F. W., Greenwood, J., and Lund, R. D. (2005). High resolution imaging of fluorescein patterns in RCS rat retinae and their direct correlation with histology. Exp Eye Res.

Zhang, H. (1994). Scanning Electron-Microscopic study of Corrosion Casts on Retinal and Choroidal Angioarchitechture in Man and Animals. Progress in Retinal and Eye Research *13*, 243-270.

Zhao, M. W., Jin, M. L., He, S., Spee, C., Ryan, S. J., and Hinton, D. R. (1999). A distinct integrin-mediated phagocytic pathway for extracellular matrix remodeling by RPE cells. Invest Ophthalmol Vis Sci *40*, 2713-2723.

Appendix I Abbreviations

AAV	adeno-associated virus
ABCR	ATP-binding cassette transporter
ADAMs	a disintegrin and metalloproteinase domain
AMD	age-related macular degeneration
AOI	area of interest
AREDS	age-related eye disease study
ATP	adenosine triphosphate
BRB	blood-retinal barrier
BSA	bovine serum albumen
BSE	bovine spongiform encephalopathy
CAM	chicken chorioallantoic membrane
CCD	charged coupled device
cGMP	cyclic guanosine monophosphate
CNTF	ciliary neurotrophic factor
CNV	choroidal neovascularisation
COOH	carbon, oxygen, oxygen, hydrogen
cSLO	confocal scanning laser ophthalmoscopy
DAB	diaminobenzidine
DHA	docosahexaenoic acid
DMEM	Dulbecco's modified Eagle medium
DVCs	development of vascular complexes
ECM	extracellular matrix
EM	electron microscopy
EPC-1	early population doubling level cDNA-1 (PEDF)
ERG	electroretinogram
FA	fluorescein angiography
FAK	focal adhesion kinase
FCS	foetal calf serum
FDA	Federal Drug Administration
FFB	Foundation Fighting Blindness
FGF	fibroblast growth factor
FITC	fluorescein-isothiocyanate
GAS6	growth arrest specific gene6
Gb	gigabyte
GCL	ganglion cell layer
GDNF	glial cell line-derived neurotrophic factor
GFP	green fluorescent protein
HIV	human immunodeficiency virus
HRP	horseradish peroxidase
IgG	mouse immunoglobulin
INL	inner nuclear layer
iNOS	inducible nitric oxide synthase
IPL	inner plexiform layer
IPM	inter photoreceptor matrix
IRBP	retinoid binding protein
LCA	Leber Congenital Amaurosis
NADPH-d	nicotinamide adenine dinucleotide phosphate-diaphorase

nNOS	neuronal nitric oxide synthase
NO	nitric oxide
OFL	optic fibre layer
ONL	outer nuclear layer
OPL	outer plexiform layer
OS	outer segments
P23H	Pro23His rat
P25	postnatal day 25
PBS	phosphate buffered saline
PC	personal computer
PDE	phosphodiesterase
PDT	photodynamic therapy
PEDF	pigment epithelial derived factor
RCS	Royal College of Surgeons
rd	retinal degeneration mouse (C57Bl/6J-rd le)
rds	retinal degeneration slow mouse
RGD	Arg-Gly-Asp attachment site
RGS	regulators of G protein signalling
RP	retinitis pigmentosa
RPE	retinal pigmented epithelium
SDS	sodium dodecyl sulfate
SEM	standard error of the mean
SLO	scanning laser ophthalmoscopy
T1H2	transplantation at 1 month, harvested at 2 months
T1H3	transplantation at 1 month, harvested at 3 months
T1H7	transplantation at 1 month, harvested at 7 months
T3H4	transplantation at 3 month, harvested at 4 months
VC	vascular complex
VEGF	vascular endothelial growth factor